National Library of Canada

Acquisitions and Bibliographic Services Branch

395 Wellington Street
Ottawa, Ontario
K1A 0N4

Bibliothèque nationale du Canada

Direction des acquisitions et des services bibliographiques

395, rue Wellington
Ottawa (Ontario)
K1A 0N4

Your file Votre référence

Our file Notre référence

NOTICE

The quality of this microform is heavily dependent upon the quality of the original thesis submitted for microfilming. Every effort has been made to ensure the highest quality of reproduction possible.

If pages are missing, contact the university which granted the degree.

Some pages may have indistinct print especially if the original pages were typed with a poor typewriter ribbon or if the university sent us an inferior photocopy.

Reproduction in full or in part of this microform is governed by the Canadian Copyright Act, R.S.C. 1970, c. C-30, and subsequent amendments.

AVIS

La qualité de cette microforme dépend grandement de la qualité de la thèse soumise au microfilmage. Nous avons tout fait pour assurer une qualité supérieure de reproduction.

S'il manque des pages, veuillez communiquer avec l'université qui a conféré le grade.

La qualité d'impression de certaines pages peut laisser à désirer, surtout si les pages originales ont été dactylographiées à l'aide d'un ruban usé ou si l'université nous a fait parvenir une photocopie de qualité inférieure.

La reproduction, même partielle, de cette microforme est soumise à la Loi canadienne sur le droit d'auteur, SRC 1970, c. C-30, et ses amendements subséquents.

Canada

PREPARATION OF HIGHLY SELECTIVE POLYAMIDE MEMBRANES FOR GAS SEPARATION APPLICATIONS

ABDULREZA TABE MOHAMMADI

A Ph.D. Thesis Submitted to the School of Graduate Studies
and Research in Partial Fulfilment of the requirements
for the Degree of Doctorate of Philosophy in
the Department of Chemical Engineering
University of Ottawa

December 1994

National Library
of Canada

Acquisitions and
Bibliographic Services Branch

395 Wellington Street
Ottawa, Ontario
K1A 0N4

Bibliothèque nationale
du Canada

Direction des acquisitions et
des services bibliographiques

395, rue Wellington
Ottawa (Ontario)
K1A 0N4

Your file Votre référence

Our file Notre référence

ISBN 0-612-07864-7

Canada

UNIVERSITÉ D'OTTAWA
UNIVERSITY OF OTTAWA

TABLE OF CONTENTS

List of Figures iv

List of Tables vi

List of Publications and Presentations viii

Acknowledgements x

Nomenclature xi

Abstract xiii

Chapter One: Introduction 1

1.1. Objectives 2

1.2. Membrane Gas Separation Processes 2

1.3. Historical Background and Recent Developments 4

1.4. Applications 9

1.4.1. Air Separation 11

1.4.2. Hydrogen Separation and Recovery 13

1.4.3. Natural and Landfill Gas Treatments 15

1.5. Transport Models 16

1.6. Membrane Materials Selection and Membrane Formation 17

1.7. Overview of the Objectives 19

Chapter Two: Theory 21

2.1. Gas Transport Through Membranes 21

2.1.1. Introduction 21

2.1.2. Gas Permeation Mechanisms 25

2.2. Resistance Model 28

2.2.1. Resistance in an Uncoated Membrane 30

2.2.2. Resistance in a Coated Membrane 31

2.2.3. Ideal Separation Factor (ISF) 32

2.2.4. Actual Separation Factor (ASF) 32
2.3. Calculation of the Local Resistances 33
2.3.1. Local Resistances of an Uncoated Membrane 33
2.3.2. Local Resistances of a Coated Membrane 35
2.3.3. Procedure to Solve for the Local Resistances 37
2.4. Permeation Rate Measurement in a Constant Volume System 39

Chapter Three: Experimentals 41
3.1. Preparation of Dry Membranes 41
3.1.1. Material 41
3.1.2. Preparation of Uncoated and Coated Asymmetric Membrane 42
3.1.3. Preparation of Homogeneous Dense Membranes 44
3.2. Apparatus for Gas Permeation Experiments 46
3.2.1. Constant Pressure System 47
3.2.2. Experimental Procedure for the Constant Pressure System 47
3.2.3. Calibration of the Gas Chromatograph 49
3.2.4. Constant Volume System 50
3.2.5. Process Control Algorithm 57
3.2.6. Experimental Procedure for the Constant Volume System 59
3.2.7. Range of the Permeation Rates Measurable Using the Constant Volume System 61
3.2.8. Testing the Performance of the Constant Volume System Devices 63
3.3. Measurement of Leak Rate into the Constant Volume System 63
3.4. Measurement of Permeation Rate 65

Chapter Four: Results and Discussions 66
4.1. Performance of the Constant Volume System 66
4.1.1. Leak Rate into the System 67
4.1.2. Upstream Pressure Control 71

4.2. Effect of Pressure on the Performance of Asymmetric Membrane 72
4.2.1. Uncoated Membrane 74
4.2.2. Coated Membrane 82
4.2.3. Measurement of the Permeation Rate of the Low Permeable Gases Through Silicone-Coated Asymmetric Membranes Using Constant Volume System 91

4.3. Determination of the Local Resistances and the Effect of Coating 99
4.4. Gas Mixture Separation 106
4.4.1. CO_2/CH_4 Separation 106
4.4.2. O_2/N_2 (Air) Separation 109
4.5. Gas Permeation Through Homogeneous Membranes 110
4.5.1. Intrinsic Permeability and Intrinsic Separation Factor 110
4.5.2. Performance of Homogeneous Membrane with Additive 113
4.5.3. Performance of Homogeneous Membrane without Additive 116
4.6. Scanning Electron Microscopy Results 119

Conclusions **123**
References 125
Appendices 134
Appendix A: Sample Calculations 135
Appendix B: Computer Program 156

LIST OF FIGURES

Figure 1.1:	A typical membrane separation process.	3
Figure 2.1:	A schematic diagram of uncoated and coated membranes with their electrical analogue.	29
Figure 3.1:	Chemical structure of aromatic polyamide polymer.	42
Figure 3.2:	Schematic diagram of the separation cell and the constant pressure gas separation system.	48
Figure 3.3:	Schematic diagram of constant volume gas separation system.	51
Figure 3.4:	Schematic diagram of gas separation cell.	53
Figure 3.5:	Calibration curves to be used as a guideline for choosing correct downstream volume at different permeation rates in the constant volume system.	62
Figure 4.1:	Variation of the downstream pressure and leak rate with time during leak test (ii).	69
Figure 4.2:	Fluctuation of upstream pressure with respect to the set point.	73
Figure 4.3:	Permeation rates of the experimental gases at different operating pressures through uncoated asymmetric membranes.	77
Figure 4.4:	Permeabilities of the experimental gases at different operating pressures through uncoated asymmetric membranes.	78
Figure 4.5:	Overall resistance of uncoated membranes toward the permeation of the experimental gases.	80
Figure 4.6:	Ideal separation factor of the uncoated asymmetric membranes toward the experimental gases.	81
Figure 4.7:	Permeation rates of the experimental gases through coated asymmetric membranes.	85
Figure 4.8:	Permeabilities of the experimental gases through coated asymmetric	

membranes. 87

Figure 4.9: Overall resistance of coated asymmetric membranes toward the permeation of the experimental gases. 89

Figure 4.10: Ideal separation factors of the coated asymmetric membranes toward the experimental gases. 90

Figure 4.11: Comparison of the ideal separation factors before and after coating. 92

Figure 4.12: Variation of the permeation rate and the downstream pressure with time of nitrogen and methane measured by the constant volume system. 95

Figure 4.13: Comparison of the permeability and separation factors of P membranes with other membranes found in the literature for O_2/N_2 and CO_2/CH_4 systems. 98

Figure 4.14: Comparison of the matrix and the pore resistances for helium at different operating pressures. 102

Figure 4.15: Mole fraction of carbon dioxide in the permeate versus that in the feed in CO_2/CH_4 separation experiments. 108

Figure 4.16: Permeation rate versus carbon dioxide feed mole fraction in CO_2/CH_4 separation experiments. 108

Figure 4.17: Intrinsic separation factor of homogeneous PA membranes with no additive toward O_2/N_2 system. 118

Figure 4.18: Scanning electron micrographs of the cross-section of an asymmetric PA membrane. 120

Figure 4.19: Scanning electron micrographs of the cross-section of a homogeneous PA membrane prepared with the addition of lithium nitrate. 121

Figure 4.20: Scanning electron micrographs of the cross-section of a homogeneous PA membrane prepared without the addition of lithium nitrate. 122

LIST OF TABLES

Table 1.1: Ideal separation factors of different membranes toward some gas mixtures. 10

Table 1.2: A list of applications of membrane gas separation processes. 11

Table 1.3: List of commercial membrane suppliers and their applications. 12

Table 1.4: Comparison of hydrogen recovery systems. 14

Table 3.1: Preparation conditions of homogeneous aromatic polyamide dense membranes with the addition of lithium nitrate. 45

Table 3.2: Preparation conditions of homogeneous aromatic polyamide dense membranes without the addition of lithium nitrate. 46

Table 4.1: Leak rate into the constant volume system; the permeation rates of oxygen, nitrogen, and methane; and the composition of impurities in the permeate. 67

Table 4.2-a: Permeation rate, permeability, overall resistance, and ideal separation factor data pertinent to the uncoated aromatic polyamide membrane "a". 75

Table 4.2-b: Permeation rate, permeability, overall resistance, and ideal separation factor data pertinent to the uncoated aromatic polyamide membrane "b" 76

Table 4.3-a: Permeation rate, permeability, overall resistance, and ideal separation factor data pertinent to the silicone-coated aromatic polyamide membrane "a". 83

Table 4.3-b: Permeation rate, permeability, overall resistance, and ideal separation factor data pertinent to the silicone-coated aromatic polyamide membrane "b". 84

Table 4.4: Permeation rate, permeability, and ideal separation factor data of oxygen, nitrogen carbon dioxide, and methane through silicone-coated aromatic polyamide membrane using the constant volume system. 94

Table 4.5-a: Comparison of the permeability, permeability coefficient, and ideal separation factor of silicone-coated aromatic polyamide membrane and typical asymmetric and homogeneous membranes for O_2/N_2 system. 96

Table 4.5-b: Comparison of the permeability, permeability coefficient, and ideal separation factor of silicone-coated aromatic polyamide membrane and typical asymmetric and homogeneous membranes for CO_2/CH_4 system. 97

Table 4.6: Values of the local ideal separation factors to be used in Equations 2.27, 2.28, and 2.32 to 2.36. 100

Table 4.7-a: Pore ideal separation factor, α_3, matrix resistance, R_2, pore resistance, R_3, coating layer resistance, R_1, and coated pore resistance, R_{3c}, pertinent to the uncoated and silicone-coated aromatic polyamide membrane "a". 101

Table 4.7-b: Pore ideal separation factor, α_3, matrix resistance, R_2, pore resistance, R_3, coating layer resistance, R_1, and coated pore resistance, R_{3c}, pertinent to the uncoated and silicone-coated aromatic polyamide membrane "b". 102

Table 4.8: Composition of carbon dioxide and methane in the feed and permeate, permeation rate, and actual separation factor for CO_2/CH_4 separation. 107

Table 4.9: Composition of oxygen and nitrogen in the feed (air) and permeate, permeation rate, and actual separation factor for O_2/N_2 separation. 109

Table 4.10: Permeation rate, permeability coefficient, and intrinsic separation factor of the experimental gases through homogeneous aromatic polyamide membrane. 111

Table 4.11: Permeation rates of single gases through homogeneous aromatic polyamide membranes made from solutions with the addition of lithium nitrate. 114

Table 4.12: Permeation rates of oxygen and nitrogen through homogeneous membranes made from solutions without the addition of lithium nitrate. 117

LIST OF PUBLICATIONS AND PRESENTATIONS

The results obtained in the present study were/will be published in the following journals and were presented in the following conferences. A patent application was also filed based on the present results.

Patent:

- "Membrane for gas separation"; A. Tabe Mohammadi, T. Matsuura, S. Sourirajan, and B. Laverty, UK patent application number 94101375, May 1994.

Publications:

1. "Design and construction of gas permeation system for measurement of low permeation rates and permeation compositions"; A. Tabe Mohammadi, T. Matsuura, and S. Sourirajan, Accepted for publication in Journal of Membrane Science, September 1994.
2. "Investigation of polymer morphology of integral-asymmetric membranes and its comparison with homogeneous films"; K.C. Khulbe , S. Gagné, A. Tabe Mohammadi, and T. Matsuura, J. Memb. Sci., 98, 201 - 208, 1995.
3. "Gas separation by silicone-coated dry asymmetric aromatic polyamide membranes"; A. Tabe Mohammadi, T. Matsuura, and S. Sourirajan, Submitted to Journal of Gas Separation and Purification, December 1993.
4. "Production of high purity oxygen from air using aromatic polyamide membranes"; A. Tabe Mohammadi, T. Matsuura, and S. Sourirajan, Proceedings of the Third International Symposium on Separation Technology, Elsevier, Amsterdam, April 1994.

Presentations:

1. "High selectivity gas separation based on silicone-coated aromatic polyamide membranes"; A. Tabe Mohammadi, T. Matsuura, and S. Sourirajan, in the 6th North American Membrane Society (NAMS) Annual Meeting, Breckenridge, Colorado, May 21 - 25, 1994.
2. "Production of high purity oxygen from air using aromatic polyamide membranes"; A. Tabe

Mohammadi, T. Matsuura, and S. Sourirajan, in the 3rd International Symposium on Separation Technology, Antwerp, Belgium, August 22 - 27, 1993.

3. "Development of asymmetric PPO flat-sheet membranes for gas separation"; S. Gagné (speaker), A. Tabe Mohammadi, T. Matsuura, and S. Sourirajan, in Gordon Research Conferences, Membranes: Materials and Processes, Plymouth, New Hampshire, August 1 - 6, 1993.

4. "Effect of silicone-rubber coating on separation of gas mixtures by aromatic polyamide membranes"; A. Tabe Mohammadi, T. Matsuura, and S. Sourirajan, in 5th North American Membrane Society (NAMS) Annual Meeting, Lexington, Kentucky, May 17 - 25, 1992.

ACKNOWLEDGEMENTS

I wish to express my gratitude to my project supervisors Dr. Takeshi Matsuura and Dr. Srinivasa Sourirajan for their guidance and encouragements throughout this work.

I would also like to thank all IMRI staff without them this work would not have been possible.

The acknowledgement is extended to Louis Tremblay, Joe Gasperetti, Adriano Bonaldu, and Frank Ziroldo of the machine shop for all their valuable helps in the course of this project.

Special thanks to Dr. André Tremblay of the Chemical Engineering Department of the University of Ottawa for his helps during the construction of the constant volume system.

The financial support came from the British Gas Co. which is gratefully acknowledged.

NOMENCLATURE

A	Effective membrane surface area	m^2
c_0, c_l	Molar concentration at the upstream and downstream surfaces of membrane, respectively	mol m^{-3}
d	Membrane pore diameter	m
D, D_K	Diffusion coefficient, Knudsen diffusion coefficient	m^2 s^{-1}
D_m	Molecular diameter of a gas	m
J	Flux	mol m^{-2} s^{-1}
K_n	Knudsen number	-
l	Membrane thickness	m
M	Molecular mass	kg mol^{-1}
n	Number of moles	-
P	Permeability coefficient	mol m m^{-2} s^{-1} Pa^{-1}
p, p_i, $\bar{p}$	Total pressure, partial pressure, mean pressure	Pa
Q	Permeation rate	mol s^{-1}
R	Membrane resistance (with subscript)	Pa s mol^{-1}
	Gas constant	Pa m^3 mol^{-1} K^{-1}
r	Membrane pore radius	m
S	Solubility coefficient	mol m^{-3}
t	Thickness of adsorbed monolayer on the membrane surface	m
T	Absolute temperature	K
x	Feed mole fraction	-
y	Permeant mole fraction	-
$\alpha_{a/b}$	Ideal, actual, or intrinsic separation factor of gas "a" over gas "b"	-

Ideal separation factor is defined as the ratio of permeation rates of gas "a" over gas "b".

Actual separation factor is defined as the mole concentration ratio of gas "a" to gas "b" in permeate over that in feed.

Intrinsic separation factor is defined similar to the ideal separation factor exept

	it is measured through a homogeneous membrane.	
α_H	Adsorption constant	-
η	Viscosity	Pa s
λ	Mean free path of molecules	m
ε	Porosity	-
μ	Tortuosity factor	-

SUBSCRIPTS:

1,2,3,4	regions in a membrane related to the coating layer, skin layer matrix, skin layer pores, and porous sub-layer respectively.
a, b	components
c	coated
t	total

ABSTRACT

The use of reverse osmosis (RO) and ultrafiltration (UF) membranes for separation of gas mixtures is a relatively new development. Most of asymmetric RO and UF membranes which are useful in liquid separation fail to be effective in gas separation because some of the pores on the membrane surface are too large and have no separation capacity.

The selectivity of these membranes can be improved by blocking the large pores with a second material. This process is known as coating and has proven to be highly effective in upgrading RO & UF membranes for gas separation.

In this study membranes were prepared from an aromatic polyamide (PA) polymer and coated by silicone rubber. In a set of experiments, the permeation rates of six experimental gases through these membranes were measured at different pressures. The ideal separation factors higher than those reported in the literature were obtained. These results show that PA membranes are highly capable of separating the gases under investigation. The resistance model was employed to analyze the data and to explain the performance of this polymeric membrane.

In another set of experiments, mixtures of CH_4/CO_2 with known compositions, and O_2/N_2 (air), were separated using coated PA membranes. The actual separation factors of 64 to 166 for CO_2/CH_4 and 8.7 for O_2/N_2 systems obtained in this set of experiments were higher than those reported in the literature.

A "membrane-self-sealing" gas separation cell design allowed for a leak-free system with a leak rate of $<1.2\times10^{-9}$ cm^3/s. This level of leak is few orders of magnitude lower than similar existing systems. This cell design facilitates experiments involving the separation of air in which a perfect sealing is necessary in order to prevent the oxygen enriched permeate to mix with the leaking air.

The new separation cell was installed in a fully automated system which operates gas permeation experiments using a process control computer program. The system is designed such that measurement of permeation rates as low as 1×10^{-8} cm^3/s becomes possible. The new system is ideal for experiments involving homogeneous membrane and/or low permeable gases such as nitrogen and methane.

CHAPTER ONE

INTRODUCTION

The production of a gas at a specific purity from a multi-component mixture is the subject of all gas separation techniques. The most commonly used techniques include adsorption, absorption, cryogenic distillation, scrubbing, and membrane separation. It is only more than ten years that the membrane separation processes have emerged as a new gas separation technique. To be superior to, or competitive with other techniques, membrane processes take advantage of many features including: low capital investment, simplicity and ease of installation and operation, low maintenance requirements, low weight and space requirements, and high process flexibility.

In this section, fundamental aspects of membrane gas separation and the objectives of the present study will be introduced and discussed.

1.1. OBJECTIVE AND TASKS

The objective of thepresent research was to develop methods to improve the gas separation properties of aromatic polyamide membranes.

The following tasks were found essential to achieve the objective:

- Design of an accurate and leak-free separation system for measurement of low permeation rates and determination of the permeate composition.
- Determination of the intrinsic properties of aromatic polyamide membranes.
- Development of a new solution method to calculate the values of a membrane's local resistances accurately using the resistance model .
- Comparison of the separation characteristics and morphology of homogeneous and asymmetric aromatic polyamide membranes.

1.2. MEMBRANE GAS SEPARATION PROCESSES

It is difficult, if not impossible, to establish a correct and complete definition for a membrane. The most general and widely accepted one may be the following [Lonsdale, 1989]:

"A membrane is a phase or a group of phases that lies between two phases, which is physically and/or chemically distinctive from both of them and which, due to its properties and the force field applied, is able to control the mass transport between these phases."

Separation is achieved because of the difference in the relative rate of permeation of the

feed components across the membrane. Therefore, the membrane allows for the preferred transport of species from the bulk phase in one side to the bulk phase on the other side of the membrane. The driving force for the selective transport is the gradient of chemical potential or electrical potential. A gradient in the chemical potential could be due to either or both of concentration gradient or pressure gradient.

Figure 1.1 shows a typical membrane gas separation process. A gas mixture is fed into the upstream at high pressure. Component(s) that diffuses faster is enriched in the "permeate" side. The slower component(s) concentrates in the "retentant" or the "residue" stream.

Membrane separation is a non-equilibrium process. This is because, the separation is based on the relative rate of permeation of the feed components. If a membrane system is permitted to go to the equilibrium, permeation would be continued until the pressure and the concentration of the gases on both sides were equal.

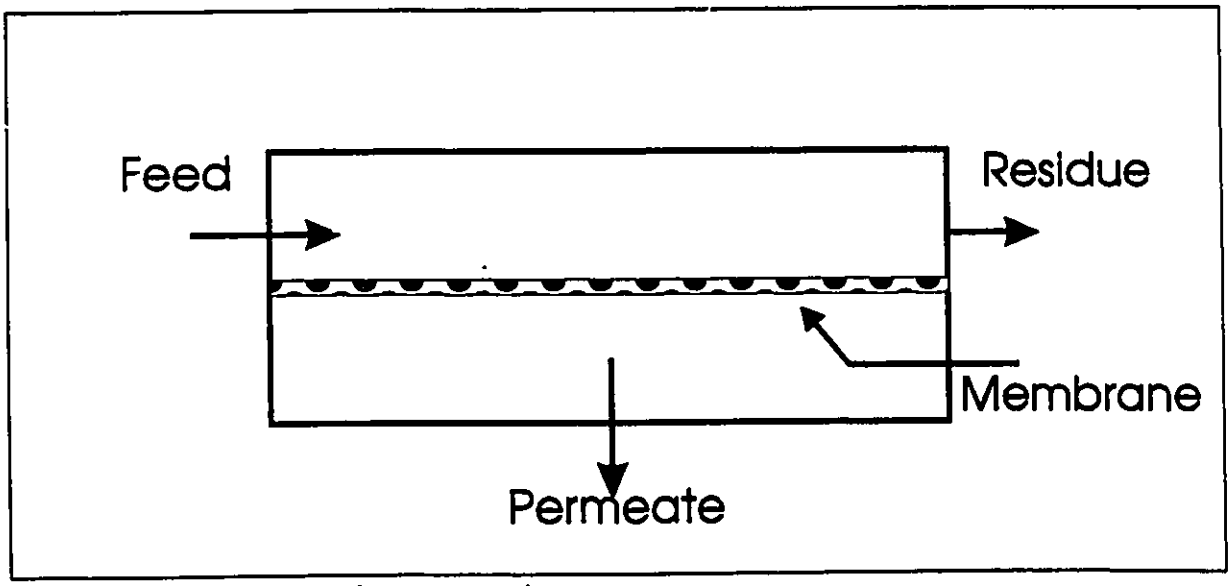

Figure 1.1: A typical membrane separation process.

1.3. HISTORICAL BACKGROUND AND RECENT DEVELOPMENTS

The gas separation properties of membranes have been known for more than a century. In fact it has been well established that virtually all materials exhibit different permeabilities toward different gases. The root of membrane gas separation techniques goes back to the works of Mitchell [Meares, 1986] who in 1831 measured the rates of escape of ten different gases through natural rubber balloons. He found that each gas permeates with a specific velocity.

At approximately the same time, Fick, who was a physiologist, studied gas transport across membranes made of nitrocellulose [Paul, 1994]. The formulation of what is known today as the Fick's first law of diffusion is the fruit of that study. Few decades later in 1866, Thomas Graham performed a gas separation experiment via Knudsen diffusion [Stanley, 1986]. He later observed separation of gases using natural rubber as well.

All the early studies on the gas permeation were focused on the steady flux across the membrane. On 1920, H. A. Daynes for the first time realized the importance of the transient permeation experiments [Paul, 1994]. He plotted the flux versus time at both transient and steady-state and showed that the extrapolation of the line obtained, after steady-state conditions are established, to the time axis gives a time lag, Θ, that is directly related to the diffusion coefficient:

$$\Theta=\frac{l^2}{6D} \qquad (1.1)$$

Where, l is the membrane thickness, and D is the diffusivity of the gas. Because it was possible to measure the permeability coefficient, P, from the steady-state part of the same curve, one could calculate the solubility coefficient as the ratio P/D. Hence, all three quantities could be determined

from single experiment.

In the 1930s and 1940s, R. M. Barrer introduced widely the Fick's method to experimental practices. In recognition of the major contributions of Barrer to the field of gas permeation, the following definition for the units of permeability coefficient is widely used:

1 Barrer = 10^{-10} cm^3 (STP) cm/cm^2 s cmHg

The progress of the membrane separation technique was very slow in the early stages. From the works of Mitchell and Graham it took more than a century until the emergence of the first large scale application of membrane for concentration of uranium 235 [Werner, 1986]. In early 40s, U^{235} was concentrated from its natural occurrence of 0.17% to 3% (weight) using membranes. This process was costly because of the low selectivity of membrane and the number of stages required to reach certain purity.

The major problem with the early membranes was their insufficient selectivities and low fluxes. Therefore, the processes were costly and uncompetitive with the more traditional methods. The reason behind it comes from a very natural characteristic of all membranes: high selectivity comes at the cost of low permeability. The search for techniques for producing membranes with both high selectivity and high permeability was, and still is, the main subject of many research activities. The first breakthrough in the process came about with the introduction of asymmetric cellulose acetate membrane by Loeb and Sourirajan [1960]. They could successfully produce a membrane with a very thin dense layer and a relatively thick and porous sublayer. The dense top layer was responsible for the actual separation, while the porous sublayer provided mechanical support for the top selective layer. The Loeb-Sourirajan type membranes proved to hold the selectivity of the symmetric membranes while exhibiting large permeabilities for the desalination and liquid/liquid separation

applications. However, it was not still satisfactory for the separation of gas mixtures, because these membranes were prepared by water quenching and had to be kept in water. If dried, the membranes shrank and lost their separating properties. The early attempts to separate gases using direct air dried cellulose acetate membranes were not successful [Sourirajan, 1963].

The problem of drying the RO membranes was solved by Vos and Burris [1969]. They used surfactant to reduce the interfacial tension between the membrane pore walls and the water held in the pores. Thus, water could be evaporated without having the pores collapse. This technique was adapted by Gantzel and Merten [1970] to demonstrate a much higher selectivity of dried CA membranes toward the H_2/N_2 system compared with older generation membranes. Later, Schell et al. used the solvent exchange technique to produce dry CA membrane [Schell, 1976]. The drying techniques were the beginning of the penetration of RO membranes into the gas separation market.

In the early 70's, the newly developed membranes were tested in laboratory scale in many places to separate gases. However, there still were few major barriers to overcome before the commercialization of membranes. One problem was that while the asymmetric membranes proved to be effective in liquid/liquid separation, their selectivities were not enough toward gases. That was because of the presence of relatively large pores in the structure of the membranes. Two developments helped membrane to become a competitor in the field of gas separation industry: first was the introduction of composite membrane, and second the development of coating technique. In the mid 70's, Ward et al. [1976] of General Electric produced the first ultrathin supported composite membrane. A composite membrane has a similar structure as an asymmetric membrane except that the selective and the supporting layers are usually made of different polymers and mechanically attached to each other. With composite membranes higher permeability was gained without loss of

selectivity. The other improvement was the coating technique developed by Henis and Tripodi [1980a &b]. They plugged the large pores of a selective membrane with a non-selective highly permeable rubbery membrane. The coating layer reduced the permeability of the desired gas insignificantly but increased the selectivity tremendously. These accomplishments eventually led to the introduction of PRISM® by Monsanto (now Permea). It was a hollow fibre system spun from polysulfone with a dense skin on the exterior surface. PRISM® was used in large scale for removal of hydrogen from ammonia.

Although by mid 80's feasible and economical techniques were available to prepare dry membranes, only a small number of polymers proved to be of practical use to the industry. Since late 80's, in parallel with efforts to improve asymmetric and hollow fibre membranes preparation techniques, fundamental studies were conducted to understand the relationship between the preparation parameters and the membrane performance. The Group at the National Research Council Canada studied the effect of preparation variables on the performances of a series of cellulose acetate membranes [Rangarajan, 1984; Minhas, 1985, 1987; Lui, 1988a&b]. These variables included shrinkage temperature, and the solvent used in the solvent exchange drying process. According to these studies, the pore size and pore size distribution of the final product is greatly influenced by the preparation parameters. Recently, van't Hof et al. [1992] have developed the dual bath coagulation method for drying the wet membranes without the necessity of solvent evaporation. In this technique, the polymer solution is in contact with two non-solvent baths. The first bath initiates formation of a dense skin layer, while the second gives the actual precipitation of polymer.

From the early stages of synthetic membrane preparation, it was well known that the glassy polymers, in general, are more selective and less permeable than the rubbery polymers [Chern, 1985].

This concept, along with the coating technique [Henis, 1980a&b], was used to coat polyethersulfone glassy polymers [Haesloop, 1985]. The coated polyethersulfone found an application in the production of oxygen enriched air. Later, the effect of the number of coating on the selectivities of polysulfone membranes was studied [Chen, 1990]. The latter study concluded that the membrane's selectivity increases with the number of layers up to 3 layers. Additional layers were not found to be of any advantage.

Beside cellulose acetate and polysulfone, another group of polymers attracted attentions in the 80's. This group was the family of polyimide polymers. The selectivities of a series of polyimides have been upgraded in the past few years. Kim et al. [1988a&b] achieved separation factors higher than the existing membranes with polyimide based membranes.

While many studies were focused on the improvement of the selectivities of different membranes, only limited number of them became involved with the membrane geometry. In principal, two types of geometries found a ground in the gas separation field: asymmetric, and composite membranes whose geometries were discussed earlier. For some applications, composite membranes offered advantages over asymmetric polymeric membranes in the sense that the properties of both the dense selective layer and the porous support layer could be individually optimized. Therefore, it seemed natural to explore the possibility of making composite membranes out of different materials. Kneifel and Peinemann [1992] prepared composite hollow fibre membranes with polyetherimide selective layer coated by silicone rubber. The major advantage of this membrane, as other hollow fibres, was the higher surface area per unit volume. The production of polymer-ceramic composite membrane was another development in this respect [Martin, 1991; Rezac, 1992]. These membranes were composed of a homogeneous separating polymeric films with thicknesses less than 1μm. The

ceramic supporting layer had a negligible resistance to the permeation of gases. Accordingly, their selectivities were comparable with asymmetric membranes while higher permeabilities were achieved.

A remarkable development was the introduction of gas separation in electronically conductive polymers. Different preparation techniques were reported by Anderson et al. [1991; Kaner, 1991] from UCLA and Martin [1991] from Colorado State University. The main step in both approaches is doping, undoping and redoping the polymer with counterions of appropriate sizes. This new class of membranes gives a control over the morphology of membrane after synthesis to optimize a particular separation. The selectivities achieved by these researchers, surpass the previously reported values.

Table 1.1 shows a series of selected separation factors achieved in the recent years.

1.4. APPLICATIONS

Membrane processes have been proven to be efficient and economical in many large scale industrial applications. These applications could be categorized in three principal classes: hydrogen recovery and recycle in several industrial process streams; natural and landfill gas treatment; and oxygen and nitrogen enrichment from air. Some of the applications of membrane processes in gas separation are listed in Table 1.2. In addition, in Table 1.3 a list of commercial membrane suppliers and the applications these membranes are used is given [Zolandz, 1994]. Some of the most important membrane gas separation applications are discussed here.

Table 1.1: Ideal separation factors of different membranes toward some gas mixtures.

Gas Pair	α	Polymer	Reference
O_2/N_2	10	Polyimide	[Yamamoto, 1990]
	6	Polyimide	[Kim, 1988a]
	6	Polycarbonate	[Koros, 1989a]
	2.9	polyvinylalcohol	[Zhang, 1989]
	7	Polysulfone	[Pfromm, 1993]
	6.6	Polyethersulfone	[Kumazawa, 1993]
	6.4	Radel A PSF	[Ghosal, 1993]
	2.6	Polyetherimide	[Kneifel, 1992]
	4 - 5	Composite polymer-ceramic	[Rezac, 1992]
	30	**polyaniline**	**[Anderson, 1991]**
	7.9	Polypyrrole	[Martin, 1991]
He/N_2	170	Polyetherimide	[Kneifel, 1992]
	27	Polysulfone	[Pfromm, 1993]
	247	Prism Polysulfone	[Murphy, 1989]
	366	Prism PES	[Murphy, 1989]
	30 - 45	Composite polymer-ceramic	[Rezac, 1992]
H_2/N_2	37	Polyimide	[Yamamoto, 1990]
	29	Coated PES	[Chen, 1990]
	3590	**Polyaniline**	**[Anderson, 1991]**
CO_2/CH_4	67	Polyimide	[Yamamoto, 1990]
	50	Polyimide	[Kim, 1988a]
	30	Polycarbonate	[Koros, 1989a]
	50 - 70	Polyimide film	[O'Brien, 1987]
	50	Polyethersulfone	[Van't Hof, 1992]
	32.3	Radel A PSF	[Ghosal, 1993]
	336	Polyaniline	[Anderson, 1991]
	45	Ultem (PEI)	[Ogden, 1986]
	70	Polyimide	[Kim, 1988b]
He/CH_4	110	Polycarbonate	[Koros, 1989a]
	170	Polyimide	[Kim, 1988b]
	135	Polyimide	[Kim, 1988a]
	921	Polyimide	[Kim, 1988a]
	75	Radel A PSF	[Ghosal, 1993]
H_2/CH_4	73	Polyimide	[Yamamoto, 1990]
	47	Dacron Polyester	[Kammermeyer, 1976]

1.4.1. Air Separation

The products of membrane air separation process are oxygen (permeate) and nitrogen (residue). Both of these streams can be the desired product. Most of the oxygen and nitrogen produced nowadays is obtained via cryogenic techniques, but membrane processes show very good prospects especially for small applications. The current state of membrane technology allows the production of high purity nitrogen (>95%). However, membrane processes are only used to enrich

Table 1.2: A List of Applications of Membrane Gas Separation Processes.

O_2/N_2	Nitrogen production Oxygen enrichment
H_2O/Air	Air dehumidification
H_2/Hydrocarbons	Refinery hydrogen recovery
H_2/CO	Syngas ratio adjustment
H_2/N_2	Hydrogen recovery in ammonia production
CO_2/Hydrocarbons	Acid gas treating landfill gas upgrading Sour gas treating
H_2O/Hydrocarbons	Natural gas dehydration
H_2S/Hydrocarbons	Sour gas treating
He/Hydrocarbons	Helium separations
He/N_2	Helium recovery
Hydrocarbons/Air	Pollution control hydrocarbon recovery

Table 1.3: List of Commercial Membrane Suppliers and Their Applications.

Company	CO_2	H_2	O_2	N_2	Other[a]
A/G Technology (AVIR)	X		X	X	
Asahi Glass (HISEP)			X	X	
Cynara (Dow)	X				
Dow (Generon)			X	X	
Du Pont/L'Air Liquid (MEDAL)		X		X	
Grace Membrane Systems	X	X			X
Hoechst-Celanese (Separex)	X	X			X
International Permeation	X				X
Membrane Technology & Research					X
Nippon Kokan K.K.					X
Osaka Gas			X		
Oxygen Enrichment Co.			X		
Perma Pure					X
Permea (Air Products)	X	X	X	X	X
Techmashexport (USSR)			X		
Teijin Ltd.			X		
Toyobo			X		
Ube Industries		X	X	X	X
Union Carbide (Lind)	X	X	X		
UOP/Union Carbide	X				

[a]: Includes solvent recovery, dehumidification, and/or helium recovery membranes.

oxygen content of air to around 40%. That is mainly because many physical properties of oxygen and nitrogen are very close. Therefore, the separation factor for this pair is not very high. The selectivity of the present membranes toward O_2/N_2 system is typically between 2 and 8 [Paul, 1994]; where selectivity is defined, in an ideal form, as the ratio of the permeation rate of the faster gas to the slower one. High quality nitrogen has applications such as inert gas blanketing and ammonia production. Oxygen enriched air is useful in different fields of medicine as well as in enhanced

combustion engines.

The production of high purity oxygen by membrane processes, at the current level of selectivity, can hardly compete with cryogenic or adsorption systems. However, nitrogen has successfully been produced at high purity. That is because the product, in this case, is the retentate and the membrane selectivity need not to be high. In addition, the produced nitrogen remains essentially at the same pressure as the feed which eliminates the cost of recompression.

Membrane systems can also be combined with other processes for air separation to reduce the overall cost as well as the weight and/or the volume of the system. Hybrid systems of membrane in conjunction with adsorption [Beaver, 1988], cryogenics [Agrawal, 1986], and catalytic oxygen remover [Beaver, 1988] are reported in the literature.

1.4.2. Hydrogen separation and recovery

Hydrogen recovery was the first large scale application of membrane processes with the first operation in 1969 [Hwang, 1975]. The application of membrane processes is widespread in the ammonia, refinery, and petrochemical industries. In most cases hydrogen used to be burned for its fuel value, while, membrane allowed an economical way of separating it from waste gases. In ammonia industry, hydrogen is recovered from the unreacted gas stream and recycled into the feed. Detailed comparison of membrane and other processes in hydrogen recovery is given by Islaski [1984], as well as Baldus and Tillman [1986].

In different syngas processes membranes are used to adjust the H_2/CO ratio by removing hydrogen. Syngas has applications in the production of acetic acid, ethylene glycol, ethanol, ethylene,

and many other useful products. The stoichiometric ratio of H_2/CO must be adjusted for each specific application.

In the refinery industry, membranes are used to separate or recover hydrogen from the product or purge streams. There are many refinery production lines with hydrogen either as the byproduct or mixed in the purge streams. Some of these processes are catalytic cracking, hydrocracking, hydrotreating, and methanol synthesis.

Table 1.4 [Zolandz, 1992] compares the membrane processes, for the recovery of hydrogen, with pressure swing adsorption and cryogenic systems. As seen in this table, the membrane technology is competitive with other processes in a wide range of operating conditions. However, the competitive systems deliver the purified hydrogen at a pressure similar to the feed pressure, while, recompression is necessary in membrane processes.

Table 1.4: Comparison of Hydrogen Recovery Systems. [Zolandz, 1992]

	Membrane	PSA	Cryogenic
Relative investment	**1**	**1 to 3**	**2 to 3**
Maximum operating pressure (psia)	**2000**	**600**	**1000**
Minimum hydrogen content in feed (%)	**15 to 20**	**50**	**20**
Maximum hydrogen purity (%)	**99**	**99.999**	**98.5**
Maximum hydrogen recovery (%)	**95**	**85**	**95**
Product pressure/feed pressure	**Lower**	**Same**	**Same**
Retentate pressure/feed pressure	**Same**	**Lower**	**Lower**
Fractionation of heavies	**No**	**No**	**No**
Modularity	**Yes**	**No**	**No**
Ease of operation	**Very easy**	**Average**	**Average**

1.4.3. Natural and Landfill Gas Treatments

Natural gas usually contain carbon dioxide and hydrogen sulfide impurities. Both are corrosive and hydrogen sulfide is toxic as well. For economical and environmental reasons, both these gases must be removed before entering pipelines. The recovered carbon dioxide can be used in the enhanced oil recovery where it is injected into the dead oil wells to pressurize the remaining oil for further production.

The commercial use of membrane systems for removal of acid gases goes back to 1984 with the installation of SACROC® unit by Cynara a subsidiary of Dow [Parro, 1984]. Membrane processes have also found applications in off-shore installations, where membrane systems can offer major savings by weight reduction of the gas to be transported to the shore. The industrial installation of membrane for natural gas treatments is summarized by Verghese [1990].

Landfills generate methane at atmospheric pressure contaminated with high percentages of carbon dioxide. Although the collection of the landfill gases is costly, they have to be removed because of the environmental impacts. Refining and selling the landfill gases reduces the collection costs and helps the local industries where the price of energy is essential.

While membranes are good for bulk removal of acid gases, they are inferior to, or must be combined with, other processes for small contaminations of these gases. That is because, at small concentrations the partial pressure of acid gases, and therefore the driving force of the process, decreases [Schendel, 1986]. A number of membrane hybrid systems have received attention in the literature for acid gas removal from natural gas. Membrane/potassium carbonate system at SACROC® installation discussed earlier is an example of these hybrids [Parro, 1984]. PRISM, from permea, has

also been combined with a traditional amine and cryogenic processing units [Backhouse, 1986]. Baldus and Tillman also show that a membrane/cryogenic hybrid with a membrane selectivity of 20 is advantageous over a membrane alone system [Baldus, 1986]. They show that if the selectivity of the membrane increases to 50, the membrane alone system is economical and efficient.

1.5. TRANSPORT MODELS

There are many models describing the transport mechanism of gases through polymeric membranes. The most important ones are solution diffusion, dual sorption, free volume, and surface force - pore flow models. The first three assume a non porous dense top layer membrane, while the last one takes into account the presence of pores with known size and size distribution.

The solution-diffusion model explains the gas transport as the solution of molecules in one face, diffusion through, and release at the other face of the membrane. The extent of separation depends on both solubility and diffusivity of the gas in the polymer.

The dual sorption model assumes permeation of gas molecules through two distinct mechanisms. One involves the solution of molecules in the polymer matrix obeying Henry's law. The other considers transport of molecules through membrane's microcavities according to Langmuir type isotherm. The molecules are exchanged rapidly between the two mechanisms.

The free volume model suggests the movement of gas molecules from one "hole" to another within the polymer. The "hole" is created by fluctuations of local density.

The surface force pore - flow model explains the transport of molecules through reverse osmosis membranes with a well defined pore size and pore size distribution. This model considers the

adsorption of molecules at the wall of the membrane pores and transport of the adsorbed layer to the other side of the membrane by different flow mechanisms. At the other surface, the molecules are desorbed due to the trans-membrane pressure difference.

1.6. MEMBRANE MATERIALS SELECTION AND MEMBRANE FORMATION

The permeability of different gases through a particular membrane varies by many orders of magnitude depending on the material used in the membrane. The large variation indicates that, in principle, many materials can be used as a membrane. Membranes can be classified as "rubbery" and "glassy" according to their glass transition temperature, T_g. Rubbery polymers have T_g lower than the ambient temperature and their polymer chains are more flexible. The glass transition temperature is higher than ambient temperature in glassy polymers and they have more rigid morphology. The rubbery membranes are the most permeable membranes with the least selectivities. On the other hand, the glassy polymers are inherently more selective than rubbery ones. The higher selectivity of the glassy polymers are due to their significantly lower chain mobility. However, as it was mentioned earlier, the high selectivity is commonly accompanied with low permeability.

It the next chapter it will be shown that the permeability is inversely proportional to the thickness of the membrane. This implies that membranes with the lowest thicknesses are more suitable for gas separation. On the other hand, it dictates the approach toward the development of new membrane geometries. The major geometries which fulfil this requirement and are now in use include supported ultrathin films, asymmetric membranes, composite membranes, and coated structure.

The asymmetric membranes are mostly manufactured by either wet phase inversion technique, or dry/wet phase inversion technique. In general, the polymer solution is brought into contact with a non-solvent fluid. The solvent is exchanged with the non-solvent and, as a result, the polymer precipitates and form a porous film. Because the polymer chains at the interface contact the non-solvent first, a thin dense layer forms at the interface that reduces the rate of penetration of the non-solvent into the sublayers. Therefore, the polymer chains underneath the dense skin layer precipitate more slowly and form a more porous structure.

In a dry/wet phase inversion process, the local concentration of the polymer at the interface is increased as the solvent evaporates at elevated temperature (drying). The film is then immersed in a non-solvent bath where the actual precipitation occurs.

In composite structure, the selective and the supporting porous layers are formed separately and are mechanically attached. This structure allows for the tailoring the properties of both selective layer and the support layer to fit a particular application.

The defects in an asymmetric membrane can be repaired by applying a non-selective and highly permeable membrane on top of the base membrane. This technique is known as coating and results in an increase in the selectivity of the membrane. In the coating method, usually, a glassy membrane is coated with a rubbery polymer.

Addition of different additives known as "pore formers" to the polymer solution is also a common practice in the preparation of the asymmetric membranes. Lithium and ferric salts are examples of these additives. Generally, the addition of the salts into the solutions improves the rate of water quench uptake and in some cases slows the rate of solvent departure from the nascent membrane during the wet phase immersion process [Koros, 1993]. The presence of the excess water

promotes an unstable situation leading to a lower resistance to the passage of penetrants across the membrane structure in an actual permeation process.

1.7. OVERVIEW OF THE OBJECTIVE

While the list of organic and inorganic materials suitable for membranes is rather long, only a small number of these materials has penetrated into the market. Examples of successful materials include cellulose acetate, polyimide, and polysulfone with cellulose acetate as the pioneer in the field [Ruston, 1990]. In addition, in the most of the fundamental studies in the field of membrane gas separation homogeneous films were used, while, only membranes possessing asymmetric structure are of commercial value. That is because, high selectivity and high permeability are only achievable with asymmetric geometry.

The polyamide (PA) family of membranes has been successfully used for brackish and sea water desalination applications. Also, due to their high glass transition temperature and yield stress the polyamide hollow fibres exhibited a high collapse pressure and could operate at high temperatures [Ekiner, 1990]. The potential application of polyamides to gas separation have been studied by many academic and industrial researchers. However, it was well understood that the pore size of PA membranes, although optimum for desalination purposes, were not good enough for gas separation applications.

In the view of the above discussion, it was the objective of this study to prepare polyamide membranes with selectivities comparable with those of the commercially available membranes. Also, according to the preliminary results, one of the most established working assumptions in the field

could be doubtful. That is, to assume that the morphology of the skin layer in an asymmetric membrane is the same as the morphology of a homogeneous film made of similar material [Sada, 1989]. This assumption, in turn, leads to a might be false conclusion that the selectivity of an asymmetric membrane can not surpass that of a homogeneous one. The selectivity of a homogeneous membrane is known as the intrinsic selectivity of that membrane. Accordingly, it became the secondary objective of the study to compare the performance of the skin layer in an asymmetric membrane and that of a homogeneous film both made of polyamide.

In practice, the measurement of the permeation rates of the low permeable gases through homogeneous dense membranes has always been very difficult. That is because, these permeation rates are so small that they can not be detected by the most accurate conventional flow meters. The problem escalates when the feed involves air, in which, the permeate mixes with the leaking air and the true composition of the permeate can not be obtained. The design of a new separation system to overcome the above obstacles was necessary not only for the present study, but also for the other research activities with similar tasks. In particular the new separation system had to be: i) leak free, and ii) able to measure extremely low permeation rates with high accuracy.

The high values of separation factors achieved in this study not only find new industrial applications for polyamide membrane, but also offer a new approach to make a defect free membrane by means of proper coating technique. Additionally, testing the validity of the above mentioned assumption is a major contribution to the fundamental knowledge of the membrane gas separation.

CHAPTER TWO

THEORY

2.1. GAS TRANSPORT THROUGH MEMBRANES

2.1.1. Introduction

Separation between gases is possible when the mean free paths of gas molecules are larger than the membrane mean pore diameter. The mean free path of a gas molecule is defined as the distance the molecule travels before colliding with other molecules. The mathematical presentation of the mean free path is as follows [Mulder, 1991]:

$$\lambda = \frac{1}{2c_i \pi D_m^{\,2}} \qquad (2.1\text{-a})$$

where c_i is the molar concentration of the gas, and D_m is the molecular diameter of the gas. These two parameters are defined as:

$$c_i = \frac{p_i}{RT} = \frac{px_i}{RT} \qquad (2.1\text{-b})$$

$$D_m = 5.1 \times 10^{11} \frac{(MT)^{1/4}}{\eta^{1/2}} \qquad (2.1\text{-c})$$

Where p is total and p_i is partial pressures; R is gas constant; T is absolute temperature; x_i is mole fraction of gas; M is molecular mass of gas; and η is dynamic viscosity of gas. As shown in Equations 2.1-a to 2.1-c, the mean free path, λ, is proportional to the absolute temperature and inversely proportional to the pressure.

The formulation of the transport equations are based on the assumption that the pores are straight cylinders. An empirical correction factor subsequently accounts for the actual structure of the pores. For membranes holding macropores and narrow pore size distribution, the typical range of the gas transport is characterized by the Knudsen number.

$$K_n = \frac{\lambda}{d} \qquad (2.2)$$

Where d is pore diameter. For $K_n \ll 1$, where the mean free path is smaller than the pore diameter, the gas-wall impact is negligible compared with gas-gas impact. In this case, the transport is convective and no separation occurs. By decreasing the pore diameter the Knudsen number becomes greater than 1, ($K_n \gg 1$), and gas molecules transport through the pore independently by

gas-wall impact. The gas flow, then, is called to be in the Knudsen region and the transport equation is expressed as:

$$J=\frac{\pi nr^2 D_k}{RTA}\frac{\Delta p}{l} \qquad \textbf{(2.3-a)}$$

where r is the pore radius, and D_k, the Knudsen diffusion coefficient, is given by:

$$D_k=0.66r\sqrt{\frac{8RT}{\pi M}} \qquad \textbf{(2.3-b)}$$

Equations 2.3-a and 2.3-b show that the flow is inversely proportional to the square root of the molecular mass and the latter is the only parameter determining the flow of gas in the Knudsen region.

As the pore size is further decreased, the Knudsen diffusion mechanism is not valid anymore and flow through micropores appears. In fact, many membranologists do not believe in the existence of pores in this region while others define the pores as any void space between segments of polymer chains or agglomerates. The flow through the pores in this region can be derived from Fick's law:

$$J=-D\frac{dc}{dx} \qquad \textbf{(2.4)}$$

The driving force for flow of gas is concentration gradient across the membrane, dc/dx. Integration of this equation under steady state results in:

$$J=D\frac{(c_0-c_l)}{l} \qquad \textbf{(2.5)}$$

where c_0 and c_l are the gas concentration at the upstream and downstream surfaces of the

membrane. Supplying Henry's law, the concentration of gas at each surface of the membrane is proportional to the partial pressure of gas at that surface:

$$c=S.p \tag{2.6}$$

where S is the solubility coefficient of the gas. Therefore, Equation 2.5 becomes:

$$J=DS\frac{p_0-p_l}{l} \tag{2.7}$$

Defining the permeability coefficient, P, as the product of diffusion coefficient and solubility coefficient, i.e.,

$$P=D.S \tag{2.8}$$

Equation 2.8 can be written as:

$$J=P\frac{\Delta p}{l} \tag{2.9}$$

Permeability coefficient, P, is often considered as an intrinsic parameter of membranes and is usually calculated from a permeation measurement through a homogeneous membrane. Equation 2.9 shows that the flux through a microporous membrane is proportional to the partial pressure difference across the membrane and inversely proportional to the membrane thickness. An ideal separation factor is given by the ratio of the permeability coefficients of two gases:

$$\alpha_{a/b}=\frac{P_a}{P_b} \tag{2.10}$$

For example, $\alpha_{a/b}$ = 100 of a membrane toward gases "a" and "b" means that if a 50/50 mixture of these gases is fed to the membrane, ideally, for every 100 molecules of gas "a" permeating

through the membrane only 1 molecule of gas "b" permeates. However, in practice, the actual separation factor is less than the ideal separation factor. The two Equations 2.9 and 2.10 are of fundamental importance and are commonly used for describing the transport of gases through membranes.

2.1.2. Gas Permeation Mechanisms

In the light of the above introduction four principal transport mechanism can be defined for the permeation of a single gas through a porous membrane under a pressure gradient. These mechanisms include [Uhlhorn, 1989]:

1. Laminar flow
2. Knudsen diffusion
3. Surface diffusion
4. Capillary flow

If the pore radius is larger than the mean free path of the gas molecule laminar flow occurs through the pores. The permeability is then described by:

$$P=\frac{\varepsilon \mu r^2}{8\eta RTl}.\bar{p} \qquad (2.11)$$

Where P is the permeability coefficient, ε is the porosity, μ is the tortuosity factor, r is the pore radius, η is the viscosity of the gas, R is the gas constant, T is the absolute temperature, l is the membrane thickness, and $\bar{p}$ is the mean pressure across the membrane. The nature of Equation 2.11 suggests that separation between two gases can not take place under the laminar flow

regime. That is because the permeability of gases in this regime is independent of the gas properties.

Knudsen diffusion occurs if the pore radius is much smaller than the mean free path of the molecules, i.e., $r<0.05\lambda$, and is described by modifying Equations 2.3-a and 2.3-b [Mulder, 1992]:

$$P=\frac{J}{A\Delta p}=\frac{\pi n r^2}{RTl}\times 0.66r\sqrt{\frac{8RT}{\pi M}} \qquad (2.12)$$

Under Knudsen diffusion mechanism, two gases can be separated based on their difference in the molecular weight. That is, as can be seen in Equation 2.12, keeping everything constant, the permeability of gases depends only on the reciprocal of the square root of M, the molecular mass of the gas. Thus, a separation factor based on Knudsen diffusion, α_K, is defined as [Ruthven, 1984]:

$$\alpha_K=\sqrt{\frac{M_{ref}}{M_{gas}}} \qquad (2.13)$$

where M_{ref} and M_{gas} are molecular weights of a reference gas and an experimental gas respectively. Since this quantity is generally small, only low separations are achieved via Knudsen mechanism.

If the pore sizes are of the same order of magnitude as the mean free path of the molecules both Knudsen diffusion and laminar flow occurs. This case usually happens with asymmetric or composite membranes with the toplayer pore size large enough for the Knudsen diffusion mechanism to occur, and supporting sublayer of large pore size allowing laminar flow

to occur [Uhlhorn, 1989]. In this case, the permeability is a function of pressure. Then, the y-axis intercept (zero pressure) indicates the Knudsen contribution, and the slope is attributed to the occurrence of the laminar flow.

The surface flow exists always when a monolayer of adsorbed gas can be formed on the surface of the pore. This condition can be satisfied when the pore radius is larger than the monolayer thickness. In other words, both Knudsen and laminar flow can be combined with surface flow depending on the size of the pores. The permeability due to the surface flow is defined as [Matsuura, 1989]:

$$P=\frac{\pi(2r-t)^2t^3}{8r}\frac{RT}{\mu}K^2{}_H\frac{\overline{p}}{l} \qquad (2.14)$$

Where t is the thickness of the monolayer, μ is the surface viscosity, and K_H is the proportionality constant of a linear adsorption isotherm and is equal to (unit weight of polymer/volume of adsorbed gas molecules) times α_H, the adsorption constant.

A forth transport mechanism which can occur is multilayer diffusion and capillary condensation. In this mechanism the pores are filled (multilayer adsorption) until a liquid meniscus forms inside the pore (capillary condensation). This type of transport can not be expressed by one single mathematical equation but requires modelling [Lee, 1986].

It can be seen from Equations 2.11 to 2.14 that except for pure Knudsen flow all transport mechanisms are pressure dependent. It means that the gas permeability increases as the transmembrane pressure difference increases. According to the above discussion, the type of transport mechanism can be approximated based on the permeability and the selectivity data of a particular membrane toward different gases. Following is a guideline leading to the

determination of the type of the transport mechanism:

1. No selectivity indicates laminar flow through the pores. Pinholes or cracks exist in the toplayer.

2. Pressure independent permeability indicates Knudsen flow mechanism. The separation factor can be determined by Equation 2.13.

3. Pressure dependency with non-zero y-intercept indicates coupling of Knudsen flow with either laminar or surface flow mechanisms. Lower than Knudsen separation factor indicates laminar flow coupled with Knudsen, and higher than Knudsen separation factor indicates surface flow coupled with Knudsen mechanism.

4. Pressure dependency with zero y-intercept indicates either pure laminar flow or pure surface flow. The separation factor is unity in the pure laminar flow, and is higher than the Knudsen separation factor in the case of the pure surface flow.

2.2. RESISTANCE MODEL

According to the resistance model, the membrane is divided into different segments each providing a specific resistance to the permeation of gases. These resistances are analogous to the resistance to the flow of electricity in an electric circuit. Figure 2.1 shows the uncoated and coated membranes with their analogue electrical resistances.

An asymmetric membrane may be divided into a thin dense skin layer and a highly porous sublayer. The skin layer is responsible for the separation, while the porous sublayer provides mechanical support to the membrane. The skin layer, in turn, may be divided into two regions:

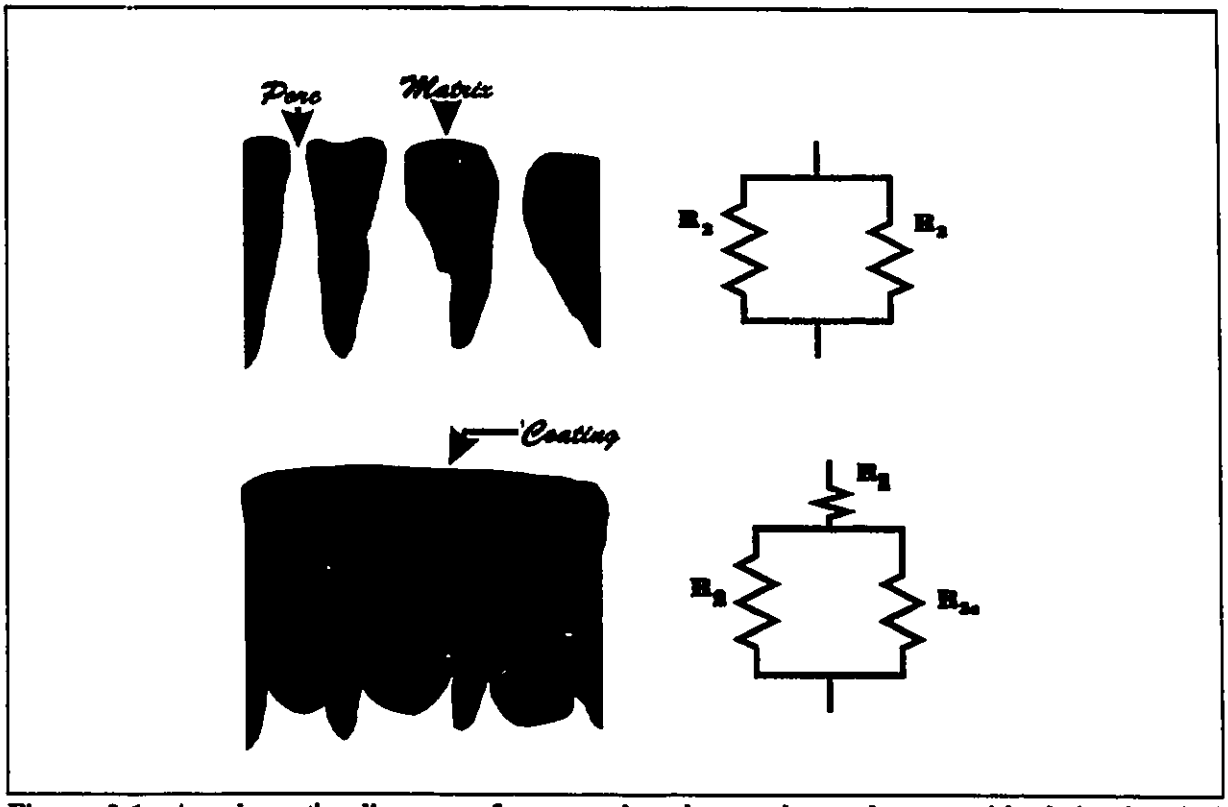

Figure 2.1: A schematic diagram of uncoated and coated membranes with their electrical analogue. Top: uncoated; bottom: coated.

"matrix" and "pores". The matrix consists of the polymer chains holding void spaces in molecular size within themselves. This region is denoted as region 2. The skin layer pores are denoted as region 3 and are very small compared with those in the porous sublayer. The porous sublayer is denoted as region 4. The permeating gas can flow through the porous sublayer with a negligible resistance compared with the resistance of the skin layer.

With reference to Equation 2.9, the permeation rate, Q, of a gas through a membrane can be described by:

$$Q=\frac{PA}{l}\Delta p \qquad (2.15)$$

where, Q is permeation rate, P is permeability coefficient of membrane, A is membrane surface

area available to the permeation of gas, l is thickness of membrane (skin layer thickness in an asymmetric membrane), and Δp is transmembrane pressure drop. Because the measurement of the true thickness of the skin layer in an asymmetric membrane is difficult, permeability, defined as P/l, is used instead of permeability coefficient, P, which is used in a homogeneous membrane.

Equation 2.15 is mathematically equivalent to the Ohm's law in an electrical circuit:

$$I=\frac{E}{R} \tag{2.16}$$

Conceptually, the current, I, can be equated to the permeation rate, Q, and the driving force for the current flow (i.e., electric potential difference, E), is analogous to pressure difference across membrane, Δp. Therefore, we can define a resistance to permeate flow, R, which is equivalent to the electrical resistance:

$$R=\frac{l}{PA} \tag{2.17}$$

so that the combination of Equations 2.15 and 2.17 gives:

$$Q=\frac{\Delta p}{R} \tag{2.18}$$

2.2.1. Resistance in an Uncoated Membrane

In an uncoated membrane, the matrix, pore, and sublayer resistances are denoted as R_2, R_3, and R_4 respectively. As it can be seen in Figure 2.1, resistances R_2 and R_3 are in parallel, and their total is in series with R_4. The total resistance, R_t, is related to the local resistances according

to the following equation:

$$R_t = \frac{1}{\frac{1}{R_2}+\frac{1}{R_3}} + R_4 = \frac{R_2 R_3}{R_2+R_3} + R_4 \qquad (2.19)$$

For a good performing asymmetric membrane $R_4 << R_2$ & R_3, i.e., the supporting sublayer introduces a negligible resistance to the permeation of gases compared with the resistances of the skin layer regions. That is because the separation should take place only within the skin layer and the permeant must flow as easily as possible through the sublayer. Therefore, ignoring the value of R_4, Equation 2.19 is simplified as:

$$R_t = \frac{R_2 R_3}{R_2+R_3} \qquad (2.20)$$

2.2.2. Resistance in a Coated Membrane

When a membrane is coated, a new region is created on top of the skin layer with its own resistance to the gas flow. This region is called region 1 and its resistance is R_1. The resistance R_1 is in series with the total of R_2 and R_{3c}, where R_{3c} is the resistance of the pores after being blocked by coating material. Note that although R_2 does not change after coating, R_3 is changed because the pores are filled with the coating material and their resistances are increased to R_{3c}. Then, equation 2.20 becomes:

$$R_{tc}=R_1+\frac{R_2R_{3c}}{R_2+R_{3c}} \tag{2.21}$$

2.2.3. Ideal Separation Factor (ISF)

As mentioned earlier, an ideal separation factor (ISF), α, of gas "a" over gas "b" is defined as the ratio of permeability of gas "a" to gas "b". It can also be defined as the ratio of the resistance to gas "b" over the resistance to gas "a", or, the ratio of the permeation rate of gas "a" to the permeation rate of gas "b". A common practice is to chose a reference gas and calculate the ISF of other gases with respect to that one. The overall and the local ideal separation factors are then defined as:

$$\alpha_t=\frac{P_{ref}}{P_{gas}}=\frac{R_{t_{gas}}}{R_{t_{ref}}}=\frac{Q_{ref}}{Q_{gas}} \tag{2.22}$$

$$\alpha_i=\frac{R_{i_{gas}}}{R_{i_{ref}}} \tag{2.23}$$

where t denotes overall, and i denotes regions 1, 2, and 3.

2.2.4. Actual Separation Factor (ASF)

Equation 2.22 defines the ideal separation factor based on single gas permeation. This definition can not be applied to gas mixtures. An actual separation factor (ASF) which is used

for gas mixtures is defined as the molar ratio of gas components in the permeate to that in the feed.

$$\alpha_{mix}=\frac{y_a/y_b}{x_a/x_b} \tag{2.24}$$

where: x_a and x_b are the mole fractions of components "a" and "b" in the feed; and,

y_a and y_b are the mole fractions of components "a" and "b" in the permeate.

In practice, the actual separation factor is usually smaller than the ideal separation factor.

2.3. CALCULATION OF THE LOCAL RESISTANCES

In this section a new solution method that was developed to solve for the local resistances is discussed. In this method the local resistances are calculated with minimum number of assumptions leading to more accurate results.

2.3.1. Local Resistances of an Uncoated Membrane

Knowing the permeation rates and the operating pressures of the permeating gas, the permeability, P/l, the overall resistance of the membrane, R_t, and the overall ideal separation factor (ISF), α_t, can be calculated using Equations 2.15, 2.18 and 2.22. Then, Equations 2.20 to 2.23 can be used to calculate the local resistances. The local resistances are first calculated for the reference gas and then for other gases.

Equation 2.20 may be written for a reference gas, e.g. helium (as it will be used in this thesis), as:

$$R_{t_{He}} = \frac{R_{2_{He}} R_{3_{He}}}{R_{2_{He}} + R_{3_{He}}} \tag{2.25}$$

Similarly, for any gas other than helium, Equations 2.22 and 2.23 can be substituted in Equation 2.20 to obtain:

$$R_{t_{gas}} = \frac{\alpha_2 R_{2_{He}} \alpha_3 R_{3_{He}}}{\alpha_2 R_{2_{He}} + \alpha_3 R_{3_{He}}} = \alpha_t R_{t_{He}} \tag{2.26}$$

Equations 2.25 and 2.26 are solved simultaneously for $R_{2\,He}$ and $R_{3\,He}$. Rearrangement of the above two equations gives:

$$R_{2_{He}} = \frac{(\alpha_2 - \alpha_3) R_{t_{He}} R_{t_{gas}}}{\alpha_2 (R_{t_{gas}} - \alpha_3 R_{t_{He}})} \tag{2.27}$$

$$R_{3_{He}} = \frac{(\alpha_2 - \alpha_3) R_{t_{He}} R_{t_{gas}}}{\alpha_3 (\alpha_2 R_{t_{He}} - R_{t_{gas}})} \tag{2.28}$$

The quantities involved in Equations 2.27 and 2.28 can be found as follows:

i) $R_{t\,He}$ and $R_{t\,gas}$ from experimental data using equation 2.18.

ii) α_2 is not recorded in the literature. However, it is assumed that after coating, the overall ISF, α_{tc}, is dominated by that of the polymer matrix. In other words, α_{tc} approaches α_2 after coating. In practice it is assumed that $\alpha_2 \approx \max(\alpha_{tc})$. It means that, the highest experimental separation factor achieved from the coated membrane is used for α_2. This assumption can be justified

because the pore resistance becomes enormous when the pore is filled with the coating material and the gas flows primarily through the polymer matrix. Hence, the permeating gas "feels" only the matrix resistance, R_2, and separation occurs within the matrix only.

iii) α_3 is unknown and has to be chosen randomly as will be discussed later in more details.

2.3.2. Local Resistances of a Coated Membrane

For a coated membrane, Equation 2.21 can be written for helium as the reference gas as:

$$R_{tc_{He}} = R_{1_{He}} + \frac{R_{2_{He}} R_{3c_{He}}}{R_{2_{He}} + R_{3c_{He}}} \tag{2.29}$$

Then Equations 2.22 and 2.23 are substituted in Equation 2.21 to obtain similar expression for other gases with respect to helium as the reference gas:

$$R_{tc_{gas}} = \alpha_1 R_{1_{He}} + \frac{\alpha_2 R_{2_{He}} \alpha_{3c} R_{3c_{He}}}{\alpha_2 R_{2_{He}} + \alpha_{3c} R_{3c_{He}}} = \alpha_{tc} R_{t_{He}} \tag{2.30}$$

As in case of uncoated membrane, we have two equations and two unknowns which should be solved for $R_{1\ He}$ and $R_{3c\ He}$. However, the solution is more complicated than for uncoated membrane. An analytical solution of Equations 2.29 and 2.30 results in the following equations:

$$aR_{1_{He}}^2 + bR_{1_{He}} + c = 0 \tag{2.31}$$

where:

$$a=\alpha_1(\alpha_{3c}-\alpha_2) \tag{2.32}$$

$$b=(\alpha_2-\alpha_{3c})(R_{tc_{gas}}+\alpha_1 R_{tc_{He}})-\alpha_2(\alpha_1-\alpha_{3c})R_{2_{He}} \tag{2.33}$$

$$c=(\alpha_{3c}-\alpha_2)R_{tc_{He}}R_{tc_{gas}}+\alpha_2(R_{tc_{gas}}-\alpha_{3c}R_{tc_{He}})R_{2_{He}} \tag{2.34}$$

Then:

$$R_{1_{He}}=\frac{-b\pm\sqrt{b^2-4ac}}{2a} \tag{2.35}$$

The coated pore resistance, R_{3c}, can then be calculated using the following equation:

$$R_{3c_{He}}=\frac{R_{2_{He}}(R_{1_{He}}-R_{tc_{He}})}{R_{tc_{He}}-(R_{1_{He}}+R_{2_{He}})} \tag{2.36}$$

The quantities involved in above equations are found as follows:

i) The value of the coating layer separation factor, α_1, can usually be found in the literature. Otherwise, it can be determined by performing separate experiments using a homogeneous dense membrane made of the coating material alone.

ii) α_2 (matrix separation factor) does not change after coating. As in the case of an uncoated membrane, it is assumed to be equal to the maximum of the overall separation factor after coating, i.e., $\alpha_2 \approx \max(\alpha_{tc})$. For explanation see Section 2.3.1.

iii) α_{3c} is the pore separation factor after coating. Assuming that all pores are filled with the coating material, the ideal separation factor of filled pores approaches that of the coating material. Therefore, the same value as α_1 can be used for α_{3c}, i.e., $\alpha_{3c} \approx \alpha_1$.

iv) $R_{tc\ He}$ and $R_{tc\ gas}$ from experimental data using equation 2.18.

v) $R_{2\,He}$ is not changed after coating. The values that were obtained from the uncoated membranes are used here.

2.3.3. Procedure to Solve for the Local Resistances

Equations 2.27 and 2.28 include three unknowns, namely, $R_{2\,He}$, $R_{3\,He}$, and α_3. The numerical values for α_3 are under the following restrictions. The value for α_3 is limited by the overall separation factor, α_t, as the upper limit, and the Knudsen separation factor, α_K, defined by Equation 2.13, as the lower limit. This limitation is based on the fact that if $\alpha_3 > \alpha_t$ ($=R_{t\,gas}/R_{t\,He}$) the denominator of Equation 2.27 becomes negative, resulting in a negative value for R_{2He} which is not acceptable. On the other hand, if α_3 is less than the Knudsen separation factor, it means that the flow is dominated by laminar mechanism which leads to no separation.

Under the above restrictions, the procedure to solve the Equations 2.27 and 2.28, and 2.32 to 2.36 is described below.

1. Choose a gas to be paired with helium (the reference gas) for solving the above equations, e.g., hydrogen.

2. Choose a value for α_3 between α_t and α_K of the paired gas, and substitute in Equation 2.27 and 2.28. Also, substitute $R_{t\,He}$, $R_{t\,gas}$ (in this example $R_{t\,H2}$), and α_2 in the above equations. Solve for $R_{2\,He}$ and $R_{3\,He}$.

3. Solve Equations 2.32 to 2.34 by substituting α_1, α_2, α_{3c} ($= \alpha_1$), and $R_{tc\,He}$ and $R_{tc\,gas}$ (in this example $R_{tc\,H2}$) from experimental data, and $R_{2\,He}$ from step 2. Calculate a, b, and c.

4. Substitute a, b, and c in Equation 2.35 and solve for $R_{1\,He}$.

5. Substitute $R_{1\,He}$ from step 4, $R_{2\,He}$ from step 2, and $R_{tc\,He}$ from the experimental data in Equation 2.36 and solve for $R_{3c\,He}$.

6. Choose the next gas to be paired with helium. Substitute $R_{2\,He}$ obtained in step 2 in Equation 2.27 and calculate α_3 for the newly chosen gas.

7. Repeat steps 3 to 5 for the newly chosen gas and calculate the corresponding local resistances.

8. Repeat steps 6 and 7 until all gases are paired with helium.

9. Go back to the first gas and choose a new value for α_3. Repeat steps 2 to 8.

The R_2 values obtained through the above procedure is independent of the gas paired with helium. The R_3 and R_1 values depend on the gas paired with helium but are calculated with high precision. The R_{3c} value also depends on the gas paired with helium and is only accurate within the order of magnitude. That is because, after coating, R_{3c} is usually very high compared with other local resistances and the overall resistance is approximately equal to the sum of the coating layer resistance and the matrix resistance, i.e., $R_{tc} \approx R_1 + R_2$. Therefore, the denominator of Equation 2.36 becomes close to zero and the calculation of R_{3c} becomes inaccurate.

As α_3 values vary, different set of results are found for $R_{2\,He}$, $R_{3\,He}$, $R_{1\,He}$, and $R_{3c\,He}$. The criteria to choose the correct set of results are as follows.

i) The α_3 values for all gases must be between the lower and the higher limit of that particular gas as discussed above.

ii) Resistances can not take negative values.

iii) The size of the matrix void spaces is much smaller than the size of the membrane pores. Therefore, the matrix resistance can only be comparable or larger than the pore resistance, that is $R_2 \geq R_3$.

iv) The coating material is usually chosen such that it is highly permeable to all gases. Therefore, the coating layer resistance, R_1, is relatively small compared with those of the substrate membrane. That is $R_1 < R_2$ & R_3.

The α_3 values that satisfy all the above requirements are in a very narrow range and, in fact, α_3s could be determined with three significant digits. It must also be noted that the solution of the quadratic Equation 2.35 results in two different roots, one from the solution of the equation with the negative sign before the square root term, and another with the positive sign before the square root term. The criterion to choose between the two roots is that the resistance value obtained by pairing the reference gas with one gas must be in agreement with those obtained by pairing the reference gas with other gases. That is, they must be at least in the same order of magnitude.

After calculation of all the local resistances for helium the local resistances for other gases are determined. This is done by multiplying the local resistances for helium by a proper local separation factor for each gas using Equation 2.23.

A sample calculation performed based on the above procedure using the experimental data obtained in this study is given in Appendix A.

2.4. Permeation Rate Measurement in a Constant Volume System

Two types of separation system available include constant pressure system and constant volume system. In a constant pressure system the permeate side is open to atmosphere, thus, the permeate pressure is constant and equal to the atmospheric pressure. In contrast, the permeate

side of a constant volume system is closed to atmosphere and its pressure increases as the permeant accumulates in the permeate side volume. The permeation rate is measured directly using a bubble flow meter in a constant pressure system. However, it should be determined indirectly in a constant volume system. The required equation can be derived from the ideal gas law.

$$n=\frac{V}{RT}p \tag{2.37}$$

Keeping the volume and the temperature constant, and taking the derivative of the both sides with respect to time permeation rate can be defined in number of moles per unit time:

$$Q=\frac{dn}{dt}=\frac{V}{RT}\frac{dp}{dt} \tag{2.38}$$

Where, n is number of moles of the permeating gas; t is time, V is the permeate side volume, R is gas constant, T is absolute temperature, and p is pressure. The practical interpretation of this equation is that, if the downstream pressure is graphed versus time, the permeation rate at each time can be calculated by multiplying the slope of the graph by a constant (V/RT). For small time intervals, Equation 2.38 can be approximated by:

$$Q=\frac{\Delta n}{\Delta t}=\frac{V}{RT}\frac{\Delta p}{\Delta t} \tag{2.39}$$

For an accurate calculation of small permeation rates, the pressure change, Δp, can be amplified by increasing Δt. If the change of the pressure is linear with time within the experimental range, an increase in Δt does not decrease the accuracy of the permeation rate calculation.

CHAPTER THREE

EXPERIMENTAL

3.1. PREPARATION OF DRY MEMBRANES

3.1.1. Material

The aromatic polyamide polymer used in this study known as poly-m-phenylene-iso(70)-co-tere(30)-phthalamide, abbreviated PA hereafter, was laboratory synthesized according to the method reported elsewhere [Gan, 1975]. The PA polymer has an average molecular weight of 31100 Dalton, an intrinsic viscosity of 1.472 dL/g, and a density of 1.3 g/cm^3 [Nguyen, 1987]. The chemical formula of the aromatic polyamide polymer is shown in Figure 3.1. Dimethylacetamide (DMAc) used as solvent was supplied by BDH Chemicals. Silicone material

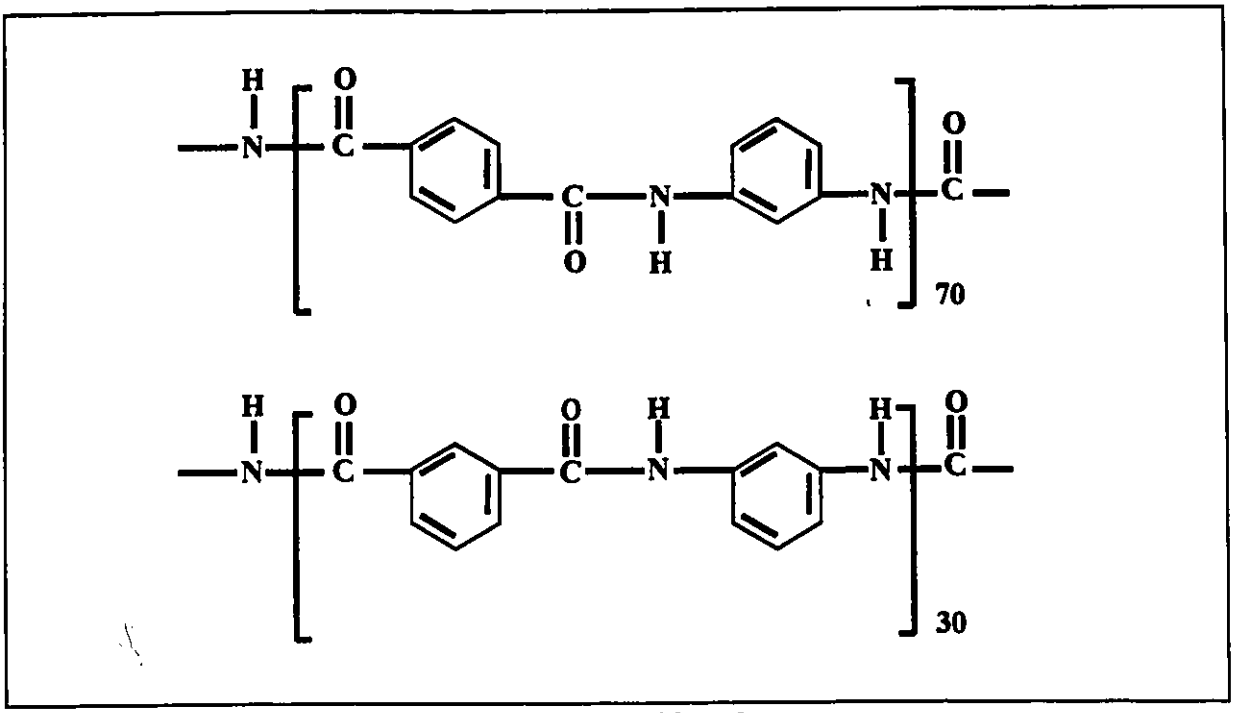

Figure 3.1: Chemical structure of aromatic polyamide polymer

poly(dimethyl-siloxane) was supplied by Beng-Pu Organic Chemical Industries, Dalian, China. Curing agents I (tetraethylorthosilicate) and II (dibutyltin dilaurate) were supplied by Aldrich Chemical Co. and hexane solvent by BDH Chemicals. All pure and mixed gas cylinders were obtained from Air Products.Lithium nitrate used as non-solvent additive was supplied by Fisher Scientific.

3.1.2. Preparation of Uncoated and Coated Asymmetric Membrane

A solution of aromatic polyamide polymer was prepared by dissolving the polymer in a mixture of lithium nitrate in DMAc. The composition of the casting solution was (wt%): polymer (16.0), solvent (77.5), and lithium nitrate additive (6.5). The solution was filtered twice using a

cloth filter or a 3μm Millipore filter and left for two days to release the trapped small air bubbles.

The filtered solution was cast over a glass plate using a casting blade to a nominal wet thickness of 254 μm. The cast film was kept in an oven at 95°C for 15 minutes for partial evaporation of the solvent. Then, it was immersed into a cold water bath (4°C) together with the glass plate for one hour, during which period gelation took place. The membrane sheet prepared in the way described above was cut into coupons of 5.5 cm diameter. The membranes were dried using the solvent exchange technique. In this technique, the membrane coupons were kept in isopropyl alcohol/water baths of progressively increasing alcohol contents for at least two hours in each bath. The alcohol contents of these baths were 25%, 50%, 75%, and 100% by volume. Finally, the membranes were transferred to a 100% normal hexane bath where they were kept for at least two hours before they were air dried. The thickness of the membranes was measured using a micrometer. The thickness was approximately 100 μm after drying was completed. The effective area of the membranes was 9.62 cm^2. The whole procedure was done at room temperature.

The dry aromatic polyamide membranes were coated by silicone rubber. For this purpose, an uncoated membrane was mounted at the bottom of a cylindrical test cell. The cell was then partially filled with 50 mL of a silicone in hexane solution and kept for one hour under approximately 50 psig pressure. The latter solution was prepared by dissolving 5 g silicone (polydimethylsiloxane), 0.25 g curing agent I and 0.15 g curing agent II in 100 ml hexane. The solution was then poured out and the hexane evaporated. The silicone layer was further cross linked by keeping the permeation cell in an oven at 60 °C for one hour.

3.1.3. Preparation of Homogeneous Dense Membranes

The homogeneous dense membranes were prepared from solutions with different polymer concentrations, and with and without the addition of lithium nitrate additive. The preparation procedures are explained below.

i) Homogeneous dense membranes with additive

The casting solutions for the homogeneous membranes were prepared in the same way as for the asymmetric membranes. Two solutions were made. One with high polymer concentration (16wt%) and the other with low polymer concentration (5.5wt%). The solvent in both cases was DMAc. The ratio of polymer to additive was the same as the one used for the preparation of asymmetric membranes. The solutions were filtered and left overnight to release the trapped air bubbles. The high concentration solution was cast over a glass plate using a casting blade. The low concentration solution could not be cast because of its low viscosity. In the latter case, the four edges of a glass plate was covered with electric tape and the solution was poured over the glass plate. The solvent was allowed to evaporate in an oven at 60 °C or 95 °C for one or two days. After the solvent evaporation step, the film together with the casting glass plate were transferred to a vacuum oven set at 40 °C for complete drying. The dry membranes were peeled off the glass plate and were cut into 5.5 cm diameter coupons. In one case, after the solvent was evaporated at 95 °C for one day, the membrane was placed in a cold water bath (4 °C) for gelation. The water in the membrane was then replaced with isopropyl alcohol and hexane by the solvent exchange technique explained in Section 3.1.2. The effective area of the membranes were 9.62 cm^2. The thickness of the homogeneous membranes measured using a

micrometer was approximately 50 μm. The preparation conditions are summarized in Table 3.1.

ii) Homogeneous dense membranes without additive

Polymer solutions of high (21.7 wt%), medium (9.6 wt%), and low (5.5 wt%) polymer concentrations were prepared by dissolving the aromatic polyamide polymer in DMAc solvent. The solutions were filtered and left overnight to release the small trapped air bubbles. The high concentration solution was cast over a glass plate using a casting blade. The medium and low concentration solutions were poured over the glass plate with electric tape at the four edges of the glass plate. The solvent was allowed to evaporate in an oven at different temperatures for two days. Then the films were transferred, together with the casting glass plates, to a vacuum oven set at 40 °C for complete drying. The dry membranes were peeled off the glass plate and were cut into 5.5 cm diameter coupons. The effective area of the membranes were 9.62 cm^2. The thickness of the homogeneous membranes measured using a micrometer was approximately 50 μm. The preparation conditions are summarized in Table 3.2.

Table 3.1: Preparation Conditions of Homogeneous Aromatic Polyamide Dense Membranes with the Addition of Lithium Nitrate.

Sample #	Polym Conc'n (wt%)	Add've Conc'n (wt%)	Evap'n Temp. (°C)	Evap'n Time (days)	Drying Time (days)	Water Gelation
1	16.0	6.5	95	1	0	Yes
2	16.0	6.5	95	1	1	No
3	16.0	6.5	60	2	1	No
4	5.6	2.0	60	2	2	No
5	5.6	2.0	23	2	2	No

Table 3.2: Preparation Conditions of Homogeneous Aromatic Polyamide Dense Membranes without the Addition of Lithium.

Sample #	Polym Conc'n (wt%)	Evap'n Temp. (°C)	Evap'n Time (days)	Drying Time (days)
1	21.7	95	2	2
2	21.7	60	2	2
3	21.7	40	2	2
4	21.7	23	2	2
5	9.6	95	2	2
6	9.6	60	2	2
7	9.6	40	2	2
8	9.6	23	2	2
9	5.6	95	2	2
10	5.6	60	2	2
11	5.6	40	2	2
12	5.6	23	2	2

3.2. APPARATUS FOR GAS PERMEATION EXPERIMENTS

Two sets of permeation systems were used in this study: constant pressure system and constant volume system. The theoretical aspects of these systems were described in Section 2.4. In this study, the constant pressure system was used for the experiments in which the permeation rates were relatively high, i.e., $>1\times10^{-4}$ cm^3/s. These experiments included all single gas permeations through asymmetric membranes, and separation of CO_2/CH_4 mixtures. The constant volume system was used for the experiments involving the measurement of low permeation rates ($<1\times10^{-4}$ cm^3/s) as well as air separation. Specifically, the latter system was used to measure the permeation rates of all gases through dense homogeneous membranes and the permeation rates

of low permeability gases, such as O_2, N_2, and CH_4 through asymmetric membranes.

3.2.1. Constant Pressure System

Figure 3.2 shows the schematic diagram of the constant pressure system and a separation cell. The cells were stainless steel cylinders with the feed, purge, and permeate lines at the top, side, and bottom, respectively. The membrane was mounted at the bottom of the cell over a porous metal sheet. The feed pressure was controlled by a pressure regulator and was measured using a pressure gauge. The permeation rate was measured by bubble flow meters of different diameters, depending on the permeation rate. The ranges of the permeation rates measurable by the bubble flow meters of 0.25 cm, 0.80 cm, and 1.60 cm diameter, were 0.005 to 0.500 cm^3/min, 0.5 to 10 cm^3/min, and 10 to 60 cm^3/min, respectively. The composition of the feed and the permeate gases were analyzed using a Varian 3600 gas chromatograph (G.C.). The G.C. was calibrated prior to the experiments.

3.2.2. Experimental Procedure for the Constant Pressure System

Six gases including helium, hydrogen, oxygen, nitrogen, carbon dioxide, and methane; and three carbon dioxide/methane mixtures with 0.25, 0.50, and 0.75 carbon dioxide mole fractions were used for single gas permeation and mixed gas separation experiments.

Before each experiment, the separation cell was flushed with the experimental gas to purge air and other gases in the cell. This was done by filling up the cell with the experimental

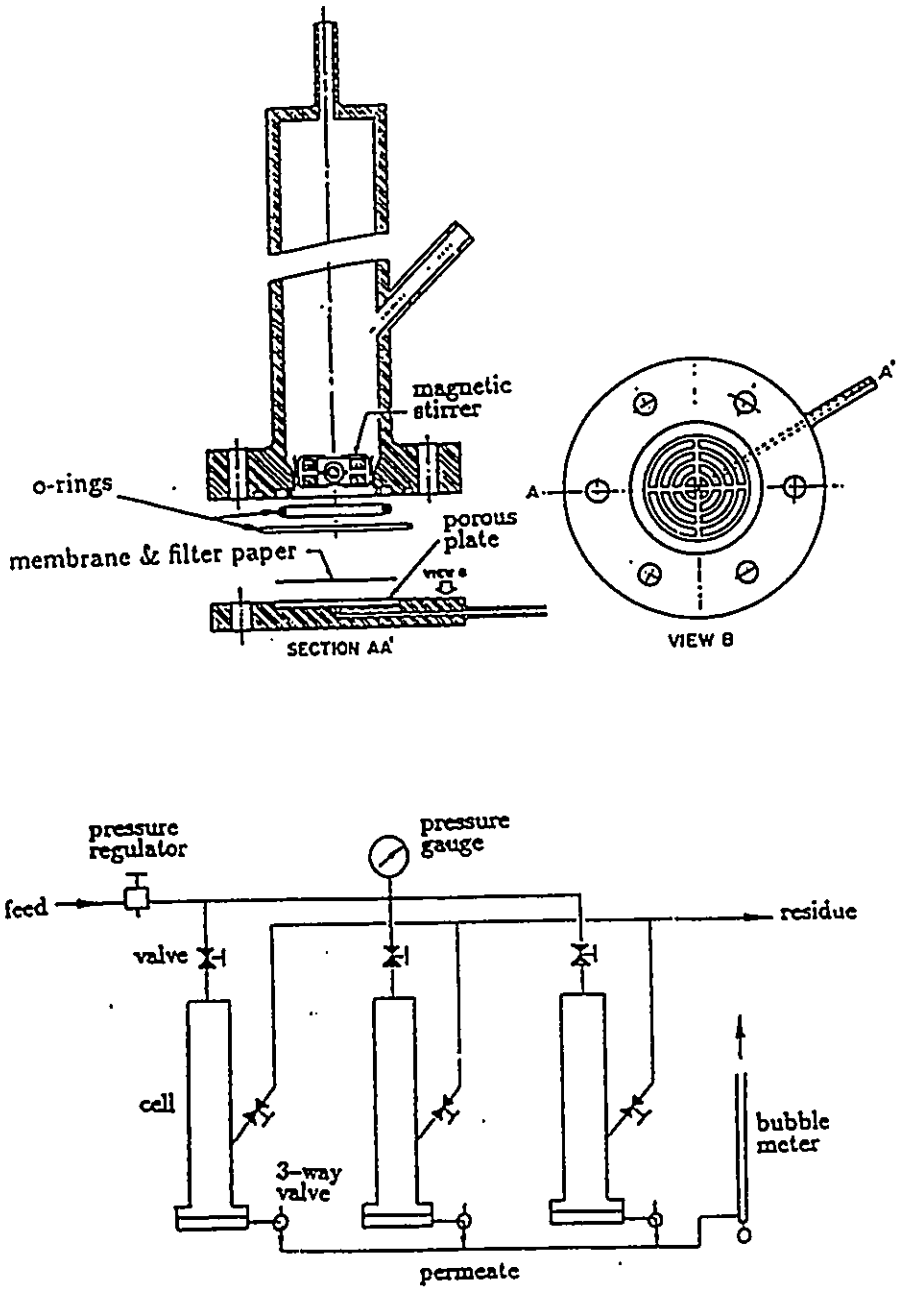

Figure 3.2: Schematic diagram of the separation cell (top), and the constant pressure system (bottom).

gas up to ≈ 100 psig and releasing the gas. The procedure was repeated five times. Then, the pressure of the gas was increased to the operating upstream pressure. The gas permeation experiments were carried out at operating pressures of 350, 700, 1050, 1400, 1750, and 2100 kPa (approximately 50, 100, 150, 200, 250, and 300 psig). The permeation rate was measured and recorded every 10 to 30 minuets until the steady-state was reached. Only the permeation rates at steady-state were used for further calculations. In case of CO_2/CH_4 mixtures the permeate mole fraction was determined by the gas chromatograph.

3.2.3. Calibration of the Gas Chromatograph

A gas chromatograph enables quantitative analysis of gas mixtures. The amount of each component is proportional to the area underneath the peak that corresponds to a particular component. The position of the peak related to each gas is usually identified by injecting pure gas sample into the carrier gas stream and recording the response.

According to Dietz [1967], a precise determination of a gas composition is only possible by dividing the area underneath each peak by a correction factor which is unique for each gas. These correction factors are called "thermal response factor" (TRF). Dietz suggested the following TRFs for the gases used in this study: $CH_4 = 35.7$, $N_2 = 42$, $O_2 = 40$, $CO_2 = 48$. He did not report the values of TRFs for H_2 and He gases. The error margin for the above factors was 3%.

In practice it was realized that the above values are not accurate enough. Therefore, Dietz' experiment was repeated many times and new values of TRFs were obtained. These new values were calculated by injecting known compositions of CO_2/CH_4 gas mixtures into the G.C. and dividing the

peak areas by different combinations of methane and carbon dioxide's TRFs. The corrected peak areas were compared with the actual gas mixture composition. The average of TRFs obtained from the tests was taken and used for further calculations. The TRF values for carbon dioxide and methane were:

TRF (CO_2) = 50.0 ± 0.0 TRF (CH_4) = 36.6 ± 0.4

The TRF values were within the error margin reported by Dietz.

3.2.4. Constant Volume System

A schematic diagram of the constant volume separation system is shown in Figure 3.3. The main advantages of this system is that it is practically leak free. In addition, it can measure permeation rates of as low as 1×10^{-8} cm^3/s and can be tailored for lower rates. Also, this system is fully automated with a process controller capable of a continuous supervision of the experiments according to the given recipes. The system includes the following components: separation cells, mass flow controllers (MFC), pressure transducers, vacuum pumps, mass spectrometer, process controller, valves, and accessories.

The gas(es) was fed into the separation cells through one or both mass flow controllers. The permeate was collected in the downstream tubing and cylinders of known volume. The composition of the feed and the permeate gases were determined by a mass spectrometer. The components of the system will be discussed in more detail below.

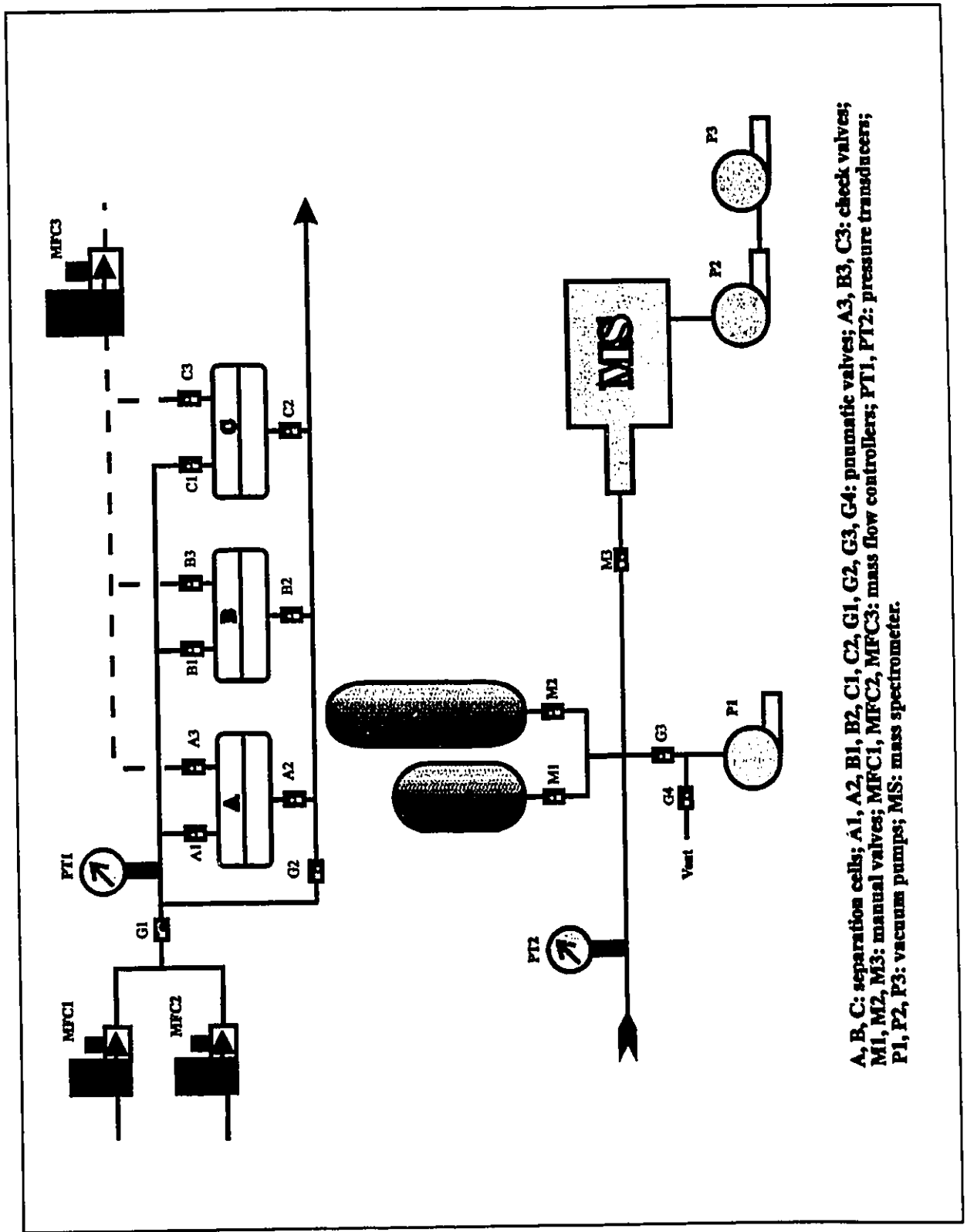

Figure 3.3: Schematic diagram of the constant volume system.

i) Separation cells

Three separation cells were constructed based on a "membrane-self-sealing" design. In this design the seal was made by the membrane itself and no "O" ring was involved.In addition, an "O" ring was installed in another cell in order to compare the performances of the cells with and without an "O" ring. These cells are denoted as A, B, and C in Figure 3.3. Figure 3.4 shows the detailed designs of the separation cells with and without an "O" ring. Each cell consisted of a stainless steel thick wall short cylinder divided into the upper and the lower parts. The feed and the purge lines were connected to the upper chamber while the permeate line was connected to the lower chamber. The membrane was mounted on top of a porous metal sheet that allowed the permeate to pass through with negligible resistance. The membrane was sandwiched between two finely machined and mirror polished surfaces of the upper and lower parts. The sealing surfaces had approximately 2 mm width and 0.050 mm depth.

ii) Mass flow controllers (MFC)

Feed and purge flow rates were controlled by three 1261C mass flow controllers provided by MKS Canada. The flow in each mass flow controller varied from 0 to 10 ± 0.1% cm^3/min. During each experiment, only one cell was used, therefore, the feed flow rate into the system was equal to the feed flow rate to the individual cell. Two mass flow controllers were installed at the feed inlet, and one at the purge side. The two inlet MFCs were used to mix and feed one or two gases into the upstream at a preset flow rate. The third MFC was used to purge the gas to keep the upstream composition and pressure constant. The flow rate ratio of the two feed gases was adjusted such that a mixture with a desired composition was obtained. The exact composition of the feed gas was determined by the mass spectrometer. Because the experiments were performed

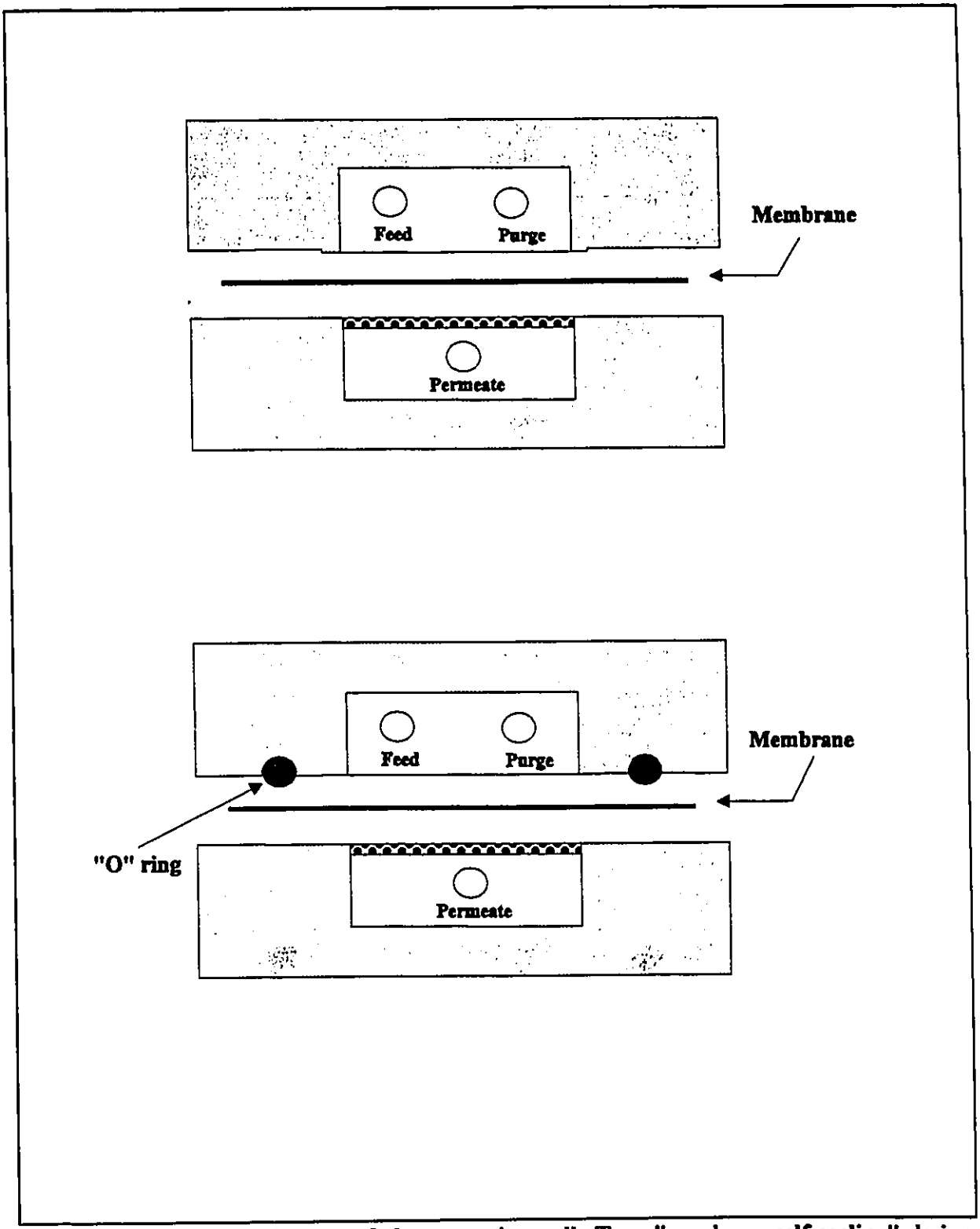

Figure 3.4: Schematic diagram of the separation cell. Top: "membrane-self-sealing" design. Bottm: cell design with "O" ring sealant.

as a continuous system, the feed flow rate was kept 3 to 4 orders of magnitude higher than the permeation rate in order to keep the composition constant. In addition, the purge flow rate was automatically adjusted by the process controller such that the upstream pressure stayed within $<\pm 0.1\%$ of the set point.

iii) Pressure transducers

The upstream and the downstream pressures were measured using two 122A type pressure transducers provided by MKS Canada. The pressure ranges were ≈ 0.27 - 2666 kPa (2 - 20000 ± 0.15% torr) and ≈ 0.13 - 1333 Pa (0.001 - 10 ± 0.15% torr) for the upstream and the downstream transducers, respectively.

iv) Mass spectrometer

A MKS 600A-PPT type partial pressure transducer mass spectrometer analyzed the composition of gases either in the feed or the permeate side. Gas sample was decomposed in the mass spectrometer chamber and its composition was displayed on a computer screen as the partial pressure of the fragmental components versus their atomic mass unit (amu). The mole fraction of the gas components was found by dividing the sum of the fragmental partial pressures by the sum of the partial pressures. The pressure in the chamber was maintained between 1.3×10^{-9} to 1.3×10^{-2} Pa (1×10^{-11} and 1×10^{-4} torr) using a turbo pump. The mass spectrometer's chamber was separated from the downstream line by an orifice allowing the required high pressure difference between the downstream and the chamber. The mass spectrometer was calibrated at the beginning and was checked frequently during the experiments. The calibration was done by injecting pure nitrogen in to the mass spectrometer's chamber and adjusting the tuning parameters until sharp and distinct peaks appeared at amu=14 and amu=28 corresponding to N and N_2. The mass

spectrometer was further fine tuned by injecting dry air into its chamber and varying the parameters until the peaks corresponding to oxygen and nitrogen were sharp and distinct.

v) Process controller

Operation of the apparatus and acquisition of the data were done by a process control computer program written in LabVIEW Graphical Programming provided by National Instrument Canada. The process control included operation of the valves and mass flow controllers according to preset parameters such as upstream and downstream pressure and feed composition. The data acquisition and analysis included receiving upstream and downstream pressures, temperature, feed and purge flow rates, and status of the valves and the vacuum pump. Based on a given recipe, the program started and stopped a certain experiment, controlled the feed flow rate and composition, and the upstream and the downstream pressures. It also calculated the derivative of the downstream pressure versus time curve and accordingly the standard temperature and pressure (STP) corrected permeation rate. The program read data every 2 milliseconds and took the average of 500 readings and updated the data log every 1 second. The accuracy of the measurement of the permeation rate was ±0.5%. The process control algorithm is discussed later in this chapter.

vi) Valves

The cells were isolated from the feed and permeate lines by pneumatic valves denoted as A1, A2, B1, B2, C1, C2 and from the purge line by check valves denoted as A3, B3, C3 in Figure 3.3. Pneumatic valves were also used to separate the system from the mass flow controllers (G1), the upstream line from the downstream line (G2), the vacuum pump from the system (G3), and the vacuum pump to vent (G4). Air at 100 psig was provided by a set of

solenoid valves to operate the pneumatic valves. Manual valves M1, M2, and M3 were used to isolate two auxiliary cylinders and the mass spectrometer.

vii) Vacuum pumps

Two Arthur 40 mechanical vacuum pumps were used in the system. The first one was used to bring down the initial downstream pressure to <0.13 Pa (<10^{-3} torr). The pump started automatically again when the downstream pressure exceeded the higher limit of ≈1333 Pa (10 torr). The second one was installed in series with a turbo pump to reduce the mass spectrometer's chamber pressure. In this case, the mechanical pump brought the pressure down to 1×10^{-3} torr, then, the turbo pump evacuated the remaining gases down to 1×10^{-11} torr.

viii) Accessories

Two auxiliary cylinders were connected to the downstream side to increase the volume and prolong the time to reach the higher limit of the downstream pressure (normally 1.3 kPa, 10 torr) when necessary. The downstream dead space was 70 cm^3. That is the volume of the lower chamber of the separation cell and the tubing. The volumes of the auxiliary cylinders were 2250 cm^3 and 3785 cm^3. The downstream dead space was determined by trapping a small amount of a gas with known pressure in the downstream and then opening an auxiliary cylinder of known volume and recording the resulting pressure. The equation: $p_1 V_1 = p_2 (V_1 + V_2)$ was used to calculate the downstream dead space. In this equation, p_1 and p_2 are the downstream pressures before and after opening the auxiliary cylinder, respectively, and V_1 and V_2 are the dead space and the auxiliary cylinder volumes, respectively. Addition of these cylinders increased the range of functionality of the system such that accurate measurement of higher permeation rates (up to 0.02 cm^3/s) became possible. The volume of the cylinders were incorporated in the calculation

of the permeation rate by the computer program.

Two power supplies with ±15, 24, and +5 VDC output were used to power the mass flow controllers, the mass spectrometer, and the analog interface boards respectively. In addition, two computers were used in the system, one to run the process controller/data acquisition and the other to run the mass spectrometer and to log the data.

The feed, permeate, and purge lines were made of ¼" stainless steel tubing. Except the valves, all connections were made by soldering the tubing and the joints. The valves were connected to the line using Cajon VCR fittings and glands. The glands were soldered to the tubing. The seals in the VCR fittings were made by stainless steel gaskets. The manufacturer claims a leak rate through the VCR valves of 1×10^{-9} cm^3/s of helium gas.

3.2.5. Process Control Algorithm

A computer program was written to control the process based on the following algorithm. Note that all the examples below are given for separation cell "A" alone. A similar procedure may be assumed for other two separation cells. The computer program is shown in the Appendices.

a) Analog read and log at each iteration:

- Read temperature in ^{o}C and log in a buffer of size 1000.
- Read upstream pressure in torr and log in a buffer of size 10000.
- Read downstream pressure in mtorr and log in a buffer of size 10000.
- Read time in ms and log in a buffer of size 1000.

b) Digital read at each iteration:

- Read the status of the valves and pumps (0: off, 1: on).

c) Analog write at each iteration:

- Write flow rate into MFC1, MFC2, and MFC3 in 0 - 5 VDC.

d) Upstream pressure control:

- Read pressure set point.

- Calculate the safety limit at 101% of the set point.

- If pressure < set point:

    - Open MFC1 at the set point.

    - Open MFC2 at the set point.

    - Close MFC3.

- If safety limit > pressure ≥ set point (normal operation):

    - Open MFC1 at the set point.

    - Open MFC2 at the set point.

    - Open MFC3 at $Q_{MFC3} = 1.2 \times (Q_{MFC1} + Q_{MFC2})$.

- If Pressure > safety limit:

    - Close MFC1.

    - Close MFC2.

    - Open MFC3 at full range.

e) Downstream pressure control:

- Read the lower pressure set point.

- Read the upper pressure set point.

- If pressure < upper set point and pressure increasing (normal operation):
    - Close G3 (disconnect pump 1).
    - Open A2 (cell A to permeate).
- If pressure > upper limit:
    - Open G3 (connect pump 1).
    - Close A2 (disconnect cell A from permeate line).
- If lower limit < pressure < upper limit and pressure decreasing:
    - Open G3 (connect pump 1).
    - Close A2 (disconnect cell A from permeate line).
- If Pressure < lower limit and decreasing:
    - Close G3 (disconnect pump 1).
    - Open A2 (connect cell A to permeate).

3.2.6. Experimental Procedure for the Constant Volume System

The sealing surfaces of the separation cells were covered with a thin layer of vacuum grease for blocking the micro-scratches to minimize air leak into the system. The membrane was then mounted on top of the porous metal and the cell was pressed between a thick metal sheet and a metal bar.

Both the upstream and the downstream lines and the upstream and the downstream chambers of the separation cell were evacuated by the vacuum pump before each experiment for at least 15 hours. This was done to release the water vapour and adsorbed gases. The process of

evacuation was prolonged to minimum 2 days if a new membrane was installed or if the separation cell was opened to air. In case of new membrane installation, a leak test was performed after at least 2 days of evacuation.

In order to minimize the amount of impurities in the feed gas, the feed and the purge lines were swept by the experimental gas. The sweep procedure was done separately for the feed and the purge lines as is discussed below.

The feed line included the tubing from the gas cylinders to the mass flow controllers and from the mass flow controllers to the upper chamber of the separation cell. To sweep the feed line, the upstream and the downstream lines were connected, i.e., valve G2 was open. Then, the gas was fed at a flow rate of 10 cm^3/min while the vacuum pump was running. The mass spectrometer was also connected to the system during the sweep procedure, and the composition of the feed gas was analyzed simultaneously. The procedure continued until the impurities in the feed were less than 1%.

In order to sweep the gas in the purge line, i.e., from the check valve A3 to the MFC3, the upstream and the downstream lines were isolated, i.e., valve G2 closed. Then, with the pressure set at a relatively small value, i.e., 1500 torr, the experimental gas was fed into the upstream until the pressure reached the set point. At this point, the purge mass flow controller was automatically opened at the full range and the impurities in the purge line were swept. This procedure was done for around half an hour.

3.2.7. Range of the Permeation Rates Measurable Using the Constant Volume System

While the system could accurately measure permeation rates as small as 1×10^{-8} cm^3/s and lower, there was a upper limit to the permeation rates measurable by the system. That was because the downstream pressure transducer was able to measure pressures between 0.001 to 10 torr. Thus, when the downstream pressure rose fast, the upper limit (10 torr) was reached quickly. At the upper limit, the controller started the vacuum pump in order to bring the pressure down to the lower limit. For highly permeable gases such as helium, the time interval between two evacuations was very small. Therefore, an accurate measurement of the permeation rate was not possible when the permeation rate was high. The solution to this problem was to open the auxiliary cylinder(s) and increase the downstream volume, thus, prolonging the time intervals. Figure 3.5 shows the time interval between two evacuations versus permeation rate for different downstream volumes. This figure can be used as a guideline to choose the correct downstream volume.

The shortest time interval between two evacuations for an accurate measurement was found empirically to be around one hour. The highest permeation rate measurable using the constant volume system was then calculated to be ≈0.02 cm^3/s which is equivalent to approximately 1.2 cm^3/min. The calculation was done by substituting $\Delta p = 10$ torr, $\Delta t = 60$ min, and the total downstream volume including both cylinders and the tubing, $V = 6105$ cm^3, $R = 62356$ cm^3 torr/mol K, and $T = 296$ K in Equation 2.39.

The recommended volume to be used according to the expected permeation rate is as

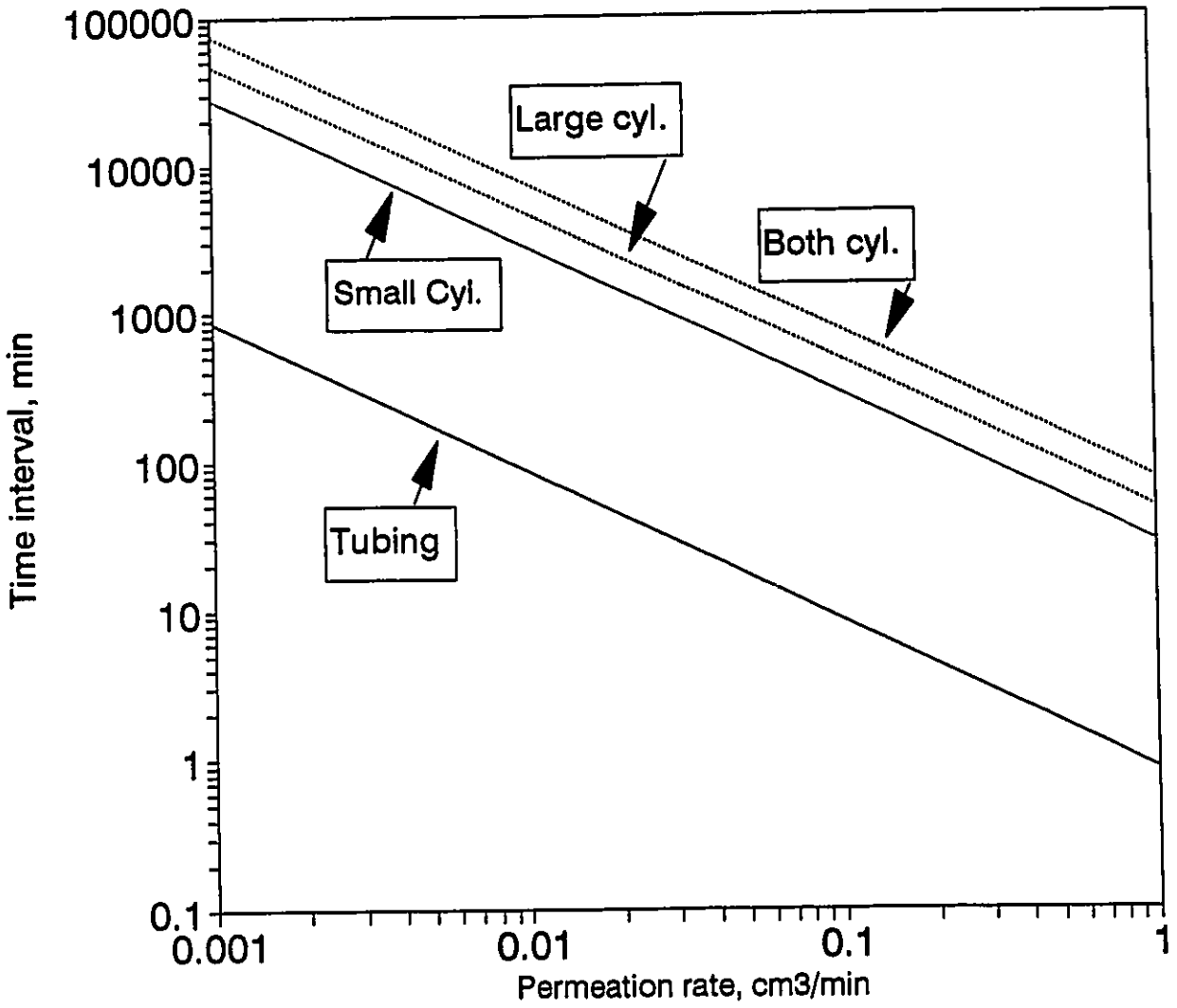

Figure 3.5: Calibration curves to be used as a guideline for choosing correct downstream volume at different permeation rates.

follows:

- For permeation rates less than 0.01 cm^3/min: close both cylinders, use the tubing only.

- For permeation rates between 0.01 cm^3/min and 0.3 cm^3/min: open the small cylinder.

- For permeation rates between 0.3 cm^3/min and 0.8 cm^3/min: open the large cylinder.

- For permeation rates between 0.8 cm^3/min and 1.2 cm^3/min: open both cylinders.

3.2.8. Testing the Performance of the Constant Volume System Devices

The performance of the process controller was tested regarding the "write into", and "read from" the electrical devices used in the system. These devices include: mass flow controllers, pumps, solenoid valves, pressure transducers, and thermocouple.

The "write" test was done by comparing the signal sent by the computer and the voltage received by each device. This test was performed on MFCs, pumps, and solenoid valves. The read test was done by comparing the voltage sent by each device and the signal received by the controller. This test was performed on the pressure transducers and the thermocouple. To interpret the signals received from the device into meaningful values, the signals were multiplied by proper coefficients. The coefficients were obtained by calibrating the transducers and the thermocouple using a pre-calibrated similar device.

3.3. Measurement of Leak Rate in to the Constant Volume Separation System

The leak rate in to the permeate line was measured for the following cases:

i) Leak through the downstream valves and joints into the permeate line (downstream).

ii) Leak through the separation cell into the permeate line (downstream).

iii) Leak during an actual permeation experiment.

The procedure is described below for the system that included the cell "A" alone (see Figure 3.3), i.e., the valves B1, B2, B3, C1, C2, C3, and the mass flow controllers MFC1 and MFC2 were closed all the times. The valve G4 was a vent valve and was also closed during all experiments.

The mass spectrometer was disconnected during the leak test by closing M3. At the end of the test, M3 was opened and the permeate composition was analyzed by the mass spectrometer.

For leak test (i), the downstream line was isolated. This was done by closing the valves G2 and A2. Then, with the vacuum pump running, the valve G3 was opened. The pressure of the downstream line was brought down to <0.13 Pa ($<1\times10^{-3}$ torr). The downstream pressure was maintained below 0.13 Pa (1×10^{-3} torr) for at least two days until the water and organic vapours were fully desorbed. Then, the vacuum pump was disconnected by closing the valve G3. The downstream pressure rise was immediately monitored by the process controller and the leak rate was calculated by the computer according to Equation 2.39.

For leak test (ii), both the upstream and the downstream lines and the upper and the lower chambers of the separation cell were evacuated. For this purpose, the valves A1, A2, G1, G2, and G3 were opened while the vacuum pump was running. The system pressure was brought down to <0.13 Pa ($<1\times10^{-3}$ torr) and maintained at that pressure for at least two days. Then, the downstream and the upstream lines were disconnected by closing the valve G2. The vacuum pump was also disconnected by closing the valve G3. The downstream pressure rise was monitored and the leak rate was calculated by the computer according to the rate of pressure rise using Equation 2.39.

For leak test (iii) a single gas permeation experiment was performed and the composition of the permeate was analyzed by the mass spectrometer and the percentage of impurities was calculated. The presence of the impurities in the permeate was attributed to the leak into the system. The leak rate was obtained by multiplying the percentage of impurities by the nominal permeation rate. The measurement of the permeation rate is explained in the next section.

3.4 Measurement of Permeation Rate

The gas permeation experiments were performed according to the following procedure. Note that, again, only the cell "A" was used to describe the procedure in the following example.

1- The downstream and upstream lines, and the upper and the lower chambers of the separation cell were evacuated to <0.13 Pa ($<1\times10^{-3}$ torr). That is, valves A1, A2, G1, G2, and G3 were opened, and A3, MFC1, and MFC2 were closed.

2-The upstream line was disconnected from the downstream line by closing valve G2, and the vacuum pump was disconnected by closing valve G3.

3- The mass flow controller(s) MFC1 and/or MFC2 were opened and gas(es) was supplied to the upstream at ≈ 666 kPa (5000 torr).

4- As the gas permeated through the membrane, the downstream pressure rose. The pressure rise was monitored and the permeation rate was calculated. When the downstream pressure reached the higher limit of ≈1333 Pa (10 torr) the cell was disconnected from the downstream by closing the valve A2, and the pump was connected again to bring the pressure down to the lower limit of <0.13 Pa ($<1\times10^{-3}$ torr), i.e., the valve G3 was opened.

5- Step 4 was repeated if necessary.

The feed flow rate was between 1 and 10 cm^3/min. The purge flow rate was set at 120% of the feed flow rate unless the upstream pressure was less than the set point. In the latter case, the purge was closed for a short period (typically around two seconds) to bring the pressure back to the set point. The composition of the permeate was analyzed by the mass spectrometer.

CHAPTER FOUR

RESULTS AND DISCUSSIONS

4.1. PERFORMANCE OF THE CONSTANT VOLUME SYSTEM

The performances of the devices used in the constant volume (CV) system were tested and reported in Chapter three: Experimental. In this section, the overall performance of the system will be discussed. The discussion includes the results of the tests on the measurement of the leak rate into the system, and on the variation of the upstream pressure with respect to the set point.

4.1.1. Leak Rate into the System

The leak rate into the permeate line was determined for the following three cases:

i) Leak through the downstream valves and joints into the permeate line (downstream).

ii) Leak through the separation cell into the permeate line (downstream).

iii) Leak during an actual permeation experiment.

The details of the operational conditions during the tests were discussed in the previous chapter. In brief, the first two tests were done when the pressure in the upstream and the downstream sides of system was effectively zero. The separation cells were disconnected from the downstream in the first test, and were connected for the second. The leak rate was calculated from the slope of the pressure increase with time as air leaked into the system. In the third test, the composition of the impurities was determined and the leak rate was calculated accordingly. The impurities were assumed to be the result of leak into the system. The results of the leak tests i, ii, and iii are summarized in Table 4.1.

Table 4.1: Leak Rate into the Constant Volume System; the Permeation Rates of Oxygen, Nitrogen, and Methane; and the Composition of Impurities in the Permeate.

	Leak or permeation rate cm^3/s	Purity of permeate	Composition of impurity
Leak test (i)	**$<1.2\times10^{-9}$**	**N/A**	**N/A**
Leak test (ii)	**$<2\times10^{-9}$**	**N/A**	**N/A**
Leak test (iii):			
O_2	**3.6×10^{-6}**	**97.2%**	**H_2O: 0.8%, N_2: 0.6%, CO_2: 1.4%**
N_2	**4.0×10^{-7}**	**97.3%**	**H_2O: 2.3%, O_2: 0.4%**
CH_4	**1.9×10^{-7}**	**95.9%**	**H_2O: 2.2%, N_2: 0.9%, CO_2: 0.9%**

Leak test (i): leak through the downstream valves and joints into the permeate line.

No pressure rise was observed during 20 hours of leak test (i). In other words, the pressure rise was less than the lowest detectable limit of the pressure transducer, i.e., less than 0.001 torr. Accordingly, the leak rate was estimated to be $<1.2\times10^{-9}$ cm^3/s. The calculation was done by substituting V = 70 cm^3, $\Delta p = 1\times10^{-3}$ torr, $\Delta t = 7.2\times10^4$ s, R = 62356 cm^3 torr/mol K, and T = 296 K in Equation 2.39.

Leak test (ii): leak through the separation cell into the permeate line.

The leak test (ii) was performed at practically zero upstream pressure. While the upstream and the downstream were isolated, it was observed that the upstream pressure rise was higher than the downstream. The upstream pressure rose to 14 torr within around 24 hours of test period. Correspondingly, leak rate to the upstream was estimated to be 1×10^{-5} cm^3/s.

The variation of the downstream pressure with time as well as the calculated leak rate are shown graphically in Figure 4.1. The downstream pressure did not change during the first 11 hours. The leak rate corresponding to this time period was estimated to be $<2\times10^{-9}$ cm^3/s. In the next 11 hours the pressure started to rise and reached ≈0.011 torr. The corresponding leak rate was $\approx3\times10^{-8}$ cm^3/s. At the end of the experiment, the composition of the gas accumulated in the permeate line was analyzed by the mass spectrometer. The results are as follows: oxygen 44.3%, nitrogen 27.1%, water 21.8%, and carbon dioxide 6.9%.

A careful examination of the leak rate, and the analysis of the gas accumulated in the downstream led to the conclusion that the leak rate into the downstream was, in fact, one order of magnitude smaller than the value calculated from the second region of the curve (i.e., smaller than 3×10^{-8} cm^3/s). Two observations supported this conclusion:

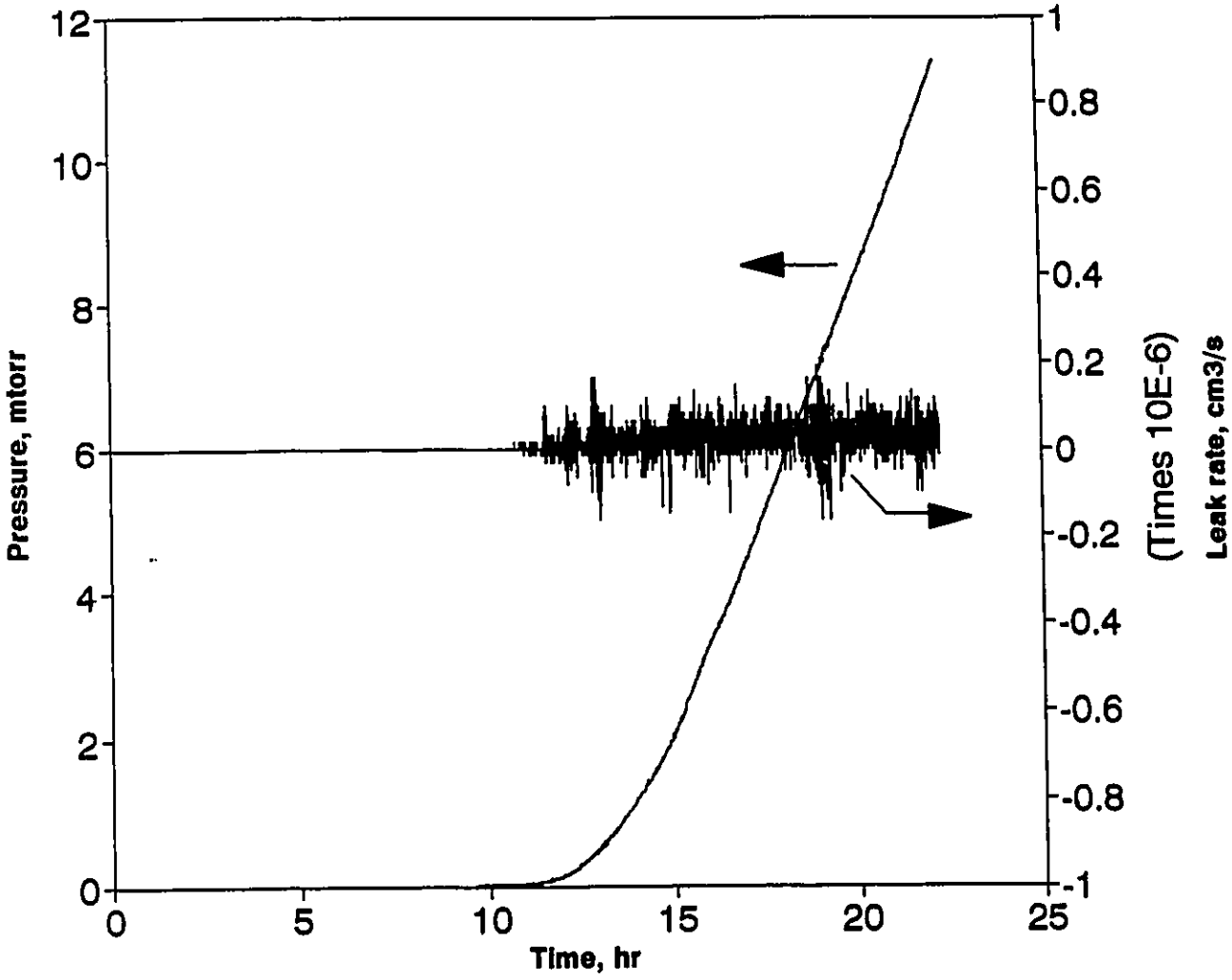

Figure 4.1: Variation of the downstream pressure and the leak rate with time during leak test (ii).

i) As mentioned before, and can be seen in Figure 4.1, in the first half of the test, no pressure rise was observed in the downstream, which indicates that the leak rate must be $<2\times10^{-9}$ cm^3/s.

ii) If air was leaking into the downstream, the composition of the accumulated gas in the permeate line must have matched that of air. That is, approximately, 21% oxygen, 79% nitrogen,

and close to zero water and carbon dioxide. However, the composition of the gas in the downstream did not match that of air. A simple explanation for this observation is that the downstream pressure rise was due to a very slow and selective permeation of low pressure air from upstream through the membrane into the downstream. The higher concentrations of oxygen, water, and carbon dioxide in the permeate which were expected from the separation characteristics of the membrane supported this explanation. Compared with similar systems, this level of leak rate is few orders of magnitude smaller [Chiou, 1987].

The higher leak rate into the upstream could be due to either/both of the following reasons:

i) Since during the normal operation of the system, the upstream is under pressure and the downstream is under vacuum, the amount of gases adsorbed in the upstream is much higher than the downstream. The higher rate of upstream pressure rise could be due to the desorption of these gases.

ii) The upstream was not as leak tight as the downstream.

The leak rate into the upstream did not affect the composition of the feed during the normal operation of the system. That is because, the feed flow rate was five to six orders of magnitude higher than the leak rate.

iii) Leak during an actual permeation experiment

To understand the extent of leak during an actual permeation experiment three tests were performed using the least permeable gases. These gases included oxygen, nitrogen, and methane. The operating conditions were reported in Chapter three. The composition of the permeating gas was analyzed by the mass spectrometer to determine the mole percentages of the impurities. The

results are summarized in Table 4.1. The permeation rates were 3.6×10^{-6} cm^3/s, 4.0×10^{-7} cm^3/s, and 1.9×10^{-7} cm^3/s for oxygen, nitrogen, and methane respectively. An analysis of the permeate composition showed 97.2%, 97.3%, and 95.9% purity for O_2, N_2, and CH_4 respectively. The impurity was mainly composed of water with traces of carbon dioxide. The permeation rates reported in Table 4.1 are corrected for the impurities. The percentage of impurities in the permeate line was around 3% for the least permeable gases, which can be compared with around 200% in similar systems and under similar conditions [Chiou, 1987]. Obviously, as the permeation rate increases this percentage decreases. The source of the impurities could be the adsorbed water and other gases in the downstream line and the membrane, the moisture content of the feed gas, and adsorbed gases remaining from the previous experiments in the downstream. The high purity of the permeate, despite the low permeation rates, indicates high degree of reliability of the system.

4.1.2. Upstream Pressure Control

The upstream pressure was controlled by the process controller according to the given set point. This was done by varying the feed and the purge flow rates. The feed and the purge flow rates, on the other hand, were designed to meet two simultaneous tasks. One was to keep the upstream pressure at the set point as accurately as possible, and the other was to keep the feed concentration constant.

The fluctuation of the upstream pressure depended on the feed flow rate, but independent of the permeation rate through the membrane, and independent of the pressure set point. That is,

the upstream pressure varied from "set point ± 0.5 torr" to "set point ± 3 torr" depending on the magnitude of the feed flow rate. For small flow rates, e.g., 1 cm^3/min, the fluctuation was around ± 0.5 torr. At high flow rates, e.g., 10 cm^3/min, the fluctuation was around ± 3 torr. The loss of gas by permeation through the membrane did not decrease the upstream pressure as the permeation rate was negligible compared with the feed flow rate. Also, at a constant flow rate changing the set point did not affect the pressure fluctuation. In other words, the fluctuation could not be defined as the percentage of the pressure set point without indicating the feed flow rate.

Figure 4.2 shows the upstream pressure fluctuation during a typical experiment. The feed flow rate was changed from 10 cm^3/min to 1 cm^3/min after three hours of operation. As a result of this change, fluctuation decreases significantly as can be seen in the figure. In general, the pressure fluctuation was negligible at all ranges of flow rates. For example, at flow rate of 10 cm^3/min and upstream pressure set point of 5000 torr the fluctuation was ±0.06% from the set point.

4.2. EFFECT OF PRESSURE ON THE PERFORMANCE OF ASYMMETRIC MEMBRANE

The constant pressure (CP) system was used to measure the permeation rates of six single gases through uncoated and silicone-coated dry aromatic polyamide membranes. The gases included helium, hydrogen, oxygen, nitrogen, carbon dioxide, and methane. The operating pressures were 350, 700, 1050, 1400, 1750, 2100 kPa gauge, (≈50, 100, 150, 200, 250, and 300 psig) for the experiments with the uncoated membranes, and 700, 1400, and 2100 kPa gauge,

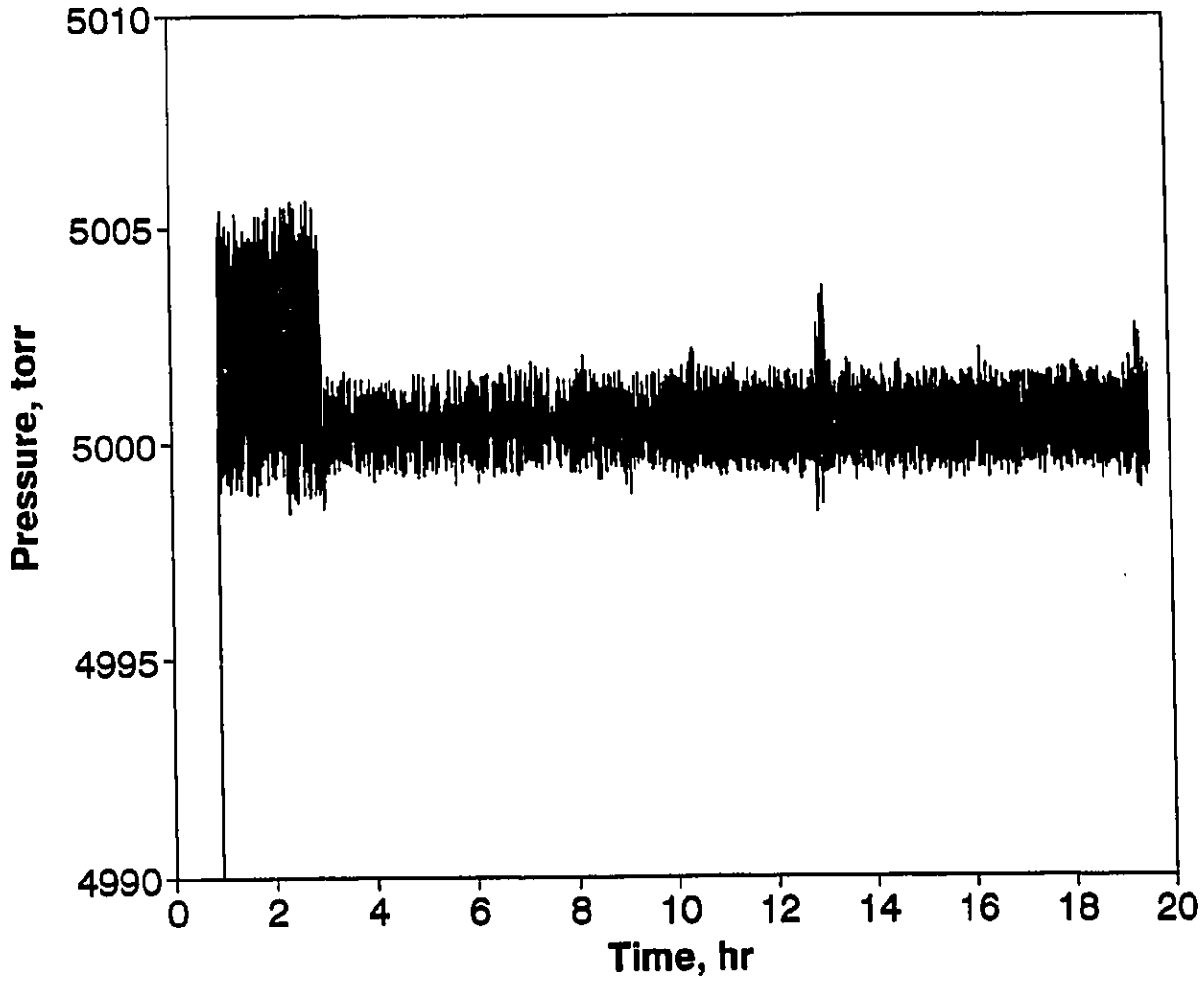

Figure 4.2: Fluctuation of upstream pressure with respect to set point. Feed flow rate: 10 cm^3/min for the first ≈ 3 hours and 1 cm^3/min for the next ≈ 17 hours.

(≈100, 200, and 300 psig) for the silicone-coated membranes. Two uncoated PA membranes, denoted as "a" and "b", prepared under the same conditions were used for all experiments. These two membranes were coated and used for the second part of the experiment. The permeation rates were recorded every 10 - 30 minutes and the steady-state values were used for further calculations. The steady-state was usually reached within 2 to 10 hours depending on the

experimental gas. The permeation rates were corrected for the pressure and temperature to standard temperature and pressure (STP) conditions. The permeability, P/l, of each membrane toward different gases was calculated from the experimental data using Equation 2.15. The overall resistance, R_t, of each membrane toward different gases was obtained from Equation 2.18. The ideal separation factor (ISF), α, was calculated using Equation 2.22 based on helium permeation data as the reference gas. A sample calculation is given in Appendix A.

4.2.1. Uncoated Membrane

The values of permeation rate, Q, permeability, P/l, overall resistance, R_t, and ideal separation factor (ISF), α, of two uncoated PA membranes at different operating pressures are shown in Tables 4.2-a & b and Figures 4.3 to 4.6. The results are discussed below.

Figure 4.3 illustrates the variation of permeation rates, Q, of the experimental gases with the operating pressure for the membranes "a" and "b". The permeation rates of gases increased as a power function of the pressure difference across the membrane: $Q = c\times(\Delta p)^{\beta}$; where "c" and "$\beta$" are constants with values between 1×10^{-3} and 6×10^{-3}, and 1.2 and 1.3 respectively within the range of the operating pressure. The shape of the permeation rate versus pressure curves was similar for both membranes. The variation of the permeation rates with the operating pressure was very close to linearity as constant "β" was close to 1.

The permeabilities, P/l, of gases are shown in Figure 4.4. The permeabilities of helium and hydrogen were higher than the other four gases. The permeability data can be divided into two groups: those for small molecule gases with high permeability including helium and hydrogen

Table 4.2-a: Permeation Rate, Permeability, Overall Resistance, and Ideal Separation Factor Data Pertinent to the Uncoated Aromatic Polyamide Membrane "a".

Δp, kPa	He	H_2	C_2	N_2	CO_2	CH_4
			Permeation rate, Q, mol/s × 10^7			
350	5.80	3.01	0.75	0.67	1.25	0.81
700	13.8	6.25	1.89	1.56	2.99	1.79
1050	24.1	10.7	3.05	2.63	4.60	2.99
1400	33.5	14.7	4.31	3.66	6.25	4.42
1750	44.2	21.9	5.54	4.91	8.79	5.98
2100	61.2	29.9	6.70	6.16	10.7	7.81
			Permeability, P/l, mol/m² s Pa × 10^{10} (GPU)			
350	17.2	8.91	2.23	1.99	3.71	2.41
	(5.14)	(2.67)	(0.67)	(0.59)	(1.11)	(0.72)
700	20.6	9.28	2.81	2.32	4.44	2.65
	(6.15)	(2.77)	(0.84)	(0.69)	(1.33)	(0.79)
1050	23.9	10.6	3.02	2.61	4.55	2.96
	(7.14)	(3.16)	(0.90)	(0.78)	(1.36)	(0.88)
1400	24.9	10.9	3.20	2.72	4.64	3.28
	(7.43)	(3.25)	(0.96)	(0.81)	(1.39)	(0.98)
1750	26.3	13.0	3.29	2.92	5.22	3.55
	(7.85)	(3.88)	(0.98)	(0.87)	(1.56)	(1.06)
2100	30.3	14.8	3.31	3.05	5.30	3.87
	(9.05)	(4.42)	(0.99)	(0.91)	(1.58)	(1.16)
			Overall resistance, R_o, Pa s/mol × 10^{-12}			
350	0.60	1.17	4.67	5.23	2.80	4.31
700	0.51	1.12	3.70	4.48	2.34	3.92
1050	0.44	0.98	3.44	3.99	2.28	3.51
1400	0.42	0.95	3.25	3.82	2.24	3.17
1750	0.40	0.80	3.16	3.56	1.99	2.93
2100	0.34	0.70	3.14	3.41	1.96	2.69
			Ideal separation factor, α, -			
350	1	1.9	7.7	8.7	4.6	7.1
700	1	2.2	7.3	8.9	4.6	7.8
1050	1	2.3	7.9	9.2	5.2	8.1
1400	1	2.3	7.8	9.1	5.4	7.6
1750	1	2.0	8.0	9.0	5.0	7.4
2100	1	2.0	9.1	9.9	5.7	7.8
Average	1	2.1 ± 0.1	8.0 ± 0.4	9.1 ± 0.3	5.1 ± 0.3	7.6 ± 0.3

GPU: cm^3/cm^2 s cmHg × 10^6

Table 4.2-b: Permeation Rate, Permeability, Overall Resistance, and Ideal Separation Factor Data Pertinent to the Uncoated Aromatic Polyamide Membrane "b".

Δp, kPa	He	H_2	O_2	N_2	CO_2	CH_4
			Permeation rate, Q, mol/s × 10^7			
350	5.36	2.95	0.82	0.71	0.85	0.80
700	13.4	6.52	1.88	1.61	1.88	1.79
1050	22.3	12.7	3.05	2.68	2.93	3.04
1400	30.4	18.3	4.29	3.71	4.02	4.46
1750	43.3	26.3	5.54	4.91	5.58	6.25
2100	54.9	34.8	6.70	6.16	7.14	7.90
			Permeability, P/l, mol/m² s Pa × 10^{10} (GPU)			
350	15.9	8.75	2.43	2.12	2.52	2.39
	(4.75)	(2.61)	(0.73)	(0.63)	(0.75)	(0.71)
700	19.9	9.68	2.79	2.39	2.78	2.65
	(5.94)	(2.89)	(0.83)	(0.71)	(0.83)	(0.79)
1050	22.1	12.6	3.02	2.65	2.90	3.01
	(6.60)	(3.76)	(0.90)	(0.79)	(0.87)	(0.90)
1400	22.5	13.6	3.18	2.75	2.98	3.31
	(6.72)	(4.06)	(0.95)	(0.82)	(0.89)	(0.99)
1750	25.7	15.6	3.29	2.92	3.31	3.71
	(7.67)	(4.66)	(0.98)	(0.87)	(0.99)	(1.11)
2100	27.2	17.2	3.31	3.05	3.54	3.91
	(8.12)	(5.14)	(0.99)	(0.91)	(1.06)	(1.17)
			Overall resistance, R_o, Pa s/mol × 10^{-12}			
350	0.65	1.19	4.28	4.90	4.13	4.36
700	0.52	1.07	3.72	4.36	3.73	3.92
1050	0.47	0.82	3.44	3.92	3.58	3.46
1400	0.46	0.76	3.27	3.78	3.48	3.14
1750	0.40	0.66	3.16	3.56	3.14	2.80
2100	0.38	0.60	3.14	3.41	2.94	2.66
			Ideal separation factor, α, -			
350	1	1.8	6.6	7.5	6.3	6.7
700	1	2.1	7.1	8.3	7.1	7.5
1050	1	1.8	7.3	8.3	7.6	7.4
1400	1	1.7	7.1	8.2	7.6	6.8
1750	1	1.6	7.8	8.8	7.8	6.9
2100	1	1.6	8.2	8.9	7.7	6.9
Average	1	1.8 ± 0.1	7.3 ± 0.4	8.3 ± 0.3	7.3 ± 0.4	7.0 ± 0.3

GPU: cm^3/cm^2 s cmHg × 10^6

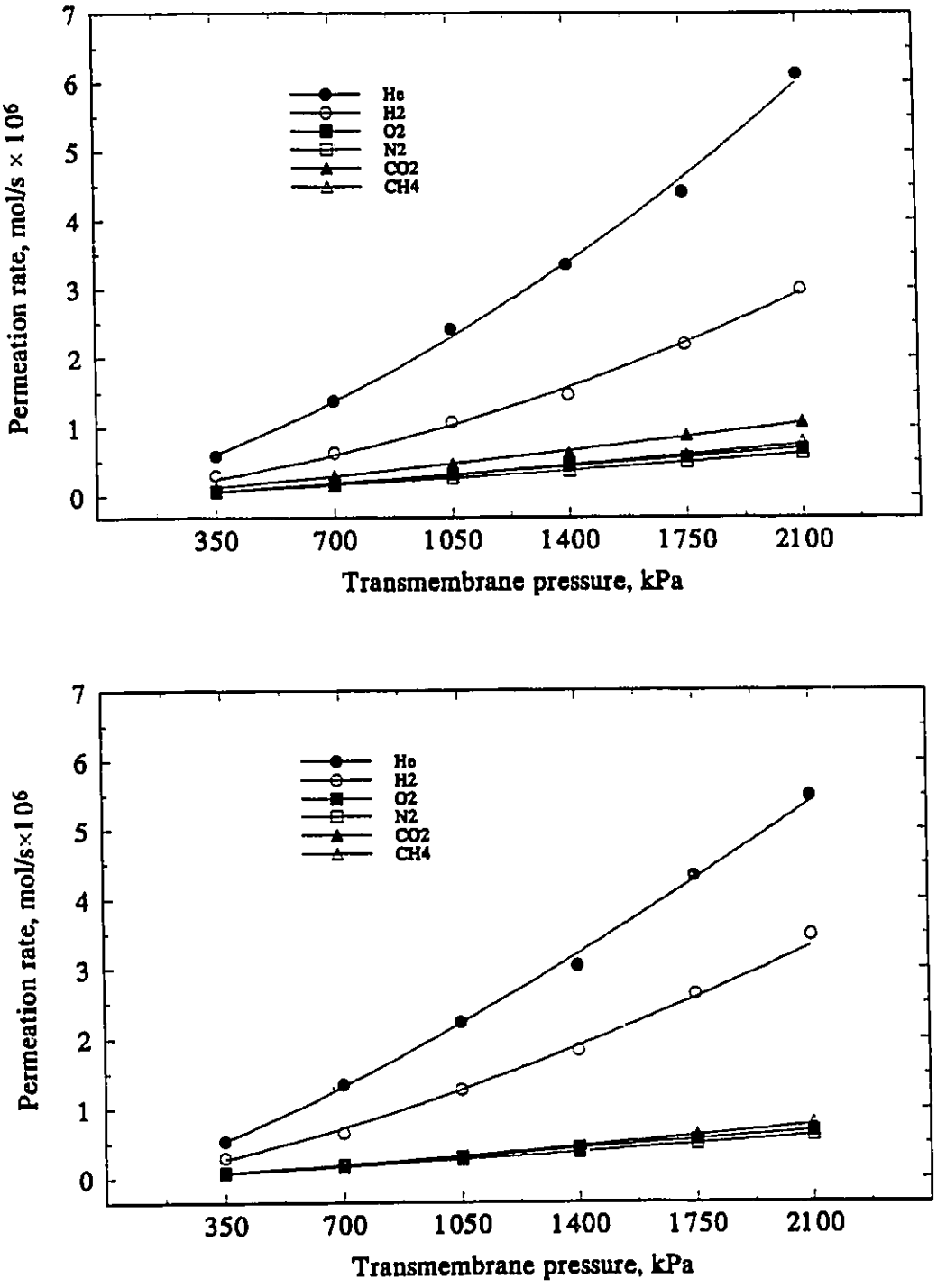

Figure 4.3: Permeation rates of the experimental gases at different operating pressure through the uncoated membrane "a" (top), and the uncoated membrane "b" (bottom).

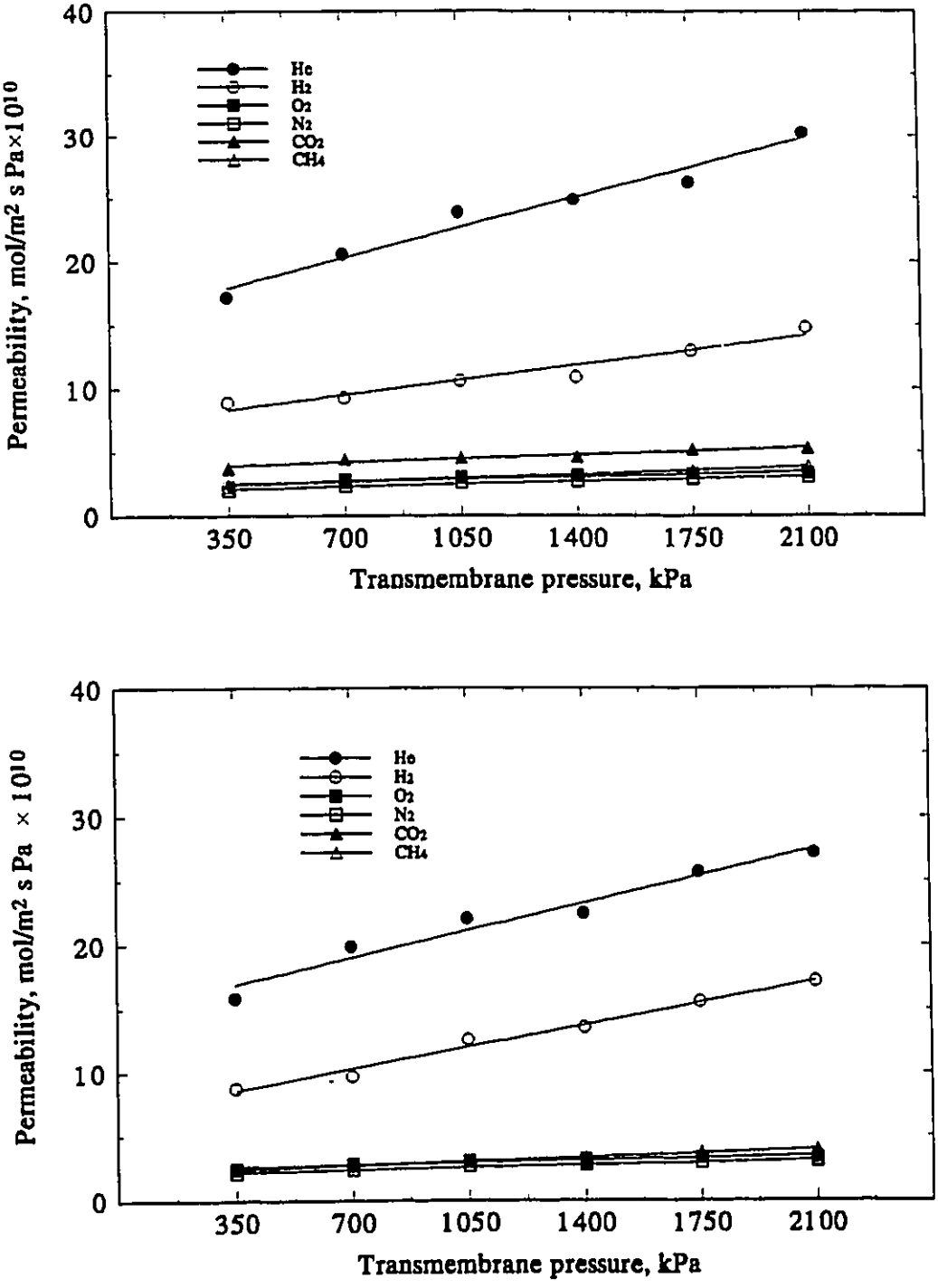

Figure 4.4: Permeabilities of the experimental gases at different operating pressure. Top: uncoated membrane "a". Bottom: uncoated membrane "b".

and those for large molecule gases with low permeabilities including oxygen, nitrogen, carbon dioxide, and methane. The significance of the gap between these two groups is that in practice an uncoated PA membrane can only be used for the separation of small molecule gases from large molecule gases but not for the separation of two small or two large ones. In general, the permeability of gases increased with the operating pressure. The increase was linear within the range of the operating pressure and the slope was greater for gases of higher permeability such as helium and hydrogen. All the permeability curves had non-zero y-intercepts. As it was discussed in Chapter two: Theory, the pressure dependency of the permeability with non-zero y-intercept was indicative of the Knudsen flow mechanism coupled with either laminar or surface flow through the pores.

The same gap between the two distinctive groups was also observed in the overall resistance curves illustrated in Figure 4.5. Both membranes showed lower overall resistance toward the permeation of small gases than the larger ones. The overall resistances decreased with increasing operating pressure as a weak power function of the operating pressure. The shape of the curves suggested that the overall resistance became independent of the operating pressure at higher pressures.

The ideal separation factors (ISF) of the two uncoated membranes are illustrated in Figure 4.6. All the ISFs are reported with respect to helium as the reference gas. The ISF between any other two gas pairs can be obtained by dividing their reported ISFs with respect to helium, e.g., the separation factor for CO_2/CH_4 system at 700 kPa is 1.7 for membrane "a". In general, the ideal separation factors were small, which indicates that a very small and negligible separation was achievable between the experimental gases using an uncoated PA membrane. It is important

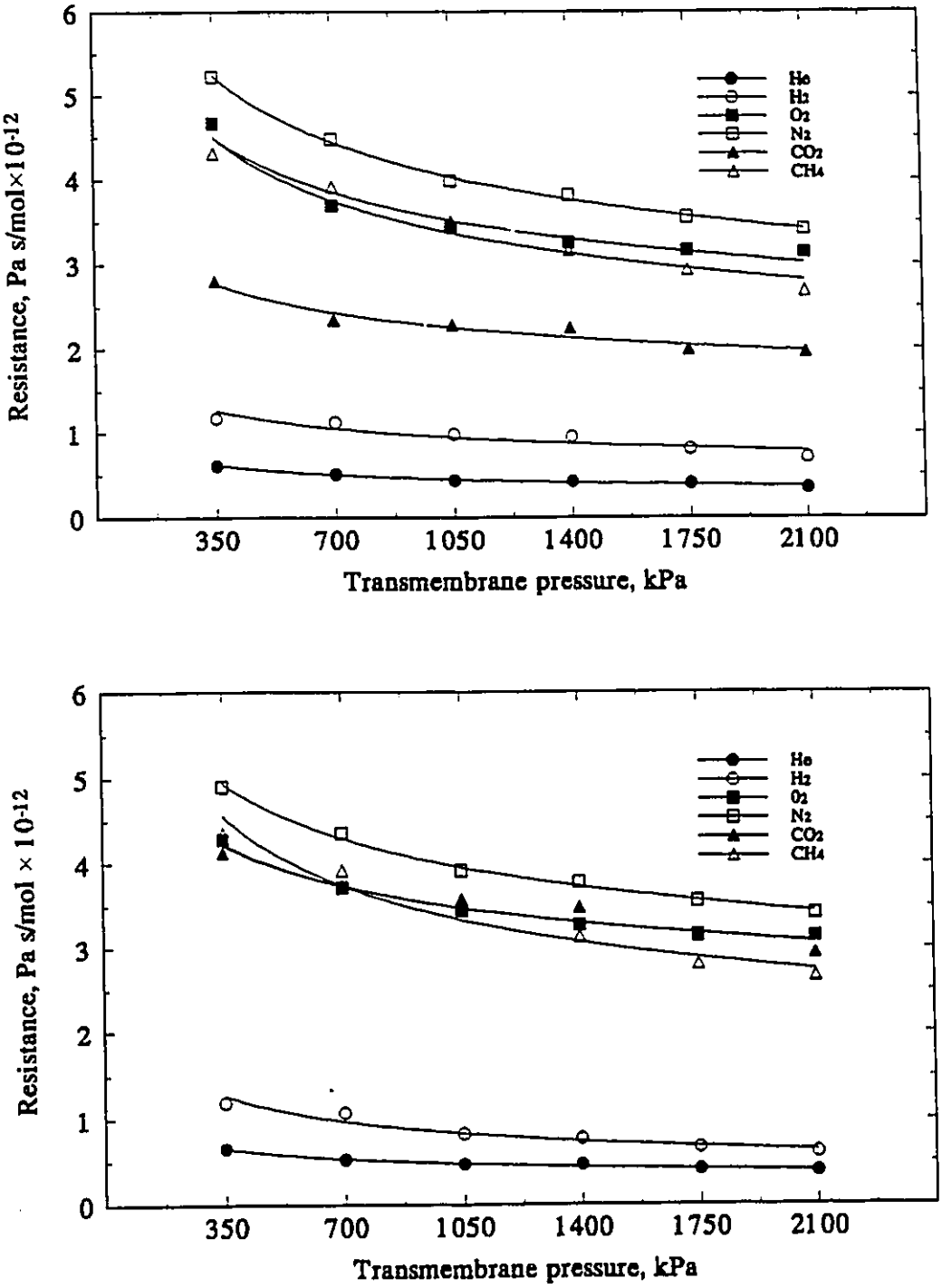

Figure 4.5: Overall resistances of the uncoated membrane "a" (top), and the uncoated membrane "b" (bottom) toward the permeation of the experimental gases.

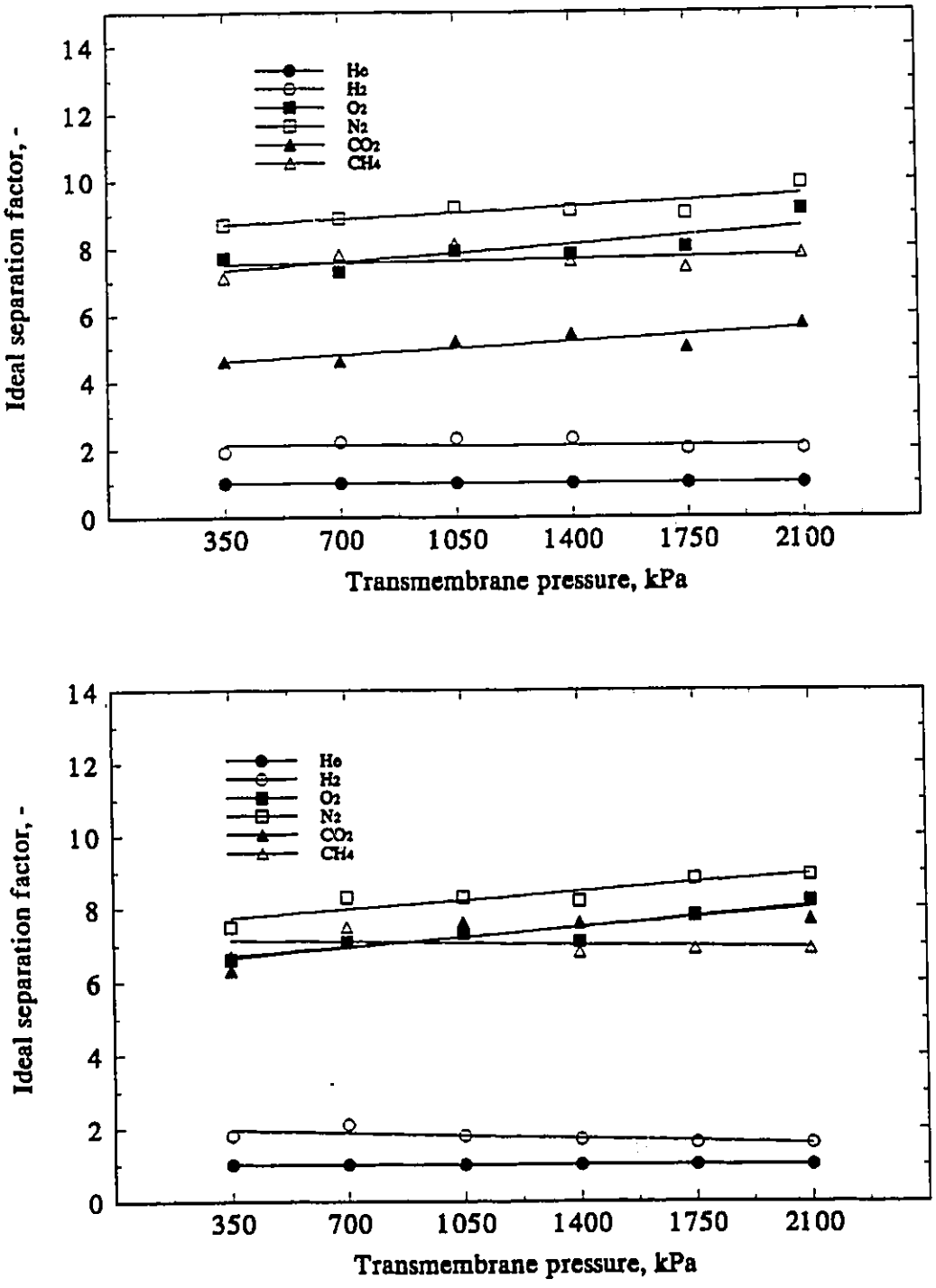

Figure 4.6: Ideal separation factor of the uncoated membranes "a" (top), and "b" (bottom) toward the experimental gases with respect to helium gas.

to remember that the further the ISF is from unity, either smaller or larger, the better separation may be achieved. A weak tendency to increase with the operating pressure was observed in the ISFs of oxygen, nitrogen and carbon dioxide, but they remained constant for other three gases. However, no single correlation could define the increasing tendency. Therefore, it was assumed that the variation in the ISFs was random and the average of the ideal separation factors was obtained over the entire range of the transmembrane pressure and used for further calculations. The averages were accurate within 3% and 6% of the experimental data.

4.2.2. Coated Membrane

Tables 4.3-a & b and Figures 4.7 to 4.10 show the permeation rate, Q, permeability, P/l, overall resistance, R_{tc}, and ideal separation factors, α_{tc}, for the PA membranes after being coated by silicone rubber.

The permeation rates of the experimental gases are shown in Figure 4.7. The permeation of nitrogen and methane practically stopped after silicone-coating. It means that, the permeation of these two gases could not be detected by the most accurate bubble flow meter. Therefore, the permeation rates of these gases were recorded as less than the lowest detectable limit of the apparatus, i.e., <5 μl/min ($<3\times10^{-9}$ mol/s). All further calculations were performed accordingly. Compared with the uncoated membrane, the permeation rates decreased for all gases after silicone-coating. However, the magnitude of the reduction differed from one gas to another. The decrease in the permeation rates was around 50%, 75%, 80%, 95%, 100%, and 100% for helium, hydrogen, carbon dioxide, oxygen, nitrogen and methane respectively. The pressure dependency

Table 4.3-a: Permeation Rate, Permeability, Overall Resistance, and Ideal Separation Factor Data Pertinent to the Silicone-Coated Aromatic Polyamide Membrane "a".

Δp, kPa	He	H_2	O_2	N_2	CO_2	CH_4
			Permeation rate, Q, mol/s × 10^7			
700	6.70	1.65	0.14	<0.03	0.67	<0.03
1400	17.4	4.46	0.30	<0.03	1.38	<0.03
2100	30.8	7.59	0.43	<0.03	2.05	<0.03
			Permeability, P/l, mol/m² s Pa × 10^{10} (GPU)			
700	9.94	2.45	0.21	<0.05	0.99	<0.05
	(2.97)	(0.73)	(0.06)	(<0.016)	(0.30)	(<0.016)
1400	12.9	3.31	0.22	<0.03	1.03	<0.03
	(3.85)	(0.99)	(0.07)	(<0.008)	(0.31)	(<0.008)
2100	15.2	3.76	0.21	<0.02	1.02	<0.02
	(4.54)	(1.12)	(0.06)	(<0.005)	(0.30)	(<0.005)
			Overall resistance, R_o, Pa s/mol × 10^{-12}			
700	1.05	4.24	50.6	>200[1]	10.5	>200[1]
1400	0.80	3.14	46.1	>390[1]	10.1	>390[1]
2100	0.68	2.77	48.5	>590[1]	10.2	>590[1]
			Ideal separation factor, α, -			
700	1	4.0	48	>190[2]	10	>190[2]
1400	1	3.9	57	>490[2]	13	>490[2]
2100	1	4.1	71	>860[2]	15	>860[2]

GPU: cm^3/cm^2 s cmHg × 10^6

1. The best estimation for the overall resistance of the membrane toward the permeation of nitrogen and methane is >590×10^{12} Pa s/mol at all operating pressures. For explanation see Section 4.3.

2. The best estimation for the ideal separation factor of nitrogen and methane is >860 at all operating pressures. For explanation see Section 4.2.

Table 4.3-b: Permeation Rate, Permeability, Overall Resistance, and Ideal Separation Factor Data Pertinent to the Silicone-Coated Aromatic Polyamide Membrane "b".

Δp, kPa	He	H_2	O_2	N_2	CO_2	CH_4
			Permeation rate, Q, mol/s × 10^7			
700	6.25	1.65	0.09	<0.03	0.40	<0.03
1400	15.2	4.46	0.21	<0.03	0.80	<0.03
2100	25.9	8.93	0.29	<0.03	1.43	<0.03
			Permeability, P/l, mol/m² s Pa × 10^{10} (GPU)			
700	9.28 (2.17)	2.45 (0.73)	0.14 (0.04)	<0.05 (<0.016)	0.60 (0.18)	<0.05 (<0.016)
1400	11.3 (3.37)	3.31 (0.99)	0.16 (0.05)	<0.03 (<0.008)	0.60 (0.18)	<0.03 (<0.008)
2100	12.8 (3.82)	4.42 (1.32)	0.14 (0.04)	<0.02 (<0.005)	0.70 (0.21)	<0.02 (<0.005)
			Overall resistance, R_o, Pa s/mol × 10^{-12}			
700	1.12	4.24	74.7	>200[1]	17.4	>200[1]
1400	0.92	3.14	65.3	>390[1]	17.4	>390[1]
2100	0.81	2.35	72.4	>590[1]	14.7	>590[1]
			Ideal separation factor, α, -			
700	1	3.8	67	>175[2]	16	>175[2]
1400	1	3.4	71	>430[2]	19	>430[2]
2100	1	2.9	89	>730[2]	18	>730[2]

GPU: cm^3/cm^2 s cmHg × 10^6

1. The best estimation for the overall resistance of the membrane toward the permeation of nitrogen and methane is >590×10^{12} Pa s/mol at all operating pressures. For explanation see Section 4.3.

2. The best estimation for the ideal separation factor of nitrogen and methane is >730 at all operating pressures. For explanation see Section 4.2.

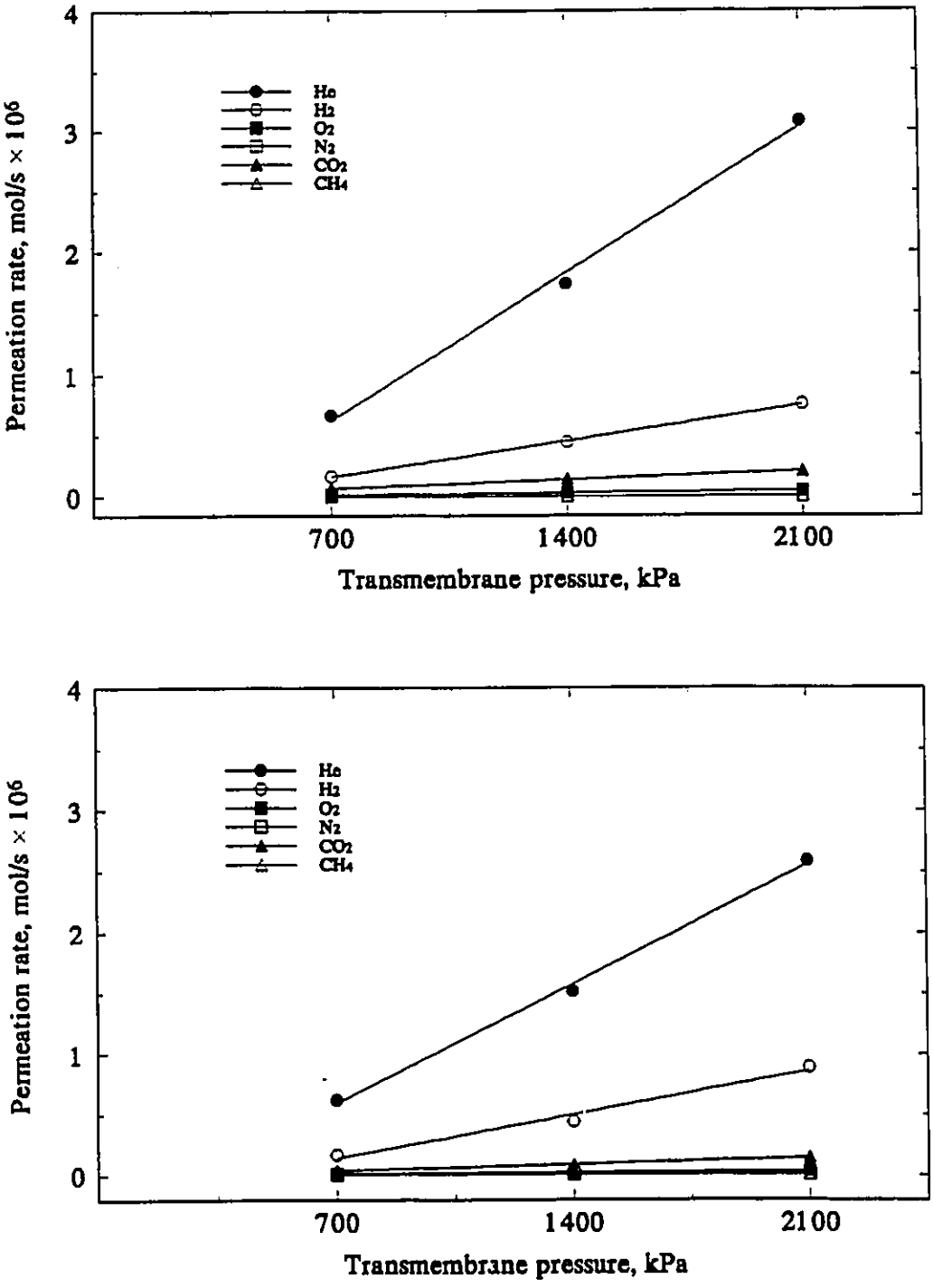

Figure 4.7: Permeation rates of the experimental gases through the coated membranes. Top: membrane "a". Bottom: membrane "b".

of the permeation rates was still obvious after coating, i.e., the permeation rates increased with increasing operating pressure. The variation was linear within the range of the operating pressure.

Figure 4.8 shows the permeability of gases through the coated membranes. The pressure dependency of the permeability was observed for helium and hydrogen for both coated membranes as can be seen in the figure. The permeability curves of these two gases had non-zero y-intercept. The non-zero y-intercept indicates that the Knudsen mechanism is still contributing to the flow of these two gases through the coated membranes. This phenomenon can be explained by considering the fact that the pores under the polymer matrix are contributing to the resistance and their resistance has been included in the matrix resistance, R_2. If gas permeation occurs in such pores by Knudsen mechanism, matrix resistance as well as the overall resistance decrease with an increase in the feed pressure. As a result the membrane permeability increases and the increase is more pronounced for smaller gases such as helium and hydrogen.

Comparison of the data in Figure 4.4 and 4.8 indicates that the permeability of gases through coated membranes was less than that of the uncoated membranes. The decrease in permeability was more pronounced for gases of larger kinetic diameter. As a result, the order of the permeability through the coated membranes became as follows:

helium > hydrogen > carbon dioxide > oxygen > nitrogen = methane = non-detectable.

The above order is precisely the reverse order of the kinetic diameter of the gas molecules (Å) [Breck, 1974].

helium (2.6) < hydrogen (2.89) < carbon dioxide (3.3) < oxygen (3.46) < nitrogen (3.64) < methane (3.8).

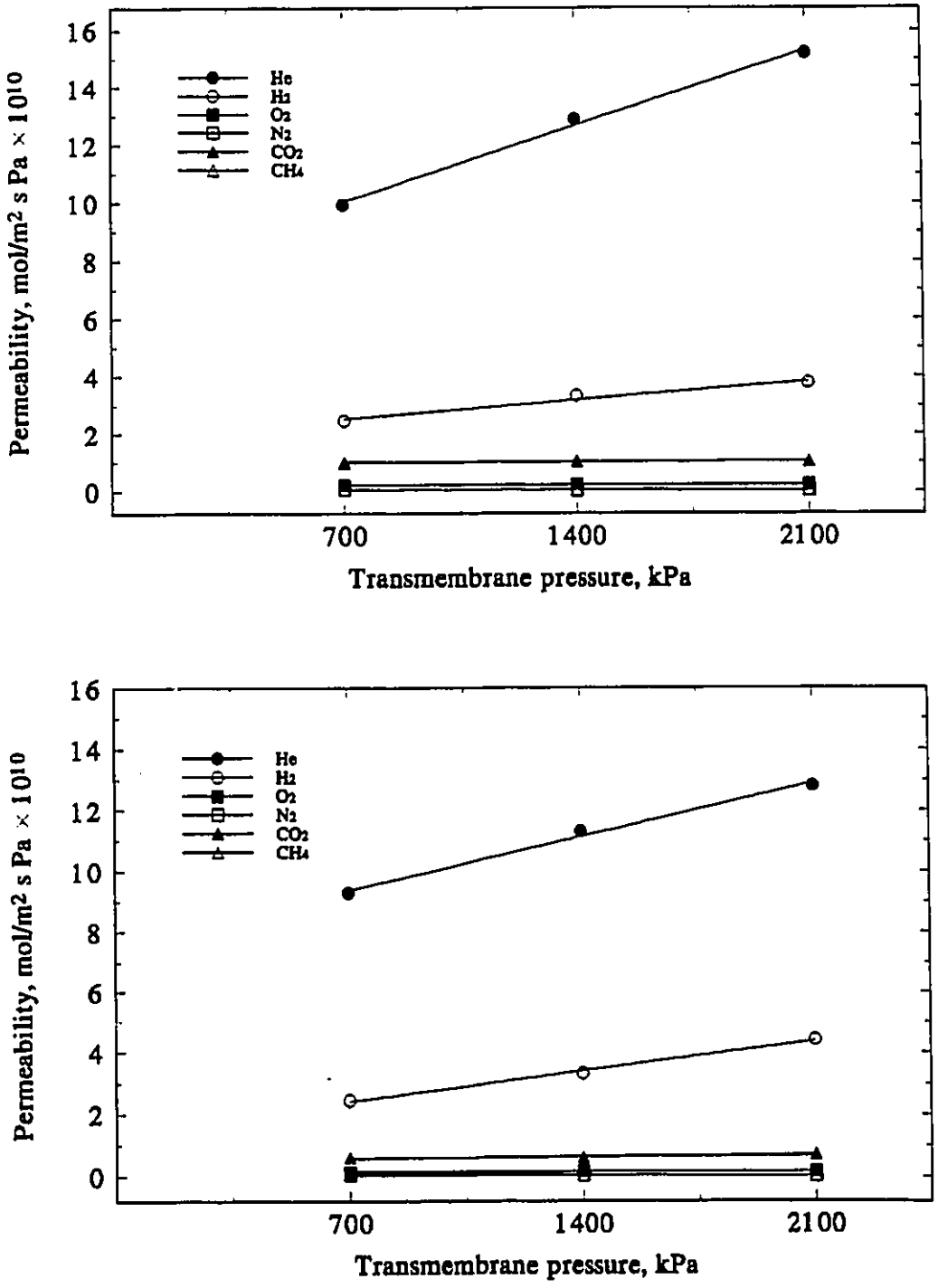

Figure 4.8: Permeabilities of the experimental gases through the coated membranes. Top: membrane "a". Bottom: membrane "b".

The overall resistances of the silicone-coated PA membranes are shown in Figure 4.9. The silicone-coating did not have a significant effect on the overall resistance of the membranes toward the permeation of helium, hydrogen, and carbon dioxide. These resistances remained within the same order of magnitude as for the uncoated membrane. The overall resistances of the silicone-coated membranes toward oxygen increased by one order of magnitude, and showed a tremendous increase for nitrogen and methane.

As shown in Tables 4.3-a & b, a slight decrease in the overall resistances of helium and hydrogen was observed as the operating pressure increased. This pressure dependency was not so obvious for oxygen and carbon dioxide. Finally, in case of nitrogen and methane, since the overall resistances were determined by approximation, the effect of pressure on the overall resistances of these gases was unknown. The cases of these two gases will be discussed later.

As the permeation of the gases decreased after coating, the ideal separation factors increased considerably. The ISFs of the silicone-coated PA membranes are shown graphically in Figure 4.10. The ISFs of nitrogen and methane approached infinity and could not be determined accurately. Therefore, the maximum estimated values of ISF for these two gases are shown in Figure 4.10. A small increase in the ISFs with the operating pressure was observed for oxygen and carbon dioxide.

The high ideal separation factors suggest that very high separations are achievable between N_2 or CH_4 and any other gases (α>860), i.e., theoretically pure gases may be produced from a mixture of N_2 or CH_4 and any other gas. Also oxygen may be separated from helium ($\alpha_{He/O2}$=70) and hydrogen ($\alpha_{H2/O2}$=17) with high purity. For example, a mixture of 50% hydrogen in oxygen results in a mixture of approximately 95% hydrogen in the permeate. A comparison

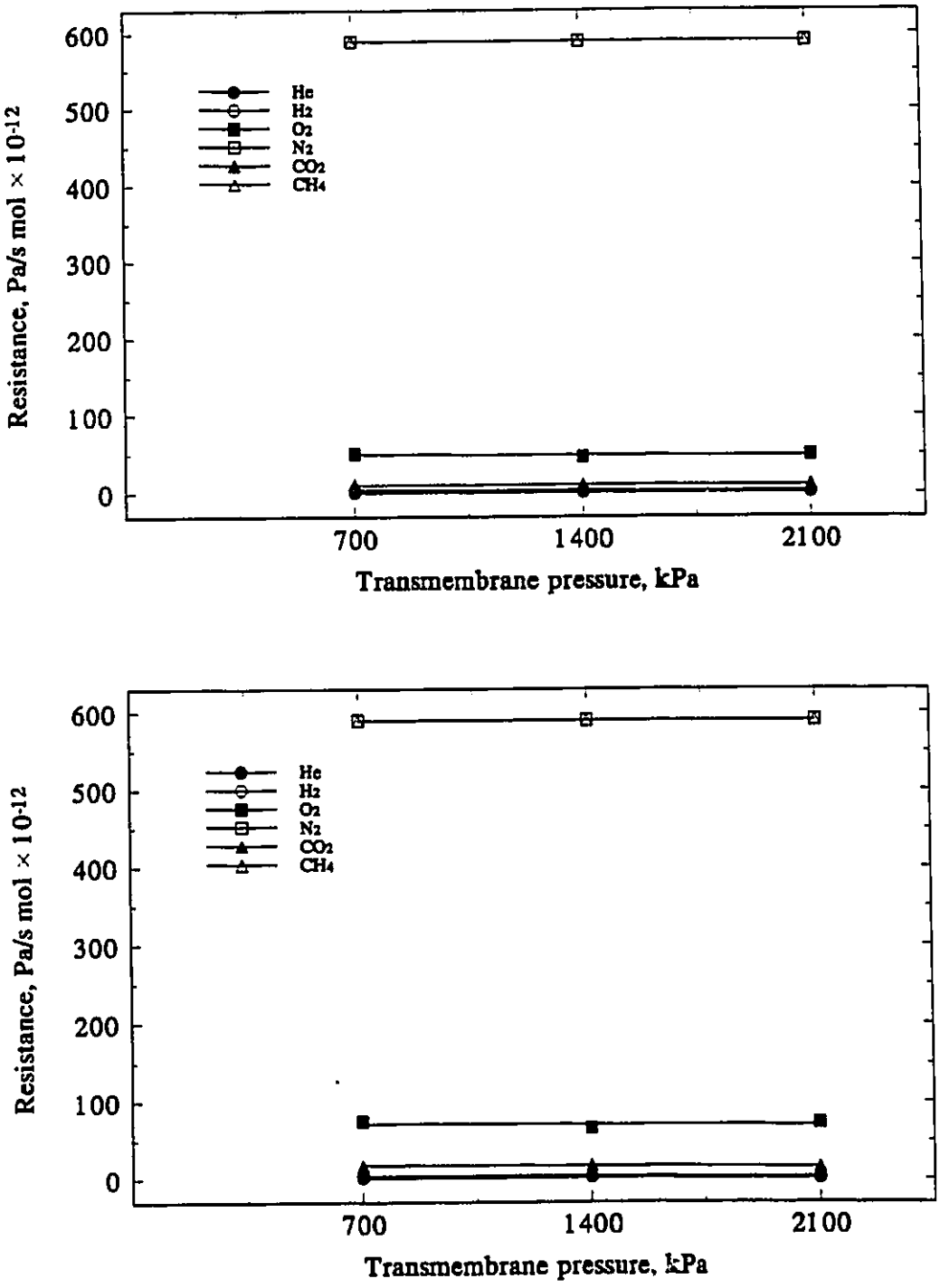

Figure 4.9: Overall resistances of the coated membranes "a" (top), and "b" (bottom) toward the permeation of the experimental gases.

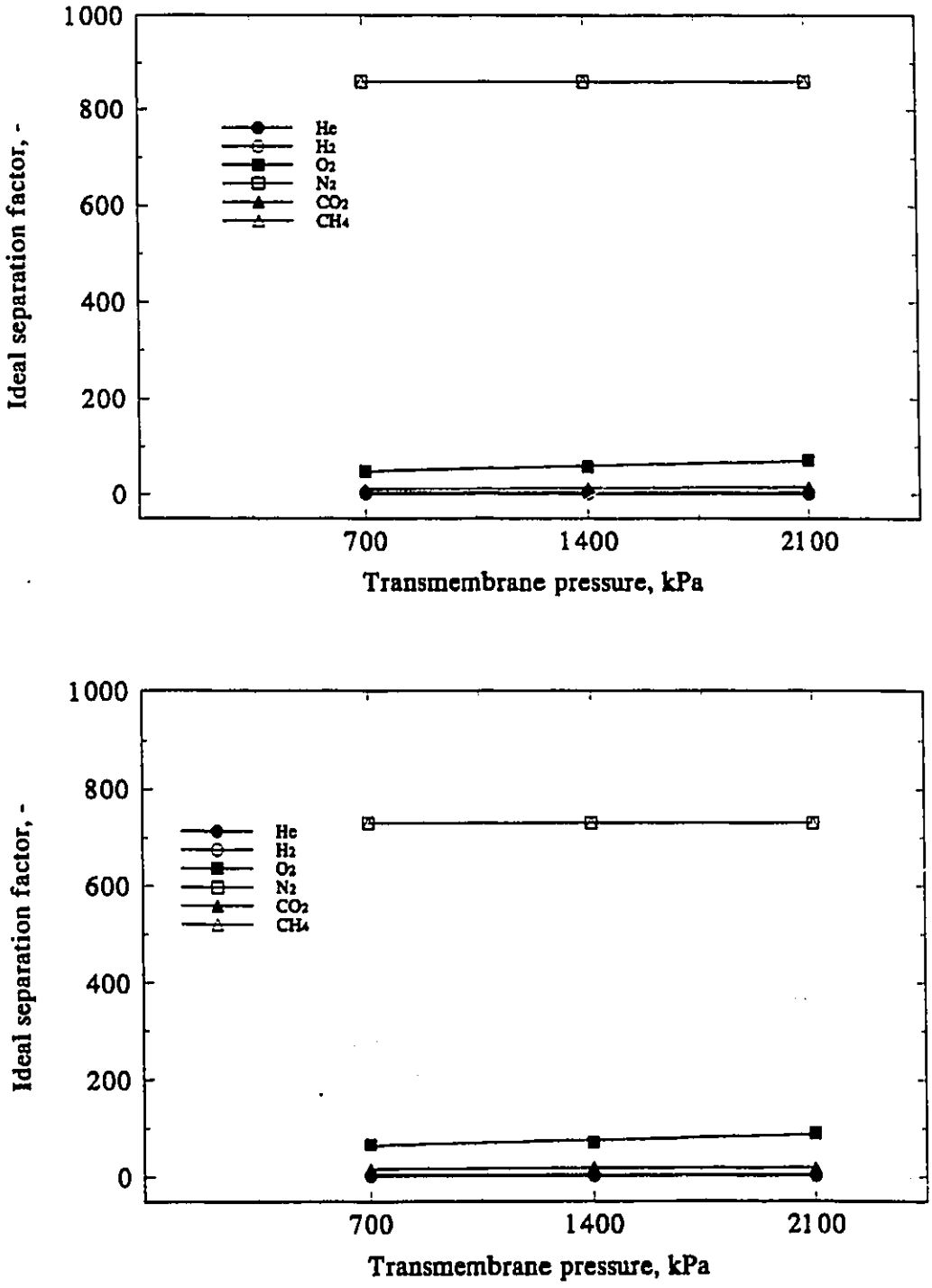

Figure 4.10: Ideal separation factor of the coated membranes "a" (top), and "b" (bottom) toward the experimental gases.

between the ideal separation factors before and after coating for membrane "a" at 700 kPa is shown in Figure 4.11.

As mentioned earlier, the permeation of nitrogen and methane was non-detectable and all the calculations were performed based on the lowest measurable limit of the bubble flow meter. Since the results obtained by the above method, in most cases, were misleading some discussions are in order in this respect. The permeability data in Tables 4.3-a & b and Figure 4.8 show that the permeability of helium, hydrogen, oxygen, and carbon dioxide increased or remained constant with an increase in the operating pressure. Assuming that the same tendency applies to nitrogen and methane, it is expected that the permeability of these gases at 700 kPa and 1400 kPa be equal or smaller than their permeability at 2100 kPa, i.e., a value of $P/l < 2\times10^{-12}$ mol/m^2 s Pa for both gases at all pressures seems closer to the real answer. Correspondingly, the overall resistance of membranes "a" and "b" toward these gases should be $R_t > 590\times10^{12}$ Pa s/mol at all pressures. Similarly, the ISF values of $\alpha > 860$ for membrane "a" and $\alpha > 730$ for membrane "b" at all pressures seem to be more appropriate. The above discussed values are shown as footnotes in Table 4.3-a & b and are reflected in Figures 4.8 to 4.11.

4.2.3. Measurement of the Permeation Rate of the Low Permeable Gases Through Silicone-Coated Asymmetric Membranes Using Constant Volume System

It was discussed in the previous section that the permeation rates of nitrogen and methane through silicone-coated asymmetric membranes were below the detectable limit of the constant pressure system and could not be determined accurately. The experiments were repeated using

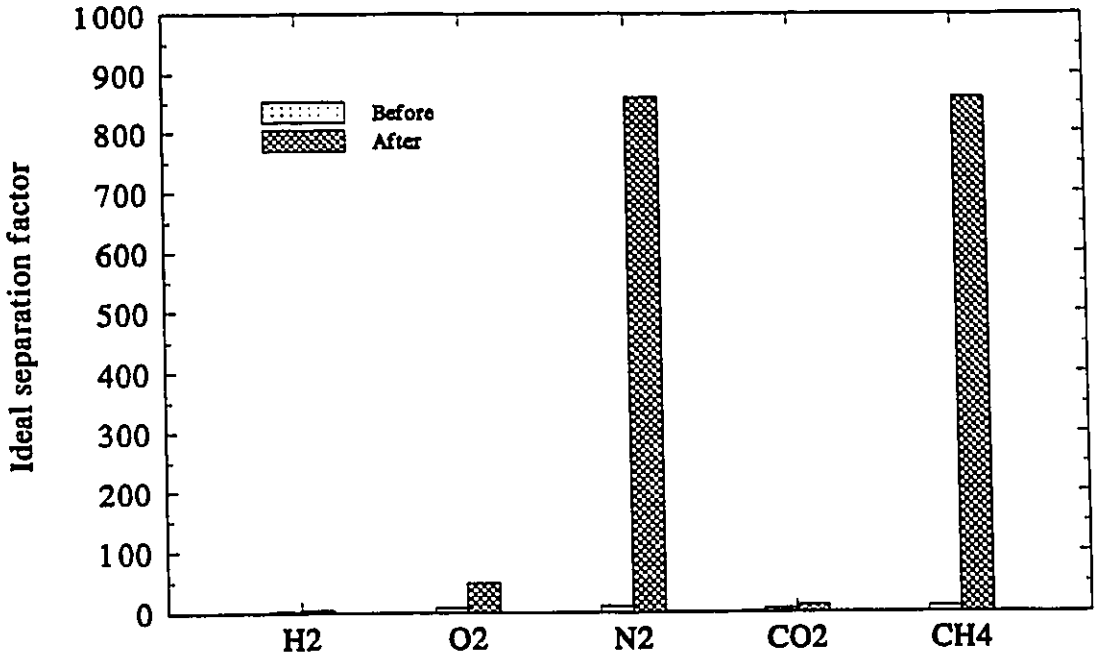

Figure 4.11: Comparison of the ideal separation factors before and after coating for membrane "a" at operating pressure of 700 kPa.

the constant volume system which allowed an accurate measurement of the permeation rates of these two gases. The CV system was also used to measure the permeation rates of oxygen and carbon dioxide in addition to nitrogen and methane. The permeation rates of helium and hydrogen were higher than the detectable limit of the CV system and could not be determined. Note that the results obtained from these two systems are not fully compatible. That is because, the experimental conditions are not similar in the two systems with respect to the downstream pressure. However, the CV results give a better insight for the analysis of data particularly regarding the ideal separation factors of O_2/N_2 and CO_2/CH_4 systems. Air separation experiments

were also performed using asymmetric membranes installed in the CV system which will be discussed later. The membrane preparation procedure and the experimental conditions were described in Sections 3.1.2 and 3.2.6, respectively.

The experiments were performed using two silicone-coated asymmetric polyamide membranes. One was the membrane denoted as "a" in the constant pressure system, and the other was a new membrane prepared under the same conditions as membrane "a". The new membrane was denoted as membrane "c". The membrane denoted as "b" in the CP system showed a high leak rate when installed in the constant volume system and, therefore, was not used in the present tests. The permeation rate, Q, permeability, P/l, and ideal separation factor, α, of the four experimental gases are shown in Table 4.4. In addition, Figure 4.12 illustrates the variation of the downstream pressure and the permeation rates for nitrogen and methane obtained using the constant volume system. Similar graphs were obtained for O_2 and CO_2.

Using the experimental data, the ideal separation factor for O_2/N_2 was calculated to be 12.0 and 12.3 for the membranes "a" and "c", respectively. The ISF values for CO_2/CH_4 system were 110 and 105 for the membranes "a" and "c", respectively. These ISF values are among the highest values reported in the literature. Tables 4.5-a & b and Figure 4.13 compare typical literature ISF data with the results obtained in this study for O_2/N_2 and CO_2/CH_4 systems. The tables include data from both asymmetric and homogeneous membranes. According to Tables 4.5-a & b and Figure 4.13 the ideal separation factors achieved in this study were among the highest reported in the literature. The permeability of gases through the membranes, on the other hand, remained within the lower limit of the literature data. The permeability of gases through asymmetric polyamide membrane must be improved by one to two orders of magnitude for the

Table 4.4: Permeation Rate, Q, Permeability, P/l, and Ideal Separation Factor, ISF, Data of Oxygen, Nitrogen, Carbon Dioxide, and Methane Through Silicone-Coated Aromatic Polyamide Membranes Using the Constant Volume System.

	Membrane "a"			
	O_2	N_2	CO_2	CH_4
Q, µl/min	5.15	0.43	22.0	0.20
Q, $cm^3/s \times 10^{-5}$	8.58	0.72	36.7	0.33
Q, $mol/s \times 10^{-9}$	3.83	0.32	16.4	0.15
P/l, $mol/m^2\ s\ Pa \times 10^{-12}$	5.92	0.49	25.3	0.23
P/l, $cm^3/cm^2\ s\ cmHg \times 10^{-8}$	1.78	0.15	7.62	0.0693
ISF	$\alpha_{O2/N2} = 12.0$		$\alpha_{CO2/CH4} = 110$	
	Membrane "c"			
Q, µl/min	3.47	0.283	11.1	0.106
Q, $cm^3/s \times 10^{-5}$	5.78	0.471	18.4	0.183
Q, $mol/s \times 10^{-9}$	2.51	0.21	8.26	0.82
P/l, $mol/m^2\ s\ Pa \times 10^{-12}$	3.87	0.32	12.8	0.13
P/l, $cm^3/cm^2\ s\ cmHg \times 10^{-8}$	1.20	0.098	3.83	0.038
ISF	$\alpha_{O2/N2} = 12.3$		$\alpha_{CO2/CH4} = 105$	

membrane to become comparable with other membranes. This matter will be discussed later in more detail.

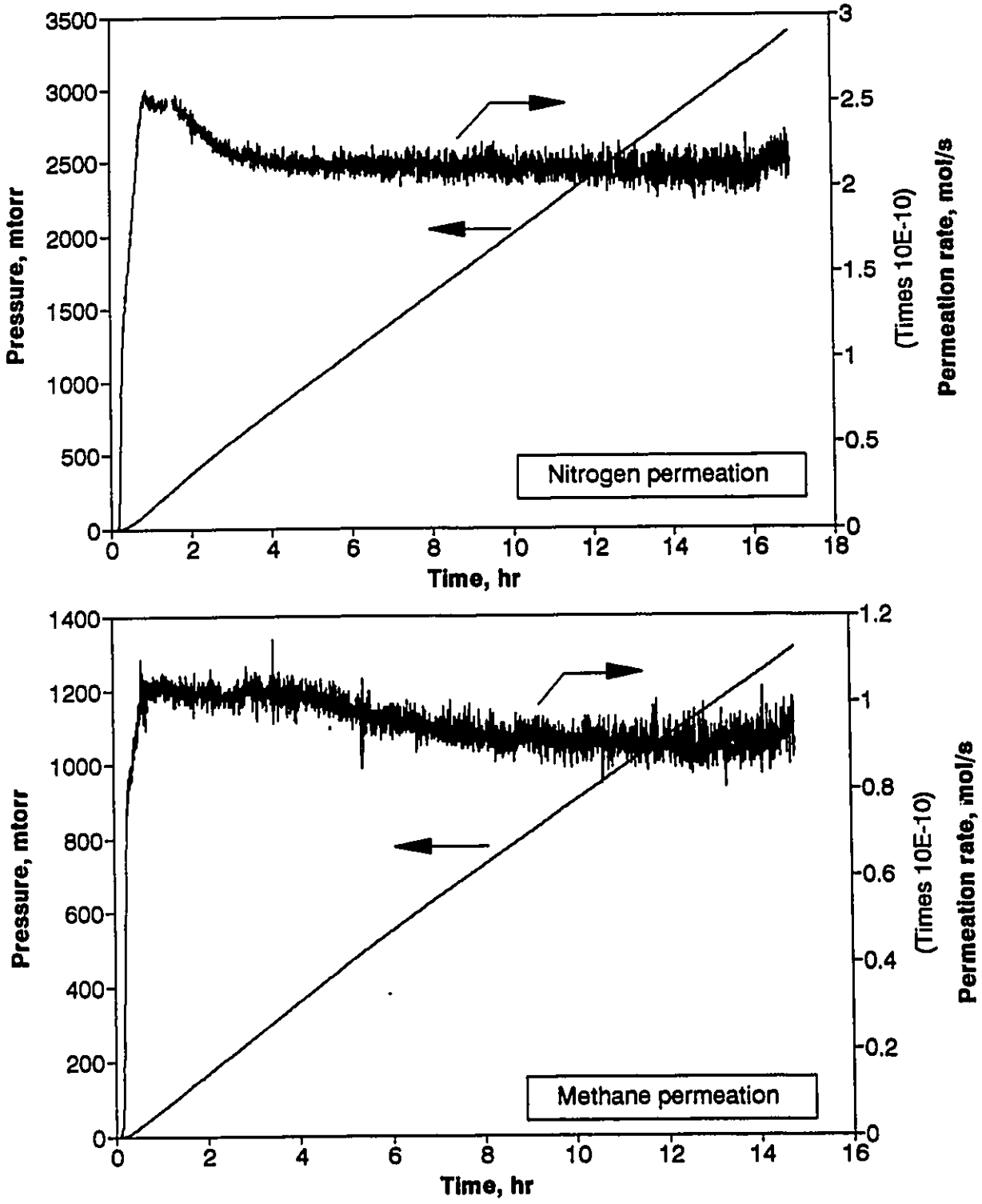

Figure 4.12: Variation of the permeation rate and the downstream pressure rise with time of nitrogen (top) and methane (bottom) measured by the constant volume system.

Table 4.5-a: Comparison of the Permeability, permeability coefficient, and Ideal Separation Factor of Silicone-Coated Aromatic Polyamide Membrane and Typical Asymmetric and Homogeneous Membranes for O_2/N_2 system.

Asymmetric membranes				
	Permeability, P/l, GPU			
Polymer	O_2	N_2	α	Reference
PA	0.0178	0.0015	12.0	Present study
PA	0.0116	0.00096	12.3	Present study
PS	9.62	1.48	6.5	[Mohr, 1991]
PS	38.5	9.9	3.9	[Mercea, 1994]
PI	10.6	1.80	5.89	[Mercea, 1994]
CA	13.8	2.96	4.66	[Mercea, 1994]
Homogeneous membranes				
	Permeability coefficient, Barrer			
PA	0.0376	0.00408	9.21	Present study
Natural rubber	24	8.7	2.76	[Bixler, 1971]
Silicone rubber	933	440	2.12	[Stern, 1987]
PS	1.4	0.25	5.6	[Mehatti, 1991]
PES	0.629	0.0974	6.5	[Süer, 1994]
PI	0.61-7.8	0.10-1.25	6.1-6.2	[Koros, 1989b]
PI	1.8	0.26	6.9	[Coleman, 1990]
PI	0.13	0.018	7.2	[Mi, 1993]
CA	0.82	0.15	5.5	[Puleo, 1989]
PAn	0.100	0.0067	14.9	[Kurwabata, 1994]
PC	1.4-32	0.19-7.8	7.5-4.1	[Koros, 1989a]
PEC	1.0-1.4		8.0-6.7	[Zolandz, 1992]
PEI (Ultem®)	0.41	0.051	8.0	[Barbari, 1989]
TBBA	0.8-1.87		6.9-6.4	[Zolandz, 1992]
TCBA	0.8-1.45		6.1-5.4	[Zolandz, 1992]
TMBA	1.3-3.9		6.0-5.0	[Zolandz, 1992]
PU	6.07	1.19	5.1	[Hsieh, 1991]
PU-PSt	1.2	0.2	6.0	[Xuesong, 1994]
PP	0.14	0.013	10.7	[Xuesong, 1994]

GPU: gas permeation unit, $cm^3(STP)/cm^2\ s\ cmHg \times 10^{-6}$;
Barrer: $cm^3(STP)\ cm/cm^2\ s\ cmHg \times 10^{-10}$;
PA: polyamide, PS: polysulfone, PI: polyimide, CA: cellulose acetate, PES: polyethersulfone, PAn: polyaniline, PC: polycarbonate, PEC: polyestercarbonate, PEI: polyetherimide, TBBA: tetrabromobisphenol, TCBA: tetrachlorobisphenol, TMBA: tetramethylbisphenol, PU: polyurethane, PSt: polystyrene, PP: polypyrrolone.

Table 4.5-b: Comparison of the Permeability, permeability coefficient, and Ideal Separation Factor of Silicone-Coated Aromatic Polyamide Membrane and Typical Asymmetric and Homogeneous Membranes for CO_2/CH_4 system.

Asymmetric membranes				
	Permeability, P/l, GPU			
Polymer	CO_2	CH_4	α	Reference
PA	0.0762	0.00693	110	Present study
PA	0.0383	0.0038	105	Present study
PS	47.0	1.47	32	[Mohr, 1991]
PVTMS	0.49	0.15	3.3	[Uchytil, 1992]
CA	1.37	0.054	196	[Chen, 1989]
CA	48.9	0.74	66	[Chen, 1989]
Homogeneous membranes				
	Permeability coefficient, Barrer			
PA	0.15	0.00194	75.5	Present study
Natural rubber	134	28.5	4.7	[Bixler, 1971]
Silicone rubber	4553	1351	3.37	[Stern, 1987]
PS	5.6	0.254	22	[Mehatti, 1991]
PS	3	0.065	46	[Kamps, 1992]
PES	2.9	0.048	60	[Kamps, 1992]
PI	0.15-32	0.002-0.63	71.6-51.1	[Koros, 1989b]
PI	0.55-22	0.008-0.5	33-64	[Stern, 1989]
PI	5.13-63.9	0.080-1.6	40-64	[Coleman, 1990]
PI	1.46-44.9	0.021-0.738	41-74	[Matsumoto, 1993]
PEI (Ultem®)	1.33	0.036	36.9	[Barbari, 1989]
CA	9	0.426	21	[Spillmann, 1989]
CA	4.75	0.148	32	[Puleo, 1989]
PAn	0.5	0.009	54	[Kuwabata, 1994]
PES-Zeolite	2.8	0.1	28	[Chiou, 1987]
TBBA	3.6-7.0		35-29	[Zolandz, 1992]
TCBA	2.6-5.5		32-25	[Zolandz, 1992]
TMBA	5.7-16.3		29-24	[Zolandz, 1992]
PC	4.2-111	0.12-4.62	34-24	[Koros, 1989a]
PEC	3.55-5.26		40-33	[Zolandz, 1992]

GPU: gas permeation unit, $cm^3(STP)/cm^2$ s cmHg $\times 10^{-6}$;
Barrer: $cm^3(STP)$ cm/cm^2 s cmHg $\times 10^{-10}$;
PA: polyamide, PS: polysulfone, PVTMS: polyvinyltrimethylsilane, CA: cellulose acetate, PES: polyethersulfone, PI: polyimide, PEI: polyetherimide, PAn: polyaniline, TBBA: tetrabromobisphenol, TCBA: tetrachlorobisphenol, TMBA: tetramethylbisphenol, PC: polycarbonate, PEC: polyestercarbonate.

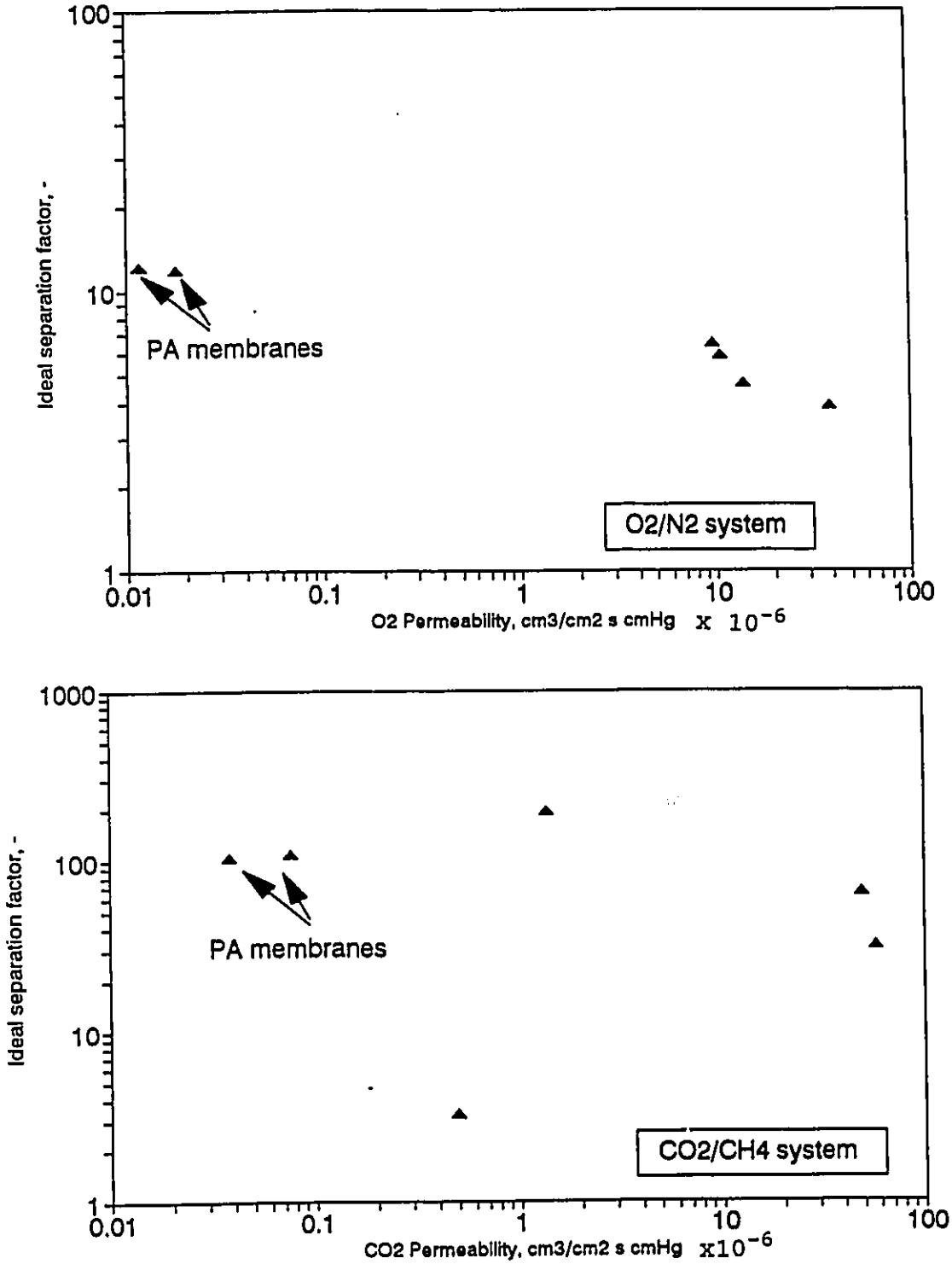

Figure 4.13: Comparison of the permeability and separation factors of PA membranes with other membranes found in the literature. Top: O_2/N_2 system. Bottom: CO_2/CH_4 system.

4.3. DETERMINATION OF THE LOCAL RESISTANCES AND THE EFFECT OF COATING

The local resistances were calculated using Equations 2.27 and 2.28, and 2.32 to 2.36. These equations were solved according to the procedure discussed in Section 2.3.3. The quantities involved in the above equations can be found as follows:

i) The overall resistances of uncoated membranes, $R_{t\,He}$ and $R_{t\,gas}$, were calculated from the experimental data. These values are summarized in Tables 4.2-a & b.

ii) The overall resistances of coated membranes, $R_{tc\,He}$ and $R_{tc\,gas}$, were calculated from the experimental data. These values are summarized in Tables 4.3-a & b.

The local separation factors α_1, α_2, α_3, and α_{3c} are summarized in Table 4.6. These values were obtained as follows:

iii) The coating layer separation factor, α_1, for silicone rubber is reported in the literature [GEPM, 1982].

iv) The matrix separation factor, α_2, was assumed to be equal to the highest ideal separation factor achieved from a coated membrane which are reported in Tables 4.3-a & b.

v) The pore separation factor, α_3, was unknown. However, the upper and the lower limits of α_3 were known to be equal to the highest ideal separation factor achieved by the uncoated membrane, and the Knudsen separation factor, α_K, respectively. The Knudsen separation factor was defined in Equation 2.13.

vi) The filled pore separation factor, α_{3c}, was assumed to be equal to the coating layer separation factor, α_1.

Table 4.6: Values of the Local Ideal Separation Factors to be Used in Equations 2.27, 2.28, and 2.32 to 2.36.

Δp, kPa	He	H_2	O_2	N_2	CO_2	CH_4
			Membranes "a" and "b"			
α_1, α_{3c}	1	0.55	0.60	1.2	0.11	0.37
α_2 (=maxα_{ic})	1	4.1	89	860	19	860
			Membrane "a"			
α_3, high	1	2.1	8.0	9.1	5.1	7.6
α_3, low	1	0.707	2.83	2.65	3.32	2.00
			Membrane "b"			
α_3, high	1	1.8	7.3	8.3	7.3	7.0
α_3, low	1	0.707	2.83	2.65	3.32	2.00

The local resistances are shown in Tables 4.7-a & b. The matrix and the pore resistances for helium are also shown graphically in Figure 4.14. The shape of the resistance curves for other gases were similar to those of helium except the distance between the two curves, one corresponding to the matrix resistance and the other corresponding to the pore resistance, varied from one gas to another.

The matrix resistances were higher than the pore resistances without exception. Both the matrix and the pore resistances decreased with an increase in the operating pressure. A comparison between the matrix and the pore resistances led to the division of the gases into two extremes. The division was made according to the magnitude of the difference between the matrix and the pore resistances for the gases. In one extreme, the matrix and the pore resistances of helium and hydrogen were close to each other. On the other extreme, the matrix resistances of nitrogen and methane were two to three orders of magnitude larger than their pore resistances. In the middle, the matrix resistances of oxygen and carbon dioxide were about one order of magnitude higher than their pore resistances.

Table 4.7-a: Pore Ideal Separation Factor, α_3, Matrix Resistance, R_2, Pore Resistance, R_3, Coating Layer Resistance, R_1, and Coated Pore Resistance, R_{3c}, Pertinent to Uncoated and Silicone-Coated Aromatic Polyamide Membrane "a".

Δp, kPa	He	H_2	O_2	N_2	CO_2	CH_4
Uncoated membrane						
Pore ideal separation factor, α_3,						
350	1	1.30	4.17	4.49	2.71	3.69
700	1	1.52	3.86	4.51	2.66	3.94
1050	1	1.65	4.60	5.16	3.33	4.54
1400	1	1.51	3.85	4.34	2.97	3.60
1750	1	1.34	4.21	5.56	2.91	3.75
2100	1	1.37	4.84	5.02	3.38	3.95
Average	1	1.4 ± 0.1	4.3 ± 0.3	4.8 ± 0.3	3.0 ± 0.2	39 ± 02
Matrix resistance, R_2, Pa s/mol × 10^{-12}						
350	1.23	5.04	109	>1000	23.4	>1000
700	1.04	4.27	92.8	>900	19.8	>900
1050	1.01	4.16	90.3	>870	19.3	>870
1400	0.80	3.28	71.1	>690	15.2	>690
1750	0.82	3.35	72.6	>700	15.5	>700
2100	0.68	2.77	60.2	>580	12.8	>580
Pore resistance, R_3, Pa s/mol × 10^{-12}						
350	1.17	1.52	4.89	5.26	3.18	4.32
700	1.00	1.52	3.85	4.50	2.66	3.93
1050	0.78	1.28	3.57	4.01	2.59	3.53
1400	0.78	1.18	3.02	3.40	2.33	2.82
1750	0.78	1.05	3.30	3.58	2.28	2.94
2100	0.68	0.94	3.31	3.43	2.31	2.70
Coated membrane						
Coating layer resistance, R_1, Pa s/mol × 10^{-12}						
700	0.01	<0.01	<0.01	0.01	<0.01	<0.01
1400	<0.01	<0.01	<0.01	<0.01	<0.01	<0.01
2100	<0.01	<0.01	<0.01	<0.01	<0.01	<0.01
Coated pore resistance, R_{3c}, Pa s/mol × 10^{-12}						
700	>400	>220	>240	>480	>44	>150
1400	>320	>170	>190	>380	>35	>120
2100	>1000	>550	>600	>1200	>110	>370

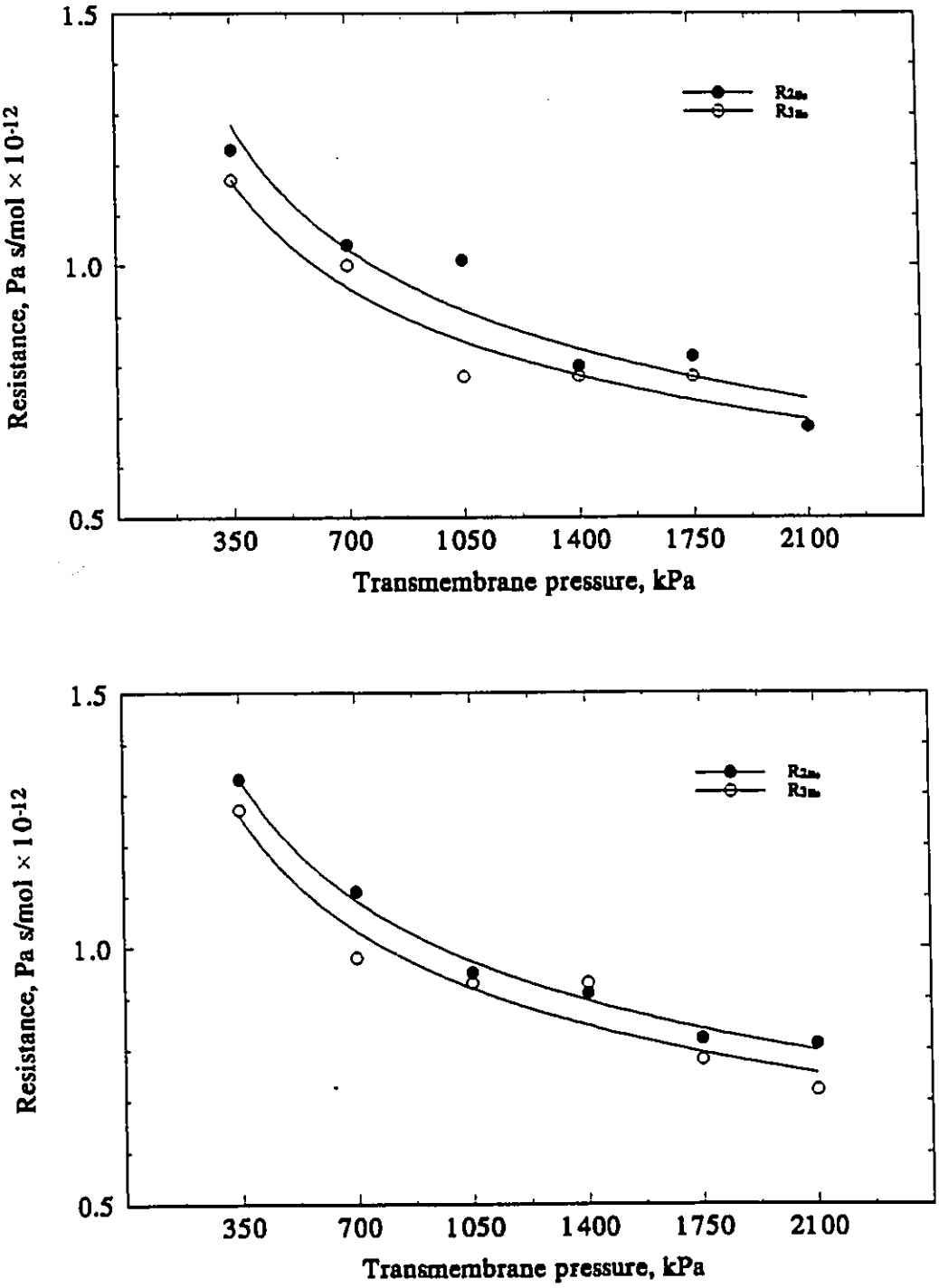

Figure 4.14: Comparison of the matrix and the pore resistances for helium at different operating pressures. Top: membrane "a". Bottom: membrane "b".

Table 4.7-b: Pore Ideal Separation Factor, α_3, Matrix Resistance, R_2, Pore Resistance, R_3, Coating Layer Resistance, R_1, and Coated Pore Resistance, R_{3c}, Pertinent to Uncoated and Silicone-Coated Aromatic Polyamide Membrane "b".

Δp, kPa	He	H_2	O_2	N_2	CO_2	CH_4
			Uncoated membrane			
			Pore ideal separation factor, α_3,			
350	1	1.20	3.50	3.88	3.89	3.45
700	1	1.43	3.96	4.48	4.63	4.03
1050	1	1.12	3.87	4.25	4.81	3.75
1400	1	1.03	3.68	4.11	4.70	3.41
1750	1	1.05	4.22	4.57	5.03	3.59
2100	1	1.02	4.57	4.77	5.07	3.72
Average	1	1.1 ± 0.1	4.0 ± 0.3	4.3 ± 0.3	4.7 ± 0.3	3.7 ± 0.2
			Matrix resistance, R_2, Pa s/mol × 10^{-12}			
350	1.33	5.47	119	>1150	25.3	>1150
700	1.11	4.56	98.9	>960	21.1	>960
1050	0.95	3.91	84.9	>820	18.1	>820
1400	0.91	3.75	81.4	>790	17.4	>790
1750	0.82	3.35	72.8	>700	15.5	>700
2100	0.81	3.31	71.8	>690	15.3	>690
			Pore resistance, R_3, Pa s/mol × 10^{-12}			
350	1.27	1.52	4.44	4.92	4.93	4.38
700	0.98	1.40	3.87	4.38	4.53	3.94
1050	0.93	1.04	3.59	3.94	4.46	3.48
1400	0.93	0.95	3.40	3.80	4.35	3.15
1750	0.78	0.82	3.30	3.58	3.94	2.81
2100	0.72	0.73	3.28	3.43	3.64	2.67
			Coated membrane			
			Coating layer resistance, R_1, Pa s/mol × 10^{-12}			
700	0.01	<0.01	<0.01	0.01	<0.01	<0.01
1400	0.01	<0.01	<0.01	0.01	<0.01	<0.01
2100	0.01	<0.01	<0.01	0.01	<0.01	<0.01
			Coated pore resistance, R_{3c}, Pa s/mol × 10^{-12}			
700	>380	>210	>230	>450	>42	>140
1400	>160	>88	>100	>190	>18	>60
2100	>74	>40	>44	>90	>8	>27

The magnitude of the difference between the matrix and the pore resistance has a significant implication. In case of helium and hydrogen the permeation through the matrix and through the pores occurred with similar ease. On the other hand, oxygen and carbon dioxide permeated mainly through the pores. Nitrogen and methane permeated almost completely through the pores and did not go through the polymer matrix.

The numerical values obtained for the local resistances explain the permselectivity behaviour of the uncoated and the coated membranes. In an uncoated membrane, because the matrix resistance was much larger than the pore resistance for most of the gases, the gas permeation took place mostly through the pores. Thus, the small selectivity of the uncoated membrane can be attributed to the low selectivity of the pore flow. When the pores were blocked by the coating material their resistances increased by three to four orders of magnitude for all gases. Therefore, the pore flow was practically stopped for all gases. Then, the only path available was the void spaces in the membrane matrix where only the small molecules could overcome its resistance. As a result, the permeation of the large gases were either stopped or hindered severely by the matrix resistance.

The coating layer resistances, R_1, were smaller than the substrate membrane resistances by one order of magnitude or more. The coating layer resistances were of the same order of magnitude for all gases. Therefore, the contribution of the coating layer resistance to the decrease in the permeation rate was small. The decrease was due to the tremendous increase in the coated pore resistance, R_{3c}, which was at least three orders of magnitude higher than both the matrix and the pore resistances.

The pore separation factors, α_3, are reported in Tables 4.7-a & b. Comparison of Tables 4.2-a & b and Tables 4.7-a & b shows that the overall separation factor of uncoated membrane is in the same order of magnitude as the pore ISF. On the other hand, comparison of Tables 4.3-a & b and Tables 4.7-a & b shows that the ISF of coated membrane is in the same order of magnitude as the separation factor of the polymer matrix. Thus, it can be concluded that the overall ISF of the uncoated membrane was controlled by the unplugged pores, and that of a coated membrane was controlled by the polymer matrix.

The pore separation factors for all gases were well above the Knudsen separation factor, α_K. The higher than the Knudsen values of the pore separation factors implies that the Knudsen mechanism alone could not be applied to the flow through the unplugged pores. Rather, a combined Knudsen-surface flow mechanism through the pores of an uncoated membrane would better explain the experimental observation. The higher than unity pore separation factor indicates also that the membranes were free of pin-holes which could cause laminar flow through the membrane. Membrane "a" had higher pore separation factors compared with the membrane "b". In membrane "a", the pore separation factor for CO_2 were very close to, and at some pressures smaller than separation factor based on the Knudsen mechanism. This observation can be explained by the plasticization effect of carbon dioxide, i.e., the presence of this gas in the membrane caused the pores to expand. The pore expansion resulted in higher permeation rate, lower resistance, and lower selectivity of CO_2 with respect to helium.

4.4. GAS MIXTURE SEPARATION

4.4.1 CO_2/CH_4 Separation

Separation experiments were conducted for CO_2/CH_4 systems in the constant pressure system. The operating pressure was 700 kPa gauge (≈100 psig). The composition of the feed and the permeant was analyzed using a gas chromatograph. Mixtures of carbon dioxide/methane with three different compositions were separated using two coated polyamide membranes denoted as "a" and "b". The mole fractions of CO_2 in the feed mixtures were 0.25, 0.50, and 0.75, with the balance of CH_4.

Table 4.8 shows the results. In this table the compositions of each gas in the feed and in the permeate, the actual separation factor, and the permeation rates are given. The results are also shown in Figures 4.15 and 4.16. According to Table 4.8 and Figure 4.15, carbon dioxide can be removed from methane with a very high efficiency in a one stage process even at relatively low carbon dioxide concentrations.

The separation factors achieved in this study were considerably higher than those reported in the literature while the permeation rate was lower [Rautenbach, 1984]. The actual separation factors reported in the literature vary between 10 - 30 [Robson, 1990] compared with 64 - 166 in the present study.

The actual separation factors of CO_2/CH_4 system reported in Table 4.8 can be compared with the ideal separation factors reported in Tables 4.3-a & b. While it is well established that, in general, the actual separation factor is lower than the ideal separation factor, the decrease is

Table 4.8: Composition of Carbon Dioxide and Methane in the Feed and Permeate, Permeation Rate, and Actual Separation Factor for CO_2/CH_4 Separation.

Feed composition (mole fraction)		Permeate composition (mole fraction)		Separation factor (α)	Permeation rate mol/s × 10^7 ($cm^3/s \times 10^3$)	
CO_2	CH_4	CO_2	CH_4			
		Membrane "a"				
0.00	1.00	0.00	1.00	-	0.0	(0.0)
0.25	0.75	0.955	0.045	64	3.3	(7.4)
0.50	0.50	0.994	0.006	166	7.1	(15.9)
0.75	0.25	0.998	0.002	166	11.1	(24.9)
1.00	0.00	1.00	0.00	-	18.6	(41.7)
		Membrane "b"				
0.00	1.00	0.00	1.00	-	0.0	(0.0)
0.25	0.75	0.956	0.044	65	1.7	(3.8)
0.50	0.50	0.985	0.015	66	3.0	(6.7)
0.75	0.25	0.995	0.005	66	4.5	(10.1)
1.00	0.00	1.00	0.00	-	7.0	(15.7)

usually more significant in case of CO_2/CH_4 separation. That is because, considering the plasticization effect of carbon dioxide, the presence of this gas in the polymeric membrane increases the mobility of polymer in the membrane matrix resulting in the decrease in the matrix, and therefore, the overall resistance of the membrane to larger CH_4 molecules. In addition, coupling effect occurs between CO_2 and CH_4 molecules such that CH_4 transport through the membrane is enhanced by that of CO_2 molecules. The combination of the plasticization and the coupling effects causes a decrease in the actual separation factor. The above discussion implies that the separation factors estimated using the values reported in Table 4.3-a & b are conservative ones.

The total permeation rate was plotted against CO_2 feed mole fraction in Figure 4.16. The figure shows that the permeation rate increases linearly with CO_2 mole fraction until the latter reaches 0.75. Then, the permeation increases in non-linear fashion.

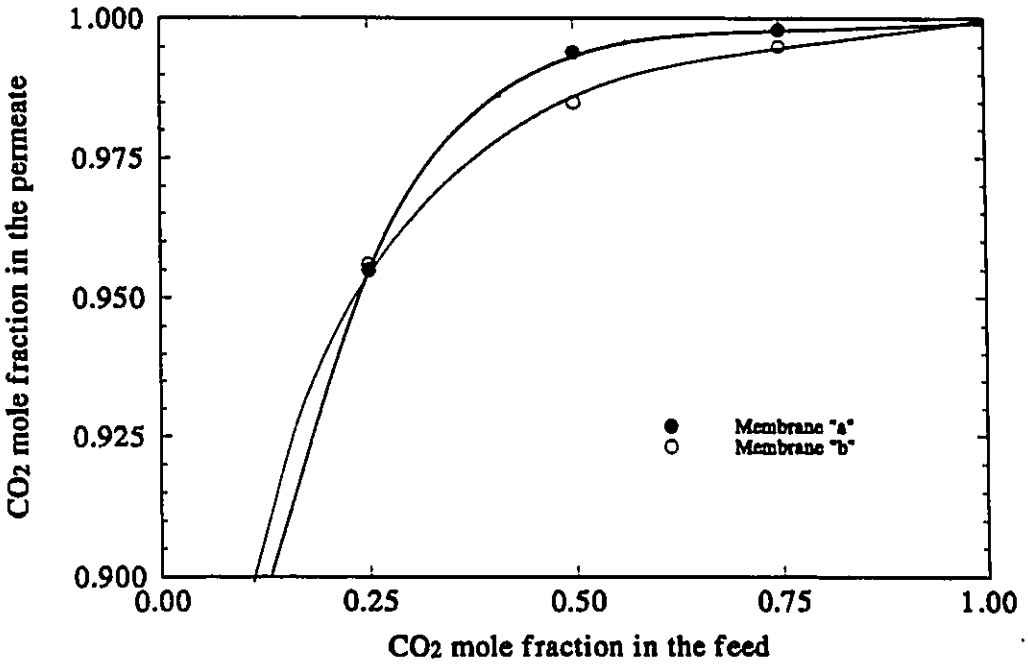

Figure 4.15: Mole fraction of carbon dioxide in the permeate versus that in the feed in CO_2/CH_4 separation experiments.

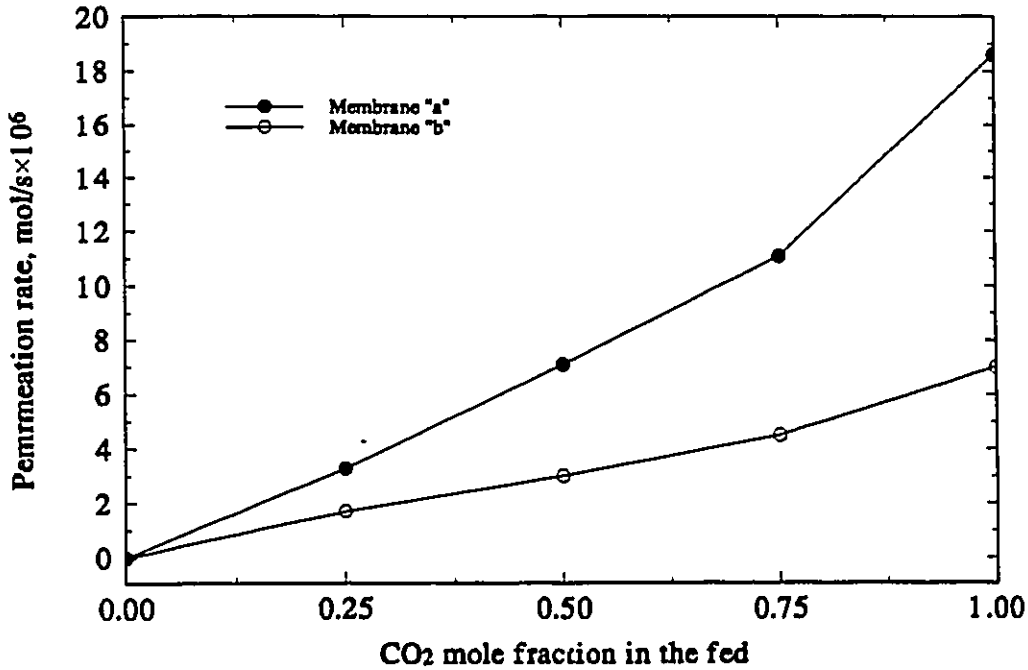

Figure 4.16: Permeation rate versus carbon dioxide feed mole fraction in CO_2/CH_4 separation experiments.

4.4.2. O_2/N_2 (Air) Separation

Air separation experiments were performed using two asymmetric silicone-coated aromatic polyamide membranes installed in the constant volume system. These two membranes were denoted as "a" and "c". The experimental procedure is described in Section 3.2.6. The downstream pressure varied from 0 to 1.3 kPa (0 to 10 torr) during the experiments. Since the downstream pressure was negligible compared with the upstream pressure the pressure drop across the membrane was assumed to be constant. The composition of the permeate was determined by the mass spectrometer at the end of each experiment.

Table 4.9 shows the experimental results. Actual separation factors of 8.7 from membrane "a" and 8.4 from membrane "c" were obtained for O_2/N_2 system. The permeation rates were 8.93×10^{-10} mol/s (2.00×10^{-5} cm^3/s), and 6.79×10^{-10} mol/s (1.52×10^{-5} cm^3/s) for membranes "a" and "c", respectively. The actual separation factor achieved corresponded to 70% oxygen in the permeate with approximately 1% impurities. The impurity was mainly composed of water and carbon dioxide. The oxygen content in the permeate obtained in this work is higher than those reported in the literature. The oxygen content in the permeate of commercial modules is between 30% and 40% which can be interpreted to a separation factor of 1.6 to 2.5.

Table 4.9: Composition of Oxygen and Nitrogen in the Feed (Air) and Permeate, Permeation Rate, and Actual Separation Factor for O_2/N_2 Separation.

Memb	Feed composition (mole fraction)		Permeate composition (mole fraction)		Separation factor (α)	Permeation rate mol/s × 10^9 ($cm^3/s \times 10^5$)
	O_2	N_2	O_2	N_2		
a	0.21	0.78	0.70	0.30	8.7	8.93 (2.00)
c	0.21	0.78	0.69	0.30 (<1% impurities)	8.4	6.79 (1.52)

4.5. GAS PERMEATION THROUGH HOMOGENEOUS MEMBRANES

A series of experiments were performed using homogeneous aromatic polyamide membrane in order to gain a better and in depth understanding of the membrane performance. The study included the determination of the intrinsic properties of the aromatic polyamide polymer, the effect of the presence of additive in the casting solution on the performance of the homogeneous membrane, the effect of polymer concentration in the casting solution on the membrane performance, and finally comparing the performance of a homogeneous and an asymmetric membrane.

4.5.1. Intrinsic Permeability and Intrinsic Separation Factors

The permeability coefficient of a gas through a membrane, P, is usually measured using a homogeneous membrane and is called the intrinsic permeability of a particular gas through a particular membrane. The ratio of the intrinsic permeabilities of two gases is called intrinsic separation factor. It is commonly believed that the intrinsic separation factor of a homogeneous membrane is the upper limit for the ideal separation factor of an asymmetric membrane made of the same material [Sada, 1994]. Usually the intrinsic separation factor is used in place of the matrix separation factor in an asymmetric membrane when analyzing the data.

In order to obtain the intrinsic permeability and the intrinsic separation factor of the experimental gases through aromatic polyamide membrane the permeation rates of six gases were measured through a homogeneous PA membrane. The membrane was prepared from a solution

of 9.6wt% polymer concentration in DMAc with no lithium nitrate additive. The solvent was evaporated at room temperature and then the membrane was transferred to a vacuum oven for further evaporation of solvent (sample number 8 Table 3.2). The details of the preparation conditions are reported in Section 3.1.2. The gases used in the experiment included helium, hydrogen, oxygen, nitrogen, carbon dioxide, and methane. The thickness of the dry homogeneous membrane was ≈50 μm. The upstream pressure was 666 kPa (5000 torr). The downstream pressure varied from ≈0 to 1.3 kPa (10 torr) during the experiment.

Table 4.10 shows the permeation rate, Q, permeability coefficient, P, and intrinsic separation factor for each experimental gas. The permeation rates reported in the table are the values after correction for the impurities. The correction was done by subtracting the permeation rate of impurities from the nominal permeation rate. The permeability coefficients were calculated

Table 4.10: Permeation Rate, Permeability Coefficient, and Intrinsic Separation Factor of the Experimental Gases Through Homogeneous Aromatic Polyamide Membrane. Pressure = 666 kPa (5000 torr), Membrane Thickness = 50 μm.

	He	H_2	O_2	N_2	CO_2	CH_4
Purity, %	100	100	97.2	97.3	98.2	95.9
			Permeation rate, Q, mol/s × 10^{10} (cm^3/s × 10^5)			
	84.8 (19.0)	48.7 (10.9)	1.61 (0.361)	0.175 (0.0392)	6.43 (1.44)	0.0835 (0.0187)
			Permeability coefficient, P, mol m/m^2 s Pa × 10^{16} (Barrer)			
	6.62 (1.98)	3.80 (1.13)	0.126 (0.0376)	0.0137 (0.00408)	0.502 (0.150)	0.0065 (0.00194)
			Intrinsic separation factor, -			
	1	1.74	52.6	484	13.1	1020
			$\alpha_{O2/N2}$ = 9.21		$\alpha_{CO2/CH4}$ = 75.5	

1. Barrer = cm^3 cm/cm^2 s cmHg $\times 10^{-10}$

using Equation 2.15. The intrinsic separation factors were calculated using Equation 2.10 with respect to helium as the reference gas. The intrinsic separation factors were calculated for O_2/N_2 and CO_2/CH_4 systems to be 9.21 and 75.5 respectively. These values are also reported in Table 4.10.

The intrinsic separation factors in Table 4.10 can be compared with the ideal separation factors in Tables 4.2-a & b for the uncoated asymmetric membranes and with those in Tables 4.3-a & b for coated asymmetric membranes. In general, the intrinsic separation factors are larger than the ideal separation factors of the uncoated membranes and smaller than those of the coated membranes. There are two exceptions to this observation. One is that the intrinsic separation factor of hydrogen is smaller but close to the ISF of the uncoated membranes. The other is that a strong conclusion can not be made in case of methane. That is because, as shown in Tables 4.3-a & b, the ISF of the coated membranes for methane were estimated to be above some values. Therefore, the ISF and the intrinsic separation factor of methane are considered to be in the same range. Neglecting these exceptions, the order: $ISF_{uncoated}$< intrinsic SF < ISF_{coated} applies to the experimental data. This order leads to an important conclusion that the intrinsic separation factor is not necessarily the upper limit for the ISF. In other words, the intrinsic separation factors can be surpassed by the ISF of an asymmetric membrane. This observation is interpreted by the difference in the morphological structure of the dense skin layer in an asymmetric membrane from that of a homogeneous dense membrane. Therefore, the assumption that the intrinsic separation factor can be used in place of the matrix separation factor is not necessarily valid.

4.5.2. Performance of Homogeneous Membranes with Additive

Five samples of homogeneous aromatic polyamide membrane were prepared using polymer solutions with lithium nitrate as an additive. The details of the preparation procedures are discussed in Section 3.1.3 and Table 3.1. The samples were tested using the constant pressure or constant volume systems depending on the magnitude of the permeation rates. All samples were tested for the permeation rate of oxygen and nitrogen. In addition to these two gases, samples number 4 and 5 were tested for carbon dioxide and methane as well. The membrane preparation conditions are summarized in Table 3.1, and the results are shown in Table 4.11.

All samples showed selectivities close to 1 toward O_2/N_2 system, i.e., no separation between these gases. The selectivity of sample number 4 toward CO_2/CH_4 was around 4.5 which is higher than the ISF of the uncoated asymmetric membranes. Except the latter result, the separation factors were lower than those of the uncoated asymmetric membranes, and therefore, much lower than those of the coated asymmetric ones.

The permeation rate data in Table 4.11 can be compared with those of the coated asymmetric membranes in Table 4.3-a & b. The comparison indicates that the permeation rate of the gases through sample number 1 was in the same range as through the coated membranes. Samples number 2 and 3 showed higher, and samples number 4 and 5 showed lower permeation rates than the coated membranes. The high permeation rates were observed from the samples prepared from the solutions with high polymer concentration, while, the low concentration solutions showed low permeation rates. The correlation between the permeation rate and the polymer concentration can be explained in the following way. At high concentration, the polymer

Table 4.11: Permeation Rates of Single Gases Through Homogeneous Membranes Made from Polymer Solutions with the Addition of Lithium Nitrate. Pressure = 666 kPa (5000 torr).

		Permeation rate, mol/s × 10^9 (cm^3/s × 10^5)				
Sample #	l[1], μm	O_2	N_2	CO_2	CH_4	$\alpha_{O2/N2}$
1	48	115 (25.7)	112 (25.0)	-	-	1.0
2	50	617 (1380)	595 (1330)	-	-	1.0
3	51	14900 (33000)	14900 (33000)	-	-	1.0
4	48	0.55 (1.23)	0.55 (1.23)	2.4 (5.33)	5.4 (1.20)	1.0
5	49	5.96 (13.4)	5.53 (12.4)	6.26 (14.0)	5.60 (12.6)	1.1
		Permeability coefficient, mol m/m^2 s Pa × 10^{14} (Barrer)[2]				
1		0.0897 (2.67)	0.0874 (2.60)			
2		4.81 (143)	4.64 (138)			
3		116 (3430)	116 (3430)			
4		0.0043 (0.128)	0.0043 (0.128)	0.019 (0.125)	0.0042 (0.554)	
5		0.0465 (1.39)	0.043 (13.0)	0.0488 (1.46)	0.044 (1.32)	

[1] l: membrane thickness
[2] Barrer = cm^3 cm/cm^2 s cmHg × 10^{10}

chains do not have enough space to relax in a uniform fashion during the solvent evaporation period. The non-uniformity of the precipitated polymer chains results in the formation of pores with a wide range of size distribution which includes pinholes and defects, thus, allowing the gas to permeate at higher rates.

The presence of the additive in the solution is also known to affect the size of the polymer nodules in favour of the formation of larger pores [Kesting, 1993]. Comparison between the

performance of membrane samples number 1 and 2 shows that the permeation rate of sample number 1 is lower than number 2. These two membranes were prepared under the same conditions except one was gelled in water (number 1) and the other was directly air dried (number 2). Since the additive is water soluble and is washed out during the gelation step, it is expected that, the lithium nitrate was not present in sample number 1, but remained in sample number 2. Apparently, the presence of the additive in the membrane during air drying causes formation of cracks and defects. The defect reduces the overall resistance of the membrane to the permeating gas causing a significant increase in the permeation rate.

The high permeation rates and low separation factors were attributed to the presence of pinholes which allow the laminar flow through the membranes. The low polymer concentration samples (number 4 and 5) showed low permeation rate but without high selectivity. The low permeation rate is attributed to two simultaneous effects. One is the formation of smaller polymer nodules, and therefore, smaller pores. The second is the high thickness of the homogeneous membranes which increases the overall resistance of the membrane and decreases the permeation rates. However, the low selectivity indicates that the pores are still large enough for the laminar flow to be dominant.

In general, the presence of the additive in the polymer solution was found to increase the flux. The increase in the permeability was accompanied by substantial reduction in the selectivity of the membrane.

4.5.3. Performance of Homogeneous Membranes without Additive

The membrane samples were prepared from polymer solutions with high (21.7 wt%), medium (9.6 wt%), and low (5.6 wt%) concentration. The solvent was evaporated at different temperatures ranging from 23 °C to 95 °C. The details of the membrane preparation conditions are reported in Section 3.2.3 and Table 3.2. The permeation rates of oxygen and nitrogen through the homogeneous membranes were measured using the constant pressure or the constant volume systems depending on the magnitude of the permeation rate. The experimental procedures are discussed in sections 3.2.2 and 3.2.6.

The results are shown in Table 4.12 and Figure 4.17. The high polymer concentration samples (21.7 wt%) showed high permeability and no selectivity toward oxygen and nitrogen. This phenomenon was also observed for the high concentration membranes with additive in the previous section (Table 4.11). Comparison of these two sets of results indicates that the membranes lose their selectivity when they are prepared from solution of high polymer concentration; and presence or absence of additive is not a dominant factor.

The high permeability and low selectivity were also observed for the membranes of low polymer concentration, i.e., 5.5 wt%. The selectivity of the membranes were close to unity except for the sample which was dried at room temperature (23 °C). In the latter case, a separation factor of 4.7 and a permeation rate lower than other samples were obtained.

The highest selectivity was achieved from the membranes prepared from the medium polymer concentration solution (9.6wt%). The separation factors for these membranes were well above unity at all evaporation temperatures. However, a decreasing tendency was observed in the

Table 4.12: Permeation Rates of Oxygen and Nitrogen Through Homogeneous Membranes Made from Polymer Solutions without the Addition of Lithium Nitrate.

Evap'n temp, °C	23	40	60	95
Thickness, μm	46	46	48	47
		Polymer concentration: 5.5%		
		Permeation rate, mol/s × 10^7 (cm^3/s × 10^5)		
O_2	0.0268	9.37	8.04	14.1
	(6.00)	(2100)	(1800)	(3170)
N_2	0.00565	8.48	4.91	16.4
	(1.27)	(1900)	(1100)	(3660)
$\alpha_{O2/N2}$	4.74	1.1	1.64	0.9
		Permeability, mol m/m^2 s Pa × 10^{16} (Barrer)[1]		
O_2	0.0209	7.31	6.27	11.0
	(0.624)	(218)	(187)	(332)
N_2	0.00441	6.61	3.83	12.8
	(0.132)	(198)	(114)	(380)
		Polymer concentration: 9.6%		
thickness, μm	50	51	48	
		Permeation rate, mol/s × 10^9 (cm^3/s × 10^5)		
O_2	1.61	3.62	4.42	
	(0.361)	(0.810)	(0.990)	
N_2	0.175	0.551	0.744	
	(0.0392)	(0.123)	(0.167)	
$\alpha_{O2/N2}$	9.21	6.59	5.93	
		Permeability coefficient, mol m/m^2 s Pa × 10^{16} (Barrer)[1]		
O_2	0.126	2.82	3.45	
	(0.0375)	(0.0842)	(0.103)	
N_2	0.136	0.430	0.580	
	(0.00407)	(0.0128)	(0.0174)	
		Polymer concentration: 21.7%		
Both gases showed high permeation rates and no selectivity				

1. Barrer = cm^3 cm/cm^2 s cmHg x10^{-10}

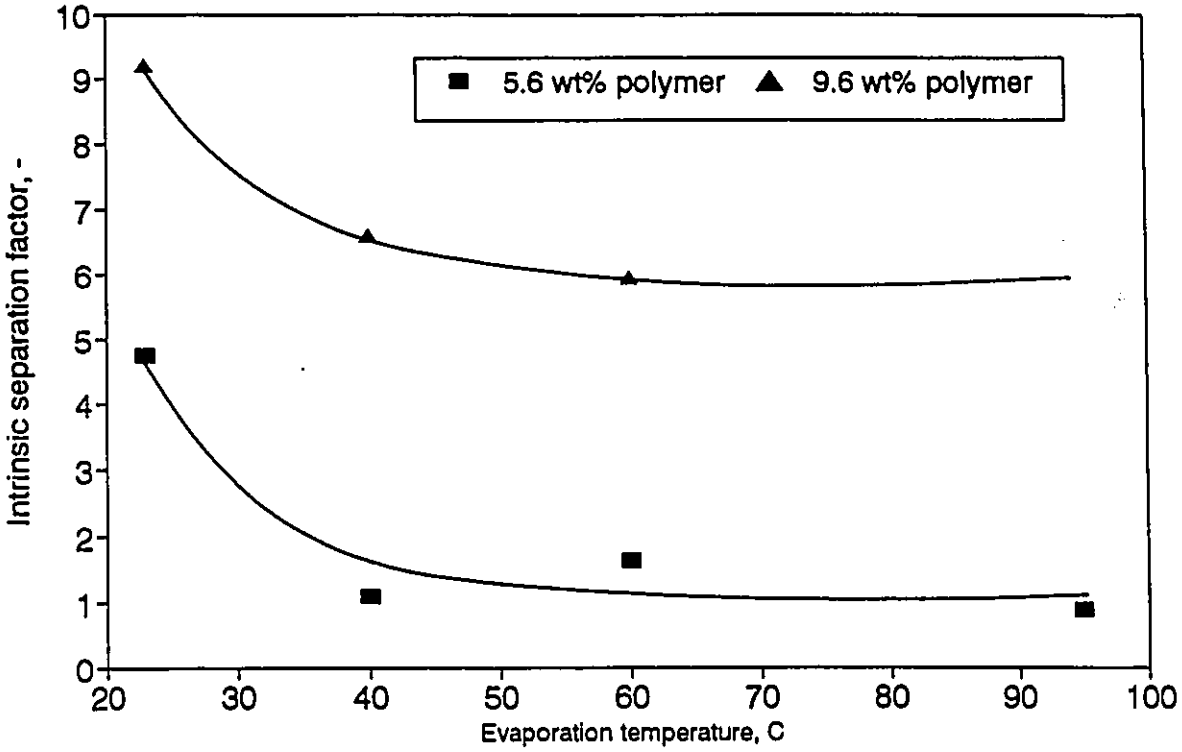

Figure 4.17: Intrinsic separation factor of homogeneous PA membranes prepared with no additive with respect to O_2/N_2 system.

separation factor with an increase in the evaporation temperature. As shown in Figure 4.17, the separation factor decreased from 9.2 to 5.9 as the evaporation temperature was increased from 23 °C to 60 °C.

When the evaporation temperature increases, the fast solvent evaporation does not allow for polymer relaxation, resulting in a non-uniform local density and polymer structure. Therefore, larger void spaces are formed which allows laminar flow to occur and reduces the selectivity.

In general, the results indicate that the selectivity of homogeneous membranes decreases as the evaporation temperature increases. Also, an optimum polymer concentration exists at which

the selectivity becomes the highest. Comparison between the results from the homogeneous membranes made with and without the addition of lithium nitrate indicates that the distribution of the polymer chains is more uniform in the absence of the additive. Also, nodules of smaller size are formed when the lithium nitrate is not added to the solution.

4.6. SCANNING ELECTRON MICROSCOPY RESULTS

In order to confirm the results discussed in the previous sections a series of scanning electron microscopic (SEM) photographs were taken for the asymmetric aromatic polyamide membrane "a", a homogeneous with additive (sample number 5, Table 3.1), and a homogeneous membrane without additive (sample number 8, Table 3.2). The SEM pictures are shown in Figures 4.18 to 4.20.

The cross-section of an uncoated asymmetric membrane is shown in Figure 4.18. The asymmetric structure of the membrane is obvious (top photomicrograph). The membrane is divided into two distinct regions. The skin layer with an average thickness of approximately 1 μm lies on top of the porous supporting sublayer. The thickness of the skin layer was not uniform and in some regions thicker skin layer was observed. Figure 4.18 (bottom) also shows a pinhole in the skin layer with an approximate diameter of 0.05 μm. Such pores of large diameter allow for laminar flow of gases through the membrane. The overall selectivity of the membrane increases when these pores are blocked. The thickness of the skin layer was larger where the pinhole existed. This observation suggests that pinholes are formed when the thickness of the skin layer exceeds a critical value, at which point the skin layer cracks.

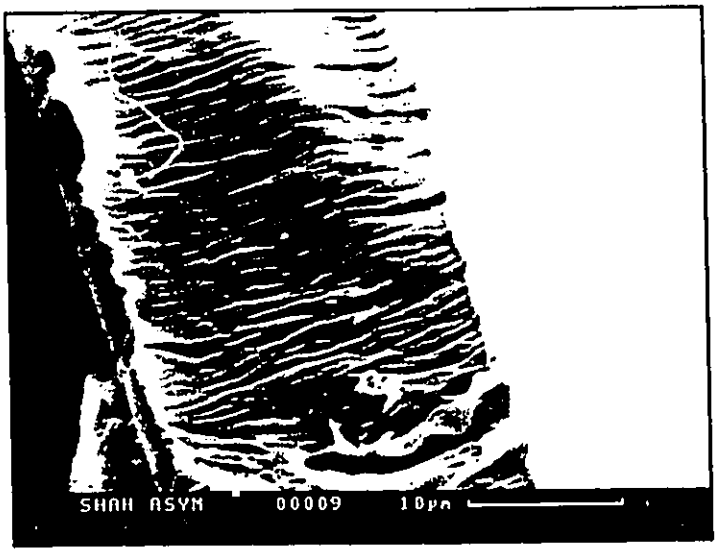

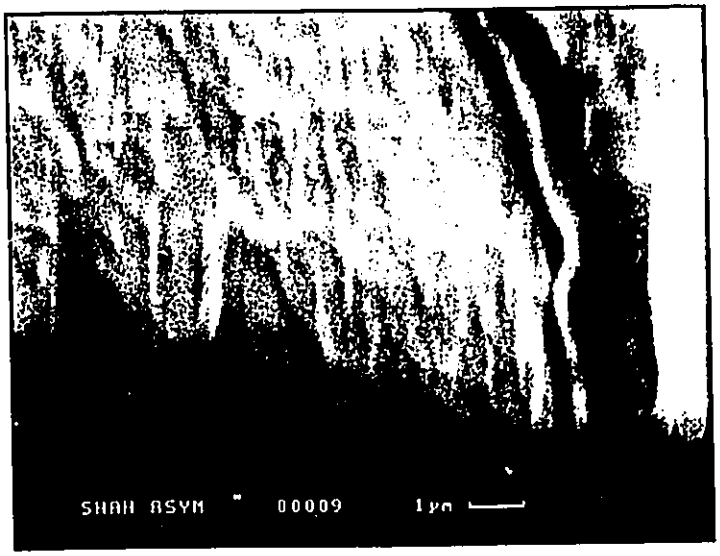

Figure 4.18: Scanning electron micrographs of the cross-section of an asymmetric PA membrane. Top: the cross-section. Bottom: A typical pinhole in the skin layer.

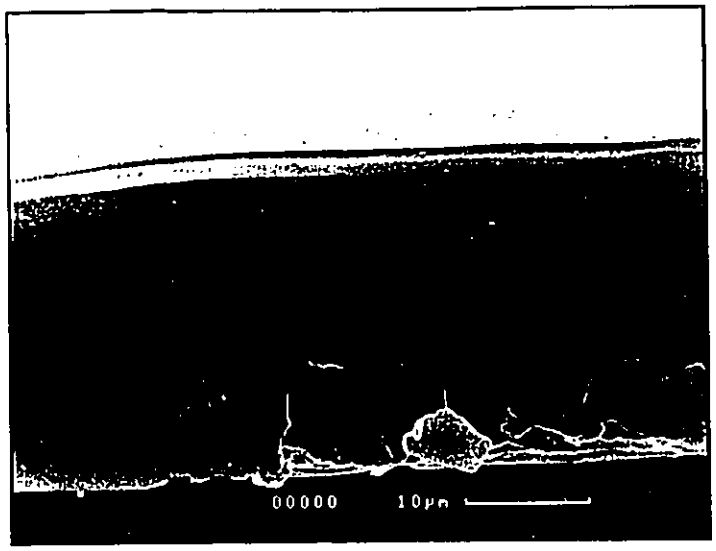

Figure 4.19: Scanning electron micrographs of the cross-section of a homogeneous PA membrane prepared without the addition of lithium nitrate.

The cross-sectional structure of a homogeneous membrane is shown in Figure 4.19. This membrane was prepared from a solution without the addition of lithium nitrate. the membrane is dense and uniform across the cross-section. The high and uniform polymer density counts for the small permeability of gases through the membrane.

The homogeneous membrane prepared from the polymer solution with additive has a uniform and dense structure across the cross-section as shown in Figure 4.20. However, many pores penetrating through the cross-section is observed. The poor overall selectivity of this membrane, shown in Table 4.11, is due to its high porosity.

Figure 4.20: Scanning electron micrographs of the cross-section of a homogeneous PA membrane prepared with the addition of lithium nitrate.

The SEM pictures confirm the discussions made in the previous sections concerning the low selectivity of uncoated membranes and the effect of the addition of lithium nitrate to the polymer solution on the overall separation factor.

A comparison between Figures 4.18 and 4.20 shows that the morphology of the skin layer in an asymmetric membrane is different from that of a homogeneous membrane prepared by adding lithium nitrate to the casting solution. On the other hand, at the magnification available, no difference was observed between the morphologies of the skin layer and the homogeneous dense membrane with no additive (Figures 4.18 and 4.19).

CONCLUSIONS

1. The selectivity of dry aromatic polyamide membranes was enhanced by coating them with silicone rubber under certain conditions. The permeation of nitrogen and methane through coated membranes reduced significantly, while, other gases permeated through with relative ease. As a result, ideal separation factors comparable with, or higher than, the highest literature values were obtained.

2. Actual separation factors of 8.4 - 8.7 for air, and 64 - 166 for CO_2/CH_4 mixture separation were achieved in the present study. These separation factors are higher than the reported literature values.

3. The intrinsic separation factor of a number of homogeneous aromatic polyamide membranes, prepared under different conditions, were all lower than the ideal separation factor of coated asymmetric PA membranes. It was concluded that, the intrinsic separation factor of a polymer is not necessarily the upper limit for the ideal separation factor of an asymmetric membrane made of that polymer. Correspondingly, the intrinsic separation factor can not be used in place of the matrix separation factor in an asymmetric membrane.

4. A new leak-free separation cell design allowed for an accurate determination of the permeate composition especially in case of an air separation experiment. In this design, the membrane acts as the sealant and no "O" ring is involved. The leak rate into the downstream of the system was measured to be $< 1.2 \times 10^{-9}$ cm^3/s.

5. A fully automated gas separation system was designed and constructed for the measurement of low permeation rates. This constant volume system can operate the permeation experiments with minimum supervision and can measure permeation rates of 1×10^{-8} cm^3/s and lower.

6. A new solution method was developed based on the resistance model to solve for the local resistances of an asymmetric membrane. In this method the number of assumptions are reduced and more accurate results can be obtained.

REFERENCES

Agrawal, R. and S. Auvil; "Process for the Generation of Gaseous and/or Liquid Nitrogen", U.S. Patent 4,595,405, (1986).

Anderson, M. R., B. R. Mattes, H. Reiss, and R. B. Kaner; "Conjugated Polymer Films for Gas Separations", Science **252**, 1412 - 1415, (1991).

Backhouse, I. W., "Recovery and Purification of Industrial Gases Using Prism® Separators" in "Membranes in Gas Separation and Enrichment", Proc. 4th BOC Prestley Conf., Leeds Univ., Royal Society of Chemistry, London (1986), Special Publication No. **62**, pp. 265-280.

Baldus, W. and D. Tillman, "Conditions Need to be Fulfilled by Membrane Systems in order to Compete with Existing Methods in Gas Separation", in "Membranes in Gas Separation and Enrichment", Proc. 4th BOC Prestley Conf., Leeds Univ.,Royal Society of Chemistry, London (1986), Special Publication No. **62**, pp. 26-42.

Barbari, T. A., W. J. Koros, and D. R. Paul, "Polymeric Membranes Based on Bisphenol-A for Gas Separations", J. Memb. Sci. **42**, 69 - 86, (1989).

Beaver, E. P., P. V. Bhat, and D. S. Sarcia, "Integration of Membranes with other Air Separation Technologies", AIChE Symp. Ser. **84**, 261, 113-123, (1988).

Breck, D. W.; "Zeolite Molecular Sieves", Wiley, New York (1974), p. 636.

Bixler, H. J. and O. S. Sweeting, in "The Science and Technology of Polymer Films", Vol. II, O.J. Sweeting Ed., John Wiley & Sons, New York (1971), p. 85.

Chen, Y., A.E. Fouda, and T. Matsuura, in "AIChE Symp. Series" **272**, 85, AIChE, New York (1989), pp. 18-23.

Chen, Y., T. Miyano, A. Fouda, and T. Matsuura, "Preparation and Gas Separation Properties of Silicone Coated Dry Polyethersulfone Membranes", J. Memb. Sci. **48**, 203 - 219, (1990).

Chern, R. T., W. J. Koros, H. B. Hopfenberg, and V. T. Stannett, "Material Selection for Membrane Based Gas Separation", Am. Chem. Soc. Symp. Series, "Materials Science of Synthetic Membranes", D. R. Loyd Ed., Washington, D.C. **269**, 25 - 46, (1985).

Chiou, J. S. and D. R. Paul, "Gas Transport in a Thermotrapic Liquid-Crystalline Polyester", J. Polym. Sci. Polym. Phys. Ed. **25**, 1699 - 1707, (1987).

Chiou, J. S., Y. Maeda, and D. R. Paul, J. Appl. Polym. Sci. **33** 1823, (1987).

Coleman, M. R. and W. J. Koros, "Isomeric Polyimides Based on Fluorinated Dianhydrides and Diamines for Gas Separation Applications", J. Memb. Sci. **50**, 285, (1990).

Ekiner, O. M. and G. Vassilatos, "Polyaramide Hollow Fibers for Hydrogen/Methane Separation - Spinning and Properties", J. Memb. Sci. **53**, 259 - 273, (1990).

Gan, L. H., P. Blais, D. J. Carlsson, J. Sprunchuk, and D. M. Wiles, J. Appl. Polym. Sci. **19**, 69, (1975).

Gantzel, P. K. and Merten U., "Gas separation with high flux Cellulose Acetate Membranes", Ind. Eng. Chem. Process Des. Devel. **9**, 331 - 332, (1970).

Ghosal, K., R. T. Chern, and B. D. Freeman, "Gas Permeability of Radel A Polysulfon", J. Polym. Sci.: Part B: Polym. Phys. **31**, 891 - 893, (1993).

Haesloop, D. G., R. J. Swedo, and L. S. Burnett, "Development and Demonstration of a Spiral Wound Thin Film Composite Membrane System for the Economical Production of Oxygen Enriched Air", Final Report, DOE contract DE AC01 - 79CS 40294, (1985).

Henis, J. M. S. and M. K. Tripodi, "A Novel Approach to Gas Separation Using Composite

Hollow Fibre Membranes", Sep. Sci. Tech. **15**, 1059 - 1068, (1980a).

Henis, J. M. S. and M. K. Tripodi; "Multicomponent Membrane for Gas Separation", U.S. Pat. 4,230,463, Oct. 28, (1980b).

Hsieh, K. H., C. C. Tsai, and D. M. Chang; "Vapour and Gas Permeability of Polyurethane Membranes. Part II: Effect of Functional Group", J. Memb. Sci. **56**, 279 - 287, (1991).

Hwang, S. T. and K. Kammermeyer; "Membranes in Separations, Techniques of Chemistry", John Wiley, NY, USA, (1976).

Islaski, W. H.; "25 Years of Purge Gas Recovery", Nitrogen **152**, (1984).

Kammermeyer, K.; "Technical Gas Permeation Processes", Chem. Ing. Tech. **48**, 8, 672 - 675, (1976).

Kamps, K. M. P., H. A. Teunis, M. Wessling, and C. A. Smolders; " ", J. Memb. Sci. **74**, 193-201, (1992).

Kaner, R. B.; "Research Update: University of California - New Class of Membranes Consisting of Cyclically Dopable, Conjugated Conductive Polymers", Memb. Sep. Tech. News **Sep**, 3 - 4, (1991).

Kesting, R. E. and A. K. Fritzsche; "Polymeric Gas Separation Membranes", John Wiely & Sons, New York (1993), pp. 296 - 299.

Kim, T. H., W. J. Koros, G. R. Husk, and K. C. O'Brien; "Relationship Between Gas Separation Properties of Aromatic Polyimides", J. Memb. Sci. **37**, 45, (1988a).

Kim, T. H., W. J. Koros, and G. R. Husk; "Advanced Gas Separation Membrane Materials: Rigid Aromatic Polyamides", Sep. Sci. Tech. **23**, 12&13, 1611 - 1626, (1988b).

Kneifel, K. and K. V. Peinemann, "Preparation of Hollow Fiber Membranes from Polyetherimid

for Gas Separation", J. Memb. Sci. **65**, 295 - 307, (1992).

Koros, W. J., "Simplified Analysis of Gas/Polymer Selective Solubility Behaviour", J. Polym. Sci.: Polym. Phys. Ed. **23**, 1611 - 1628, (1985).

Koros, W. J. and M. W. Hellums, "Gas Separation Membrane Material Selection Criteria: Differences for Weakly and Strongly Interacting Feed Components", Fluid Phase Equilibria **53**, 339 - 354, (1989a).

Koros, W. J. and M. W. Hellums, "Transport Properties Encyclopedia of Polymer Science and Engineering", 2nd ed. (supplemental vol.), John Wiley & Sons, New York, (1989b), 724 - 802.

Koros, W. J. and G. K. Fleming, "Membrane-Based Gas Separation"; J. Memb. Sci. **83**, 1-80, (1993).

Kumazawa, H., J. S. Wang, and E. Sada; "Gas Transport through Homogeneous and Asymmetric Polyethersulfone Membranes", J. Polym. Sci.: Part B: Polym. Phys. **31**, 881 - 886, (1993).

Kuwabata, S. and C. R. Martin, "Investigation of the Gas-Transport Properties of Polyaniline", J. Memb. Sci. **91** 1-12, (1994).

Lee, K. H. and S. T. Hwang, J. Coll. Interface Sci. **110**, 544, (1986).

Loeb S. and Sourirajan S.;, "Sea Water Dimineralization by Means of a Semipermeable Membrane", Report No. 6060, UCLA, (1960).

Lui A., F. D. F. Talbot, T. Matsuura, and S. Sourirajan, "Studies on the Solvent Exchange Techniques for Making Dry Cellulose Acetate Membrane for the Separation of Gas Mixtures", J. Appl. Polym. Sci. **36**, 1809 - 1820, (1988a).

Lui A., F. D. F. Talbot, T. Matsuura, and S. Sourirajan; "Studies on Gas Transport Through Dry Cellulose Acetate Membranes Prepared by Solvent Exchange Technique", Sep. Sci. Tech. **23**,

12&13, 1839 - 1852, (1988b).

Martin, C. R. ; "Gas Transport in Electronically Conductive Polymers", Memb. Sep. Tech. news **Sep.** (1991).

Matsumoto, K., P. Xu, and T. Nishikimi; "Gas Permeation of Aromatic Polyimides. I. Relationship between Gas Permeabilities and Dielectric Constants", J. Memb. Sci. **81** 15-22, (1993).

Matsuura, T. and Sourirajan S., "Preferential Sorption-Capillary Flow Mechanism and Surface Force-Pore Flow Model Applicability to Different Membrane Separation Processes", in Advances in Reverse Osmosis and Ultrafiltration, T. Matsuura and S. Sourirajan Eds., National Research Council Canada, Ottawa, Canada (1989), pp. 139 - 175.

Meares, P., "Fundamental Mechanisms of Transport of Small Molecules in Solid Polymers", 4th BOC Prestley Conf., Leeds Univ., Royal Society of Chemistry, London (1986), Special Publication No. **62**, pp. 1-25.

Mehatti, J. S., W. J. Koros, and D. R. Paul, "Gas Transport Properties of Polysulfones, I: Role of Symmetry of Methyl Group Placement on Bisphenol Rings", Polymer **32**, 5, 840, (1991).

Mercea, P. V. and S. T. Hwang; "Oxygen Separation From Air by a Combined Pressure Swing Adsorption and Continuous Membrane Column Process", J. Memb. Sci. **88**, 131 - 144, (1994).

Mi, Y., S. A. Stern, and S. Trohalaki, "Dependence of the Gas Permeability of some Polyimide Isomers on Their Intrasegmental Mobility", J. Memb. Sci. 77, 41 - 48, (1993).

Minhas, B.S., T. Matsuura, and S. Sourirajan, "Solvent Exchange Drying of Cellulose Acetate Membranes for Separation of Hydrogen - Methane Gas Mixture", Am. Chem. Soc.Symp. Series, S. Sourirajan and T. Matsuura Eds. **281**, 451 - 466, (1985).

Minhas, B. S., T. Matsuura, and S. Sourirajan "Formation of Asymmetric Cellulose Acetate Membranes for the Separation of Carbon dioxide - Methane Gas", Ind. Eng. Chem. Res. **26**, 11, 2344 - 2348, (1987).

Mohr, J. M., D. R. Paul, I. Pinnau, and W. J. Koros; "Surface fluorination of Polysulfone Asymmetric Membranes and Films", J. Memb. Sci. **56** 77-98, (1991).

Mulder, M., "Basic Principles of Membrane Technology", Kluwer Academic Press, Dordrecht, The Netherlands (1992).

Murphy, M. K., E. R. Beaver, and A. W. Rice; "Post Treatment of Graded Asymmetric Membranes for Gas Application", Presented at the AIChE 1989 Spring National Meeting, Houston, Texas, Apr. (1989).

O'Brien, K. C., W. J. Koros, and G. R. Husk; "Influence of Casting and Curing Conditions on Gas Separation and Transport in Polyimide Films", Polym. Eng. Sci. **27**, 3, 211 - 217, (1987).

Ogden, I. K., R. E. Richards, and A. A. Rizvi; "Polymers for Gas Separation Membranes", Proc. 4th BOC Prestley Conf., Leeds Univ., Royal Society of Chemistry, London (1986), Special Publication No. **62**, pp. 114 - 144.

Parro, D.; "Membrane CO_2 Separation Proves out at SACROC Tertiary Recovery Project"; Oil Gas J. **82**, 39, 85-88, (1984).

Paul, D. R. and Y. P. Yampol'skii, in "Polymeric Gas Separation Membranes", D. R. Paul and Y.P. Yampol'skii Eds., CRC Press, Boca Raton (1994), 1-15.

Pfromm, P. H., I. Pinnau, and W. J. Koros, "Gas Transport through Integral - Asymmetric Membranes: a Comparison to Isotropic Film Transport Properties", J. Appl. Polym. Sci. **48**, 2161 - 2171, (1993).

Puleo, A. C., D. R. Paul, and S. S. Kelly, "The Effect of Degree of Acetylation on Gas Sorption and Transport Behaviour in Cellulose Acetate", J. Memb. Sci. **47**, 301 - , (1989).

Rangarajan, R., M. A. Mazid, T. Matsuura, and S. Sourirajan; "Permeation of Pure Gases Under Pressure Through Asymmetric Porous Membranes. Membrane Characterization and Prediction of Performance", Ind. Eng. Chem. Process Des. Dev. **23**, 79 - 87, (1984).

Rezac, M. E. and W. J. Koros, "Preparation of Polymer - Ceramic Composite Membranes with Thin Defect-Free Separating Layer", J. Appl. Polym. Sci. **46**, 1927 - 1938, (1992).

Robeson, L. M. "Correlation of Separation Factor Versus Permeability for Polymeric Membranes", J. Memb. Sci. **62**, 165 - 185, (1991).

Ruston, M., "Recent Advances in Cellulosic Membranes for Gas Separation and Pervaporation", in: The Membrane Alternative: Energy implications for Industry, Watt Committee Report number 21, J.A. Howell Ed., Elsevier, London, (1990).

Sada, E., H. Kumazawa, and P. Xu, "Permeation of Carbon Dioxide through Homogeneous and Asymmetric Polysulfone Membranes", J. Polym. Sci.: Part B: Polym. Phys. **27**, 919 - 927, (1989).

Schell, W. J., R. W. Lawrence, and W. M. King; "Membrane Application of Coal Conversion Processes", Final Report to the Energy Research and Development Adminstration, Report Number FE-2000-4, (1976).

Schendel, R.L.,"Separation of Acid Gas and Hydrocarbons", Proc. 4th BOC Prestley Conf., Leeds Univ., Royal Society of Chemistry, London (1986), Special Publication No. **62**, pp. 311-328.

Sourirajan S., "Separation of Gases by Flow Under Pressure Through Porous Membranes", Nature **199**, 590 - 591, (1963).

Spillmann, R. W., Chem. Eng. Prog. **85** 41-62, (1989).

Stanley, M., "Thomas Graham and Gaseous Diffusion", Proc. 4th BOC Prestley Conf., Leeds Univ., Royal Society of Chemistry, London (1986), Special Publication No. **62**, pp. 161-174.

Stern, S. A., V. M. Shah, and B. J. Hardy "Structure-Permeability Relationships in Silicone Polymers", J. Polym. Sci.: Polym. Phys. Ed. **25**, 1263, (1987).

Stern, S. A., Y. Mi, Y. Yammamoto, and A.K. St.Clair, J. Polym. Sci. Polym. Phys. Ed. **27**, 1887, (1989).

Süer, M. G., N. Baç, and L. Yilmaz, "Gas Permeation Characteristics of Polymer-Zeolite Mixed Matrix Membrane", J. Memb. Sci. **91**, 77 - 86, (1994).

Uchytil, P., X. Q. Nguyen, and Z. Brož, "Characterization of Membrane Skin Defects by Gas Permeation Method ", J. Memb. Sci. **73**, 47-53, (1992).

Uhlhorn, R. J. R., K. Keizer, and A. J. Burggraaf, "Formation of and Gas Transport Mechanisms in Ceramic Membranes", in "Advances in Reverse Osmosis and Ultrafiltration", T. Matsuura and S. Sourirajan Eds., National Research Council Canada, Ottawa, Canada, (1989), pp. 239 - 258.

van't Hof, J. A., A. J. Reuvers, R. M. Boom, H. H. M. Rolevink, and C. A. Smolders; "Preparation of Asymmetric Gas Separation Membranes With High Selectivity by a Dual-Bath Coagulation Method", J. Memb. Sci. **70**, 17 - 30, (1992).

Verghese, J., "The Future of Membranes in the Offshore Industries", in Membrane Alternative: Energy Implications for Industry", Ed. J.A. Howell, Elsevier, London, (1990).

Vos, K.D. and F.O. Burris, "Drying Cellulose Acetate Reverse Osmosis Membranes", Ind. Eng. Chem. Prod. Res. Devel. **8**, 84 - 89, (1969).

Ward, W. J. III, Browal W. R., and Salemme R. M., "Ultrathin Silicone/Polycarbonate Membranes for Gas Separation Processes", J. Memb. Sci. **1**, 99 - 108, (1976).

Werner, U., "Some Technical and Economical Aspects of Gas Separation by Means of Membranes", Proc. 4th BOC Prestley Conf., Leeds Univ., 1986. 4th BOC Prestley Conf., Leeds Univ., Royal Society of Chemistry, London (1986), Special Publication No. **62**, pp. 43 - 63.

Xuesong, G., T. Zhoushi, and L. Fengcai, "Gas Permeation Properties of some Polypyrrolones", J. Memb. Sci. **88**, 37 - 45, (1994).

Yamamoto, N., Y. Mi, and S.A. Stern, "Structural Permeability Relationships of Polyimide Membranes II", J. Polym. Sci.: Part B: Polym. Phys. **28**, 2291 - 2304, (1990).

Zhang, W., M. Satoh, and J. Komiyama, "A New Apparatus and Procedure for Gas Permeability Measurements on Water Swollen Gel Membranes", J. Memb. Sci. **40**, 343 - 350, (1989).

Zolandz, R.R. and G.K. Fleming, in "Membrane handbook", W. S. Ho and K. K. Sirkar Eds., Van Nostrand Reinhold, New york (1992), pp. 19 - 53.

APPENDICES

Appendix A: Sample Calculations

Appendix B: Constant Volume System Process Control Computer Program

APPENDIX A: SAMPLE CALCULATIONS

A.1. Raw Permeation rate Data for uncoated and Coated Membranes

Table A.1: Raw Permeation Rate Data for Uncoated Membranes "a" and "b".

	He	H_2	O_2	N_2	CO_2	CH_4
Δp, kPa			Permeation Rate, cm^3/min			
			Membrane "a"			
350	0.780	0.404	0.100	0.090	0.167	0.108
700	1.85	0.840	0.245	0.210	0.402	0.240
1050	3.24	1.44	0.410	0.352	0.618	0.409
1400	4.50	1.97	0.580	0.493	0.840	0.610
1750	5.94	2.94	0.746	0.658	1.18	0.832
2100	8.24	4.02	0.900	0.828	1.46	1.06
			Membrane "b"			
350	0.720	0.396	0.110	0.096	0.167	0.108
700	1.80	0.877	0.253	0.216	0.253	0.240
1050	3.00	1.71	0.410	0.360	0.394	0.402
1400	4.09	2.45	0.576	0.499	0.543	0.593
1750	5.81	3.53	0.746	0.660	0.749	0.803
2100	7.36	4.69	0.902	0.828	0.940	1.05

Table A.2: Raw Permeation Rate Data for Coated Membranes "a" and "b".

	He	H_2	O_2	N_2	CO_2	CH_4
Δp, kPa			Permeation Rate, cm^3/min			
			Membrane "a"			
700	0.927	0.222	0.019	<0.005	0.092	<0.005
1400	2.34	0.600	0.040	<0.005	0.185	<0.005
2100	4.12	1.00	0.058	<0.005	0.275	<0.005
			Membrane "b"			
700	0.830	0.223	0.013	<0.005	0.054	<0.005
1400	2.02	0.623	0.028	<0.005	0.107	<0.005
2100	3.48	1.20	0.039	<0.005	0.190	<0.005

A.2. Sample Calcuiations

The sample calculations are divided into two parts. In the first part, the calculations of the permeation rates, the permeabilities, the overall resistances, and the separation factors are given. In the second part, the calculations of the local resistances on uncoated and coated membranes are presented.

A.2.1. Permeation Rates, Permeabilities, Overall Resistances, and Separation Factors

All sample calculations below were done based on the data from membrane "a" for H_2 gas at 700 kPa except otherwise mentioned. Where necessary, helium gas data were used as the reference gas. Similar treatment may be applied to other gases.

i) Permeation rate:

The permeation rates were measured in cm^3/s and converted into mol/s. The results are reported in Table 4.2-a & b.

$$Q_{H_2}=0.84\frac{cm^3}{\min}\times\frac{1\ \min}{60\ s}\times\frac{1\ mol}{22400\ cm^3}=6.25\times10^{-7}\frac{mol}{s}$$

ii) Permeability

The data are given in Table 4.2-a. Rearrangement of Equation 2.15 gives:

$$P/l = \frac{Q}{A\Delta p}$$

Substituting Q = 6.25 × 10^{-7} mol/s, A = 9.62 × 10^{-4} m^2, and Δp = 7 × 10^5 Pa gives

P/l = 9.28 × 10^{-10} mol/m^2 s Pa

iii) Overall resistance:

The data are given in Table 4.2-a. Rearrangement of Equation 2.18 gives:

$$R_t = \frac{\Delta p}{Q}$$

Substituting Δp = 7 × 10^5 Pa and Q = 6.25 × 10^{-7} mol/s gives:

R_t = 1.12 × 10^{12} Pa s/mol

iv) Ideal separation factor

The data are given in Table 4.2-a. Using Equation 2.22 with helium as the reference and hydrogen as the experimental gases and substituting Q_{He} = 13.8 × 10^{-7} mol/s, and Q_{H2} = 6.25 × 10^{-7} mol/s gives:

α = 2.2

v) Actual separation factor

The data and the results are shown in Table 4.8. the following calculation is done based on the CO_2 feed mole fraction of 0.25. Equation 2.24 may be written for CO_2 and CH_4 as:

Substituting y_{CO2}= 0.955, y_{CH4}= 0.045, x_{CO2}= 0.25, and x_{CH4}= 0.75 gives:

$$\alpha = \frac{y_{CO_2}/y_{CH_4}}{x_{CO_2}/x_{CH_4}}$$

$\alpha = 64$

vi) Permeability coefficient

The data are given in Table 4.10. Rearrangement of Equation 2.15 results in:

$$P = \frac{Ql}{A\Delta p}$$

Substituting $Q = 48.7 \times 10^{-10}$ mol/s, $l = 50 \times 10^{-6}$ m, $A = 9.62 \times 10^{-4}$ m^2, and $\Delta p = 6.66 \times 10^5$ Pa gives:

$P = 3.80 \times 10^{-16}$ mol m/m^2 s Pa.

A.2.2. Calculation of Local Resistances

Equations 2.27 and 2.28 were used to calculate the matrix resistance, R_2, and the pore resistance, R_3, of the uncoated membranes. Equations 2.32 to 2.36 were used to calculate the pore resistance, R_1, and coated pore resistance, R_{3c}, of the coated membranes.

$$R_{2_{Ha}} = \frac{(\alpha_2 - \alpha_3) R_{t_{Ha}} R_{t_{gas}}}{\alpha_2 (R_{t_{gas}} - \alpha_3 R_{t_{Ha}})} \qquad (2.27)$$

$$R_{3_{He}} = \frac{(\alpha_2 - \alpha_3) R_{t_{He}} R_{t_{gas}}}{\alpha_3 (\alpha_2 R_{t_{He}} - R_{t_{gas}})} \tag{2.28}$$

$$a = \alpha_1 (\alpha_{3c} - \alpha_2) \tag{2.32}$$

$$b = (\alpha_2 - \alpha_{3c})(R_{tc_{gas}} + \alpha_1 R_{tc_{He}}) - \alpha_2 (\alpha_1 - \alpha_{3c}) R_{2_{He}} \tag{2.33}$$

$$c = (\alpha_{3c} - \alpha_2) R_{tc_{He}} R_{tc_{gas}} + \alpha_2 (R_{tc_{gas}} - \alpha_{3c} R_{tc_{He}}) R_{2_{He}} \tag{2.34}$$

$$R_{1_{He}} = \frac{-b \pm \sqrt{b^2 - 4ac}}{2a} \tag{2.35}$$

$$R_{3c_{He}} = \frac{R_{2_{He}} (R_{1_{He}} - R_{tc_{He}})}{R_{tc_{He}} - (R_{1_{He}} + R_{2_{He}})} \tag{2.36}$$

In the following sample calculations, the procedure explained in Section 2.3.3 will be followed.

Step one: Pair a gas with helium. In this example hydrogen is paired with helium to solve the above equations. The calculations are done for membrane "a" at 700 kPa.

Step two: choose a value for α_3. Equations 2.27 and 2.28 are solved for $R_{2\,He}$ and $R_{3\,He}$. The unknowns in equations can be found as follows:

$\alpha_2 = 4.1$ (from Table 4.6, H_2 data).

$\alpha_3 = 1.52$ (randomly chosen between $\alpha_{3,\,Low} = 0.707$ and $\alpha_{3,\,High} = 2.1$. The latter values are reported in Table 4.6 for hydrogen).

$R_{t\,He} = 0.51 \times 10^{12}$ Pa s/mol (from Table 4.2-a for helium at 700 kPa).

$R_{t\,H2} = 1.12 \times 10^{12}$ Pa s/mol (from Table 4.2-a for hydrogen at 700 kPa).

Substituting these values in Equations 2.27 and 2.28 gives:

$R_{2\,He} = 1.04 \times 10^{12}$ Pa s/mol

$R_{3\,He} = 0.998 \times 10^{12}$ Pa s/mol

Step three: Solve Equations 2.32 to 2.34. The unknown in these equations can be found for hydrogen as follows:

$\alpha_1 = 0.55$ (from Table 4.6)

$\alpha_2 = 4.1$ (from Table 4.6)

$\alpha_{3c} = 0.55$ (from Table 4.6)

$R_{tc\,He} = 1.05 \times 10^{12}$ Pa s/mol (from Table 4.3-a)

$R_{tc\,H2} = 4.24 \times 10^{12}$ Pa s/mol (from Table 4.3-a)

$R_{2\,He} = 1.04 \times 10^{12}$ Pa s/mol (from step two)

Substituting these values in the above equations gives:

a = 1.9525

b = -17.1021

c = 0.15085

Step four: calculation of $R_{1\,He}$. The values of a, b, and c are substituted in Equation 2.35. Two different roots are possible to this equation. These two roots are 8.75 and 0.0088. While the second root is high and unacceptable, the first root is reasonable. The other way to check the correct answer is that at the end of the procedure, when helium is paired with all gases and a series of answers are obtained a comparison of the results show that the root one results are very close to each other, while, the root two results differ in few orders of magnitude. In this example the acceptable value for $R_{1\,He}$ is calculated to be:

$R_{1\,He} = 0.00883 \times 10^{12}$ Pa s/mol

Step five: calculation of $R_{3c\,He}$. Equation 2.35 is used to calculate $R_{3c\,He}$. The unknown in this equation are found as follows.

$R_{1\,He}$= 0.00883 × 10^{12} Pa s/mol (from step four)

$R_{2\,He}$= 1.04 × 10^{12} Pa s/mol (from step two)

$R_{tc\,He}$= 1.05 × 10^{12} Pa s/mol (from Table 4.3-a)

Then $R_{3c\,He}$ is calculated:

$R_{3c\,He}$= 846 × 10^{12} Pa s/mol

Step six: Choose the next gas to be paired with helium. Helium is paired with another gas, e.g., oxygen. The $R_{2\,He}$ and $R_{3\,He}$ values calculated above are substituted in Equations 2.27 and 2.28, and the corresponding value for $\alpha_{3\,O2}$ is calculated.

$\alpha_{3(O2)}$= 3.86

Step seven: repeat steps three to five for the newly chosen gas. The results are as follows.

a = 53.04

b = -4528.73

c = 59.901

$R_{1\,He}$= 0.0132 × 10^{12} Pa s/mol (this value is slightly different from that calculated in step four)

$R_{3c\,He}$= 185 × 10^{12} Pa s/mol (this value is different from that calculated in step five)

Step eight: repeat step six and seven. The whole procedure is repeated for other gases until are gases are paired with helium.

Step nine: choose a new value for $\alpha_{3\,H2}$. Repeat steps 2 to 8 and calculate the corresponding values of $R_{2\,He}$, $R_{3\,He}$, $R_{1\,He}$, and $R_{3c\,He}$. New values are also calculated for α_3s for the gases.

Apparently, infinite series of answers are possible for $R_{2\,He}$, $R_{3\,He}$, $R_{1\,He}$, $R_{3c\,He}$, and α_3s.

However, only a narrow range of α_3s satisfy the conditions explained in Section 2.3.3. In fact, α_3s can be calculated with three significant digits. In addition, while the values of $R_{2\,He}$ and R_{3He} are definite, $R_{1\,He}$ values are slightly different when they are obtained by pairing helium with different gases. In this case, the average of the values are calculated and reported for $R_{1\,He}$. In our example this average is $R_{1\,He}= (1.04 \pm 0.00) \times 10^{12}$ Pa s/mol. However, $R_{3c\,He}$ is very sensitive to $R_{1\,He}$ value, and the results obtained by pairing helium with different gases differ by one order of magnitude. In this case, the $R_{3c\,He}$ is calculated by substituting the average of $R_{1\,He}$ in Equation 2.36. In the present example, the value $R_{1\,He}= 1.04 \times 10^{12}$ was substituted in Equation 2.36 to obtain $R_{3c\,He}= 400 \times 10^{12}$ Pa s/mol. Some sample results are shown in Table A.3 at the end of this section. In the above sample calculation, the value of $\alpha_{3\,H2}$ was chosen such that the best set of answers were obtained.

When $R_{2\,He}$, $R_{3\,He}$, $R_{1\,He}$, and $R_{3c\,He}$ are calculated, R_2, R_3, R_1, and R_{3c} values for other gases can be obtained using Equation 2.23.

$$\alpha_i = \frac{R_{i_{gas}}}{R_{i_{He}}} \qquad (2.23)$$

For example substituting $R_{2\,He}= 1.04 \times 10^{12}$ Pa s/mol (calculated in step two), and $\alpha_{2\,He}= 4.1$ (from Table 4.6) gives:

$R_{2\,H2}= 4.27 \times 10^{12}$ Pa s/mol.

Similarly, substitution of $R_{3\,He}= 0.998 \times 10^{12}$ Pa s/mol and $\alpha_{3\,H2}= 1.52$ in the same equation gives:

$R_{3\,H2}= 1.52 \times 10^{12}$ Pa s/mol.

Also, substitution of $R_{1\,He}= 0.01 \times 10^{12}$ Pa s/mol and $\alpha_{1\,H2}= 0.55$ in the same equation gives:

$R_{1\,H2}= 0.005 \times 10^{12}$ Pa s/mol.

Finally, substitution of $R_{3c\,He}$= 400 × 10^{12} Pa s/mol and $\alpha_{3c\,H2}$= 0.55 in the same equation gives: $R_{3c\,H2}$= 220 × 10^{12} Pa s/mol.

Table A.3: Results from the local resistances calculations. The results in the boxes are the best solutions.

Membrane "a"

p=350 kPa Gas	α_i	$R_{i\,Ni}$	$R_{i\,Ni}$	$R_{i\,gas}$	$R_{i\,gas}$
H2	1.7	2.739512	0.768263	11.22733	1.3062
O2	6.2	2.744005	0.76791	243.7152	4.763787
N2	6.82	2.735602	0.768571	2355.001	5.240166
CO2	3.85	2.733835	0.76871	52.02909	2.958158
CH4	5.62	2.738913	0.76831	2355.001	4.318142
H2	1.6	2.038328	0.850291	8.359096	1.360333
O2	5.64	2.040774	0.849866	181.4535	4.795173
N2	6.17	2.038931	0.850186	1753.371	5.245783
CO2	3.55	2.038963	0.85018	38.73727	3.018238
CH4	5.08	2.037024	0.850518	1753.371	4.319057
		2.038804	0.850208		
H2	1.5	1.64878	0.943256	6.75451	1.415543
O2	5.11	1.646584	0.943976	146.6223	4.822282
N2	5.56	1.6461	0.944136	1416.8	5.246945
CO2	3.26	1.64899	0.943187	31.30139	3.076446
CH4	4.58	1.646753	0.943921	1416.8	4.322124
		1.647441	0.943695		
H2	1.4	1.400887	1.049502	5.739565	1.470084
O2	4.62	1.399656	1.050193	124.5906	4.851277
N2	5	1.398994	1.050567	1203.909	5.2503
CO2	2.98	1.399709	1.050164	26.59798	3.129179
CH4	4.12	1.400224	1.049874	1203.909	4.326247
		1.399894	1.05006		
H2	1.3	1.229268	1.172093	5.040911	1.523464
O2	4.17	1.23188	1.169729	109.4247	4.886804
N2	4.49	1.230921	1.170594	1057.362	5.261811
CO2	2.71	1.226899	1.174256	23.36032	3.175837
CH4	3.69	1.228485	1.172806	1057.362	4.324294
		1.229491	1.171895		
H2	1.2	1.105415	1.315116	4.325026	1.577714
O2	3.73	1.103852	1.314496	98.22617	4.904063
N2	4	1.103677	1.314744	949.1517	5.259048
CO2	2.46	1.104595	1.313443	20.96963	3.234315
CH4	3.29	1.102786	1.316011	949.1517	4.325567
		1.103665	1.314762		
H2	1.53	1.746167	0.91409	7.16538	1.397937
O2	5.27	1.748066	0.913571	155.5412	4.815118
N2	5.74	1.745272	0.914336	1502.982	5.24455
CO2	3.35	1.751632	0.9126	33.20542	3.060843
CH4	4.73	1.747131	0.913826	1502.982	4.321728
		1.747654	0.913685		
H2	1.52	1.712195	0.923684	7.024386	1.403529
O2	5.22	1.714992	0.922872	152.4806	4.820013
N2	5.68	1.710908	0.924059	1473.408	5.244765
CO2	3.32	1.715894	0.922611	32.55203	3.065602
CH4	4.68	1.712335	0.923643	1473.408	4.321391
		1.713265	0.923374		
H2	1.51	1.679767	0.933405	6.889182	1.409201
O2	5.17	1.683184	0.932354	149.5457	4.824879
N2	5.62	1.677876	0.93399	1445.048	5.244839
CO2	3.29	1.681713	0.932806	31.92548	3.070377
CH4	4.63	1.678902	0.933673	1445.048	4.320926
		1.680288	0.933245		
H2	0.8	0.818876	2.244767	3.499538	1.621838
O2	2.52	0.862148	1.973272	75.96558	5.108789
N2	2.67	0.862254	1.972715	734.0495	5.412884
CO2	1.71	0.861781	1.975194	16.21737	3.466678
CH4	2.2	0.86267	1.970539	734.0495	4.460054
		0.853546	2.027297		
H2	0.707	0.778959	2.611631	3.30428	1.666107
O2	2.18	0.813018	2.289997	71.72705	5.13736
N2	2.3	0.812885	2.291053	693.0928	5.420151
CO2	1.49	0.812305	2.295677	15.31252	3.511315
CH4	1.89	0.812442	2.294578	693.0928	4.45395
		0.805922	2.356587		

Table A.3 (Membrane "a" continued)

p=700 kPa

Gas	α_{ij}	$R_{1/m}$	$R_{1/m}$	$R_{1/gas}$	$R_{1/gas}$	$R_{1/m}$	$R_{X/m}$	a	b	c
H2	1.7	1.321585	0.830484	5.424959	1.410767	-0.23022	40.89737	1.9525	-17.1021	-4.04065
O2	4.6	1.321617	0.830471	117.7195	3.818222	-0.25998	148.8037	53.04	-4528.73	-1180.98
N2	5.42	1.323231	0.829835	1137.514	4.498861	-0.27152	1022.208	1030.56	-507774	-137947
CO2	3.11	1.323862	0.829588	25.13113	2.58145	-0.2633	164.6307	2.0779	-200.527	-52.9429
CH4	4.74	1.323161	0.829863	1137.514	3.934428	-0.27263	3312.835	318.0631	-507516	-138389
	Average	1.322691	0.830048			-0.25953	131.6104			
H2	1.6	1.1457	0.919156	4.694869	1.471277	-0.08108	88.65233	1.9525	-17.1021	-1.39951
O2	4.17	1.143194	0.920775	101.8534	3.836322	-0.08547	168.1079	53.04	-4528.73	-387.468
N2	4.89	1.143854	0.920347	984.2014	4.498709	-0.09279	1229.032	1030.56	-507774	-47125.5
CO2	2.85	1.144264	0.920082	21.74399	2.621947	-0.08723	184.9432	2.0779	-200.527	-17.5073
CH4	4.28	1.14509	0.919548	984.2014	3.93752	-0.09476	3978.326	318.0631	-507516	-48095.3
	Average	1.14442	0.919981			-0.08827	211.6871			
H2	1.5	1.02035	1.01965	4.181577	1.530155	0.02832	-783.947	1.9525	-17.1021	0.482763
O2	3.78	1.019555	1.020445	90.76388	3.856287	0.035874	190.4586	53.04	-4528.73	162.3941
N2	4.41	1.018909	1.021093	877.0442	4.499002	0.031781	1504.719	1030.56	-507774	16136.34
CO2	2.61	1.020383	1.019617	19.37656	2.662674	0.034597	208.0661	2.0779	-200.527	6.935049
CH4	3.86	1.019897	1.020103	877.0442	3.937902	0.030317	4871.127	318.0631	-507516	15385.85
	Average	1.019819	1.020182			0.032177	519.9513			
H2	1.4	0.926493	1.134501	3.796515	1.58938	0.112072	-75.9947	1.9525	-17.1021	1.892152
O2	3.41	0.925443	1.136079	82.39977	3.872	0.128473	217.8129	53.04	-4528.73	580.9435
N2	3.96	0.924353	1.137725	796.2225	4.496516	0.126095	1905.198	1030.56	-507774	64011.28
CO2	2.38	0.926932	1.133843	17.59096	2.702451	0.1267	235.6118	2.0779	-200.527	25.37345
CH4	3.47	0.925979	1.135271	796.2225	3.940129	0.12416	6152.213	318.0631	-507516	63008.23
	Average	0.92584	1.135484			0.1235	-1299.92			
H2	1.3	0.853584	1.267021	3.499327	1.647383	0.178284	-41.0362	1.9525	-17.1021	2.986972
O2	3.06	0.851697	1.2712	75.92132	3.880713	0.201173	251.8508	53.04	-4528.73	908.9132
N2	3.55	0.852358	1.269732	733.6217	4.502134	0.197931	2514.641	1030.56	-507774	100464
CO2	2.16	0.85411	1.265864	16.20792	2.739327	0.198595	268.8419	2.0779	-200.527	39.74174
CH4	3.11	0.853494	1.267218	733.6217	3.944123	0.196595	8122.667	318.0631	-507516	99762.94
	Average	0.853049	1.268207			0.194516	-299.616			
H2	1.2	0.795314	1.421627	3.258612	1.70799	0.231961	-28.6289	1.9525	-17.1021	3.861966
O2	2.75	0.795949	1.419601	70.79047	3.908739	0.256214	292.0568	53.04	-4528.73	1156.842
N2	3.17	0.795019	1.42257	684.0428	4.50571	0.255158	3573.461	1030.56	-507774	129495.4
CO2	1.95	0.795927	1.419673	15.11257	2.771651	0.256114	309.5498	2.0779	-200.527	51.22152
CH4	2.77	0.794784	1.423325	684.0428	3.937166	0.255271	11641.63	318.0631	-507516	129533.2
	Average	0.795399	1.42136			0.250944	-173.752			
H2	1.1	0.747677	1.604344	3.066434	1.763594	0.276365	-22.2829	1.9525	-17.1021	4.577301
O2	2.44	0.74738	1.605711	66.55266	3.913417	0.304225	347.1783	53.04	-4528.73	1372.846
N2	2.81	0.747427	1.605496	643.0931	4.506845	0.302667	5942.45	1030.56	-507774	153592.2
CO2	1.75	0.748519	1.600478	14.20787	2.806754	0.303032	360.3623	2.0779	-200.527	60.57529
CH4	2.46	0.747911	1.603267	643.0931	3.945494	0.302118	19233.86	318.0631	-507516	153300.7
	Average	0.747783	1.603859			0.297682	-124.033			
H2	1	0.708005	1.823605	2.900984	1.826582	0.313714	-18.4327	1.9525	-17.1021	5.173023
O2	2.16	0.708591	1.819726	62.99362	3.942032	0.342608	418.056	53.04	-4528.73	1545.353
N2	2.47	0.707461	1.82722	608.7024	4.507787	0.34257	15876.99	1030.56	-507774	173827.3
CO2	1.55	0.707353	1.827942	13.44808	2.828773	0.34381	429.3025	2.0779	-200.527	68.69759
CH4	2.16	0.707557	1.826582	608.7024	3.942032	0.342453	52083.83	318.0631	-507516	173762.7
	Average	0.707793	1.825015			0.337031	-97.5058			
H2	0.9	0.674455	2.091589	2.766722	1.879361	0.34557	-15.85	1.9525	-17.1021	5.676818
O2	1.88	0.673843	2.097491	60.02845	3.931801	0.377021	524.5765	53.04	-4528.73	1699.888
N2	2.16	0.674598	2.090215	580.0502	4.517388	0.375387	-30336.7	1030.56	-507774	190466.6
CO2	1.37	0.674678	2.089443	12.81506	2.865195	0.376202	516.3809	2.0779	-200.527	75.1445
CH4	1.89	0.67481	2.088179	580.0502	3.952714	0.375185	-97138.1	318.0631	-507516	190367.6
	Average	0.674477	2.091383			0.369873	-81.1913			
H2	1.51	1.031241	1.009001	4.225556	1.524486	0.018706	-20025.3	1.9525	-17.1021	0.319228
O2	3.82	1.030944	1.009286	91.72313	3.856746	0.024682	187.9009	53.04	-4528.73	111.7445
N2	4.46	1.03063	1.009587	886.3134	4.502902	0.020092	1470.368	1030.56	-507774	10201.84
CO2	2.63	1.029547	1.010629	19.58134	2.655299	0.025575	205.9446	2.0779	-200.527	5.127018
CH4	3.9	1.030623	1.009593	886.3134	3.937515	0.019599	4769.229	318.0631	-507516	9946.794
	Average	1.030597	1.009619			0.021731	455.2792			
H2	1.52	1.042454	0.998493	4.270474	1.518931	0.00883	845.689	1.9525	-17.1021	0.150854
O2	3.86	1.042601	0.998358	92.78975	3.853734	0.013229	185.4098	53.04	-4528.73	59.90141
N2	4.51	1.042625	0.998336	896.62	4.502679	0.008131	1437.55	1030.56	-507774	4128.499
CO2	2.66	1.043649	0.997399	19.80905	2.655682	0.011694	202.8343	2.0779	-200.527	2.344648
CH4	3.94	1.041579	0.999297	896.62	3.933604	0.008653	4671.499	318.0631	-507516	4391.593
	Average	1.042581	0.998377			0.010107	403.2281			

Table A.3 (Membrane "a" continued)

p=1050 kPa

Gas	α_i	$R_{i\,He}$	$R_{i\,He}$	$R_{i\,gas}$	$R_{i\,gas}$
H2	2	2.208585	0.549466	9.050388	1.099079
O2	6.37	2.205378	0.549665	196.4596	3.500566
N2	7.27	2.20015	0.549991	1898.374	3.995152
CO2	4.39	2.214145	0.549123	41.94082	2.412478
CH4	6.4	2.208799	0.549453	1898.374	3.517053
Average		2.207412	0.549539		
H2	1.9	1.606775	0.605927	6.598095	1.150584
O2	5.82	1.608986	0.605614	143.2269	3.524421
N2	6.61	1.610675	0.605375	1383.991	4.002822
CO2	4.07	1.611415	0.60527	30.57654	2.464673
CH4	5.81	1.608606	0.605668	1383.991	3.518366
Average		1.609291	0.605571		
H2	1.8	1.286663	0.668662	5.27944	1.203105
O2	5.31	1.289683	0.66785	114.6025	3.54916
N2	5.99	1.287191	0.66852	1107.395	4.003667
CO2	3.76	1.28624	0.668777	24.4657	2.513153
CH4	5.27	1.288563	0.66815	1107.395	3.522425
		1.287668	0.668392		
H2	1.7	1.087973	0.738778	4.463638	1.25536
O2	4.83	1.088726	0.738431	96.89361	3.566698
N2	5.43	1.089777	0.737948	936.2753	4.009766
CO2	3.47	1.088667	0.738458	20.68515	2.562411
CH4	4.77	1.088318	0.738619	936.2753	3.522392
Average		1.088692	0.738447		
H2	1.6	0.952633	0.817658	3.903639	1.308874
O2	4.38	0.951289	0.818651	84.73752	3.583043
N2	4.9	0.951798	0.818274	818.812	4.008427
CO2	3.19	0.952497	0.817759	18.09003	2.609568
CH4	4.31	0.952318	0.81789	818.812	3.52578
		0.952107	0.818046		
H2	1.5	0.854512	0.907055	3.501853	1.361264
O2	3.97	0.854053	0.907573	76.01582	3.602811
N2	4.42	0.853988	0.907646	734.5349	4.01119
CO2	2.92	0.853119	0.90863	16.2281	2.649927
CH4	3.89	0.854879	0.906642	734.5349	3.530211
		0.85411	0.907509		
H2	1.4	0.780113	1.009223	3.19582	1.414427
O2	3.58	0.77902	1.011058	69.37268	3.616892
N2	3.97	0.779019	1.011059	670.3427	4.010911
CO2	2.67	0.780152	1.009157	14.8099	2.697515
CH4	3.49	0.779038	1.011027	670.3427	3.525965
		0.779468	1.010305		
H2	1.3	0.72176	1.12711	2.956978	1.466978
O2	3.22	0.721055	1.128833	64.18807	3.633593
N2	3.56	0.721378	1.128041	620.2443	4.017264
CO2	2.42	0.720395	1.130455	13.70307	2.730837
CH4	3.13	0.721483	1.127786	620.2443	3.532033
		0.721214	1.128445		
H2	1.2	0.674768	1.264644	2.76465	1.51953
O2	2.88	0.674071	1.267101	60.01314	3.646872
N2	3.17	0.673986	1.2674	579.9022	4.014092
CO2	2.19	0.674239	1.266507	12.81179	2.773142
CH4	2.79	0.674461	1.265724	579.9022	3.532907
Average		0.674305	1.266275		
H2	1.1	0.636113	1.427184	2.581087	1.612403
O2	2.56	0.635401	1.430785	56.02848	3.752501
N2	2.81	0.635482	1.430372	541.3988	4.118956
CO2	1.96	0.634673	1.43449	11.96114	2.873009
CH4	2.2	0.605999	1.606273	541.3988	3.224806
Average		0.629534	1.465821		
H2	1.65	1.014442	0.777023	4.160789	1.281716
O2	4.6	1.013679	0.777471	90.31956	3.57327
N2	5.16	1.014809	0.776807	872.7508	4.008277
CO2	3.33	1.015434	0.776441	19.2817	2.586737
CH4	4.54	1.015768	0.776247	872.7508	3.526662
Average		1.014826	0.776798		

Table A.3 (Membrane "a" continued)

p=1400 kPa

Gas	α_i	$R_{i\,ss}$	$R_{i\,ss}$	$R_{i\,gas}$	$R_{i\,gas}$	$R_{i\,ss}$	$R_{ki\,ss}$	a	b	c
H2	2	1.857871	0.542681	7.622781	0.960223	-0.81464	12.33317	1.9525	-12.709	-11.649
O2	6 11	1.859155	0.542572	165.4701	2.93348	-1.02783	108.4925	53.04	-4117.67	-4288.31
N2	7.06	1.861522	0.542371	1598.925	3.389586	-1.0571	781.2741	1030.56	-507516	-537646
CO2	4.41	1.862907	0.229973	35.32508	2.117291	-1.03669	130.5188	2.0779	-192.451	-201.746
CH4	5 85	1.854619	0.542959	1598.925	2.808651	-1.05326	2533.404	318.0631	-507436	-534816
	Average	1 859215	0.480111			-0.99791	54.52133			
H2	1 9	1.408537	0.598446	5.766147	1.006625	-0.48854	15.12543	1.9525	-12.709	-6.6749
O2	5 57	1.405197	0.59905	125.1676	2.950999	-0.58935	123.1753	53.04	-4117.67	-2445.16
N2	6 4	1.406767	0.598766	1209.485	3.390735	-0.60471	961.9857	1030.56	-507516	-307279
CO2	4 08	1.403449	0.254197	26.72117	2.161594	-0.59038	149.3355	2.0779	-192.451	-114.344
CH4	5.31	1.407937	0.598554	1209.485	2.813251	-0.6073	3112.323	318.0631	-507436	-308284
	Average	1.406377	0.529802			-0.57606	63.82715			
H2	1.8	1.153759	0.660406	4.736833	1.050989	-0.29034	19.83593	1.9525	-12.709	-3 85451
O2	5 09	1.157107	0 659314	102.8239	2.971963	-0 34764	140 246	53 04	-4117.67	-1437.87
N2	5 81	1.154922	0 660026	993.5796	3.392359	-0.35382	1213.21	1030.56	-507516	-179700
CO2	3.78	1 155166	0.279888	21.95118	2.207077	-0.34743	171.285	2.0779	-192.451	-67.1137
CH4	4 82	1.155672	0 659781	993 5796	2.814315	-0.35533	3926.19	318 0631	-507436	-180348
	Average	1.155325	0.583883			-0.33891	80.16881			
H2	1.7	0.989665	0.729656	4.06086	1.097064	-0.15659	28.6238	1.9525	-12.709	-2.03799
O2	4 63	0.991259	0.728792	88.15038	2.987887	-0.18522	161.7374	53 04	-4117.67	-764.497
N2	5 26	0.989935	0.729509	851.7902	3.394447	-0.18932	1603.645	1030.56	-507516	-96122
CO2	3.49	0.991979	0.308921	18.81862	2.252209	-0.18705	198.7021	2.0779	-192.451	-36.0709
CH4	4.36	0.989431	0.729783	851.7902	2.813648	-0.18924	5202.482	318.0631	-507436	-96040
	Average	0.990454	0.642332			-0.18149	108 4013			
H2	1.6	0.875154	0.807562	3.591976	1.142247	-0.06006	49.86906	1.9525	-12.709	-0.77035
O2	4 2	0.875225	0 807501	77.97216	2.998398	-0.07118	188.6628	53.04	-4117.67	-293.379
N2	4.76	0.876274	0 80661	753.4389	3.398184	-0.07594	2266.451	1030.56	-507516	-38544.4
CO2	3.21	0 876715	0.341931	16.64574	2.291633	-0.07344	233.7112	2.0779	-192.451	-14.1445
CH4	3 95	0.877091	0.805919	753.4389	2.819922	-0.07699	7322.448	318 0631	-507436	-39067.5
	Average	0.876092	0.713904			-0.07152	167.0387			
H2	1.5	0.790701	0.895855	3.237451	1.19056	0.012972	169.3985	1.9525	-12.709	0.164538
O2	3.8	0.790036	0.896711	70.27638	3.016086	0.012753	223.0105	53.04	-4117.67	52.50472
N2	4.28	0 789367	0.897574	679.0751	3.397066	0.010799	3755.704	1030.56	-507516	5480.613
CO2	2.93	0.788309	0.381249	15.00282	2.325561	0.01389	281.804	2.0779	-192.451	2.672825
CH4	3.55	0.789699	0.897145	679.0751	2.81766	0.010353	12148.2	318.0631	-507436	5253.269
	Average	0.789622	0.793707			0.012154	350.3317			
H2	1.4	0.725846	0.996762	2.974753	1.235308	0.070195	-133.794	1.9525	-12.709	0.88249
O2	3.43	0.72532	0.997755	64.57391	3.026506	0.076639	267.8409	53.04	-4117.67	315.2627
N2	3.85	0.725019	0.998324	623.9726	3.397098	0.075038	9120.683	1030.56	-507516	38077.38
CO2	2.68	0.725141	0.423298	13.78544	2.364733	0.076389	342.9079	2.0779	-192.451	14.68898
CH4	3.2	0.726422	0.995677	623.9726	2.823562	0.073597	28665.82	318.0631	-507436	37343.93
	Average	0.72555	0.882363			0 074372	-6678.64			
H2	1.3	0 674475	1.113193	2.764034	1.281728	0.116261	-49.7767	1.9525	-12.709	1.451164
O2	3.08	0 673565	1.115681	59.99975	3.03671	0.127806	330.2433	53.04	-4117.67	525.3985
N2	3.45	0 673962	1.114592	579.7729	3.401509	0.126022	-27818.2	1030.56	-507516	63941.74
CO2	2.44	0 674771	0.471771	12.80894	2.405705	0.126287	429 8897	2.0779	-192.451	24.2709
CH4	2.86	0 674001	1.114487	579.7729	2.819802	0.125994	-89617 8	318 0631	-507436	63929.04
	Average	0.674155	0.985945			0.124474	-332.047			
H2	1 2	0.632779	1.249028	2.593423	1.326954	0.154153	-31.274	1.9525	-12.709	1.912735
O2	2.76	0 632614	1.249672	56.29625	3.051993	0.16834	418.9232	53.04	-4117.67	691.6647
N2	3 08	0 632779	1.249027	543.9562	3.405848	0.167152	-5864.39	1030 56	-507516	84803.73
CO2	2.2	0 632116	0.53082	12.0183	2.432748	0.168583	570 6946	2.0779	-192.451	32.38495
CH4	2.55	0 632421	1.250425	543.9862	2.819777	0.167557	-18828.9	318.0631	-507436	85015.8
	Average	0 632542	1.105795			0.165157	-174.533			
H2	1.1	0 598261	1.409562	2.453064	1.371727	0.185877	-23.1625	1.9525	-12.709	2.294854
O2	2 46	0.598733	1.406948	53.24944	3.067681	0.201908	558.7403	53 04	-4117.67	829.2292
N2	2.73	0.59823	1.409735	514.5451	3.404378	0.201664	-3358.74	1030.56	-507516	102305.8
CO2	1.98	0.59838	0.597524	11.36786	2.469109	0.202063	806.5376	2.0779	-192.451	38.80252
CH4	2.26	0 597938	1.411355	514.5451	2.818276	0.202029	-10830.9	318.0631	-507436	102503.7
	Average	0 598308	1.247025			0.198708	-120.585			
H2	1 51	0.798136	0.886499	3.277082	1.18262	0.006477	137.2954	1.9525	-12.709	0.082239
O2	3.85	0.799726	0.884546	71.13666	3.015289	0.003196	218.0611	53.04	-4117.67	13.16126
N2	4.34	0.799271	0.885103	687.388	3.399053	0.000913	3470.722	1030.56	-507516	463.5413
CO2	2.97	0.799656	0.375179	15.18648	2.32608	0.002673	273.864	2.0779	-192.451	0.514323
CH4	3 6	0.799654	0.884633	687.388	2.819491	0.000403	11223.9	318.0631	-507436	204.3685
	Average	0.799288	0.783192			0.002732	315.3345			

Table A.3 (Membrane "a" continued)

p=1750 kPa

Gas	α_i	$R_{i\,He}$	$R_{i\,He}$	$R_{i\,gas}$	$R_{i\,gas}$
H2	1.9	4.292683	0.441103	17.65716	0.837821
O2	7.22	4.270073	0.441343	383.2896	3.183721
N2	8.08	4.300674	0.441019	3703.697	3.562945
CO2	4.63	4.362517	0.440378	81.82586	2.041638
CH4	6.65	4.307176	0.44095	3703.697	2.932375
	Average	4.306624	0.440959		
H2	1.8	2.243902	0.486772	9.215531	0.875871
O2	6.6	2.25051	0.486463	200.0444	3.211525
N2	7.33	2.248189	0.486571	1933.014	3.566739
CO2	4.29	2.249166	0.486525	42.70612	2.087491
CH4	6.03	2.246684	0.486642	1933.014	2.934166
	Average	2.24769	0.486595		
H2	1.7	1.560976	0.537815	6.387189	0.91492
O2	6.01	1.559054	0.538044	138.6487	3.234511
N2	6.63	1.556192	0.538385	1339.752	3.568188
CO2	3.96	1.551963	0.538893	29.59917	2.131226
CH4	5.46	1.561071	0.537804	1339.752	2.938508
	Average	1.557851	0.538188		
H2	1.6	1.219512	0.595238	4.996951	0.952668
O2	5.47	1.220487	0.595006	108.4704	3.256935
N2	6	1.219022	0.595355	1048.141	3.572507
CO2	3.65	1.213366	0.596713	23.1566	2.173275
CH4	4.94	1.221455	0.594776	1048.141	2.941364
	Average	1.218768	0.595418		
H2	1.5	1.014634	0.660317	4.158511	0.990707
O2	4.96	1.014929	0.660193	90.27011	3.275939
N2	5.41	1.01364	0.660739	872.273	3.573151
CO2	3.36	1.014294	0.660462	19.27115	2.219184
CH4	4.45	1.013857	0.660647	872.273	2.939098
	Average	1.014271	0.660472		
H2	1.4	0.878049	0.734694	3.602692	1.02793
O2	4.48	0.877466	0.735102	78.20479	3.289378
N2	4.87	0.878372	0.734468	755.6867	3.57573
CO2	3.08	0.8799	0.733403	16.6954	2.261447
CH4	4.01	0.87974	0.733514	755.6867	2.944287
	Average	0.878705	0.734236		
H2	1.3	0.780488	0.820513	3.197546	1.067529
O2	4.03	0.779564	0.821536	69.41014	3.30934
N2	4.36	0.780166	0.820869	670.7047	3.580328
CO2	2.8	0.780109	0.820932	14.81789	2.299293
CH4	3.58	0.77912	0.82203	670.7047	2.939811
	Average	0.779289	0.821176		
H2	1.2	0.707317	0.920635	2.900386	1.104572
O2	3.61	0.706719	0.92165	62.9596	3.32292
N2	3.89	0.707365	0.920554	608.3737	3.580653
CO2	2.54	0.707995	0.919489	13.44081	2.33801
CH4	3.2	0.70766	0.920055	608.3737	2.945525
	Average	0.707411	0.920476		
H2	1.1	0.650407	1.038961	2.66604	1.143289
O2	3.22	0.650785	1.037998	57.87257	3.346718
N2	3.45	0.650591	1.038492	559.2181	3.585769
CO2	2.28	0.649796	1.040523	12.35482	2.369726
CH4	2.83	0.64969	1.040794	559.2181	2.94137
	Average	0.650254	1.039353		
H2	1.49	0.998565	0.667306	4.09524	0.994104
O2	4.91	0.998551	0.667312	88.89668	3.275874
N2	5.36	0.999382	0.666942	859.0017	3.576107
CO2	3.33	0.997706	0.66769	18.97794	2.221723
CH4	4.41	0.999992	0.66667	859.0017	2.942282
	Average	0.998839	0.667184		
H2	1.34	0.815965	0.784648	3.345471	1.051424
O2	4.21	0.815859	0.784745	72.6212	3.303353
N2	4.56	0.815927	0.784683	701.733	3.577979
CO2	2.91	0.816085	0.784537	15.5034	2.283315
CH4	3.75	0.816007	0.784609	701.733	2.942417
	Average	0.815969	0.784644		

Table A.3 (Membrane "a" continued)

p=2100 kPa

Gas	α_1	R_{1/N_2}	R_{1/H_2}	$R_{1/gas}$	$R_{1/gas}$	R_{1/N_2}	R_{H_2/N_2}	a	b	c
H2	2	6.095122	0.360086	25.15108	0.719902	-3.09252	9.900073	1.9525	-11.1612	-53.1893
O2	8.77	6.083435	0.360127	545.9624	3.156772	-5.03696	94.9011	53.04	-4323.47	-23122.8
N2	9.48	6.138221	0.359937	5275.592	3.412337	-5.39171	560.3764	1030.56	-507393	-2765675
CO2	5.54	6.179212	0.359797	116.5538	1.99413	-5.16415	107.7764	2.0779	-194.091	-1057.73
CH4	7.48	6.176057	0.359808	5275.592	2.692435	-5.47495	1800.791	318.0631	-507398	-2787511
	Average	6.134409	0.359951			-4.83206	54.3313			
H2	1.9	2.36495	0.397088	9.65984	0.754947	-1.22143	9.701388	1.9525	-11.1612	-16.5455
O2	8.02	2.35091	0.397486	209.6892	3.186669	-1.62082	107.9878	53.04	-4323.47	-7146.91
N2	8.59	2.345361	0.397645	2026.21	3.413153	-1.65751	698.2632	1030.56	-507393	-843840
CO2	5.16	2.360991	0.3972	44.76511	2.050276	-1.63644	122.7723	2.0779	-194.091	-323.184
CH4	6.78	2.358031	0.397282	2026.21	2.693967	-1.67561	2252.201	318.0631	-507398	-851096
	Average	2.356059	0.39734			-1.56236	46.46777			
H2	1.8	1.517184	0.4382	6.215242	0.788952	-0.66004	11.47691	1.9525	-11.1612	-8.21743
O2	7.33	1.512308	0.438609	134.9162	3.21279	-0.8147	128.3716	53.04	-4323.47	-3557.53
N2	7.8	1.515679	0.438326	1303.685	3.418794	-0.83313	901.0244	1030.56	-507393	-423441
CO2	4.8	1.518434	0.438096	28.80234	2.103873	-0.82274	145.4191	2.0779	-194.091	-161.093
CH4	6.15	1.515959	0.438303	1303.685	2.695588	-0.83517	2915.553	318.0631	-507398	-423986
	Average	1.515913	0.438307			-0.79316	52.23106			
H2	1.7	1.141943	0.48415	4.694167	0.822158	-0.38063	14.896	1.9525	-11.1612	-4.53121
O2	6.7	1.145279	0.483553	101.8978	3.24027	-0.45693	155.88	53.04	-4323.47	-1986.58
N2	7.1	1.154446	0.481937	984.6302	3.433719	-0.47335	1214.671	1030.56	-507393	-240405
CO2	4.45	1.14166	0.484201	21.75346	2.15212	-0.45433	176.6587	2.0779	-194.091	-88.6102
CH4	5.57	1.141266	0.484272	984.6302	2.693777	-0.46094	4000.652	318.0631	-507398	-233948
	Average	1.144919	0.483622			-0.44524	65.45276			
H2	1.6	0.930269	0.535843	3.815837	0.857138	-0.21182	21.57948	1.9525	-11.1612	-2.45181
O2	6.1	0.932859	0.534987	82.83158	3.267839	-0.24844	195.8312	53.04	-4323.47	-1077.38
N2	6.4	0.932554	0.535088	800.395	3.428553	-0.25209	1863.619	1030.56	-507393	-127973
CO2	4.1	0.923318	0.538177	17.68315	2.196417	-0.23951	222.904	2.0779	-194.091	-46.6057
CH4	5.05	0.93446	0.534462	800.395	2.705343	-0.25431	6002.009	318.0631	-507398	-129059
	Average	0.930692	0.535711			-0.24123	90.65386			
H2	1.5	0.794352	0.594428	3.28867	0.885289	-0.09835	38.6436	1.9525	-11.1612	-1.11661
O2	5.6	0.809405	0.586269	71.38821	3.305081	-0.12678	248.5881	53.04	-4323.47	-548.976
N2	5.8	0.800821	0.590857	689.8186	3.423119	-0.12063	3436.405	1030.56	-507393	-61224.1
CO2	3.8	0.798084	0.592356	15.24018	2.242733	-0.11585	284.3624	2.0779	-194.091	-22.5134
CH4	4.6	0.807911	0.587055	689.8186	2.714888	-0.12785	10577.11	318.0631	-507398	-64875.7
	Average	0.802115	0.590193			-0.11789	151.5984			
H2	1.4	0.699695	0.661383	2.877895	0.923182	-0.01668	161.8312	1.9525	-11.1612	-0.18675
O2	5	0.699738	0.661345	62.47138	3.297078	-0.0184	365.779	53.04	-4323.47	-79.5775
N2	5.2	0.701821	0.659495	603.656	3.428962	-0.0218	21918.26	1030.56	-507393	-11060.8
CO2	3.5	0.706029	0.655822	13.33659	2.307955	-0.02474	387.3893	2.0779	-194.091	-4.80392
CH4	4.1	0.702345	0.659033	603.656	2.703604	-0.02234	68754.97	318.0631	-507398	-11334.6
	Average	0.701916	0.659416			-0.02079	434.3684			
H2	1.3	0.629987	0.738639	2.582488	0.960431	0.044976	-79.4277	1.9525	-11.1612	0.498042
O2	4.5	0.629578	0.739202	56.05889	3.324569	0.051084	598.4902	53.04	-4323.47	220.7207
N2	4.65	0.630471	0.737975	541.6926	3.433388	0.049458	-5584.02	1030.56	-507393	25092.1
CO2	3.17	0.629354	0.73951	11.96763	2.341974	0.051275	628.4517	2.0779	-194.091	9.946602
CH4	3.66	0.629986	0.73864	541.6926	2.703983	0.049992	-17925.7	318.0631	-507398	25365.02
	Average	0.629875	0.738793			0.049357	-517.376			
H2	1.2	0.576512	0.82877	2.362572	0.995207	0.093209	-32.9096	1.9525	-11.1612	1.023358
O2	4.03	0.575917	0.830003	51.28511	3.342237	0.104309	1467.751	53.04	-4323.47	450.3985
N2	4.14	0.576218	0.829379	495.5639	3.433464	0.103654	-2582.4	1030.56	-507393	52581.97
CO2	2.88	0.576456	0.828886	10.94851	2.388497	0.103794	1327.712	2.0779	-194.091	20.12318
CH4	3.26	0.576083	0.829658	495.5639	2.703646	0.103877	-8356.71	318.0631	-507398	52703.64
	Average	0.576237	0.829339			0.101769	-167.072			
H2	1.36	0.669418	0.690922	2.745403	0.939377	0.009934	-692.437	1.9525	-11.1612	0.110688
O2	4.8	0.669776	0.690541	59.59534	3.315449	0.011258	433.3814	53.04	-4323.47	48.6666
N2	4.96	0.668782	0.6916	575.8651	3.425964	0.011194	-19063.1	1030.56	-507393	5679.729
CO2	3.36	0.67093	0.689319	12.7226	2.320815	0.010039	463.7242	2.0779	-194.091	1.948319
CH4	3.91	0.669147	0.691211	575.8651	2.70071	0.010846	-63157	318.0631	-507398	5503.024
	Average	0.669611	0.690719			0.010654	1691.971			
H2	1.37	0.676657	0.683376	2.772023	0.937002	0.003547	2235.25	1.9525	-11.1612	0.039568
O2	4.84	0.67555	0.684509	60.17319	3.310283	0.00554	417.956	53.04	-4323.47	23.95148
N2	5.02	0.676745	0.683286	581.4488	3.433393	0.003242	-35789.7	1030.56	-507393	1644.984
CO2	3.38	0.675692	0.684363	12.84596	2.311726	0.005319	451.1177	2.0779	-194.091	1.032254
CH4	3.95	0.675872	0.684179	581.4488	2.701574	0.004124	-105941	318.0631	-507398	2092.482
	Average	0.676103	0.683943			0.004354	998.1087			

Table A.3 (Membrane "b")

Membrane "b"

p=350 kPa

Gas	α_1	R_{1He}	R_{1He}	R_{2gas}	R_{1gas}
H2	1.7	5.326829	0.740339	21.76825	1.259158
O2	5.83	5.300231	0.740856	472.5304	4.318173
N2	6.63	5.352152	0.739852	4566.024	4.910718
CO2	5.81	5.271876	0.741413	100.8773	4.303359
CH4	5.89	5.29556	0.740947	4566.024	4.362614
		5.30933	0.740681		
H2	1.6	3.144309	0.819386	12.86983	1.311599
O2	5.3	3.13333	0.820134	279.3695	4.34467
N2	5.99	3.142391	0.819516	2699.525	4.910297
CO2	5.41	3.129786	0.820378	59.61067	4.434843
CH4	5.33	3.145099	0.819332	2699.525	4.369263
		3.138983	0.819749		
H2	1.5	2.281452	0.908972	9.350284	1.363672
O2	4.81	2.281445	0.908973	202.9696	4.372841
N2	5.4	2.276979	0.909684	1961.279	4.909219
CO2	5.02	2.278232	0.909484	43.33058	4.563755
CH4	4.81	2.284677	0.908461	1961.279	4.372841
		2.280557	0.909115		
H2	1.4	1.819207	1.011356	7.460467	1.415718
O2	4.35	1.821705	1.010586	161.9467	4.398839
N2	4.86	1.81907	1.011398	1564.878	4.914565
CO2	4.64	1.82129	1.010713	34.57289	4.692095
CH4	4.32	1.816858	1.012083	1564.878	4.368502
		1.819626	1.011227		
H2	1.3	1.531142	1.129492	6.276796	1.468494
O2	3.91	1.529928	1.130153	136.2524	4.416777
N2	4.36	1.533811	1.128044	1316.596	4.925102
CO2	4.26	1.530203	1.130003	29.08759	4.812141
CH4	3.87	1.529546	1.130362	1316.596	4.371593
		1.530926	1.12961		
H2	1.2	1.334414	1.267316	5.466737	1.521933
O2	3.5	1.332965	1.268626	118.6682	4.438972
N2	3.88	1.333318	1.268306	1146.681	4.920917
CO2	3.89	1.333053	1.268547	25.33366	4.9336
CH4	3.45	1.333002	1.268593	1146.681	4.375558
		1.33335	1.268278		
H2	1.1	1.191528	1.4302	4.884082	1.573678
O2	3.12	1.19104	1.429463	106.0203	4.463522
N2	3.44	1.190788	1.431267	1024.466	4.921319
CO2	3.53	1.190819	1.431223	22.63355	5.050075
CH4	3.06	1.191023	1.430928	1024.466	4.377685
		1.19124	1.430616		
H2	1.15	1.257724	1.345217	5.155696	1.547313
O2	3.31	1.258414	1.344428	111.9163	4.45357
N2	3.66	1.258011	1.344889	1081.439	4.924492
CO2	3.71	1.257094	1.345938	23.89225	4.991766
CH4	3.25	1.256191	1.346975	1081.439	4.372841
		1.257487	1.34549		
H2	1.25	1.424309	1.195647	5.837587	1.495011
O2	3.71	1.42683	1.193877	126.7183	4.437194
N2	4.11	1.422382	1.197009	1224.469	4.915598
CO2	4.07	1.420985	1.198	27.05223	4.867757
CH4	3.66	1.424502	1.195512	1224.469	4.377394
		1.423802	1.196009		

Table A.3 (Membrane "b" continued)

p=700 kPa

Gas	α_1	$R_{2\,ss}$	$R_{1\,ss}$	$R_{1\,ps}$	$R_{1\,pp}$	$R_{1\,ss}$	$R_{2\,ss}$	a	b	c
H2	1.7	1.751062	0.739648	7.16762	1.258271	-0.50272	22.13993	1.9525	-17.2388	-9.15974
O2	5.15	1.749007	0.740015	155.7397	3.810271	-0.61644	241.6603	53.04	-6662.88	-4127.42
N2	5.91	1.749782	0.739876	1504.9	4.372563	-0.62601	810.4579	1030.56	-507846	-318322
CO2	5.68	1.751367	0.739593	33.24779	4.202396	-0.62224	334.2938	2.0779	-331.013	-206.774
CH4	5.31	1.7482	0.74016	1504.9	3.928648	-0.62704	2626.245	318.0631	-507538	-318370
	Average	1.749884	0.739858			-0.59889	97.04666			
H2	1.6	1.425497	0.818621	5.857553	1.308124	-0.24399	31.61311	1.9525	-17.2388	-4.32237
O2	4.68	1.424659	0.818897	126.9367	3.829984	-0.29803	304.7958	53.04	-6662.88	-1540.46
N2	5.34	1.423144	0.819398	1226.579	4.37011	-0.30102	950.4032	1030.56	-507846	-152964
CO2	5.29	1.429304	0.81737	27.09885	4.329192	-0.3047	442.6482	2.0779	-331.013	-101.054
CH4	4.81	1.428672	0.817577	1226.579	3.936373	-0.30801	3068.842	318.0631	-507538	-156355
	Average	1.426255	0.818373			-0.29115	133.2426			
H2	1.5	1.216686	0.908123	4.999558	1.359922	-0.0702	54.67186	1.9525	-17.2388	-1.21977
O2	4.24	1.215842	0.908594	108.3302	3.84925	-0.09219	402.9967	53.04	-6662.88	-614.67
N2	4.82	1.216278	0.908351	1046.786	4.375799	-0.09497	1128.315	1030.56	-507846	-48238.7
CO2	4.9	1.217756	0.907528	23.12667	4.448426	-0.09544	639.4633	2.0779	-331.013	-31.6112
CH4	4.34	1.219404	0.906615	1046.786	3.940034	-0.099	3646.205	318.0631	-507538	-50247.6
	Average	1.217193	0.907842			-0.09036	215.5357			
H2	1.4	1.071374	1.010412	4.385219	1.416835	0.054831	183.9414	1.9525	-17.2388	0.939343
O2	3.83	1.071023	1.010724	95.33597	3.870505	0.050971	574.4159	53.04	-6662.88	339.4733
N2	4.34	1.072536	1.00938	921.224	4.385899	0.048306	1364.037	1030.56	-507846	24529.75
CO2	4.52	1.071455	1.010339	20.35262	4.567803	0.049601	1086.429	2.0779	-331.013	16.41335
CH4	3.89	1.069566	1.012025	921.224	3.93114	0.050692	4446.643	318.0631	-507538	25727.11
	Average	1.071191	1.010576			0.05088	553.0975			
H2	1.3	0.964417	1.128437	3.953793	1.467106	0.149198	-146.655	1.9525	-17.2388	2.328539
O2	3.45	0.965428	1.127056	85.83267	3.893137	0.155558	944.1178	53.04	-6662.88	1035.181
N2	3.88	0.963529	1.129655	829.3943	4.378369	0.157015	1705.368	1030.56	-507846	79713.91
CO2	4.15	0.964345	1.128536	18.32383	4.683049	0.155957	3081.196	2.0779	-331.013	51.57316
CH4	3.49	0.96434	1.128543	829.3943	3.938275	0.155829	5523.708	318.0631	-507538	79081.23
	Average	0.964412	1.128446			0.154711	-1061.81			
H2	1.44	1.123853	0.967791	4.611825	1.392572	0.009267	95.1459	1.9525	-17.2388	0.159588
O2	3.99	1.123072	0.968371	99.99887	3.86229	-0.00052	492.7812	53.04	-6662.88	-3.45316
N2	4.52	1.122255	0.968979	966.2812	4.375326	-0.00126	1264.943	1030.56	-507846	-640.093
CO2	4.67	1.123899	0.967757	21.34807	4.520525	-0.00242	854.3347	2.0779	-331.013	-0.80182
CH4	4.07	1.124835	0.967064	966.2812	3.939729	-0.00453	4087.773	318.0631	-507538	-2297.11
	Average	1.123583	0.967992			0.000108	340.9199			
H2	1.43	1.110106	0.978223	4.559459	1.396693	0.021157	108.3082	1.9525	-17.2388	0.363844
O2	3.96	1.112916	0.976051	98.88263	3.870901	0.009526	506.2869	53.04	-6662.88	63.46271
N2	4.48	1.11081	0.977676	955.495	4.379201	0.010148	1285.7	1030.56	-507846	5153.754
CO2	4.63	1.109309	0.978843	21.10977	4.525826	0.012047	906.3478	2.0779	-331.013	3.987464
CH4	4.03	1.112063	0.976708	955.495	3.939326	0.008234	4162.434	318.0631	-507538	4178.997
	Average	1.111041	0.9775			0.012222	377.1805			

Table A.3 (Membrane "b" continued)

p=1050 kPa

Gas	α_1	$R_{1\,ss}$	$R_{1\,ss}$	$R_{2\,ss}$	$R_{1\,ss}$
H2	1.7	10.74286	0.491503	43.72745	0.835837
O2	7.02	10.59227	0.491823	949.2056	3.451513
N2	7.98	10.77511	0.491436	9172.099	3.923515
CO2	7.41	10.54867	0.491918	202.6394	3.643264
CH4	7.04	10.66725	0.491663	9172.099	3.461346
	Average	10.66523	0.491669		
H2	1.6	3.455882	0.543981	14.14252	0.87063
O2	6.39	3.436495	0.544465	306.9961	3.477077
N2	7.21	3.438648	0.544411	2966.48	3.923274
CO2	6.96	3.45284	0.544057	65.5385	3.787238
CH4	6.37	3.463108	0.543803	2966.48	3.466194
	Average	3.449395	0.544143		
H2	1.5	2.125217	0.603457	8.713647	0.905179
O2	5.81	2.130627	0.603022	189.1499	3.506058
N2	6.51	2.125367	0.603445	1827.741	3.928475
CO2	6.51	2.125866	0.603405	40.38031	3.928475
CH4	5.74	2.11932	0.603934	1827.741	3.463817
		2.12528	0.603452		
H2	1.4	1.566667	0.671429	6.425382	0.939873
O2	5.25	1.564449	0.671837	139.4778	3.524522
N2	5.86	1.569605	0.67089	1347.763	3.934038
CO2	6.06	1.565918	0.671566	29.77616	4.068305
CH4	5.17	1.569191	0.670966	1347.763	3.470815
	Average	1.567166	0.671338		
H2	1.3	1.25933	0.749858	5.161808	0.974978
O2	4.73	1.258011	0.750326	112.049	3.547421
N2	5.25	1.26069	0.749376	1082.721	3.937413
CO2	5.61	1.257066	0.750663	23.92057	4.207407
CH4	4.63	1.25979	0.749694	1082.721	3.472423
		1.258978	0.749983		
H2	1.2	1.064844	0.841358	4.365936	1.009616
O2	4.24	1.063968	0.841905	94.77275	3.56731
N2	4.68	1.065086	0.841207	915.7817	3.937502
CO2	5.17	1.064912	0.841315	20.23239	4.349762
CH4	4.13	1.065502	0.840948	915.7817	3.474762
		1.064862	0.841347		
H2	1.1	0.930693	0.949495	3.816612	1.04423
O2	3.78	0.930703	0.949485	82.8484	3.588353
N2	4.15	0.930952	0.949226	800.5576	3.939594
CO2	4.73	0.93133	0.948833	17.68674	4.490187
CH4	3.66	0.930727	0.949459	800.5576	3.474437
		0.930881	0.9493		
H2	1.12	0.934087	0.926323	3.909751	1.037999
O2	3.87	0.95398	0.926424	84.8702	3.586659
N2	4.25	0.9536	0.926783	820.094	3.938837
CO2	4.81	0.952502	0.927821	18.11836	4.457837
CH4	3.75	0.95382	0.926575	820.094	3.475445
		0.953598	0.926785		

Table A.3 (Membrane "b" continued)

p=1400 kPa

Gas	α_1	$R_{1\,He}$	$R_{1\,He}$	$R_{1\,gas}$	$R_{1\,gas}$	$R_{1\,He}$	$R_{2\,He}$	a	b	c
H2	1.6	8.882114	0.485124	36.11476	0.6551	-4.0923	11.50439	1.9525	-12.9433	-85.6663
O2	6.77	8.920279	0.485011	783.9546	2.771892	-7.41677	127.4472	53.04	-5821.32	-46093
N2	7.79	8.764241	0.485481	7575.292	3.189518	-7.7049	542.5031	1030.56	-507640	-3972498
CO2	7.32	8.724031	0.106052	167.3611	2.997082	-7.41326	186.0395	2.0779	-330.598	-2565
CH4	6.47	8.75173	0.485519	7575.292	2.64906	-7.78792	1739.4	318.0631	-507474	-3971459
	Average	8.808479	0.409437			-6.88303	68.36033			
H2	1.5	3.167108	0.538165	12.96861	0.681136	-1.50742	10.39338	1.9525	-12.9433	-23.9476
O2	6.15	3.175188	0.537932	281.5138	2.792659	-2.18727	145.2616	53.04	-5821.32	-12986.5
N2	7.03	3.157426	0.538445	2720.246	3.192259	-2.22173	631.7826	1030.56	-507640	-1132924
CO2	6.86	3.152981	0.11762	60.09846	3.115063	-2.18984	227.3076	2.0779	-330.598	-733.922
CH4	5.84	3.16268	0.538293	2720.246	2.65189	-2.23778	2039.96	318.0631	-507474	-1137211
	Average	3.163077	0.454091			-2.06881	54.2485			
H2	1.4	1.984693	0.598782	8.128613	0.707438	-0.7734	11.53786	1.9525	-12.9433	-11.1783
O2	5.56	1.979548	0.599252	176.4504	2.80954	-1.03748	175.5622	53.04	-5821.32	-6096.57
N2	6.33	1.988023	0.59848	1705.026	3.198631	-1.06279	753.2198	1030.56	-507640	-540679
CO2	6.4	1.980566	0.130851	37.66918	3.234003	-1.04748	297.8753	2.0779	-330.598	-348.576
CH4	5.25	1.980114	0.5992	1705.026	2.652893	-1.05851	2442.444	318.0631	-507474	-537523
	Average	1.982589	0.505313			-0.99593	56.98633			
H2	1.3	1.473773	0.668725	6.045613	0.869139	-0.41176	13.82103	1.9525	-12.9433	-5.66062
O2	5.02	1.477265	0.668009	131.234	3.356212	-0.54734	218.3963	53.04	-5821.32	-3202.13
N2	5.67	1.474088	0.66866	1268.104	3.790781	-0.55173	921.6302	1030.56	-507640	-280396
CO2	5.94	1.471829	0.669126	28.01626	3.971295	-0.54672	422.5576	2.0779	-330.598	-181.366
CH4	4.71	1.475744	0.66832	1268.104	3.148956	-0.55501	2981.831	318.0631	-507474	-281753
	Average	1.47454	0.668568			-0.52251	66.41723			
H2	1.2	1.188837	0.750326	4.876136	0.900169	-0.19393	17.67829	1.9525	-12.9433	-2.58348
O2	4.5	1.190121	0.749815	105.8478	3.375635	-0.26518	285.5988	53.04	-5821.32	-1547.44
N2	5.06	1.190147	0.749805	1022.799	3.795714	-0.26893	1162.292	1030.56	-507640	-136594
CO2	5.48	1.187548	0.75084	22.59673	4.110773	-0.26553	696.3334	2.0779	-330.598	-87.9287
CH4	4.2	1.1bv856	0.74992	1022.799	3.150593	-0.26948	3767.487	318.0631	-507474	-136777
	Average	1.189302	0.750141			-0.25261	83.54463			
H2	1.1	1.007106	0.846762	4.124943	0.932236	-0.04763	24.68514	1.9525	-12.9433	-0.6209
O2	4	1.004612	0.848533	89.54145	3.389949	-0.08212	404.7254	53.04	-5821.32	-478.432
N2	4.48	1.006132	0.847452	865.232	3.796743	-0.08548	1546.312	1030.56	-507640	-43399.5
CO2	5.02	1.006023	0.847529	19.11559	4.254386	-0.08545	1774.265	2.0779	-330.598	-28.2657
CH4	3.72	1.006545	0.847159	865.232	3.152653	-0.08634	5008.768	318.0631	-507474	-43819.3
	Average	1.006084	0.847487			-0.07741	115.6304			
H2	1	0.881106	0.962487	3.611898	0.812023	0.057661	40.48808	1.9525	-12.9433	0.739827
O2	3.55	0.882224	0.961156	78.40461	2.882681	0.038981	645.1242	53.04	-5821.32	226.8379
N2	3.95	0.881719	0.961756	757.6176	3.20749	0.038632	2214.716	1030.56	-507640	19609.75
CO2	4.56	0.880069	0.210469	16.73806	3.702824	0.039733	-3921.56	2.0779	-330.598	13.13236
CH4	3.27	0.879636	0.964247	757.6176	2.655315	0.040471	7244.729	318.0631	-507474	20537.57
	Average	0.880951	0.812023			0.043096	190.9198			
H2	1.04	0.926566	0.913526	3.800211	0.94975	0.019285	32.28416	1.9525	-12.9433	0.248884
O2	3.73	0.927267	0.912846	82.49239	3.406314	-0.00562	521.5069	53.04	-5821.32	-32.7261
N2	4.16	0.927127	0.912982	797.1175	3.798999	-0.00667	1890.911	1030.56	-507640	-3387.14
CO2	4.75	0.927104	0.913004	17.61073	4.337799	-0.00704	13008.45	2.0779	-330.598	-2.32691
CH4	3.45	0.92634	0.913746	797.1175	3.150612	-0.0062	6147.316	318.0631	-507474	-3146.44
	Average	0.926881	0.913221			-0.00125	151.6319			
H2	1.03	0.914653	0.92541	3.751078	0.952916	0.029298	34.01465	1.9525	-12.9433	0.377538
O2	3.68	0.914281	0.925791	81.42584	3.404593	0.007234	550.8616	53.04	-5821.32	42.10878
N2	4.11	0.915894	0.924143	786.8115	3.802413	0.004534	1959.116	1030.56	-507640	2301.603
CO2	4.7	0.914122	0.925954	17.38304	4.348258	0.005869	-88510.1	2.0779	-330.598	1.940102
CH4	3.41	0.915536	0.924508	786.8115	3.1548	0.004596	6361.483	318.0631	-507474	2332.372
	Average	0.914897	0.925161			0.010306	159.9536			

Table A.3 (Membrane "b" continued)

p=1750 kPa

Gas	α_1	R_{1He}	R_{1He}	R_{2gas}	R_{1gas}
H2	1.6	8.04878	0.420918	32.6979	0.673798
O2	7.54	8.034132	0.420959	709.7836	3.175275
N2	8.46	8.011317	0.421021	6858.583	3.562709
CO2	7.61	7.843114	0.421496	151.5268	3.204754
CH4	6.65	7.93814	0.421225	6858.583	2.800475
Average		7.975097	0.421124		
H2	1.5	2.790244	0.466939	11.48081	0.699992
O2	6.86	2.804261	0.466549	249.2176	3.201299
N2	7.64	2.800297	0.466658	2408.17	3.565295
CO2	7.15	2.797669	0.466731	53.20376	3.336631
CH4	6.01	2.808518	0.466431	2408.17	2.804636
Average		2.800198	0.466662		
H2	1.4	1.738537	0.519534	7.120428	0.72758
O2	6.21	1.739355	0.51946	154.5654	3.227339
N2	6.87	1.739685	0.519431	1493.553	3.570341
CO2	6.67	1.72686	0.520585	32.9971	3.466401
CH4	5.4	1.739012	0.519491	1493.553	2.806382
Average		1.73669	0.5197		
H2	1.3	1.287805	0.58022	5.28333	0.754072
O2	5.6	1.287465	0.580289	114.6869	3.248309
N2	6.16	1.289964	0.579783	1108.211	3.57314
CO2	6.21	1.288851	0.580008	24.48372	3.602143
CH4	4.84	1.289001	0.579977	1108.211	2.807467
Average		1.288617	0.580055		
H2	1.2	1.037398	0.65102	4.253987	0.78115
O2	5.03	1.038818	0.650463	92.34264	3.274321
N2	5.49	1.037324	0.65105	892.2996	3.573762
CO2	5.74	1.038573	0.650559	19.7136	3.736501
CH4	4.31	1.035676	0.651701	892.2996	2.805631
Average		1.037558	0.650958		
H2	1.1	0.878049	0.734694	3.604032	0.807405
O2	4.49	0.879935	0.733378	78.2343	3.295678
N2	4.87	0.878372	0.734468	755.9719	3.5746
CO2	5.27	0.879482	0.733694	16.7017	3.868202
CH4	3.83	0.879347	0.733787	755.9719	2.811236
Average		0.879037	0.734004		
H2	1	0.76773	0.835102	3.147518	0.835153
O2	3.97	0.768204	0.834541	68.32417	3.315559
N2	4.28	0.766728	0.836291	660.2111	3.574456
CO2	4.79	0.767448	0.835436	14.58606	4.000385
CH4	3.37	0.768327	0.834396	660.2111	2.814467
Average		0.767687	0.835153		
H2	1.05	0.818293	0.782307	3.354176	0.821826
O2	4.22	0.81798	0.782793	72.81016	3.302958
N2	4.57	0.817802	0.782957	703.5589	3.5769
CO2	5.03	0.818697	0.782138	15.54374	3.936938
CH4	3.59	0.817687	0.783062	703.5589	2.809862
Average		0.818092	0.782691		

Table A.3 (Membrane "b" continued)

p=2100 kPa

Gas	α_{ij}	$R_{i\,He}$	$R_{i\,He}$	$R_{i\,gas}$	$R_{i\,gas}$	$R_{i\,He}$	$R_{ik\,He}$	a	b	c
H2	1.5	4.819512	0.412526	19.81287	0.618652	-2.17794	7.862335	1.9525	-9.92403	-30.8755
O2	7.67	4.83749	0.412395	430.0843	3.163372	-3.87704	150.7	53.04	-6443.12	-25777.5
N2	8.27	4.799324	0.412675	4155.871	3.410832	-3.94987	579.0555	1030.56	-507527	-2020745
CO2	7.37	4.903624	0.411907	91.81576	3.039641	-3.95337	164.2626	2.0779	-279.366	-1136.91
CH4	6.45	4.800091	0.412669	4155.871	2.660202	-3.97777	1865.922	318.0631	-507439	-2023512
	Average	4.832408	0.412434			-3.5872	48.82489			
H2	1.4	2.208034	0.458992	9.025841	0.642992	-0.89782	7.538677	1.9525	-9.92403	-10.4839
O2	6.95	2.204455	0.459147	195.9268	3.191994	-1.36978	194.6997	53.04	-6443.12	-8925.15
N2	7.44	2.204169	0.459159	1893.225	3.417041	-1.38741	716.7815	1030.56	-507527	-706132
CO2	6.88	2.188747	0.459834	41.82707	3.159844	-1.35617	209.9646	2.0779	-279.366	-382.688
CH4	5.8	2.201717	0.459266	1893.225	2.663822	-1.38963	2319.298	318.0631	-507439	-705767
	Average	2.201425	0.45928			-1.28016	41.35524			
H2	1.3	1.468937	0.512606	6.024046	0.666334	-0.43726	8.26496	1.9525	-9.92403	-4.7127
O2	6.28	1.47161	0.512282	130.7659	3.218907	-0.65372	273.1082	53.04	-6443.12	-4234.69
N2	6.67	1.468757	0.512628	1263.58	3.418808	-0.65643	924.9271	1030.56	-507527	-333599
CO2	6.41	1.468251	0.51269	27.91631	3.285541	-0.65074	285.4189	2.0779	-279.366	-182.674
CH4	5.2	1.468842	0.512618	1263.58	2.665337	-0.65812	2994.424	318.0631	-507439	-334095
	Average	1.46928	0.512565			-0.61125	43.48163			
H2	1.2	1.119919	0.575157	4.593146	0.690074	-0.19294	9.601667	1.9525	-9.92403	-1.9874
O2	5.64	1.121174	0.574826	99.70487	3.243348	-0.30835	443.8114	53.04	-6443.12	-1991.77
N2	5.95	1.119961	0.575145	963.4403	3.421617	-0.30897	1271.084	1030.56	-507527	-156911
CO2	5.93	1.119307	0.575318	21.28531	3.410116	-0.30644	436.0151	2.0779	-279.366	-85.8043
CH4	4.64	1.121037	0.574862	963.4403	2.668286	-0.31073	4111.576	318.0631	-507439	-157708
	Average	1.120279	0.575062			-0.28549	49.50055			
H2	1.1	0.916644	0.64908	3.758335	0.713975	-0.04001	11.69229	1.9525	-9.92403	-0.40015
O2	5.03	0.916298	0.649253	81.58337	3.264814	-0.10552	1083.832	53.04	-6443.12	-680.497
N2	5.28	0.917529	0.648636	788.3337	3.427081	-0.1071	1950.504	1030.56	-507527	-54367
CO2	5.45	0.916847	0.648978	17.41668	3.537422	-0.10587	860.1987	2.0779	-279.366	-29.6
CH4	4.11	0.916016	0.649395	788.3337	2.667671	-0.10585	6353.27	318.0631	-507439	-53733.5
	Average	0.916667	0.649068			-0.09288	60.01557			
H2	1	0.783592	0.737787	3.214864	0.737326	0.065204	15.04316	1.9525	-9.92403	0.638786
O2	4.46	0.784255	0.7372	69.78607	3.288474	0.025556	-3256.31	53.04	-6443.12	164.6236
N2	4.65	0.784415	0.737059	674.3373	3.428566	0.025742	3919.041	1030.56	-507527	13064.12
CO2	4.97	0.784634	0.736866	14.89815	3.66451	0.025431	9447.339	2.0779	-279.366	7.10331
CH4	3.62	0.78367	0.737718	674.3373	2.66912	0.026378	12798.91	318.0631	-507439	13385.21
	Average	0.784113	0.737326			0.033662	78.28945			
H2	1.06	0.85727	0.682554	3.516014	0.72331	0.006404	12.83482	1.9525	-9.92403	0.063474
O2	4.8	0.857787	0.682227	76.32323	3.275366	-0.04747	2354.21	53.04	-6443.12	-306.004
N2	5.02	0.857452	0.682439	737.5054	3.425487	-0.04715	2460.73	1030.56	-507527	-23934
CO2	5.26	0.858385	0.681849	16.29372	3.589255	-0.04784	1359.243	2.0779	-279.366	-13.3706
CH4	3.91	0.856928	0.682771	737.5054	2.668059	-0.04684	7997.687	318.0631	-507439	-23767
	Average	0.857564	0.682368			-0.03658	66.09729			
H2	1.02	0.806394	0.718654	3.309005	0.732478	0.046859	14.22792	1.9525	-9.92403	0.460739
O2	4.57	0.806563	0.718519	71.82963	3.281787	0.00339	-14111.3	53.04	-6443.12	21.84424
N2	4.77	0.806694	0.718416	694.084	3.42541	0.003504	3287.312	1030.56	-507527	1778.368
CO2	5.07	0.808253	0.717184	15.33441	3.640844	0.001956	3123.449	2.0779	-279.366	0.546346
CH4	3.72	0.807468	0.717803	694.084	2.671389	0.002594	10604.16	318.0631	-507439	1316.2
	Average	0.807074	0.718115			0.011661	73.76321			

APPENDIX B: COMPUTER PROGRAM

In this section, the computer program used for process control/data acquisition is presented. This program was written in "LabView Graphical Language". Knowledge of this language is essential for understanding the program. Some of the low level subroutines were already available from the package. These subroutines that are called "Virtual Instruments" (VI) are not included in this section and can be found in the LabView software package.

Each file starts with the "Position in the Hierarchy" which defines its relative position compared with the main program and other sub VIs. The relative position of each file is shown by a double bordered rectangle. The front panel and the block diagram are also shown for each VI. The block diagrams include the hidden frames as well as the higher level frames.

PROCESS CONTROL FRONT
8/10/94 4:09

Position in Hierarchy

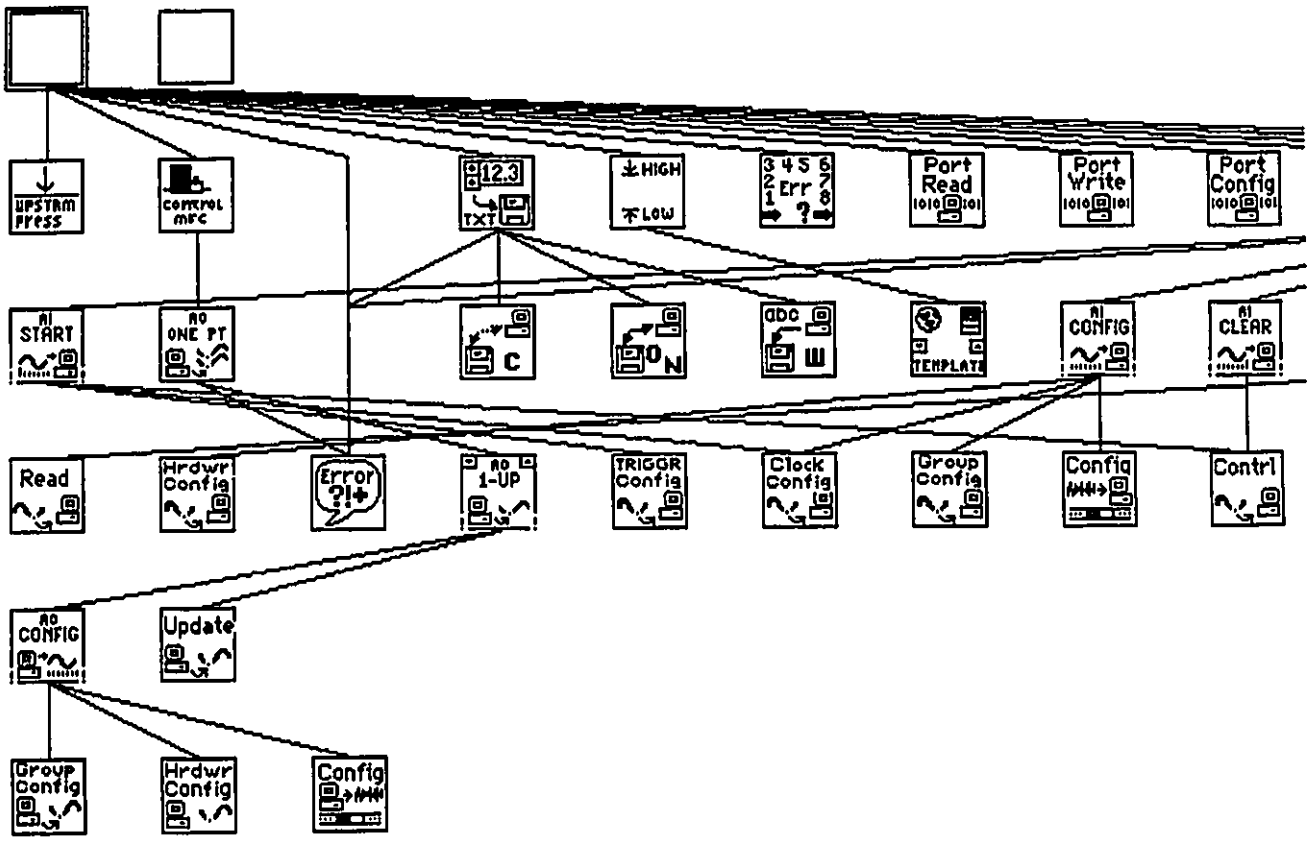

Connector Pane

PROCESS CONTROL FRONT

PROCESS CONTROL FRONT
8/10/94 4:09

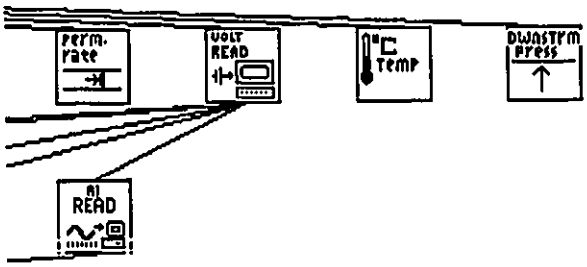

PROCESS CONTROL FRONT
8/10/94 4:09

Front Panel

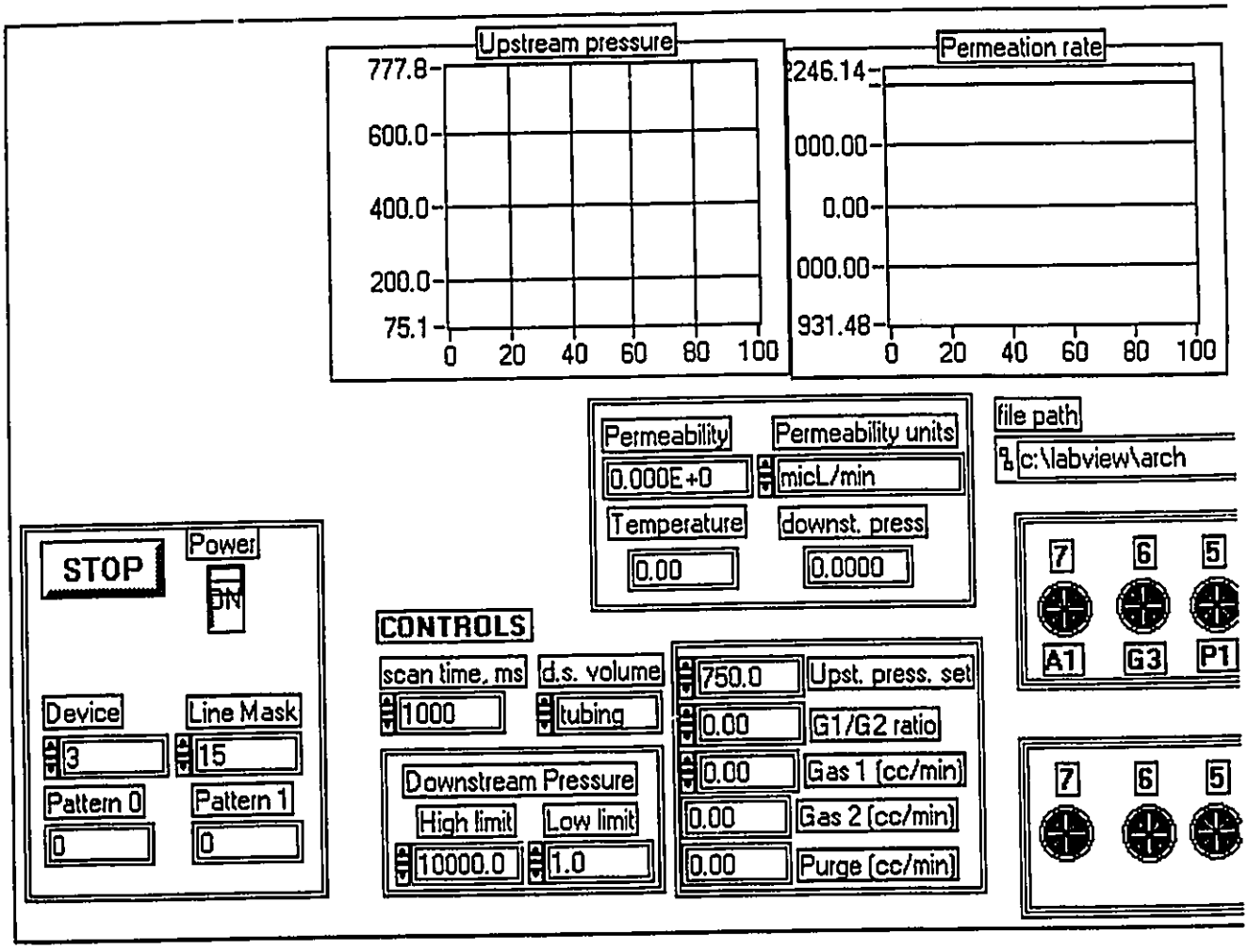

PROCESS CONTROL FRONT
8/10/94 4:09

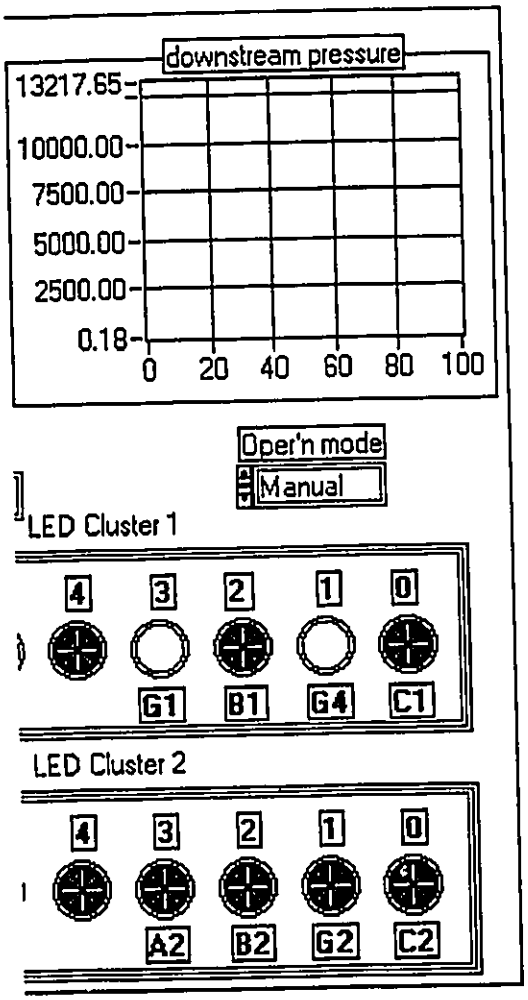

Block Diagram

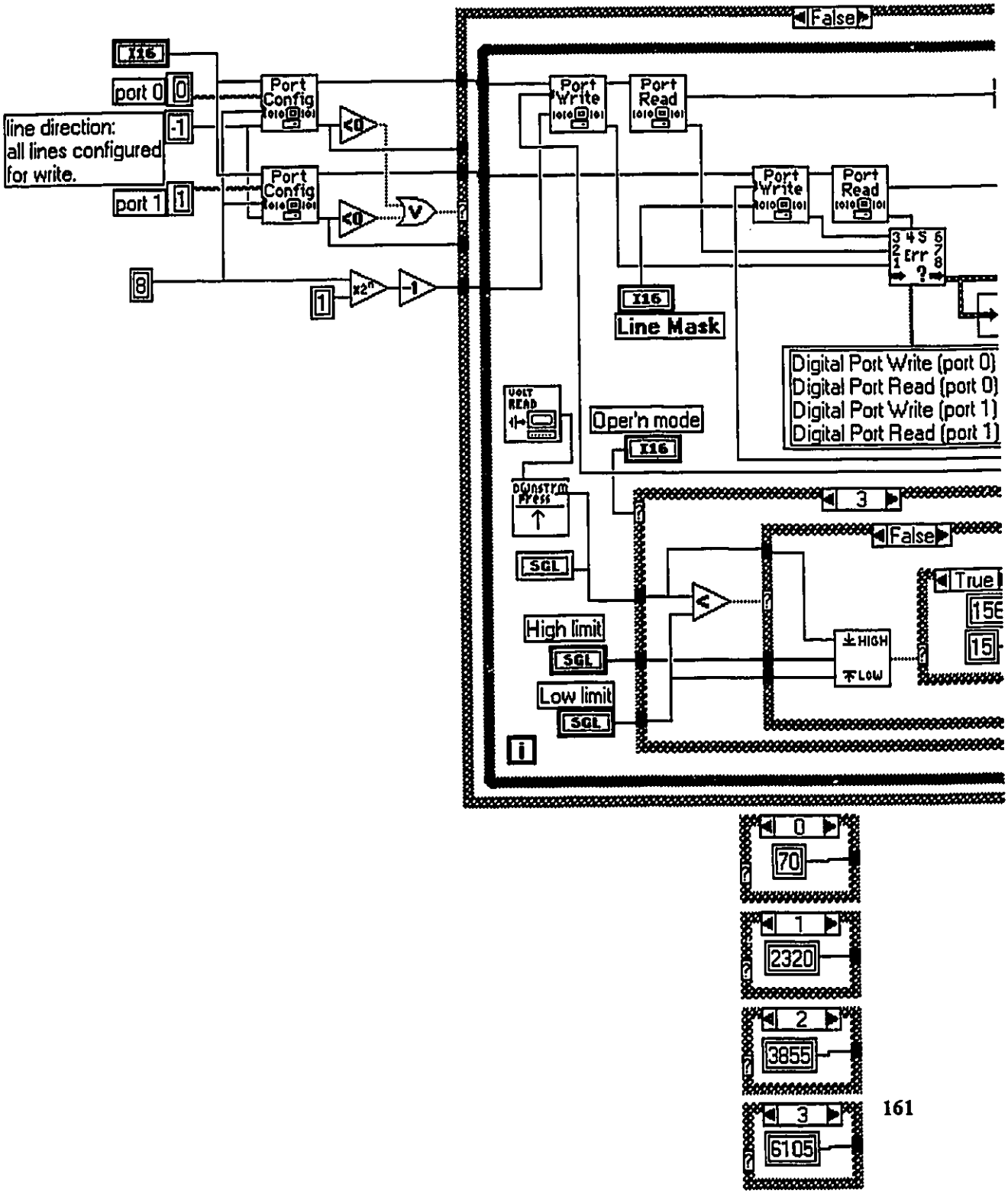

PROCESS CONTROL FRONT
8/10/94 4:09

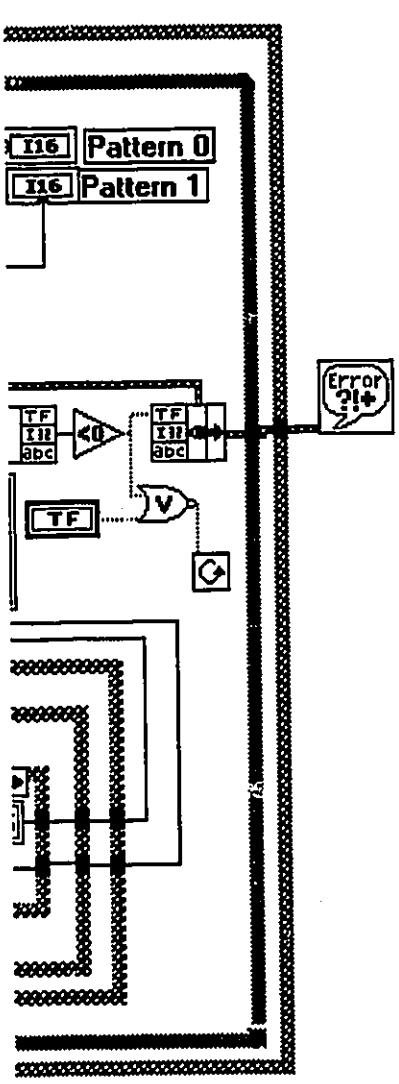

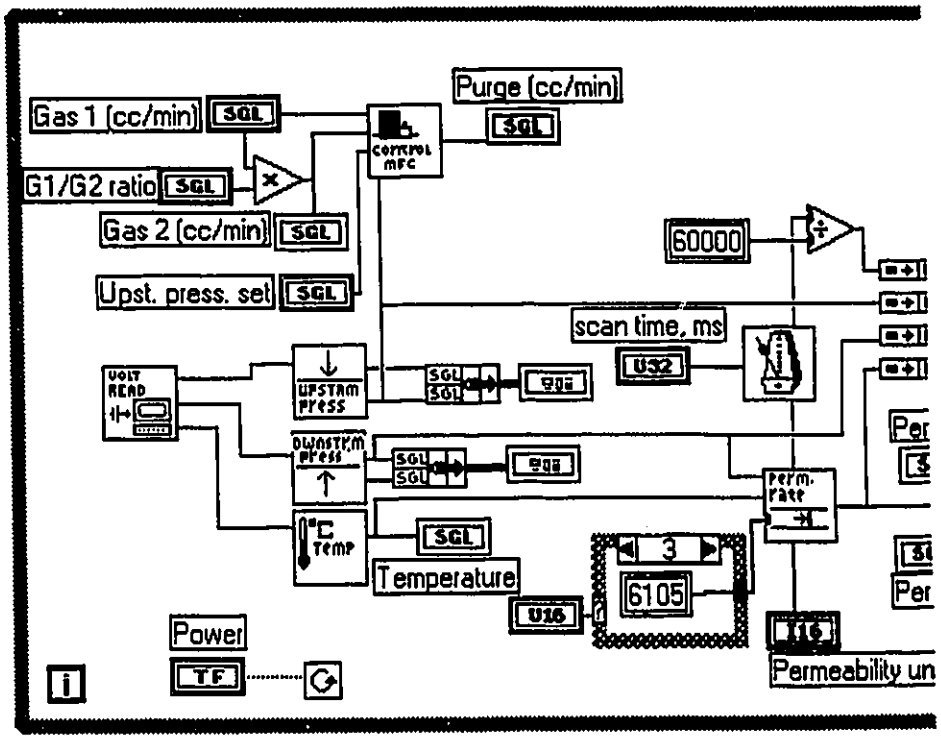

PROCESS CONTROL FRONT
8/10/94 4:09

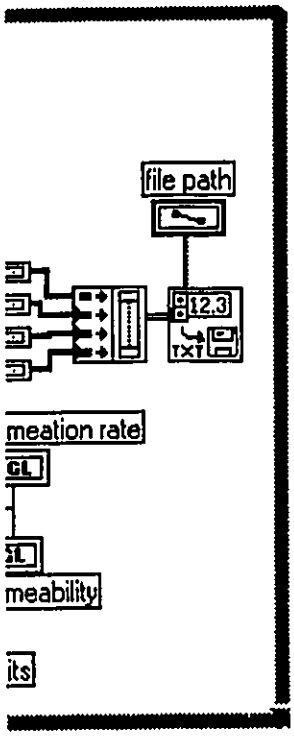

PROCESS CONTROL FRONT
8/10/94 4:09

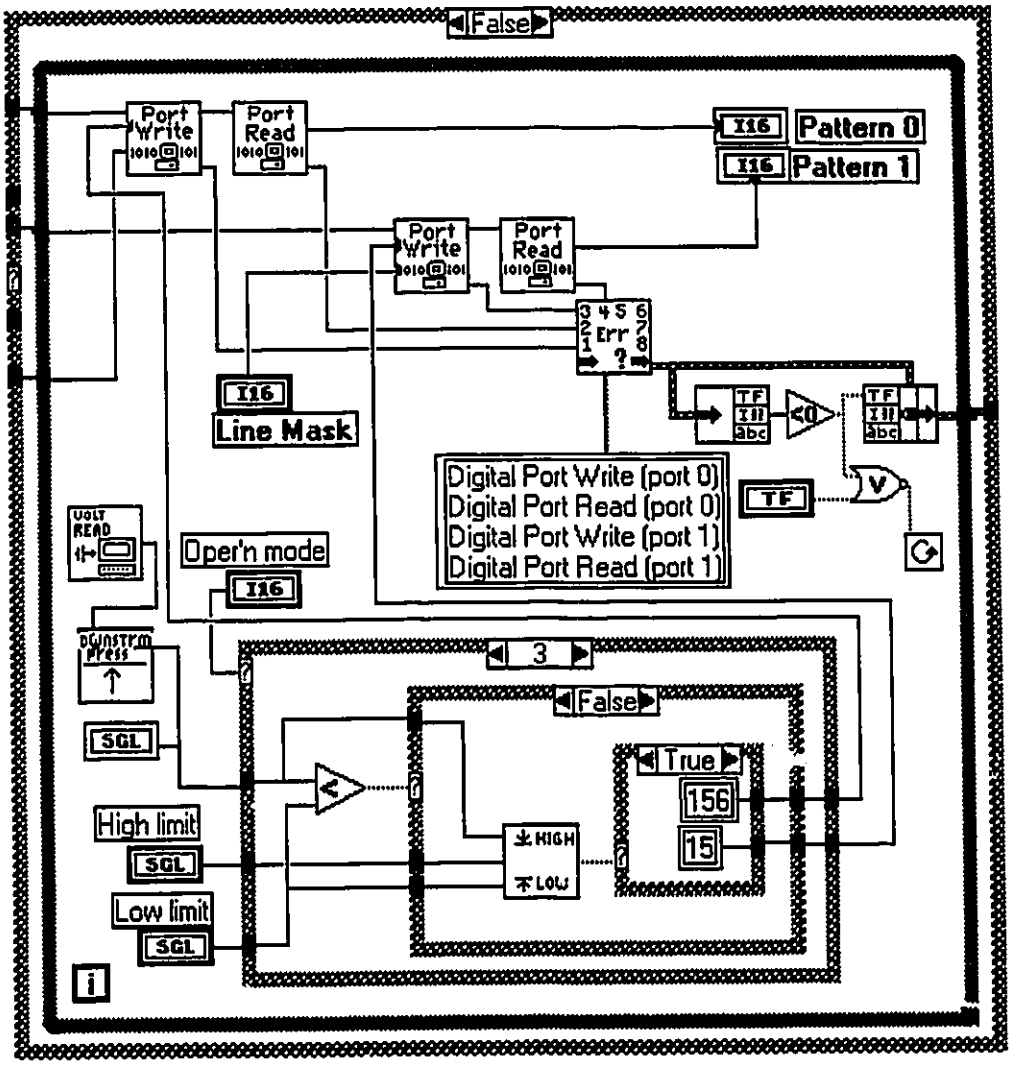

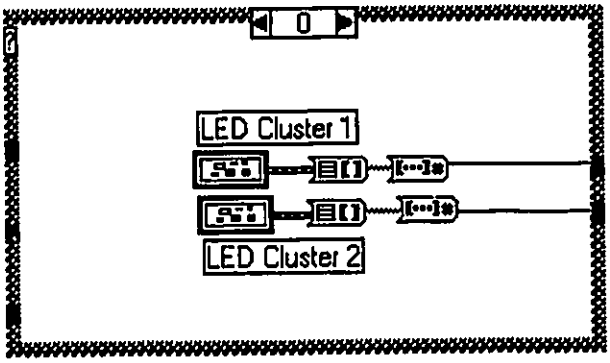

PROCESS CONTROL FRONT
8/10/94 4:09

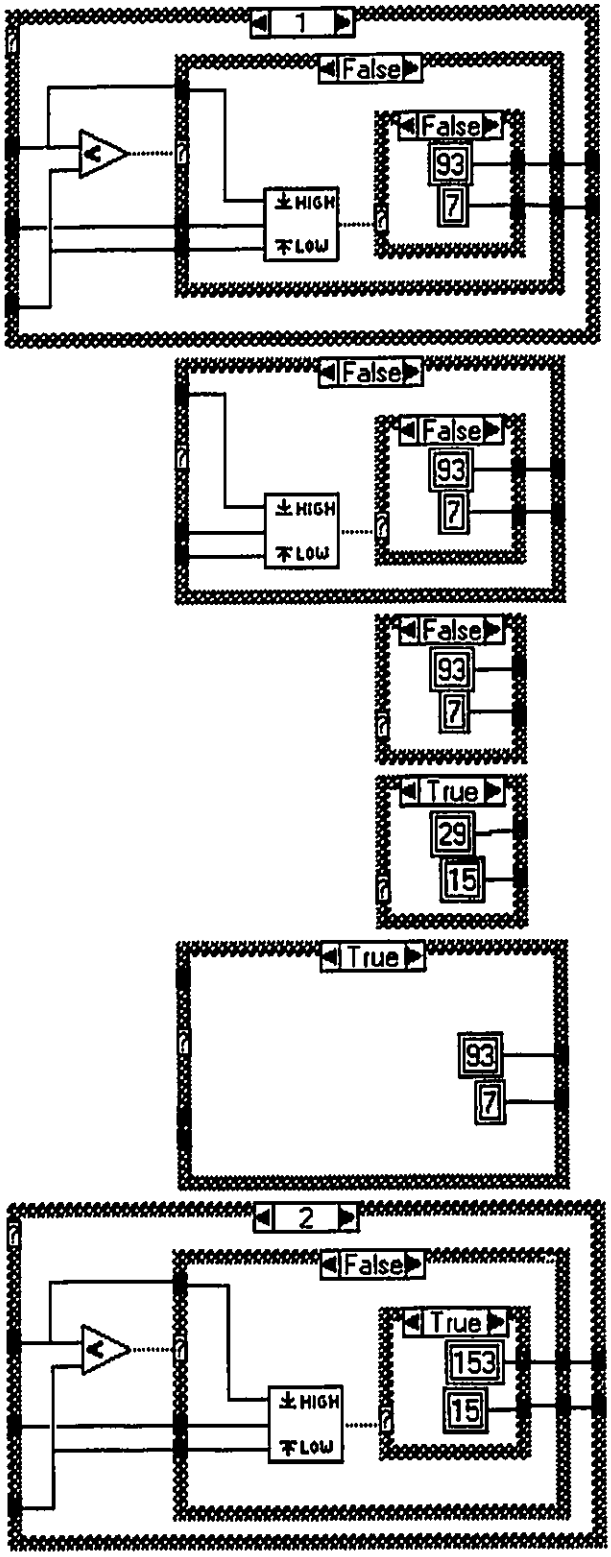

PROCESS CONTROL FRONT
8/10/94 4:09

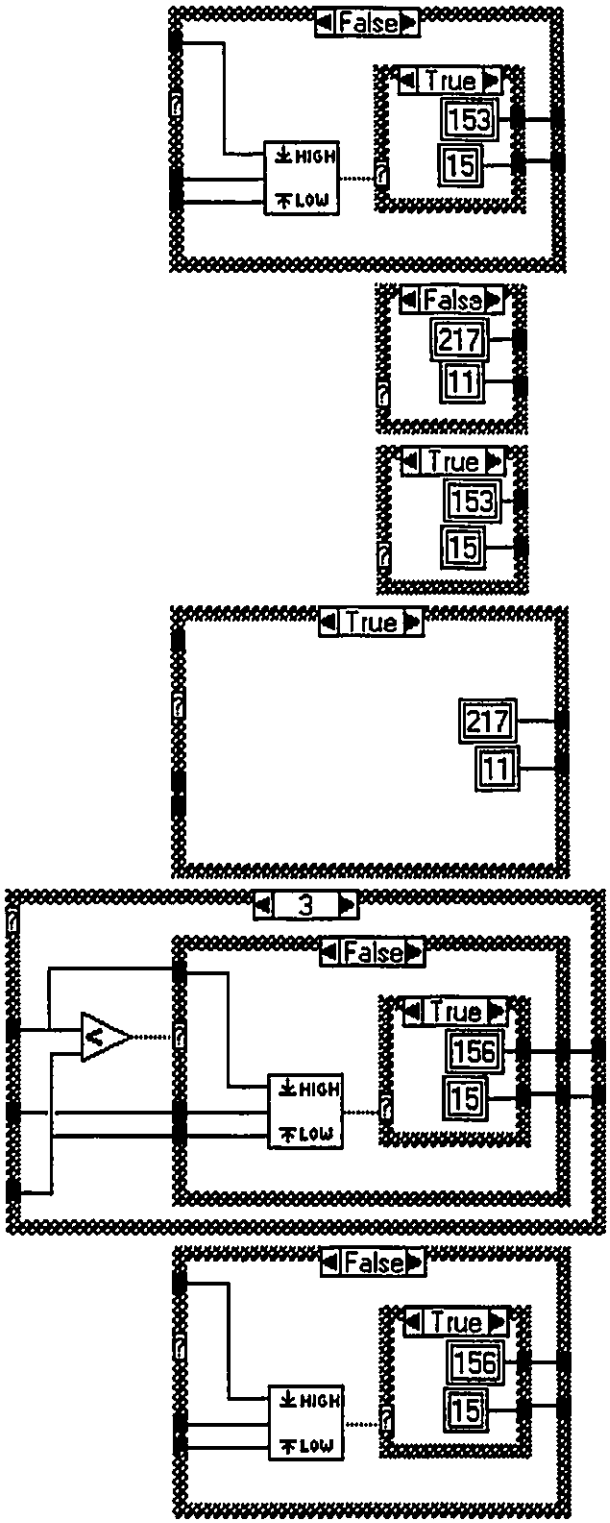

PROCESS CONTROL FRONT
8/10/94 4:09

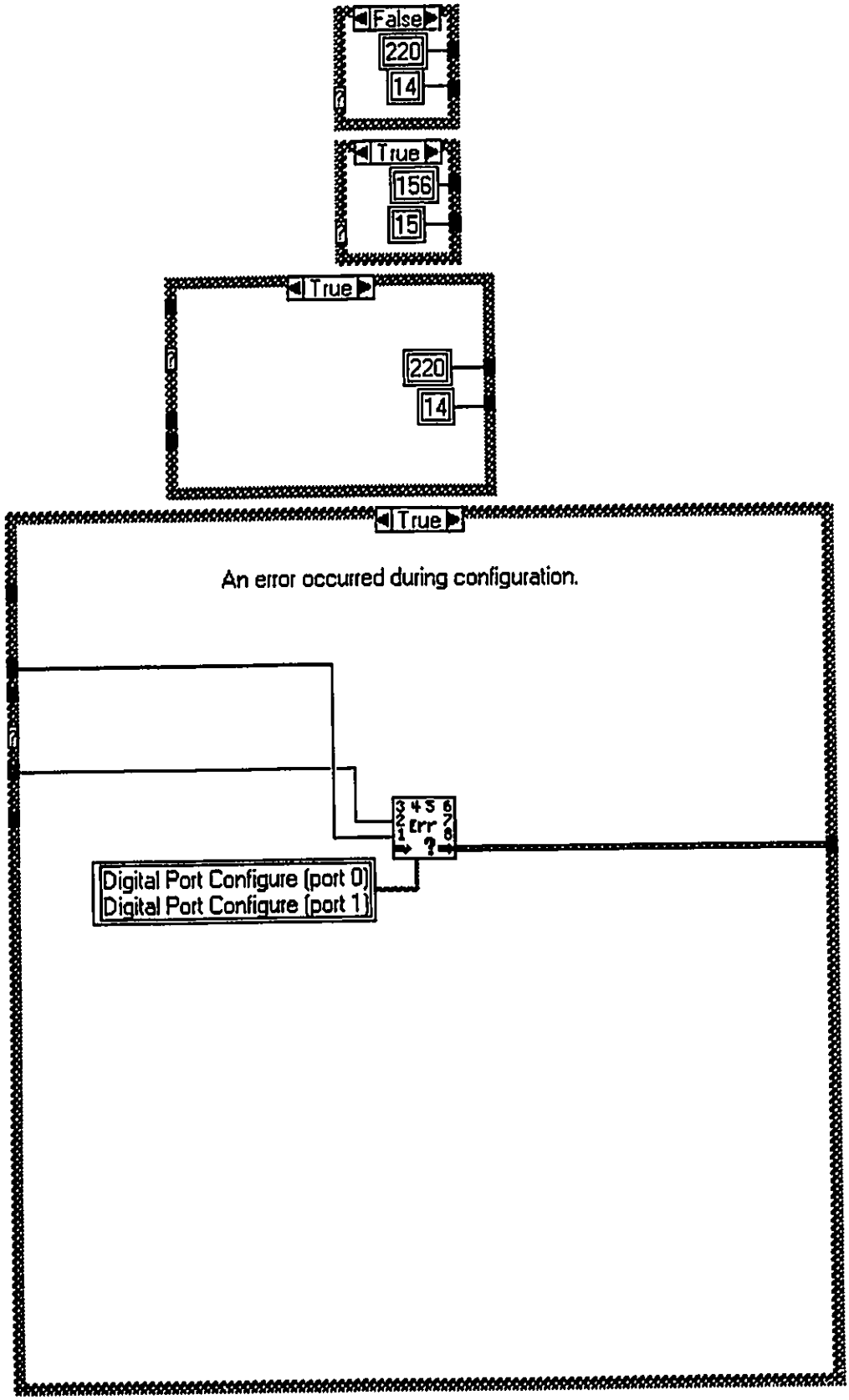

High/Low Comparison
8/10/94 4:06

Position in Hierarchy

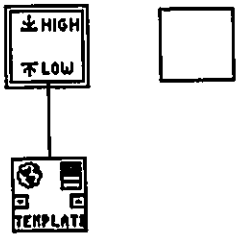

Connector Pane

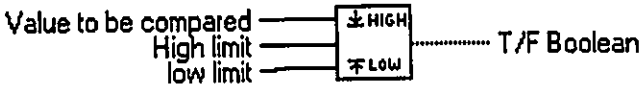

High/Low Comparison

High/Low Comparison
8/10/94 4:06

Front Panel

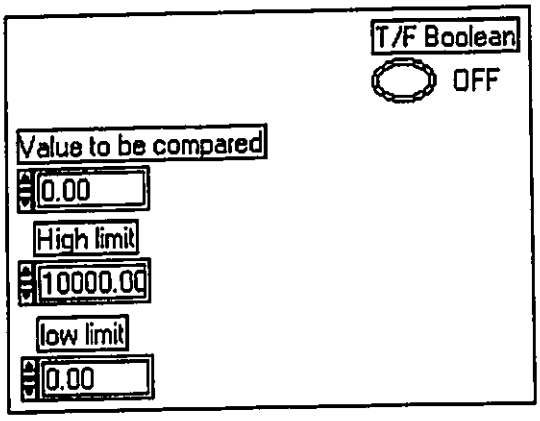

High/Low Comparison
8/10/94 4:06

Block Diagram

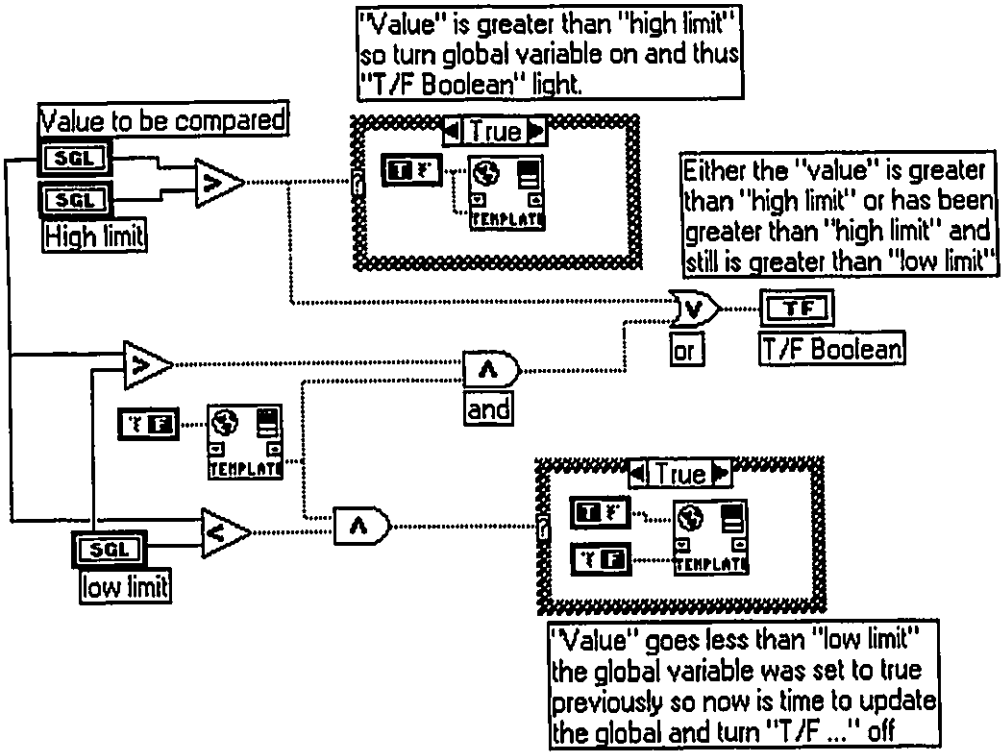

Upstream Pressure
8/10/94 4:25

Position in Hierarchy

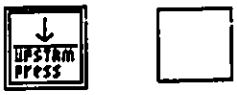

Connector Pane

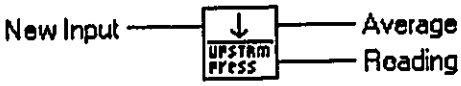

Upstream Pressure

Upstream Pressure
8/10/94 4:25

Front Panel

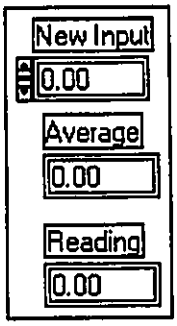

Upstream Pressure
8/10/94 4:25

Block Diagram

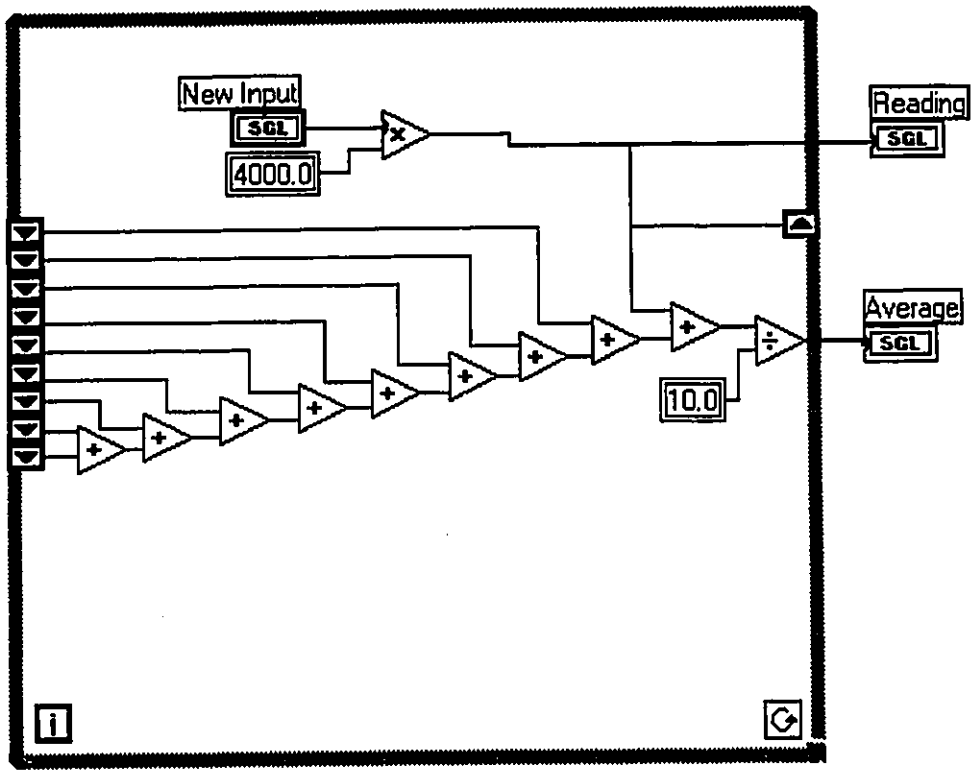

Downstream Pressure
8/10/94 4:27

Position in Hierarchy

Connector Pane

Downstream Pressure

Downstream Pressure
8/10/94 4:27

Front Panel

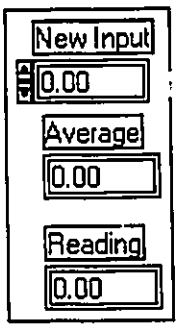

Downstream Pressure
8/10/94 4:27

Block Diagram

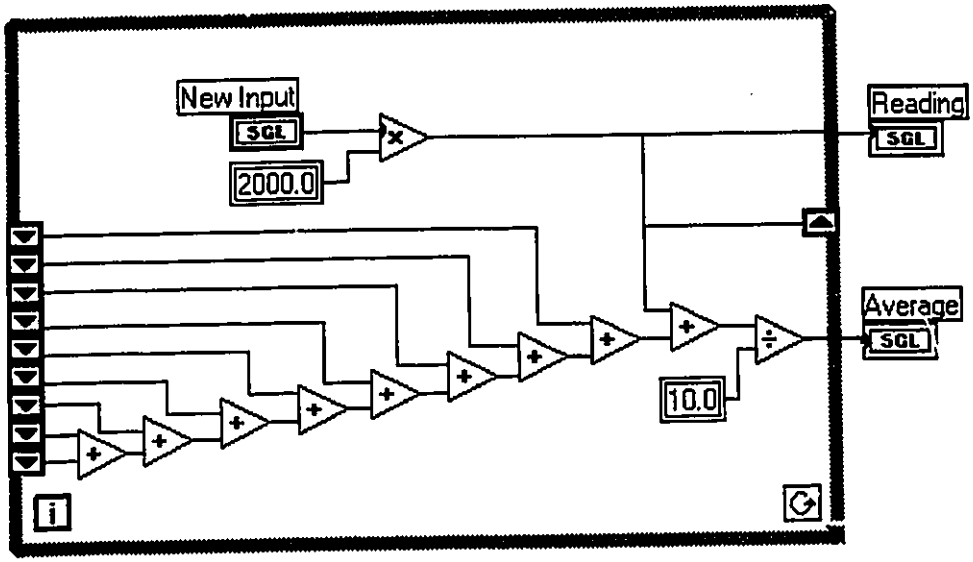

Mass Flow/Press Control
8/10/94 4:29

Position in Hierarchy

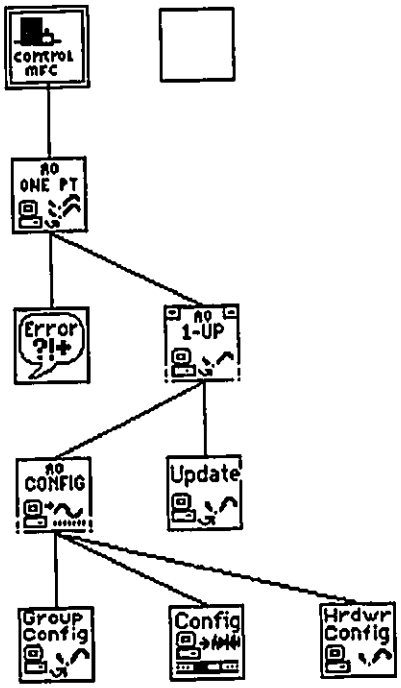

Connector Pane

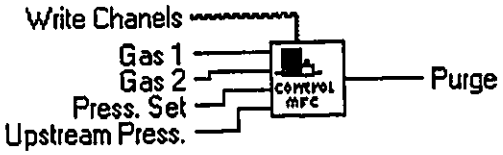

Mass Flow/Press Control

Mass Flow/Press Control
8/10/94 4:29

Front Panel

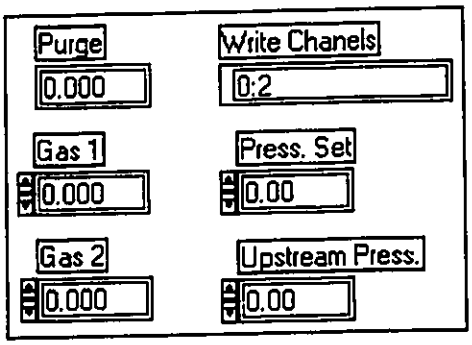

Mass Flow/Press Control
8/10/94 4:29

Block Diagram

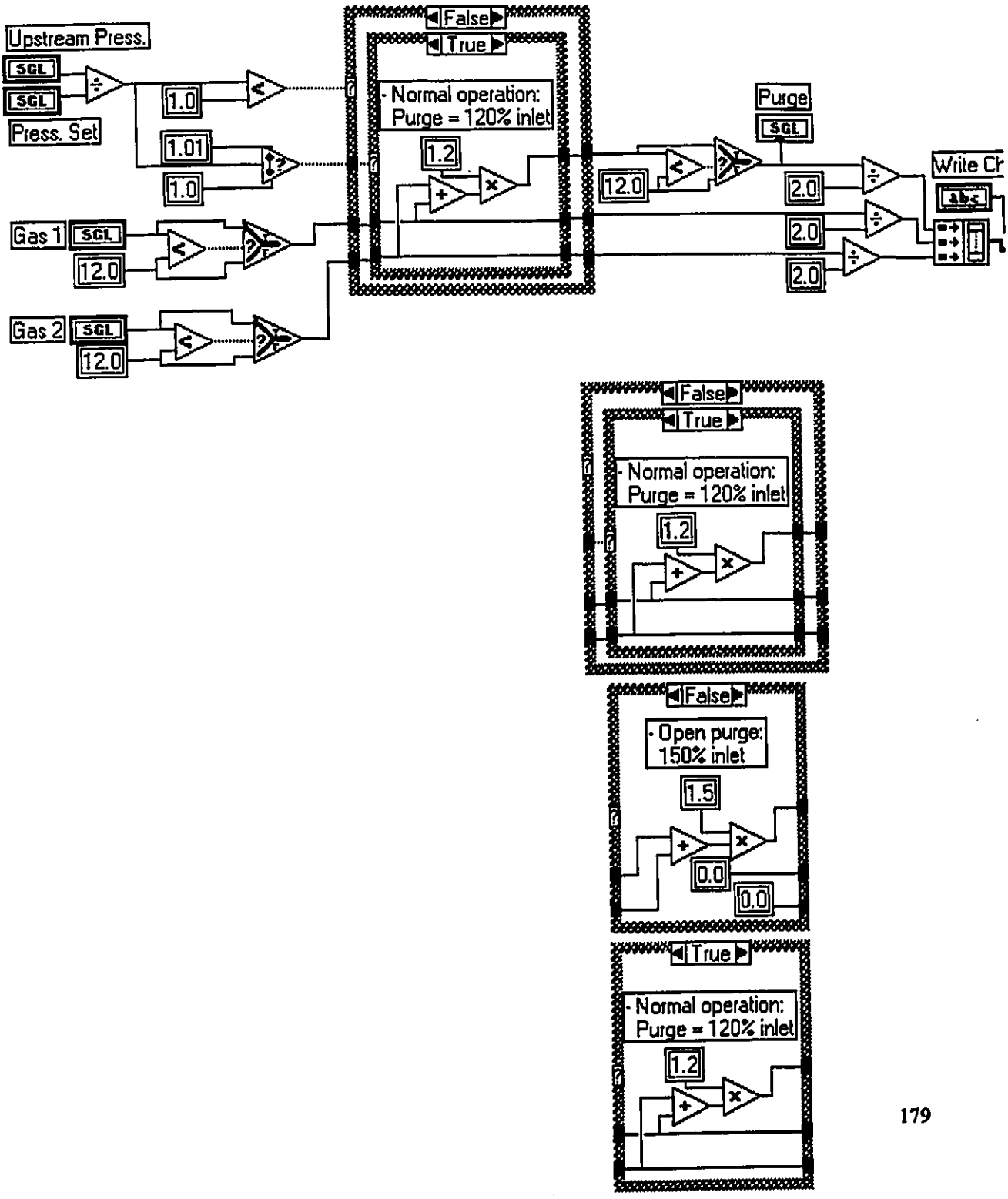

Mass Flow/Press Control
8/10/94 4:29

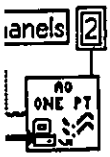

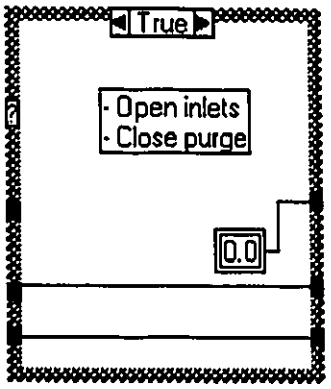
True
· Open inlets
· Close purge
0.0

read
8/10/94 4:38

Position in Hierarchy

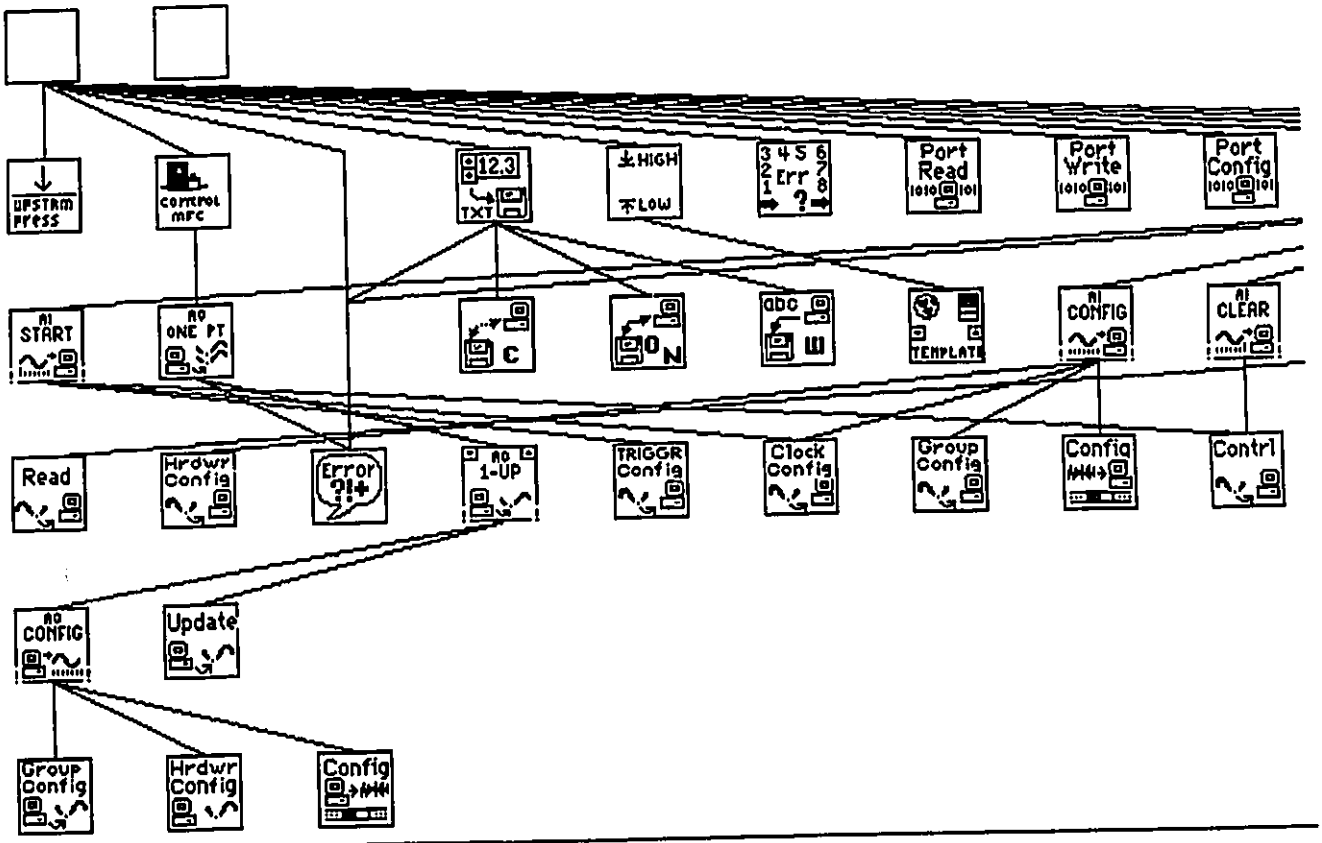

Connector Pane

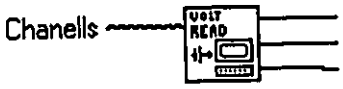

read

read
8/10/94 4:38

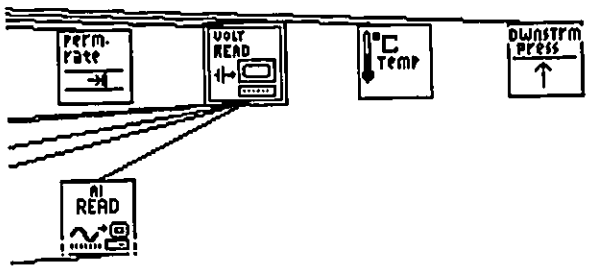

read
8/10/94 4:38

Front Panel

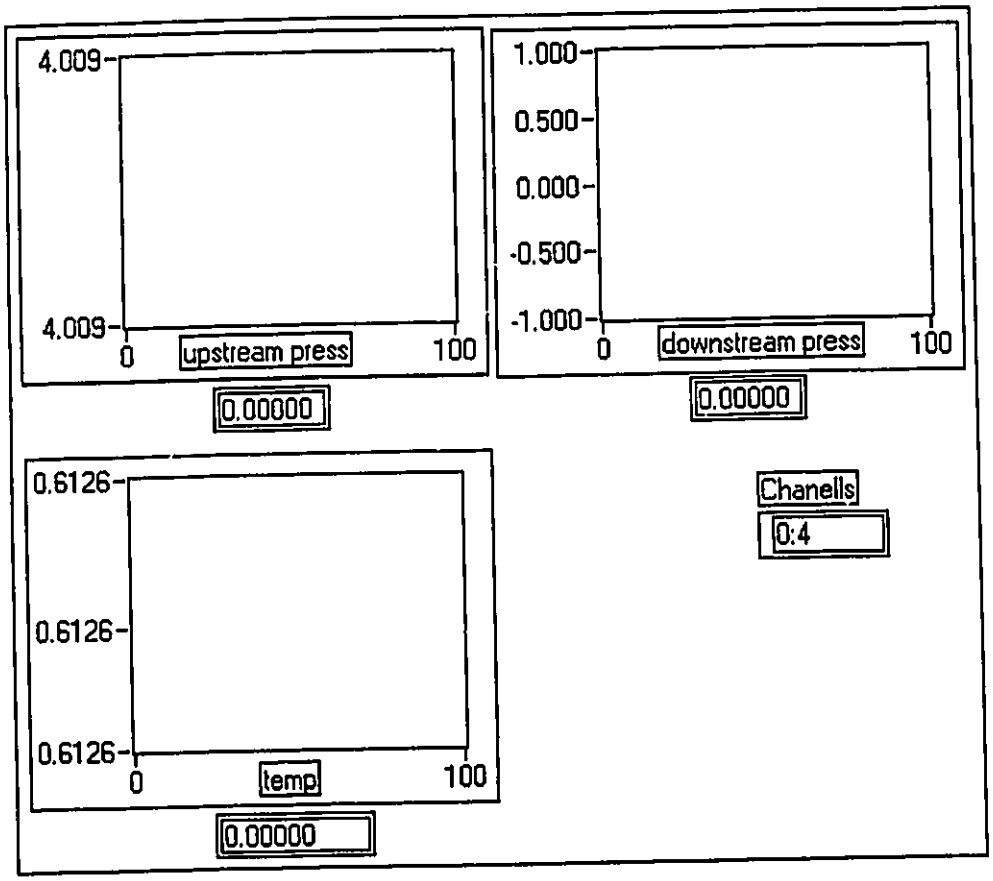

read
8/10/94 4:38

Block Diagram

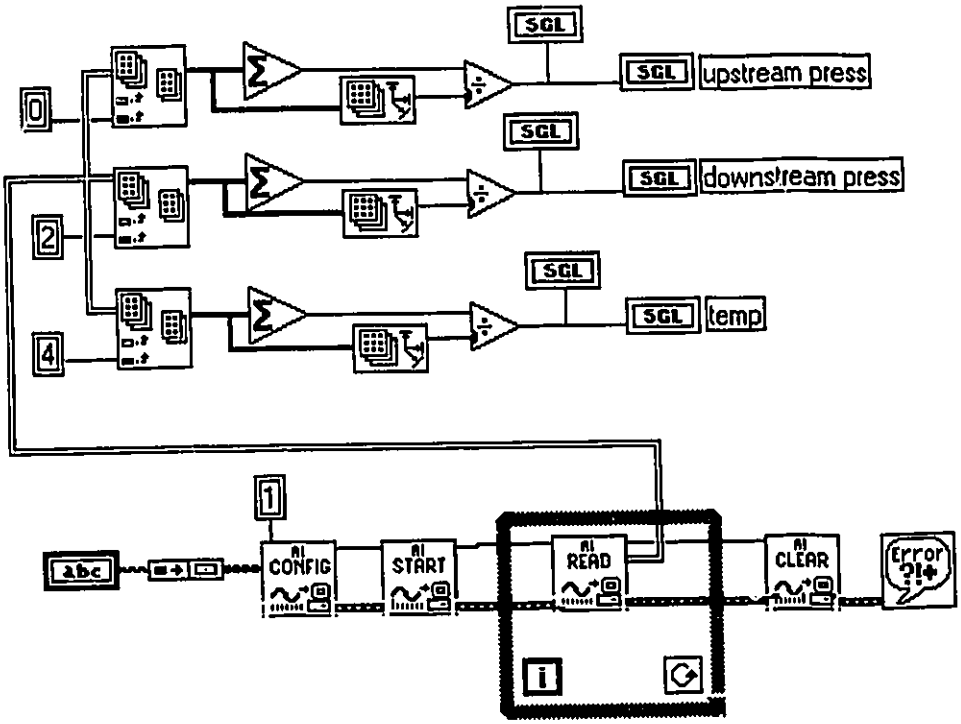

Temperature
8/10/94 4:41

Position in Hierarchy

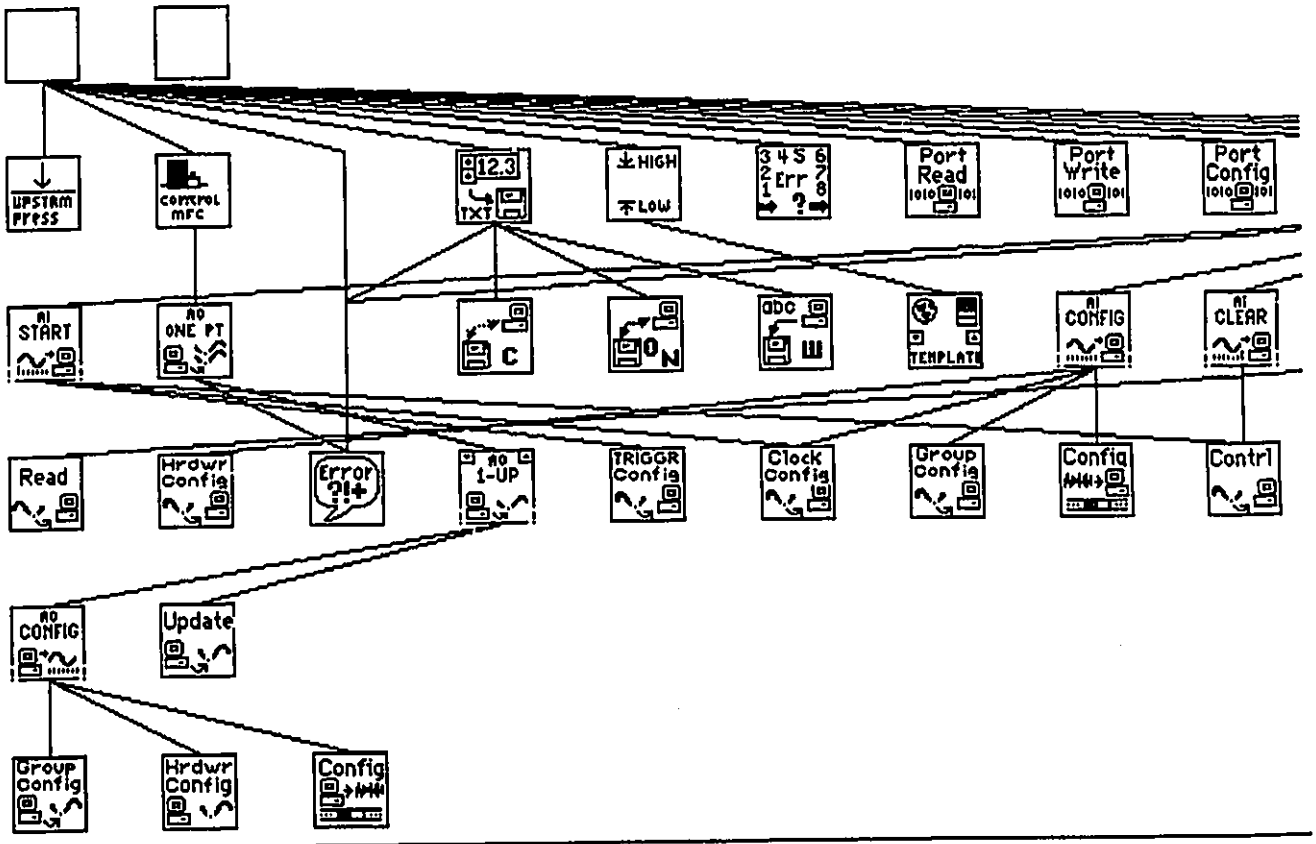

Connector Pane

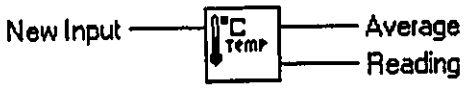

Temperature

Front Panel

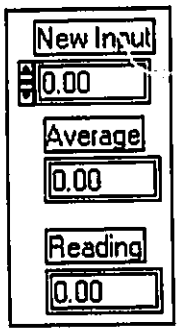

Temperature
8/10/94 4:41

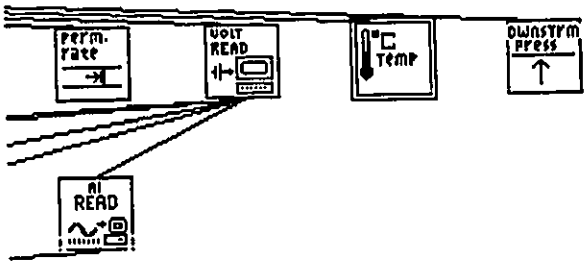

Temperature
8/10/94 4:41

Block Diagram

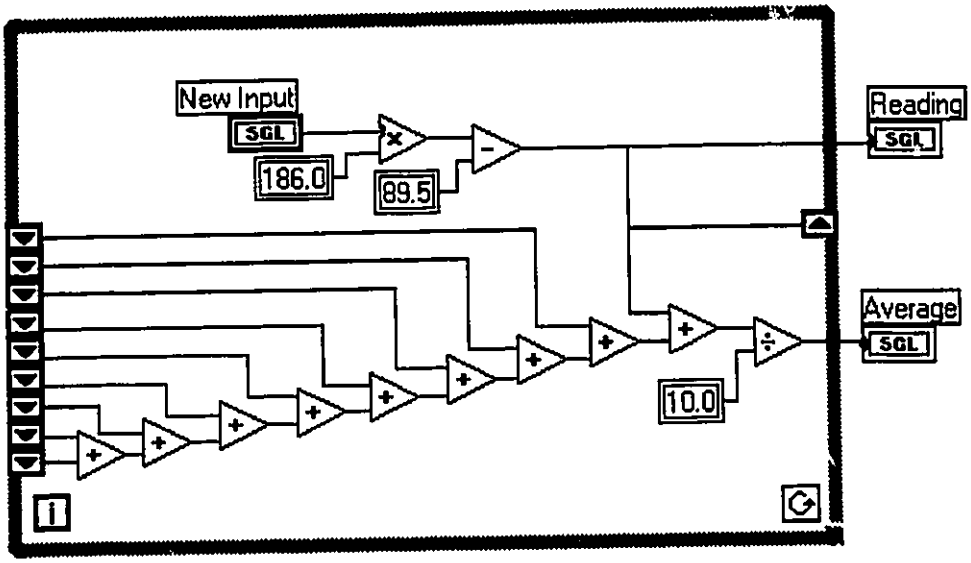

Write To Spreadsheet File
8/10/94 4:42

Position in Hierarchy

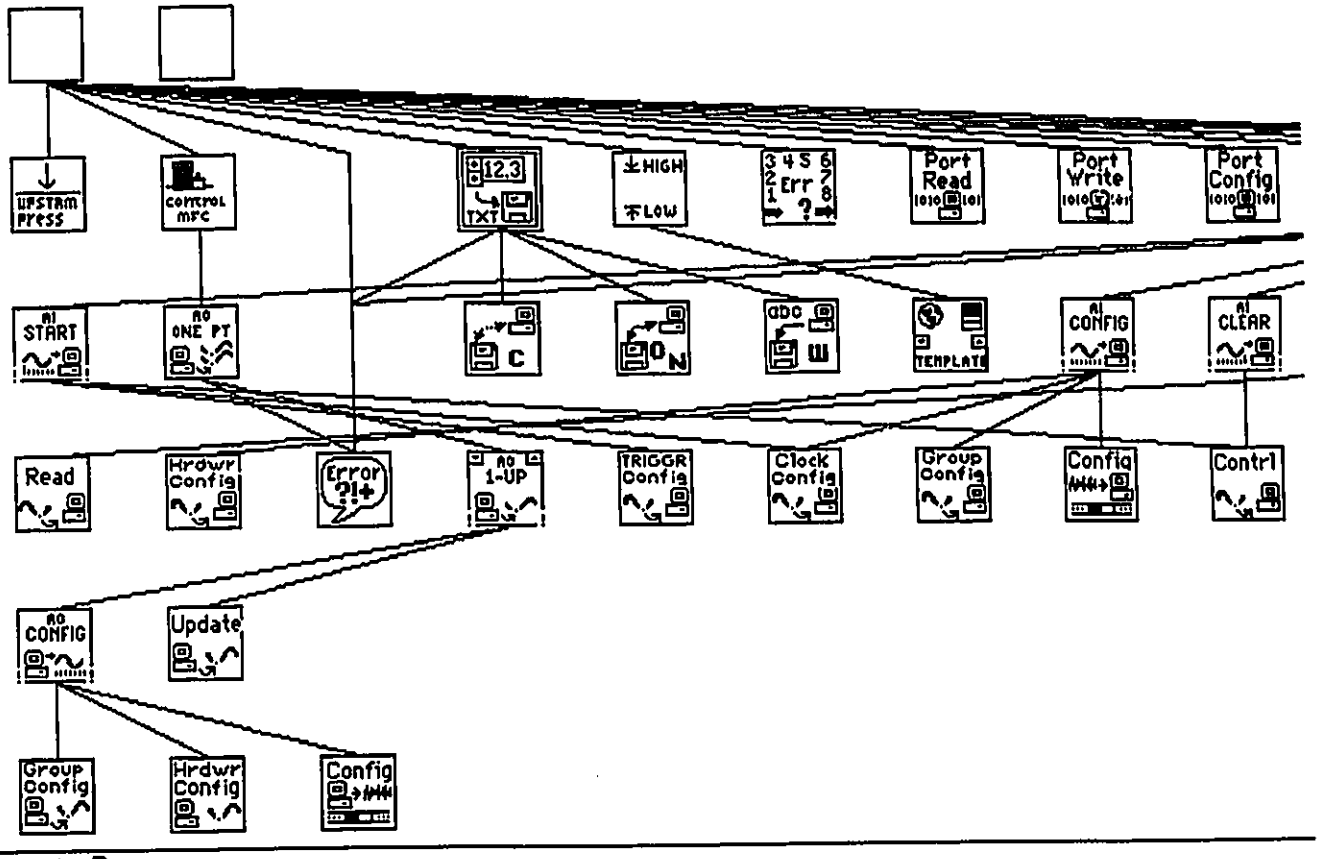

Connector Pane

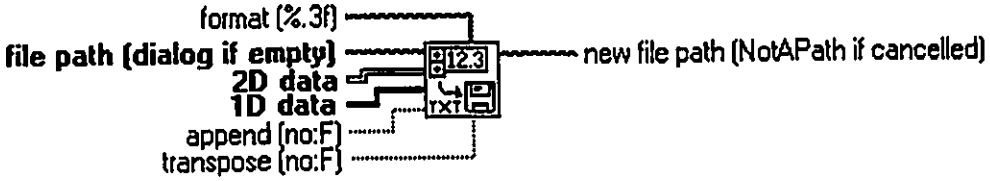

Write To Spreadsheet File

This VI creates or opens a numeric text file (e.g., readable by a spreadsheet or word processing program), converts a 1D or 2D array of single-precision numbers to text and writes or appends it to the file, then closes the file. The 1D array is used unless it is empty, in which case the 2D array is used.

If file path is empty, dialog is used to obtain the file pathname. If the file does not exist, it is created. If the file is created or opened successfully, new file path contains the file pathname; otherwise it is NotAPath.

If append is FALSE (default) and the file exists, you are asked permission to replace (overwrite) it. If append is TRUE, the data is written at the end of the file.

If you want to write to a file iteratively in a loop, consider calling the intermediate level file subVIs directly for greater efficiency.

19 Aug 92

Write To Spreadsheet File
8/10/94 4:42

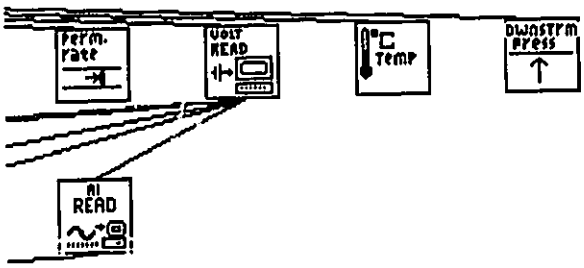

Write To Spreadsheet File
8/10/94 4:42

Front Panel

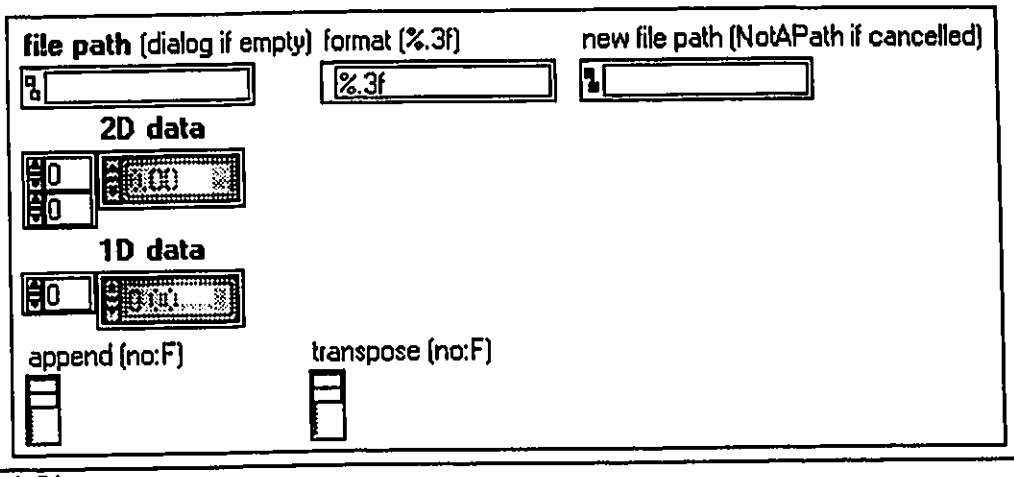

Block Diagram

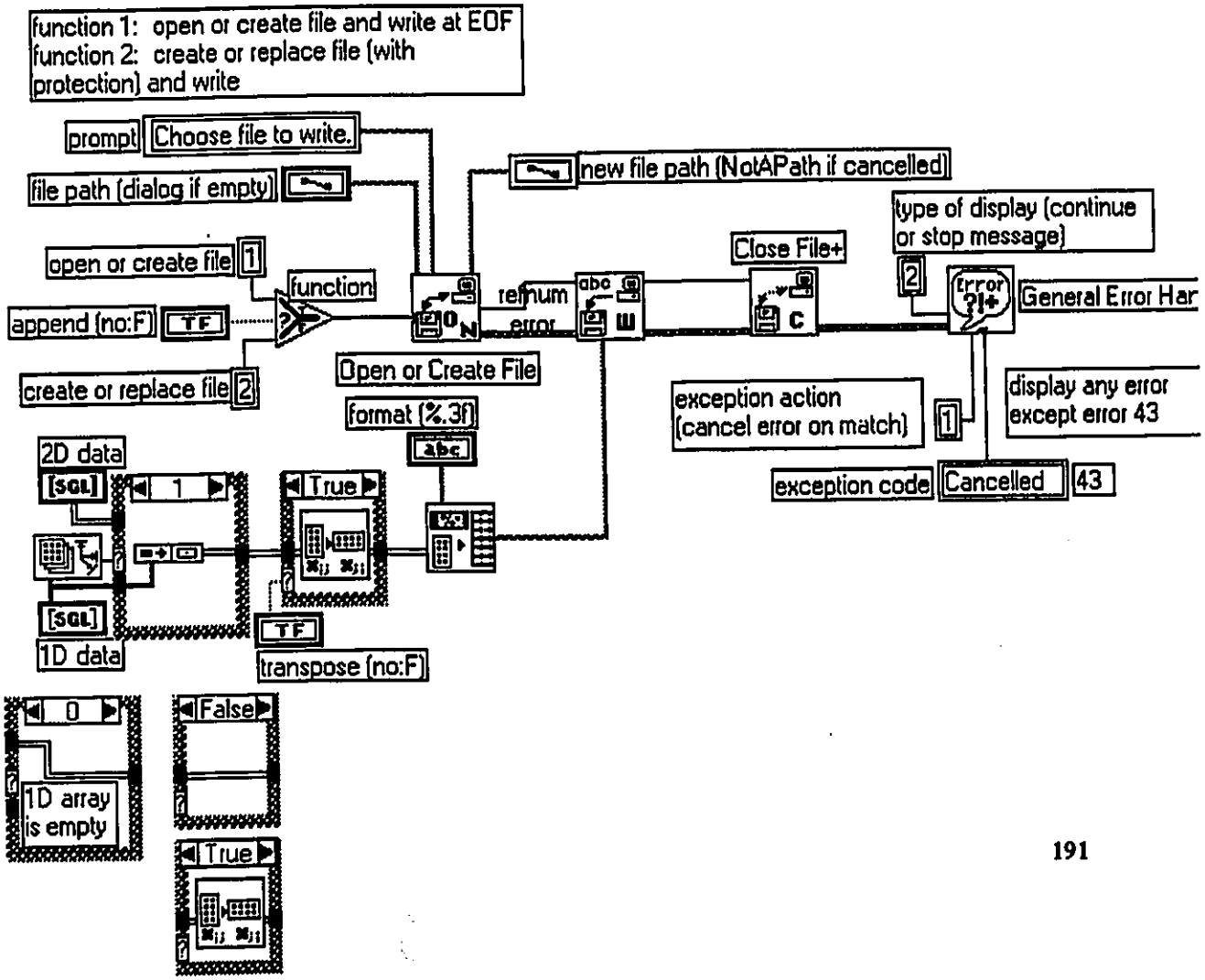

Write To Spreadsheet File
8/10/94 4:42

idler

]

Write To Spreadsheet File
8/10/94 4:42

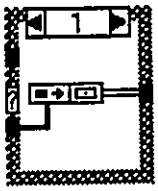

General Error Handler
8/10/94 4:49

Position in Hierarchy

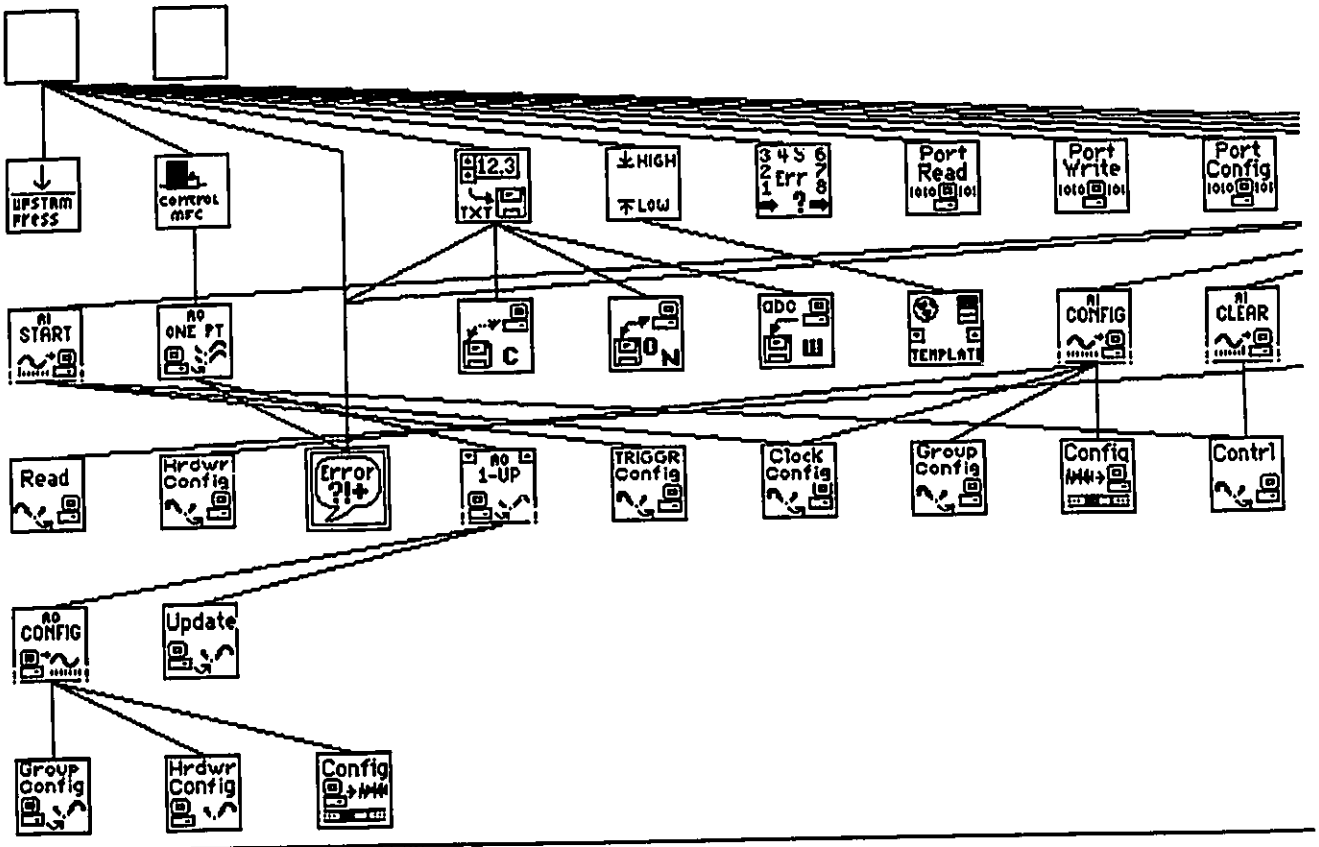

Connector Pane

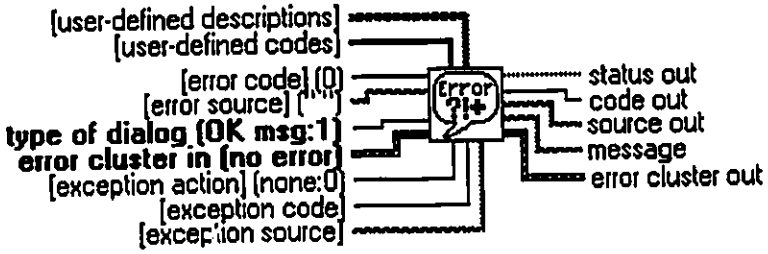

General Error Handler

This error handler is used primarily to inform the user if an input error exists, to describe the error, and to identify where i t occurred. The information need for this is derived from the inputs error cluster in, error code, and error source, and fr om an internal error description table. The table describes all errors that can be created by LabVIEW or its associated I/O operations. The handler has provisions to take alternative actions, such as to cancel or set an error status, and to test for and describe user-defined errors. See instruction on the front panel.

General Error Handler
8/10/94 4:49

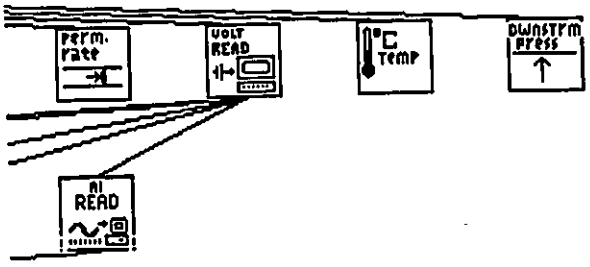

General Error Handler
8/10/94 4:49

Front Panel

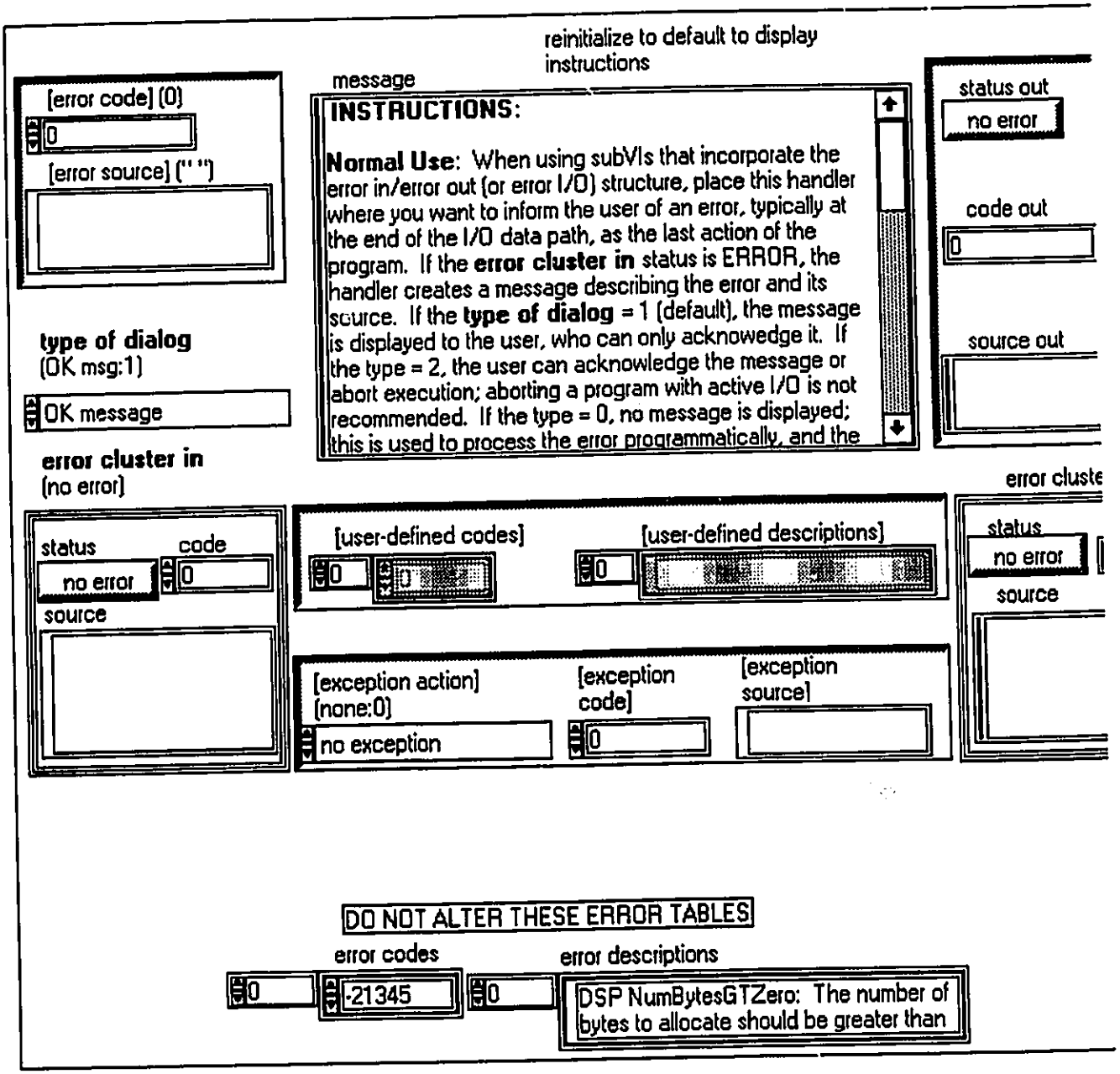

General Error Handler
8/10/94 4:49

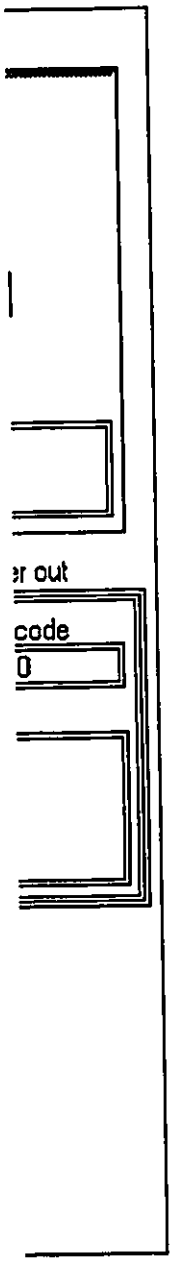

General Error Handler
8/10/94 4:49

Block Diagram

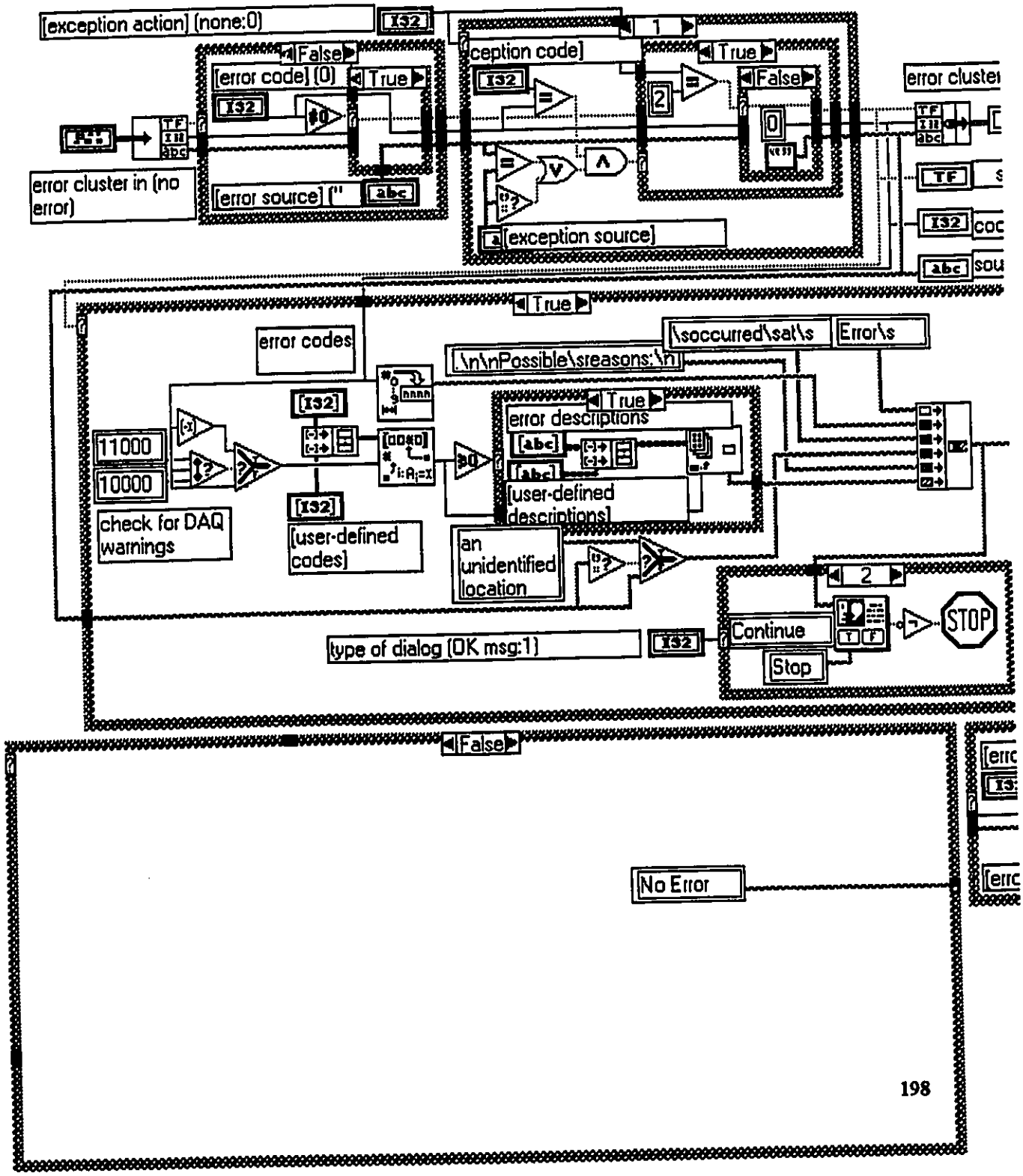

General Error Handler
8/10/94 4:49

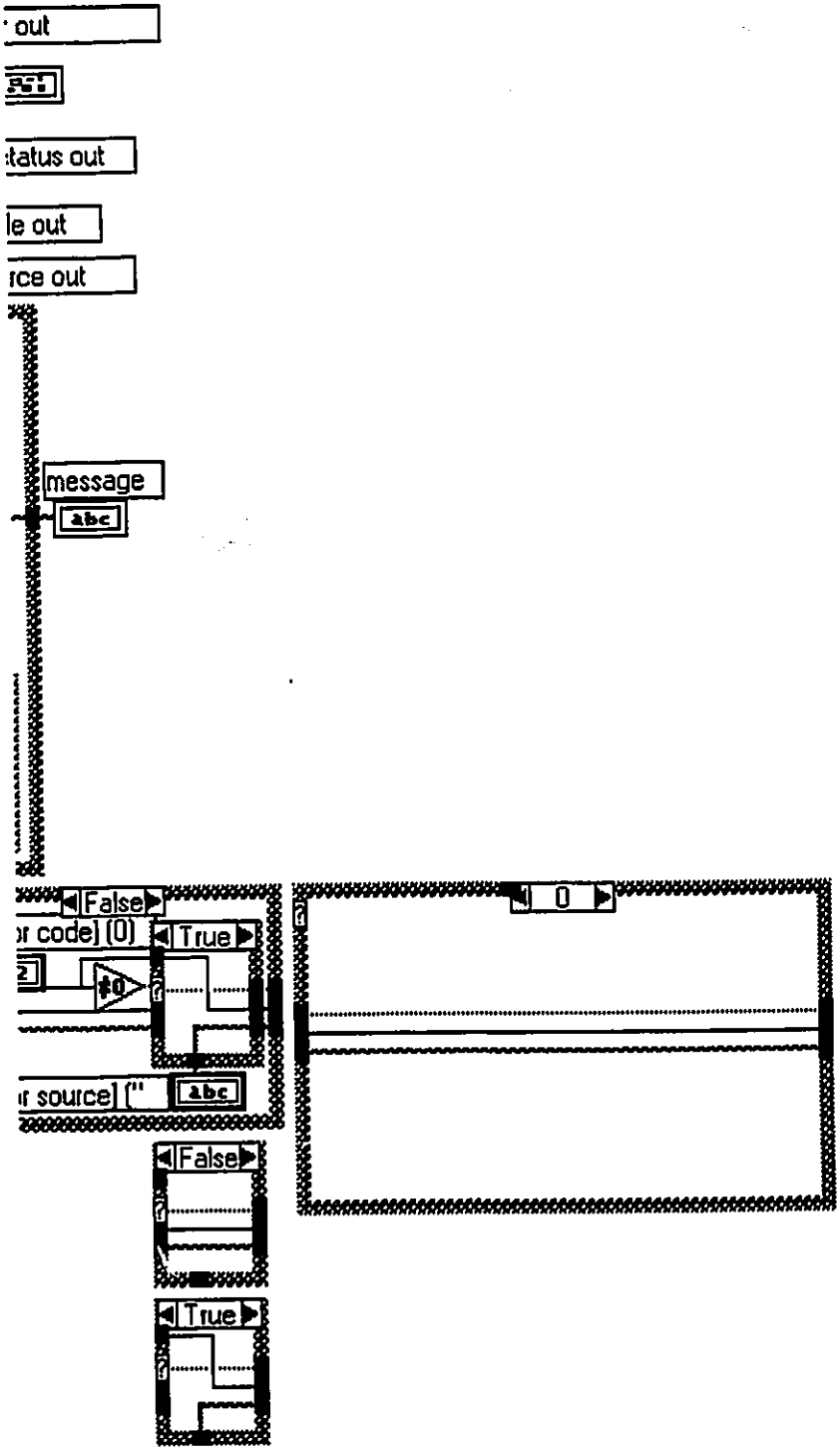

General Error Handler
8/10/94 4:49

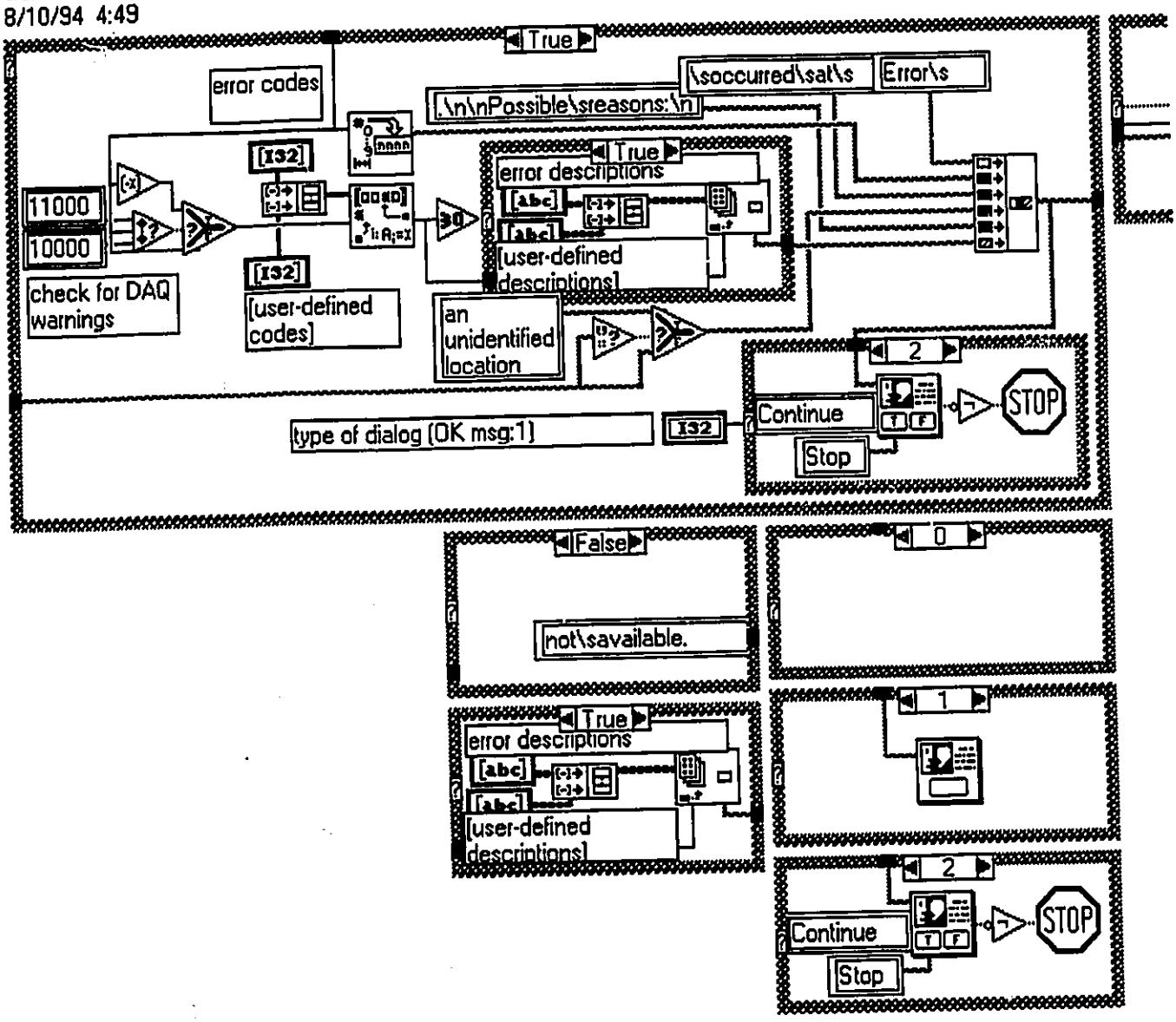

General Error Handler
8/10/94 4:49